HUNGARIAN GEOGRAPHICAL BULLETIN

Volume 75 Number 1 2026

Research Centre for Astronomy and Earth Sciences
GEOGRAPHICAL INSTITUTE

HUNGARIAN GEOGRAPHICAL BULLETIN

Quarterly Journal of the
GEOGRAPHICAL INSTITUTE
RESEARCH CENTRE FOR ASTRONOMY AND EARTH SCIENCES

Indexed by Clarivate Web of Science Core Collection, Elsevier-GEOBASE®, Elsevier-SCOPUS®, EBSCO Information Services, CAB Abstracts, Current Geographical Publications, Scimago Journal & Country Rank, Google Scholar

HUNGARIAN GEOGRAPHICAL BULLETIN 75 2026 (1)

CONTENT

Book review section

Scenario-based analysis of the projected mean changes in the monthly frequency of hot days based on the latest CMIP6 simulations along European zonal segments

Ferenc Tamás DIVINSZKI[1], Anna KIS[1] and Rita PONGRÁCZ[1]

Abstract

The potential changes in extreme hot temperature (represented by TX35, i.e. the number of days with maximum temperature above 35 °C) are analysed, using the latest global climate model simulations ensemble mean of CMIP6, available in the new tool of the IPCC, namely, the Interactive Atlas. The analysis is carried out over Europe with a special focus on Central and Southern Europe. Our aim is to evaluate the spatial patterns within the projected changes in the period 2081–2100 that can be further used in several sectors, e.g. in the health sector, which is especially affected by the potential increase of extremely hot conditions. For this purpose, the projected changes of TX35 are compared to the reference-period 1995–2014 for four available scenarios from the newest scenario-family, namely, SSP1-2.6, SSP2-4.5, SSP3-7.0, and SSP5-8.5 representing different mitigation and adaptation challenges. As the projected increase is not limited to summer, the monthly-scale analysis is extended to the period from May to September. A novel approach is used to investigate the major factors in the projected changes, namely, six zonal segments are selected over Europe, covering the relevant parts of the continent with appropriate distances between them. The most important driving factors of the projected changes of TX35 are identified as follows: (i) the differences between regions due to their north-south or east-west locations (i.e. zonal and continental effects), (ii) elevation above sea level, (iii) the different anthropogenic effects (i.e. different scenarios). The results show that the key factor in the projected changes is the difference between anthropogenic effects. Furthermore, the sea-land surface differences also have substantial effect on the projected changes of TX35, especially in the southern regions. Continentality and elevation show only smaller effects overall.

Keywords: SSP scenarios, extreme temperature, IPCC Interactive Atlas, climate change, TX35, Europe, CMIP6

Received June 2025, accepted February 2026.

Introduction

With the intensifying global warming, both climate mitigation and adaptation have become key challenges (e.g. Rojas-Downing, M.M. *et al.* 2017; Eyring, V. *et al.* 2024). As warming intensifies, more frequent and more severe extreme events occur (Wobus, C. *et al.* 2018). A recent record breaking occurred on 22nd July 2024 that became the hottest day on Earth ever measured since the regular worldwide measurements started, as the daily global mean temperature reached a record of 17.16 °C (WMO 2025). Moreover, the year 2024 was the warmest year on record, with the global mean temperature exceeding the pre-industrial average by 1.6 °C (C3S 2025), and the previous record year (i.e. 2023) by 0.12 °C.

The consequences of such heat were damaging in many sectors. For instance, heat-related mortality rose above 40,000 cases in 2023, which is the second highest after 2022 (Gallo, E. *et al.* 2024). As even greater increase is projected in the frequency of extreme events, such risks are also expected to further increase in the future (Lüthi, S. *et al.*

[1] ELTE Eötvös Loránd University, Institute of Geography and Earth Sciences, Department of Meteorology, Pázmány Péter sétány 1/a, H-1117 Budapest, Hungary. Corresponding author's e-mail: pongracz.rita@ttk.elte.hu

2023). Another example can be mentioned in the agricultural sector, namely, the consequences of extreme weather events can cause serious food supply issues (Cogato, A. *et al.* 2019). Moreover, the energy sector is also vulnerable to these extreme heat events (Schaeffer, R. *et al.* 2012).

All these examples highlight the importance of the implementation of adaptation strategies. Our study assesses the current state-of-the-art projections of extreme temperature events, with the ultimate goal to support decision-makers in creating and optimizing long-term plans. It is important to provide detailed information of the consequences of non-acting in time. More specifically, the aims of this study are to answer the following questions: (i) What are the general spatial patterns of extreme temperatures over Europe? (ii) Are these patterns changing due to climate change, and do different anthropogenic effects (i.e. scenarios with different emission pathways) have an influence on these changes? (iii) What geographical effects are dominant in shaping the patterns of extreme temperatures in different parts of the continent? The novelties of the present study include the applied new scenarios, new climate model results, a newly available tool of the IPCC, and the monthly scale, which provides more detailed information for hot conditions than the usual, more general annual/seasonal scale. For these purposes global climate model simulations applying a new generation of scenarios are used, as finer resolution regional climate model simulations taking into account these scenarios are not available yet. Since temperature-related phenomena show usually less spatial variability than e.g. precipitation-related events due to their general statistical characteristics (Wilks, D.S. 2006), the resolution of global scale models is still sufficient for a robust assessment.

In the next section data and methodology used in this study are described. Then, the third section (Results) addresses the aforementioned questions by presenting and discussing the results of a systematic analysis. A comparison of the present study to other relevant studies can be found in the fourth section (Discussion), and finally, the conclusions are summarised.

Data and methodology

The assessment reports (AR) published by the IPCC have been the key information source of climate science for the last few decades. The recently published AR6 (IPCC 2021) contains the results from the latest climate model simulations in the framework of CMIP6 (Eyring, V. *et al.* 2016), with the future projections taking into account the new SSP-scenarios (O'Neill, B.C. *et al.* 2017) paired with the previous RCPs (van Vuuren, D.P. *et al.* 2011) used in AR5 (Taylor, K.E. *et al.* 2012). The available data were then assembled in the Interactive Atlas (IA) (Gutiérrez, J.M. *et al.* 2021).

The IA provides an easy-to-use interface, where the different databases, scenarios etc. can be compared by using various diagrams, graphs, and maps. However, there are only limited options to perform scientific studies unless using the built-in option to download multi-model mean data for different datasets, different scenarios, several climate variables/indices, and time periods. Besides the more general approach using the entire year, it is also possible to focus on a specific season or month, so the annual cycle can also be evaluated from the climate change viewpoint.

In this study, multi-model monthly mean (each member has an equal weight) data were downloaded for all the four available SSP-scenarios, SSP1-2.6, SSP2-4.5, SSP3-7.0, and SSP5-8.5. The list of the individual models is shown in *Table S1* (Supplementary section).[2] Altogether 22 models provide simulation for all the four scenarios, in addition, 6 models were simulated only for two or

[2] Note, that the downloading is possible only for the multi-model ensemble mean and not the individual simulation results, thus, the inter-model spread and the ensemble uncertainty cannot be assessed; moreover, the changes are shown as a multi-year average without the time series of each annual value.

three scenarios. Both the SSP2-4.5 and SSP5-8.5 ensembles contain 27 model simulations. However, these differences of a few model simulations within the scenario-ensembles do not affect the mean results.

To study the effects of extreme heat, the focus of this study is on the climate indicator called 'days with maximum temperature above 35 °C' (indicated as TX35) by 2081–2100. The target period of projections is selected according to the most recent IPCC AR (2021), to ensure the greatest climate signals of the various scenarios by the end of the 21st century (called long term by IPCC [2021]). The projections are compared to the 1995–2014 reference period, which covers the last 20 years of the historical simulations prior to starting the scenario runs from 2015.

To cover Europe entirely, five zonal segments are selected from the Northern Hemisphere, i.e. 37.5°, 42.5°, 47.5°, 52.5°, and 57.5° (*Figure 1*), each segment represents a series of grid cells along the corresponding 1° latitude zone, e.g. the zonal segment of 37.5° represents the zone between 37° and 38°. However, the downloading process does not allow the users to select a desired area or certain grid cells to receive data from, the netCDF file of the entire global field has to be downloaded. The downloaded files contain the multi-model mean values of the entire ensemble for the target period for each month separately, but not for each simulation individually. Therefore, first, the non-European grid cells are eliminated by applying a European land contour mask to the global coverage, and then, the appropriate target segments are cut from these global data series. After re-gridding all individual simulations (the finest with a horizontal resolution of 0.5° × 0.5°, while the most coarse simulation with 2.81° × 2.77°, but the majority is closer to 1° × 1°) to a uniform custom grid (Gutiérrez, J.M. *et al.* 2021), the horizontal resolution of the multi-model ensemble mean is 1 × 1° that finally resulted in 32 (from 9°W to 23°E), 37 (from 9°W to 28°E), 47 (from 2°W to 48°E), 55 (from 10°W to 45°E), and 51 (from 7°W to 44°E) grid cells, respectively, along the segments from the southernmost (37.5°N) to the northernmost (57.5°N). Each segment begins from the westernmost land-covered grid cell near the Atlantic Ocean, and then, all the inner water-covered grid cells are kept along the segment until reaching the Aegean Sea, the Black Sea, or the river Volga in the east.

Then, the simulated data are assembled to special diagrams and graphs systematically, to help visualise and analyse the massive amount of information. Three types of diagrams are created: (i) The projected increase of TX35 is displayed for the four scenarios across the segments, with a grey shading showing the elevation of the grid cells so sea-land differences (i.e. the value of 0 m as elevation and the longitudinal location together define sea areas) can be compared from south to north. In addition, the continentality can be assessed on the basis of longitude, from west to east, as moving away from the Atlantic Ocean. (ii) The projected changes are shown as a function of elevation to analyse the orographic effect. The interpretation is based on visual and/or qualitative assessment, therefore, this applied methodology does not allow for a strict statistical separation of elevation and continentality effects. (iii) The projected warmings for the three SSPs with different mitigation/adaptation challenges are compared to the projections of SSP1-2.6 with strong mitigation and adaptation introducing as soon as possible (i.e. representing the goals of the Paris Agreement, and considered as a baseline scenario), so the anthropogenic effect as well as the impact of its reduction can be evaluated. In addition, the correlation coefficients between the monthly zonal patterns of SSP1-2.6 and the other SSPs are tested for significance using t-test (at the significance level 0.05).

To ensure full coverage of substantial increase in TX35 over the year, apart from the three summer months, results for May and September are also analysed. This is expected to be an important extension in the southernmost segments, where the increase in TX35 is still substantial before and after the summer months. Note that the analysed month

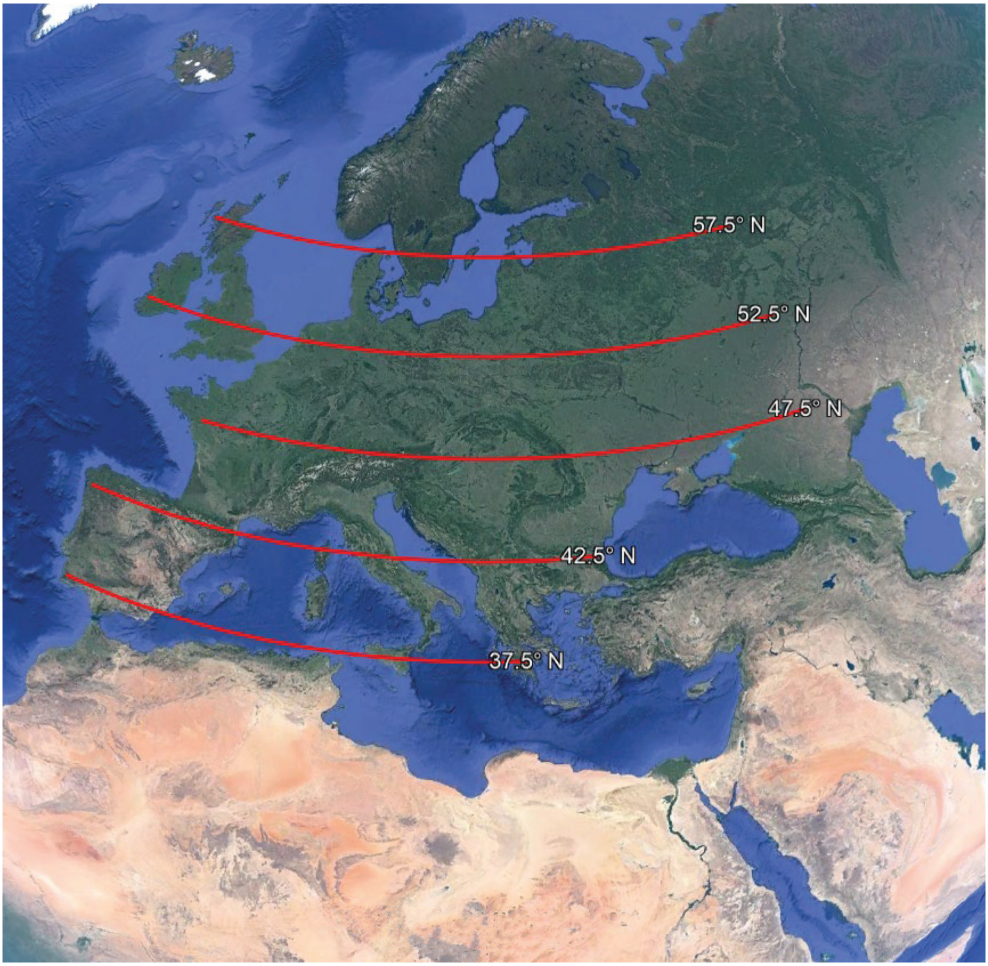

Fig. 1. Location of the selected five zonal segments in Europe. *Source*: Data SIO, NOAA, U.S. Navy, NGA, GEBCO Image Landsat / Copernicus Image IBCAO.

always provides an upper limit to the TX35 values, i.e. the total number of days of the given month. Therefore, if the values are already high in the historical period (i.e. hot conditions are quite frequent historically, shown in *Figure S1* [Supplementary section]), the possible increase is limited. However, if the values are low in the reference period (i.e. moderate/cool climatic conditions are currently present), a greater potential increase is possible. Hence, if the index values reach the upper limit (i.e. the maximum temperature will be above 35 °C every day of the month) for both cases, the latter will suffer from the higher increase only because of the lower reference value.

Results

The projected monthly increase of TX35 is analysed across the 37.5°N, 42.5°N, 47.5°N, 52.5°N and 57.5°N segments, respectively, for the period May–September (diagram type (i)). Then, the diagram type (ii) shows the projected changes in TX35 as the function of elevation. The five segments form two major groups. Group1 consists of the 37.5°N, 42.5°N and 47.5°N segments where high elevation areas with peaks are close to 1500 m. Group2 is formed by the remaining two segments: 52.5°N and 57.5°N, where the elevation is below 400 m at any longitude.

Finally, the diagram type (iii) analyses differences between scenarios instead of other geographical-location-determined climatic effects. For this purpose, the most sustainable scenario, SSP1-2.6 serves as a basis, to which all the others are compared in order to analyse the adaptation and mitigation effects on the changes of TX35. First, the correlation coefficients between the spatial patterns of SSP1-2.6 and the other SSPs along each zonal segment are tested for significance and show significant similarities (i.e. the correlation coefficients are between 0.65 and 0.99, except the 57.5°N segment, where only minor changes are projected, and the coefficient values range between 0.75 and 0.99 (*Table S2*) (Supplementary section). These imply that the spatial patterns of the SSPs are very similar at every segment, the main difference between the scenarios is the magnitude of the projected increase in TX35. These are highlighted by green dotted lines on the corresponding graphs, with the projected increase being the same, two-fold, and four-fold compared to the SSP1-2.6 scenario.

Along the 37.5°N segment (in *figures 2–4*), the TX35 values in the reference period are already high due to the southern location. Therefore, the projected increase for the 2081–2100 target period is not the greatest among the segments. However, it is still significant, especially in July, August, and September (*Figure 2, c, d*, and *e,* respectively), when the overall relative increase over land is 30–50 percent and more than 80 percent in the case of SSP1-2.6 and SSP5-8.5, respectively. In fact, the land areas of southern Spain, Italy and Greece are projected to warm much more compared to water surfaces, so higher increase of TX35 is likely to occur by late-century. This spatial pattern is also visible in the reference period; hence, the general spatial pattern will not change according to any projection either. However, the spatial differences between the land areas and water surfaces are likely to increase.

There are grid cells with elevation close to 1000 m (*Figure 3*), which makes this latitude segment belong to the same group as 42.5°N and 47.5°N, where peaks can reach up to 1500 m. The general pattern is similar in every month: there are three maximum increases for all four scenarios, at around 200 m, at 450 m, and at 800–1000 m a.s.l., which are the respective elevations for Sicily, Peloponnese, and the Iberian Peninsula. These imply that elevation does not influence much the projected change of TX35. However, as this latitude crosses the Mediterranean Sea and every land grid cell is close to the Mediterranean Sea, the effects caused by the elevation differences are dominated by a more important and stronger effect, i.e. the distance from extended water surfaces. The moderating effect of sea cover is especially highlighted in June and September (*Figure 3, b*, and *e*). For instance, in *Figure 3, e* the greatest increase projected at the water grid cells (0 m elevation) is 2.7 days, whereas it is just below 2 weeks at the land grid cells based on the SSP5-8.5 scenario. On the other hand, the difference between these grid cells is reduced in July and August to 5 days (see *Figure 3, c*, and *d*, respectively).

The scenarios show different magnitudes of increase in different months (*Figure 4*). On the basis of the calculated linear regression coefficients for the three scenarios, a general pattern is shaped across the months. The largest coefficient values can be identified in May, namely, 2.5, 5.5 and 7.7 for SSP2-4.5, SSP3-7.0 and SSP5-8.5, respectively, indicating the ratio of the mean projected increases compared to SSP1-2.6. The coefficients reduce from May to July and further to slightly less than 2 in August, when the differences between the scenarios disappear in terms of the overall fitted linear regression. This is mostly due to a spatial difference occurring

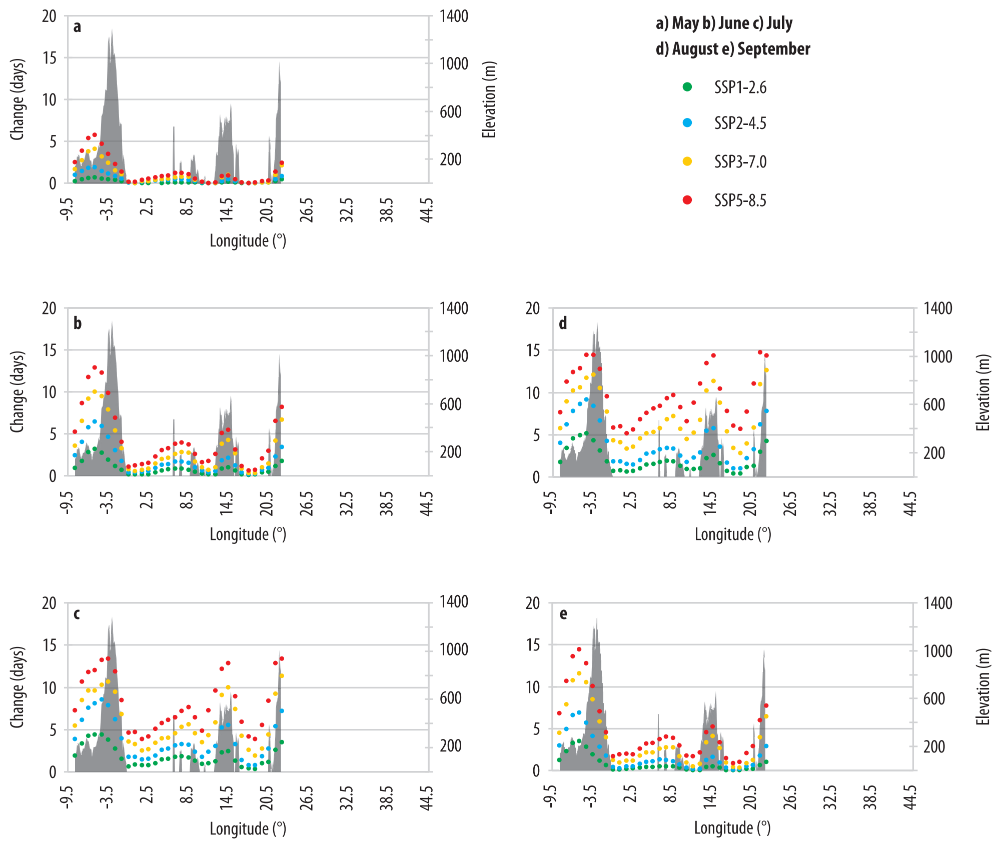

Fig. 2. Projected monthly changes of TX35 (2081–2100 vs. 1995–2014) for SSP1-2.6, SSP2-4.5, SSP3-7.0, SSP5-8.5 and elevation along the zonal segment of 37.5°N. *Source:* Authors' own elaboration.

in the segment, namely that if the projections for water and land surfaces are separated, then the different scenarios have different coefficients for these two surface types. More specifically, the coefficients for land surfaces are 1.1 and 1.08 for the SSP3-7.0 and SSP5-8.5 scenarios in August, whilst for water surfaces, they are 2.8 and 3.1, respectively. Then, the regression coefficients increase again in September; however, they still do not reach the values in May. Note that the smallest increase in monthly TX35 is found in those months when the coefficients are the largest (i.e. in May and September). Therefore, the greater the projected increase, the more reduced the relative differences between the scenarios are.

Moving northward to the *42.5°N* segment (*Figure 5*), the aforementioned spatial patterns are even more pronounced than along the 37.5°N segment. The differences are the most remarkable in August (*Figure 5, d*), and almost as much in July (*Figure 5, c*). The increase of 18.4 days in the grid cell with the centre of (42.5°N, 25.5°E) in August is the highest among every zonal segment. However, in the same month, along the same latitude but at the 5.5°E longitude, the projected increase is only 3.3 days. Both changes are projected for the SSP5-8.5, the scenario with high challenges in mitigation, low challenges in adaptation, with the highest radiative forcing change of 8.5 W/m^2 among the analysed scenarios. The changes projected by the

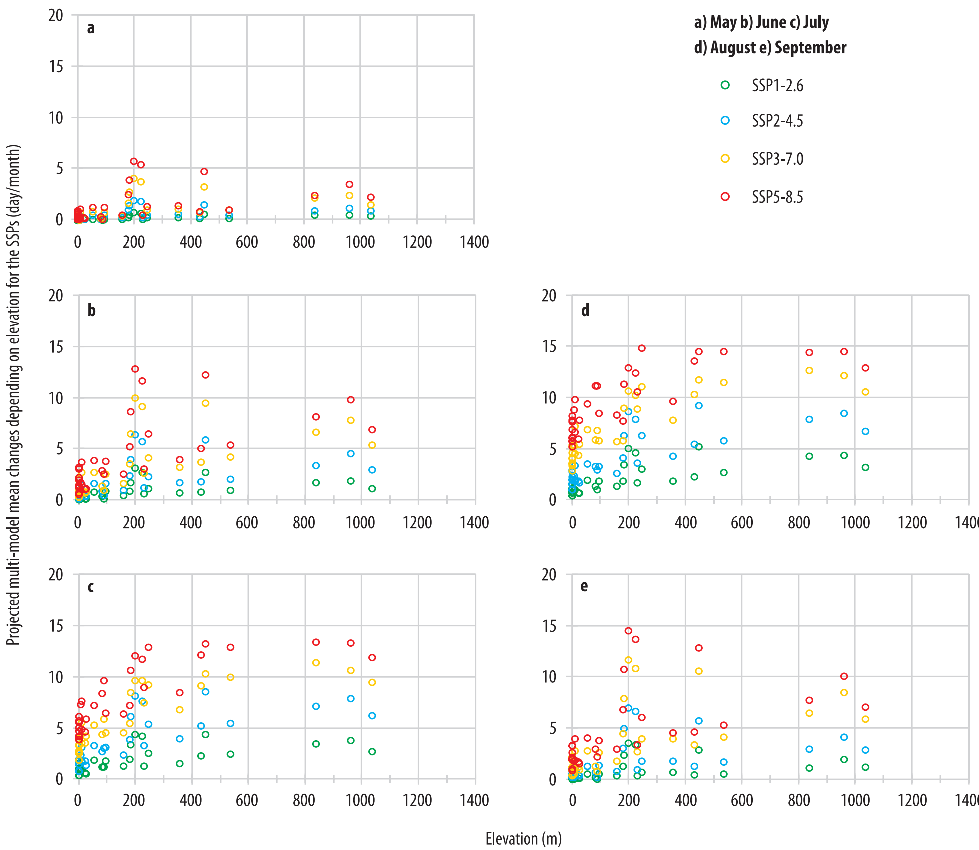

Fig. 3. Projected monthly changes of TX35 (2081–2100 vs. 1995–2014) depending on elevation at 37.5°N for SSP1-2.6, SSP2-4.5, SSP3-7.0 and SSP5-8.5. *Source:* Authors' own elaboration.

SSP1-2.6 scenario with the lowest radiative forcing change show similar spatial patterns, the increase is the greatest at 25.5°E, and the smallest at 5.5°E, however, with much lower increases, i.e. less than 4 days for the 22.5°E, and 0.2 days for the 5.5°E. Therefore, it can be concluded that the direction of the projected change of the TX35 and the spatial patterns along the segments are similar regardless the scenario. The difference is the magnitude of the projected increase, which shows that the higher the radiative forcing becomes, the greater the spatial differences (especially between land and sea). Besides the land vs. sea difference, an overall greater increase tends to be projected over land areas as moving toward east, implying a continental effect.

Analysing the effects of elevation, *Figure 6* shows that the 42.5°N segment has a much more diverse terrain than the 37.5°N segment, with grid cells being spread almost evenly within the interval of 0–1400 m elevations. The months again show similar patterns compared to each other; however, the differences across the different elevations are the most pronounced in July (*Figure 6, c*) and August (*Figure 6, d*), when the projected increase is the highest. The greatest increase is projected to occur at around 400 m above sea level, namely, more than 18 days in August, based on the SSP5-8.5 scenario. The smallest projected increases can be recognised in two different levels: (i) at the water-covered grid cells and the low elevation areas representing

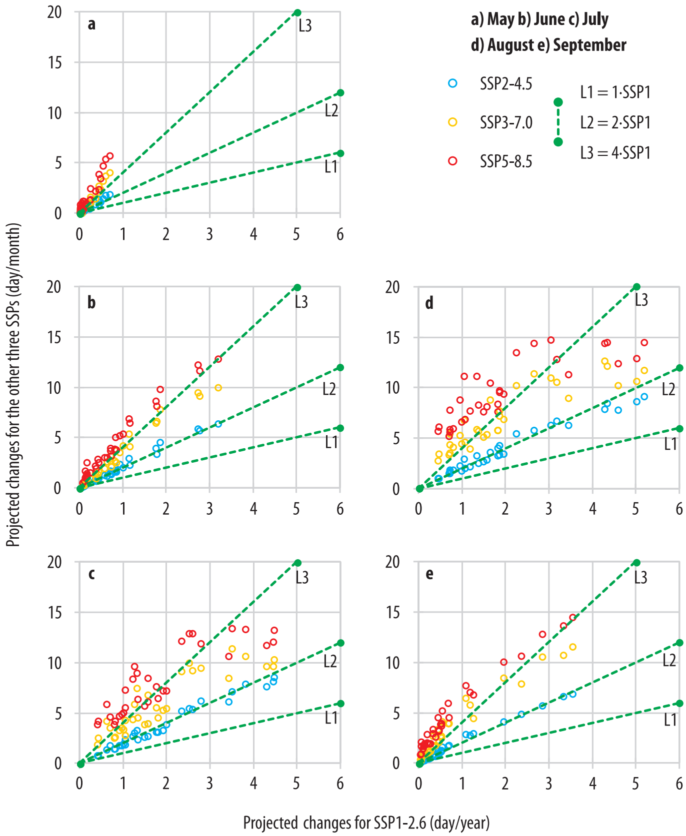

Fig. 4. Projected monthly changes of TX35 (2081–2100 vs. 1995–2014) for SSP2-4.5, SSP3-7.0 and SSP5-8.5 compared to SSP1-2.6 at 37.5°N. *Source:* Authors' own elaboration.

the shoreline lands, and (ii) at the highest elevation points around 1300 m above sea level. Here, the absolute smallest increases belong to category (i). Note that this is a general spatial distribution in the increase of TX35 for all the four scenarios, however, the actual value of the projected change is different. The lower the projected increase is, the less the influence of elevation. Similar patterns can be seen in the case of May and September (*Figure 6, a*, and *e*), when the increase is also smaller, therefore, the differences caused by elevation are not present so clearly. Also, the projections of the four scenarios are close to each other implying smaller effect from the general global warming rate (which is strongly depending on the radiative forcing change).

As for the inter-scenario comparison relative to the SSP1-2.6 scenario (*Figure 7*), there are similar patterns across the months to the 37.5°N segment, however, here, May (*Figure 7, a*) is more similar to the summer months, and only September (*Figure 7, e*) is substantially different from them. This is also reflected by the regression coefficients, which are within a narrow range from May to August (1.5-2 for SSP2-4.5, 3-3.4 for SSP3-7.0, and 3-4.5 for SSP5-8.5), but differ from these in September (2.5 for SSP2-4.5, 5.5 for SSP3-7.0, and 7.1 for SSP5-8.5). It is also worth noting that the projections for the grid cells form two major

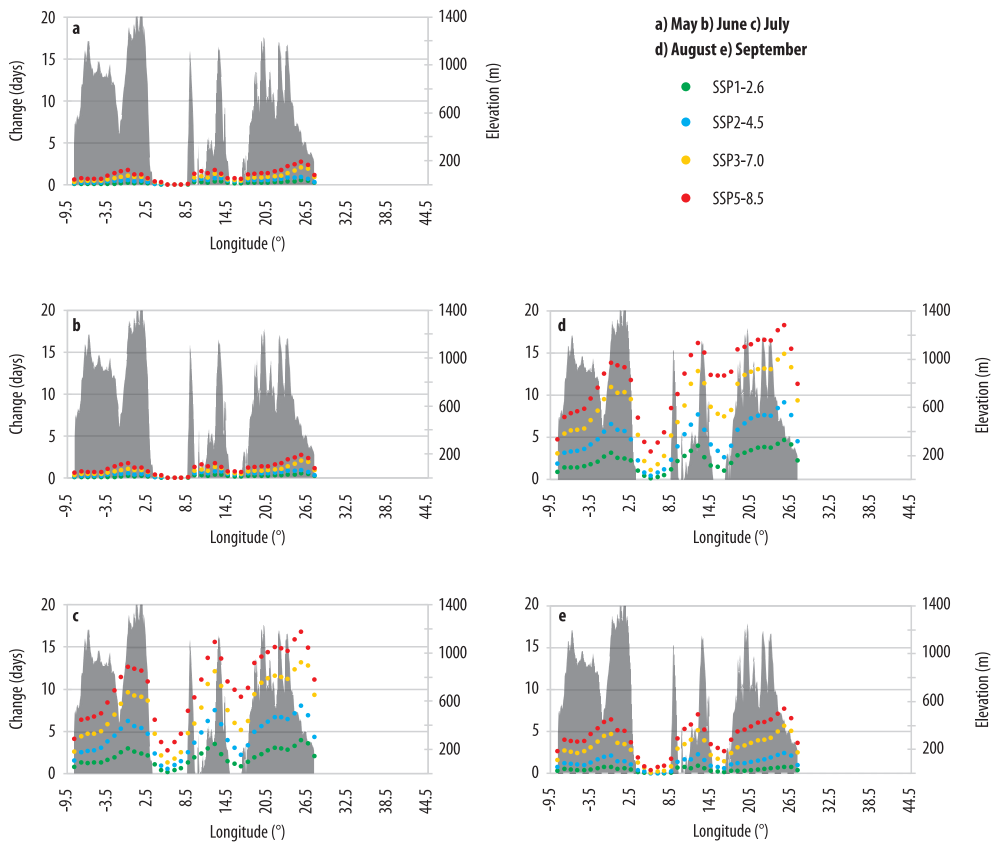

Fig. 5. Projected monthly changes of TX35 (2081–2100 vs. 1995–2014) for SSP1-2.6, SSP2-4.5, SSP3-7.0, SSP5-8.5 and elevation along the zonal segment of 42.5°N. *Source:* Authors' own elaboration.

clusters on the diagrams for the 37.5°N segment due to the limited land areas, especially in June and September (see *Figures 4, b*, and *e*), whereas at the 42.5°N segment, the points are scattered evenly along a fitted regression line on the basis of all longitudes.

Compared to the two southern segments, the continental effect is much stronger at the *47.5°N* segment (*Figure 8*). The more eastern a grid cell is, the further it is located from the Atlantic Ocean, and therefore, the projected increase is higher. Note however, that in July and August (*Figure 8, c*, and *d*), the intra-zonal increase stops from the 30.5°E towards the eastern end of the segment. This is due to the effects of the other large body of water, i.e. the Black Sea, which is lying just south of the 47.5°N segment and moderates the effects of the growing distance from the Atlantic Ocean. Furthermore, other features also shape the spatial patterns, namely, two large mountain ranges, the Alps and the Carpathians. Therefore, the complex effects of continentality and orography determine the overall intra-zonal and inter-scenario characteristics.

The effects of the orography are visualised in *Figure 9*. As expected, the greatest increase (i.e. more than 2 weeks) is linked to the lower, plain areas for every month. From around 100 m a.s.l. to 800 m, the projected change of the TX35 decreases almost linearly. However, this is abrupted by a secondary maximum

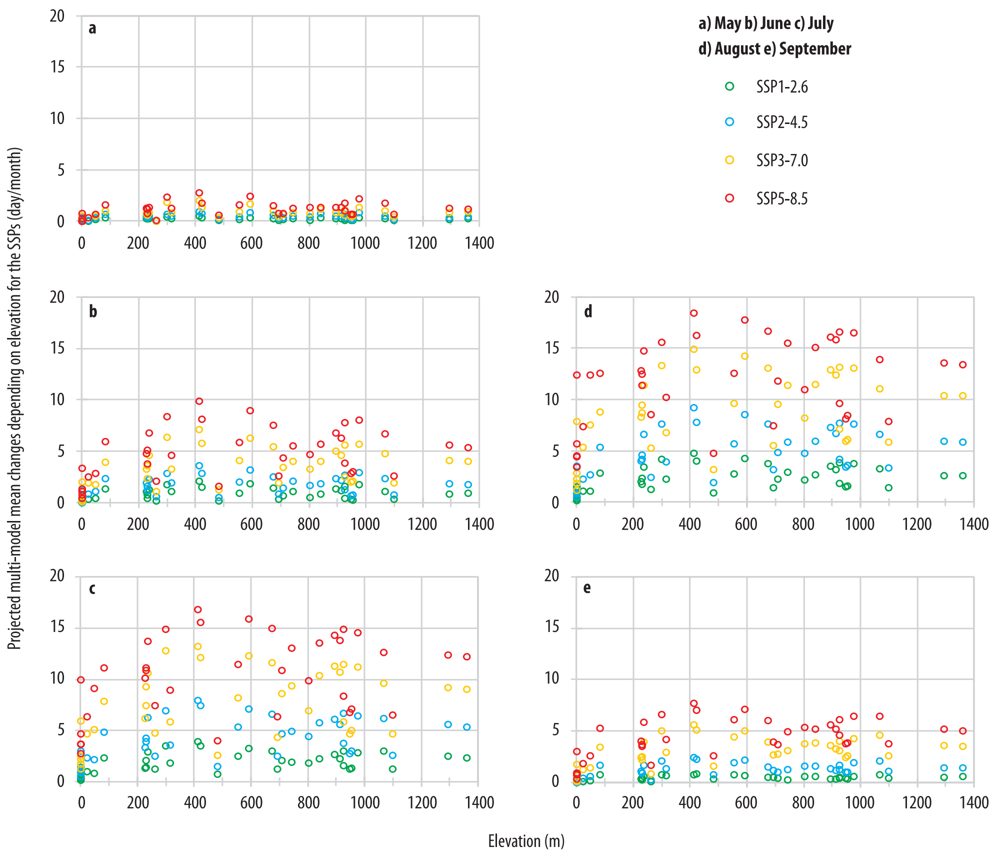

Fig. 6. Projected monthly changes of TX35 (2081–2100 vs. 1995–2014) depending on elevation at 42.5°N for SSP1-2.6, SSP2-4.5, SSP3-7.0 and SSP5-8.5. *Source:* Authors' own elaboration.

of the TX35 increase between 800 m and 1000 m, comparable to the values at 300–400 m (*Figure 9, b, c,* and *d*). The reason behind this pattern is the geographical location of the grid cells with the 800–1000 m elevation. They belong to the Carpathians, which are located on the eastern parts of the segment, thus, in addition to the orography, the continental effect also influences the projected increase of monthly TX35. Note that this pattern is more pronounced from June to August (see *Figure 9, b, c,* and *d*) and completely disappears in May (*Figure 9, a*) due to the very small projected changes at the beginning of the summer half-year. As the values of monthly TX35 in the historical period were a lot lower in the mountain areas than in the plain areas *(Figure S1)* (Supplementary section), the already existing spatial differences are likely to increase in the summer months and probably not to change in May and September for the target period 2081–2100.

As for the scenario comparisons, similarly to the 37.5°N segment, some specific points also form clusters along the 47.5°N segment (*Figure 10*), namely, in June and August (*Figure 10, b,* and *d*). However, in this case the fitted linear regressions between the projected increases of the SSP1-2.6 and the other two scenarios (SSP3-7.0 and SSP5-8.5), are more relevant for the separate clusters than in the case of the other segments. This

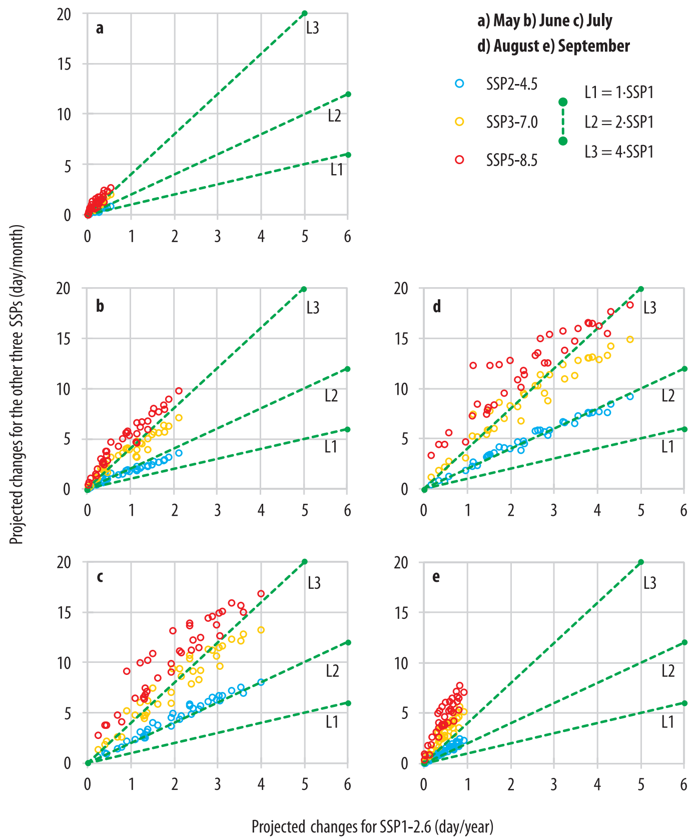

Fig. 7. Projected monthly changes of TX35 (2081–2100 vs. 1995–2014) for SSP2-4.5, SSP3-7.0 and SSP5-8.5 compared to SSP1-2.6 at 42.5°N. *Source:* Authors' own elaboration.

implies for example for August, when the regression coefficients for all the points are 2.3 for SSP3-7.0, and 2.6 for SSP5-8.5, whereas without the easterly longitudes, the coefficient values would be higher (i.e. 3.1 and 3.6, respectively). So based on *Figure 10, d*, the relative differences are far greater between the scenarios if only the first cluster is analysed (at around 0-2 days of increase in TX35 based on the SSP1-2.6) and much smaller if only the second. To reveal the reasons behind, the segment was cut into two smaller parts, a western and an eastern segment. This was due to the characteristics of the 47.5°N, as the growing continentality effect from west to east is highly influential in creating the spatial patterns. Similar diagrams are created for both subsegments, and the results show that the points in cluster1 almost entirely belong to the western part of the segment, and the points in cluster2 belong to the eastern part of the segment. The clustering can match the subsegments if the entire zonal segment is separated to the following two subsegments: (i) grid cells located west to the Alps and in the Carpathians (cluster1), (ii) grid cells located east to the Alps, except for the Carpathians (cluster2). This shows that the relative location to the Alps is a key factor when evaluating the projections. The location also explains the lower increase ratio of the higher radiative forcing change sce-

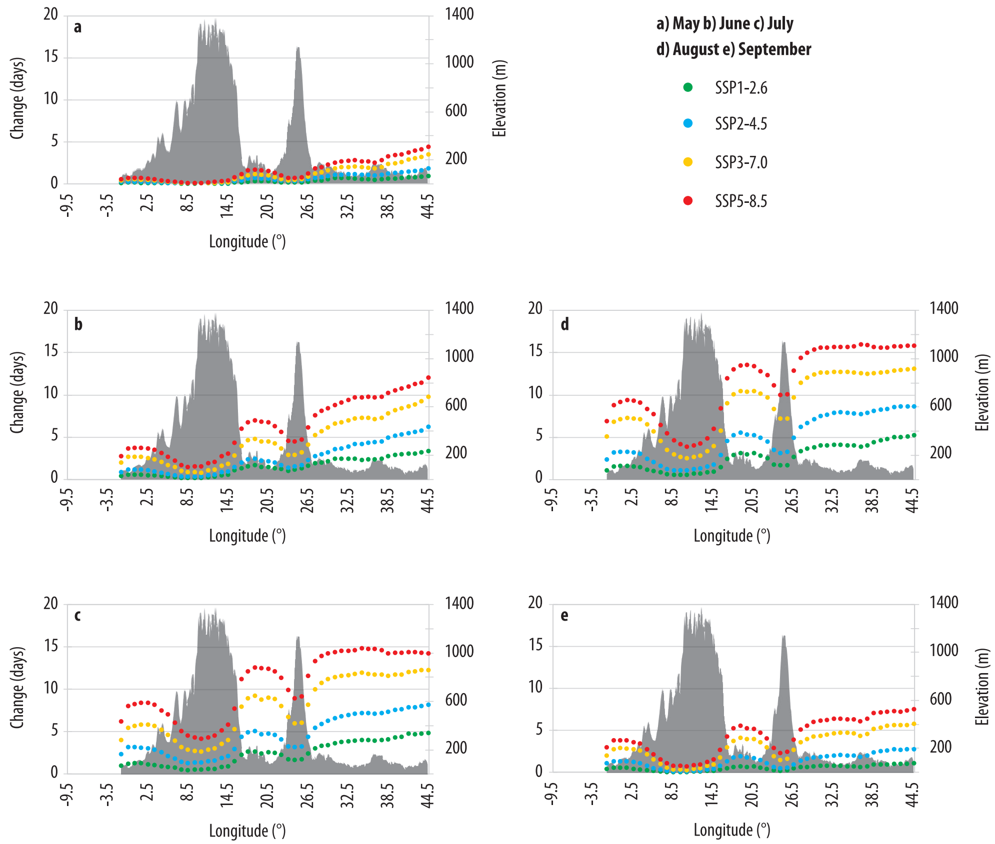

Fig. 8. Projected monthly changes of TX35 (2081–2100 vs. 1995–2014) for SSP1-2.6, SSP2-4.5, SSP3-7.0, SSP5-8.5 and elevation along the zonal segment of 47.5°N. *Source:* Authors' own elaboration.

narios relative to the SSP1-2.6 in cluster2. In these areas, especially in the east, the values of monthly TX35 were already high in the reference period (*Figure S1*) (Supplementary section). Hence, the physical upper limit of these values (20–23 days/month for SSP3-7.0 and 25–27 days/month for SSP5-8.5) driven by the added forcing levels and affected by the Black Sea, will be reached in July and August (*Figure 10, c*, and *d*) based on the high radiative forcing change scenarios.

Moving northward to the *52.5°N* segment (*Figure 11*), the greatest number of grid cells are analysed among all the latitudes. This is due to the selection process, where the main aim was to ensure that the majority of the grid cells are covered by land. Due to its northern location, the projected increase along this segment is generally lower than in the more southern segments. However, a considerable increase is projected in the eastern parts of the segment in the summer months, and an increase of up to 10 days will be likely possible based on the SSP5-8.5 scenario. The most dominant effect here is continentality, which can be explained by the facts that (i) the water surfaces are only located in the western part of the segment, and do not cover many grid points unlike along the 37.5°N and 42.5°N segments; and (ii) the 52.5°N segment lacks higher elevation areas, unlike the 47.5°N segment. As a consequence of all these, the

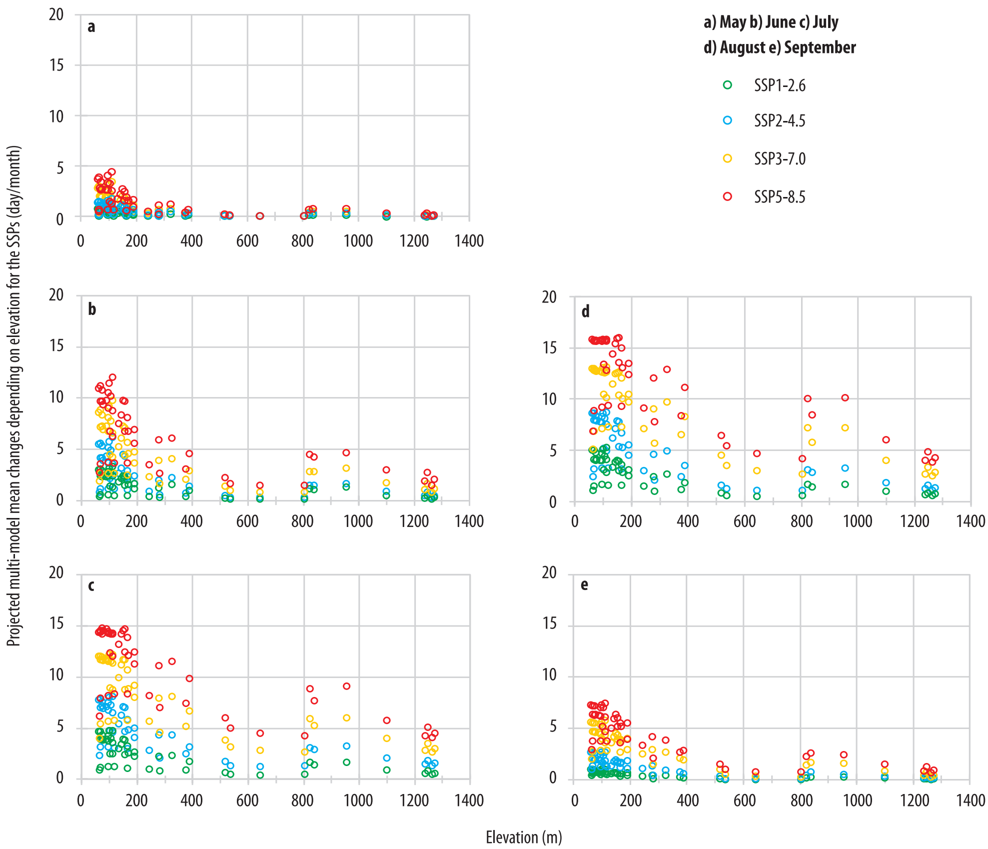

Fig. 9. Projected monthly changes of TX35 (2081–2100 vs. 1995–2014) depending on elevation at 47.5°N for SSP1-2.6, SSP2-4.5, SSP3-7.0 and SSP5-8.5. *Source:* Authors' own elaboration.

greater increase in TX35 with increasing elevation (*Figure 12*) is solely due to the higher elevation areas being in the eastern part of the segment, especially in June, July and August.

Continentality also clearly appears on the diagrams in *Figure 13*, especially for the three summer months. Note that the increase is very small in the western parts of the segment for every month, whereas an increase up to 10 days/month is projected in the east in August when SSP5-8.5 is taken into account (*Figure 13, d*). The regression coefficients are the smallest in June for all scenarios, which is different from the southern segments where the minimum was projected in August.

Finally, at the most northerly segment, at *57.5°N* (*Figure 14*), the very slight changes in the monthly TX35 are limited to the summer months only, from which the highest projected changes can be identified in July (*Figure 14, c*). This is different from the more southern segments, where the highest increase is projected in August (with much more substantial increases anyway than at the 57.5°N segment). Similar to 52.5°N, there are no high elevation areas along the segment (*Figure S2*) (Supplementary section), therefore, continentality has the major effect on the spatial distribution. The regression coefficient values show similar pattern from May to September

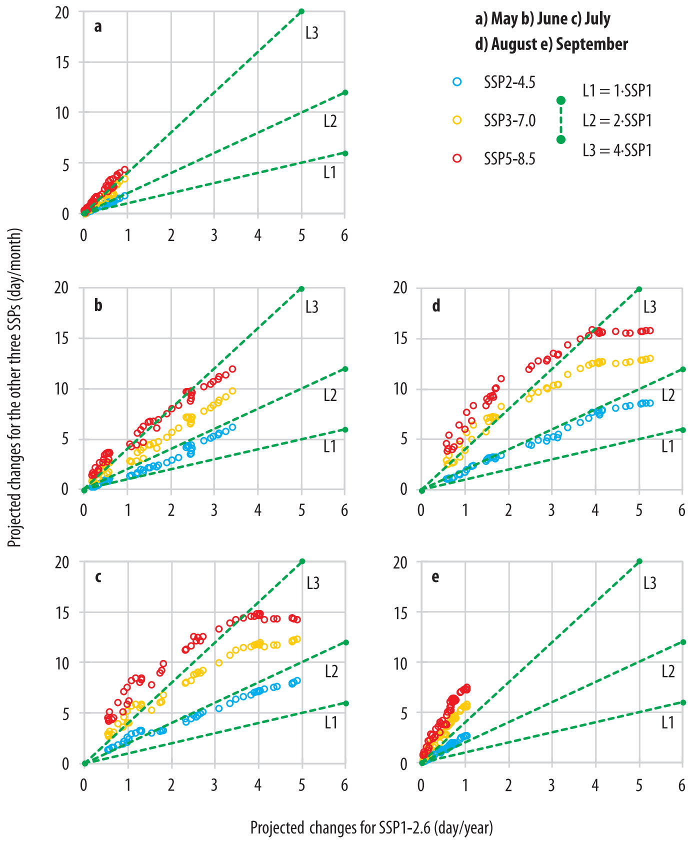

Fig. 10. Projected monthly changes of TX35 (2081–2100 vs. 1995–2014) for SSP2-4.5, SSP3-7.0 and SSP5-8.5 compared to SSP1-2.6 at 47.5°N. *Source:* Authors' own elaboration.

to the 52.5°N segment although the projected changes are even smaller here (*Figure S3*) (Supplementary section), as the minimal coefficients are identified in August. Note however, that due to the very slight projected changes, especially in May and September, the information contained in these coefficients at the 57.5°N segment is very limited.

Discussion

The trends of extreme heat events detected in the past and projected for the future have been analysed in several studies, following different approaches. For example, Cardil, A. *et al.* (2014) focused on the detected trend of air temperature at 850 hPa and high-temperature days (HTDs) in Southern Europe over the 1978–2012 period and recommended possible actions for policymakers. The main conclusion of their study is that the HTDs increased significantly in the Spanish Mediterranean Coast, Italy and Greece. The general finding of the growing risk of extreme heat events is also true for the future projections across the Mediterranean Region according to our results; however, our study area is much greater, as the above-mentioned study covers only one of the five segments of the current analysis.

A larger scale analysis for the whole European continent is given by Lorenz,

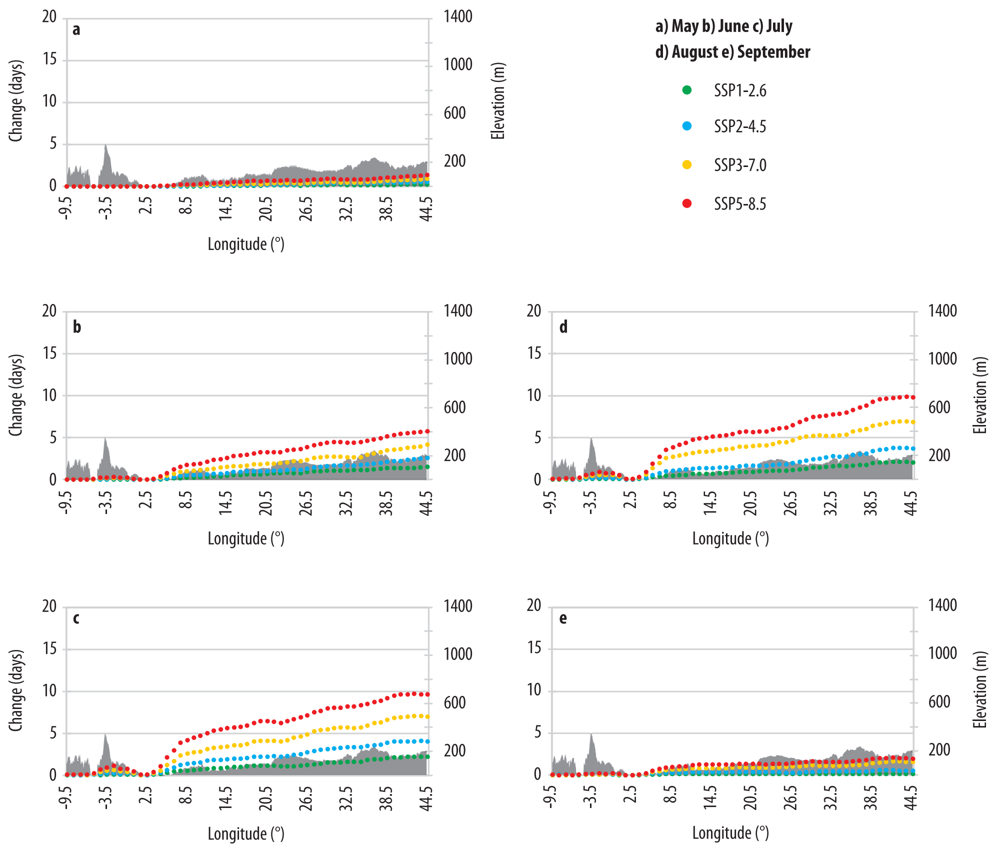

Fig. 11. Projected monthly changes of TX35 (2081–2100 vs. 1995–2014) for SSP1-2.6, SSP2-4.5, SSP3-7.0, SSP5-8.5 and elevation along the zonal segment of 52.5°N. *Source:* Authors' own elaboration.

R. *et al.* (2019), and Sulikowska, A. and Wypych, A. (2021). Both studies analysed extreme temperature increase in Europe for the past, for almost the same target period (1950–2018 and 1950–2019, respectively). However, they used slightly different datasets, Lorenz, R. *et al.* (2019) used the 4000-station data series available at the European Climate Assessment & Dataset (ECAD), whilst Sulikowska, A. and Wypych, A. (2021) used the E-OBS gridded dataset (generated from the ECAD station data) for five European subdomains. Moreover, Lorenz, R. *et al.* (2019) included both warm and cold extremes and they validated results from EURO-CORDEX simulations for their target period. Both studies' findings about increasing hot extremes resonate with our findings, however, we focused on future projections instead of past trends, for which we used the new CMIP6 simulations instead of EURO-CORDEX data where regional climate model runs were driven by the previous global models from CMIP5. Engdaw, M.M. *et al.* (2023) carried out a global analysis focusing on the frequency changes of cold and hot events for the period 1980–2020, using percentile-based climate indices instead of fix thresholds on the basis of observational data as well as simulated data from CMIP6. They found an overall significant increase in the frequency of hot events, and a decrease in

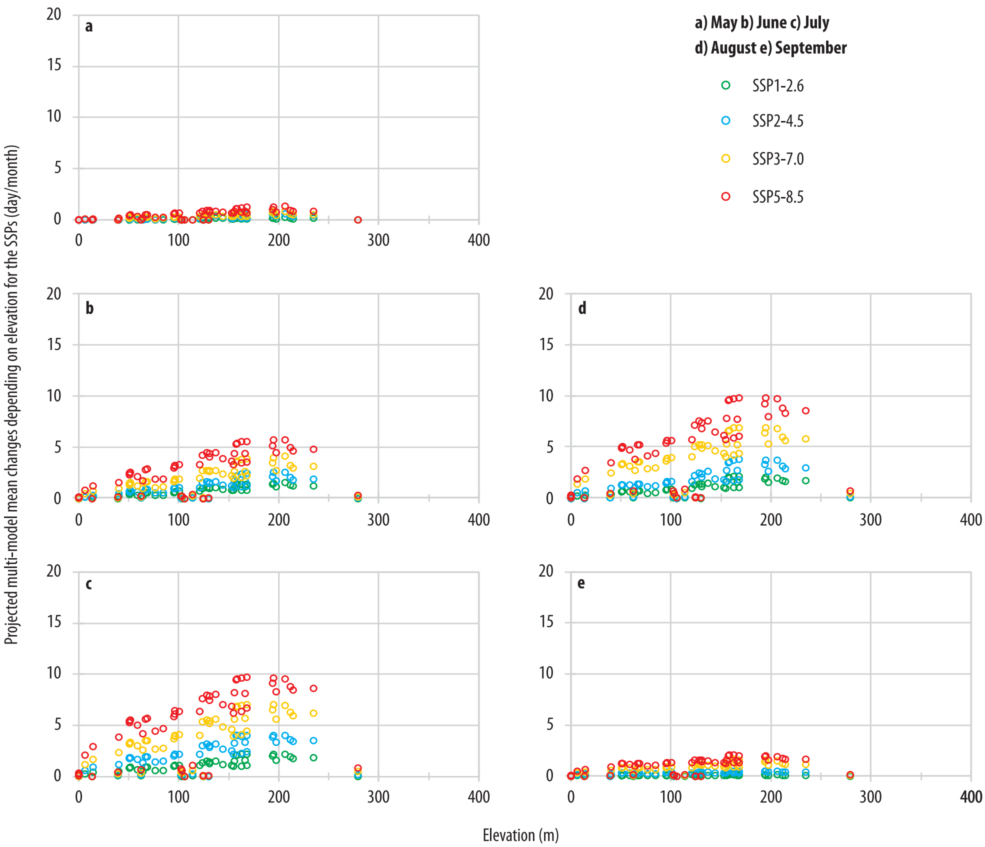

Fig. 12. Projected monthly changes of TX35 (2081–2100 vs. 1995–2014) depending on elevation at 52.5°N for SSP1-2.6, SSP2-4.5, SSP3-7.0 and SSP5-8.5. *Source:* Authors' own elaboration.

cold events for Europe, however, because the whole continent was analysed as one region, the comparison of different European areas is not possible, unlike in our study.

The studies made by Fan, X. *et al.* (2020), Alvarez, I. *et al.* (2024) and Srivastava, A.K. *et al.* (2024) all analysed both the past trends and the future changes of different temperature indices, more specifically, Fan, X. *et al.* (2020) used the CMIP6 simulations' outputs to analyse annual mean temperatures for three different past and three different future periods. Alvarez, I. *et al.* (2024), similarly to Cardil, A. *et al.* (2014), or Sulikowska, A. and Wypych, A. (2021), defined a compound heat and drought metric, the so-called Heat Index to assess the trends and projections in the Mediterranean Basin, using the CMIP6 simulations for the SSP2-4.5 and the SSP5-8.5 scenarios. On the other hand, Srivastava, A.K. *et al.* (2024) used temperature-based indices, i.e. the maximum and the mean of daily maximum temperatures to study the local hydroclimatic effects on different warming rates in the Northern Hemisphere for only one specific high emission scenario, i.e. RCP8.5. All these studies found increasing trends in their respective extreme heat indices, with Alvarez, I. *et al.* (2024) pointing out dangerous increase in heat stress over the Mediterranean. Our re-

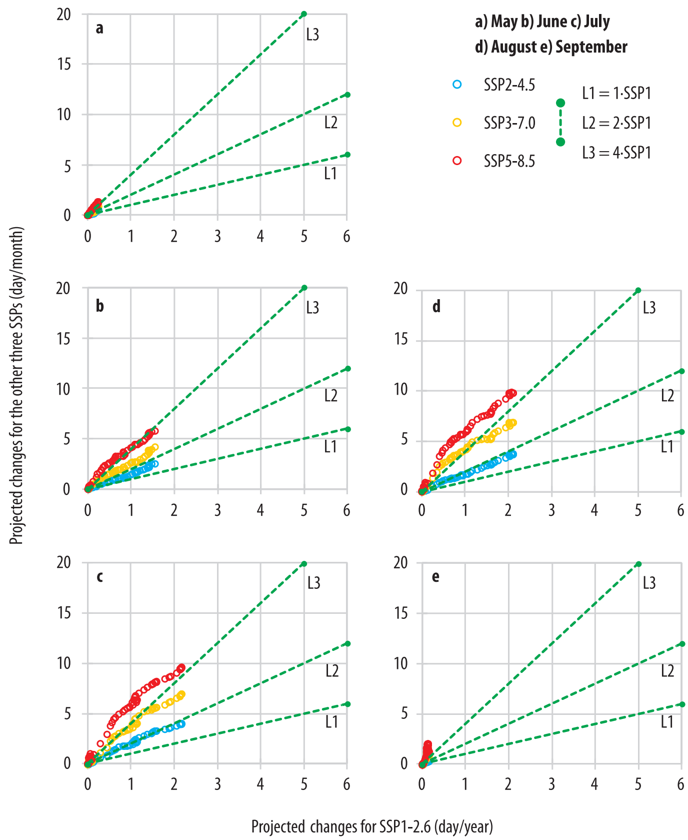

Fig. 13. Projected monthly changes of TX35 (2081–2100 vs. 1995–2014) for SSP2-4.5, SSP3-7.0 and SSP5-8.5 compared to SSP1-2.6 at 52.5°N. *Source:* Authors' own elaboration.

sults agree with these findings, however, we extended the number of scenarios taken into account, thus, providing a more systematic analysis of the projections to cover a wider range of future climatic possibilities.

A different approach was used by the studies of King, A.D. *et al.* (2018), and Tebaldi, C. and Knutti, R. (2018), who all used the time-sampling method, where instead of the analysis of a certain target period, the thresholds of global average temperature increase were set (i.e. 1.5 °C or 2 °C). Then, the exposure to extreme heat events is assessed when these certain thresholds are reached. The extreme heat indices, however, do not include TX35, and the simulations being used are from the earlier simulated data of CMIP5, using the RCP scenarios. Tebaldi, C. and Knutti, R. (2018) also analysed only the lower radiative forcing change scenarios, RCP2.6 and RCP4.5, but still, summarised similar conclusions to our study about the SSP1-2.6 and SSP2-4.5, namely, that the connections between RCP2.6 and RCP4.5 are almost linear. This is also confirmed by King, A.D. *et al.* (2018).

A limited set of CMIP6 simulations (i.e. 12 global climate models) is compared to CMIP5 simulations as well as their downscaled results of EURO-CORDEX by Coppola, E. *et al.* (2021). Their study is focusing mainly on business-as-usual scenarios (i.e. RCP8.5 and SSP5-8.5). In case of TX35, EURO-CORDEX results show an

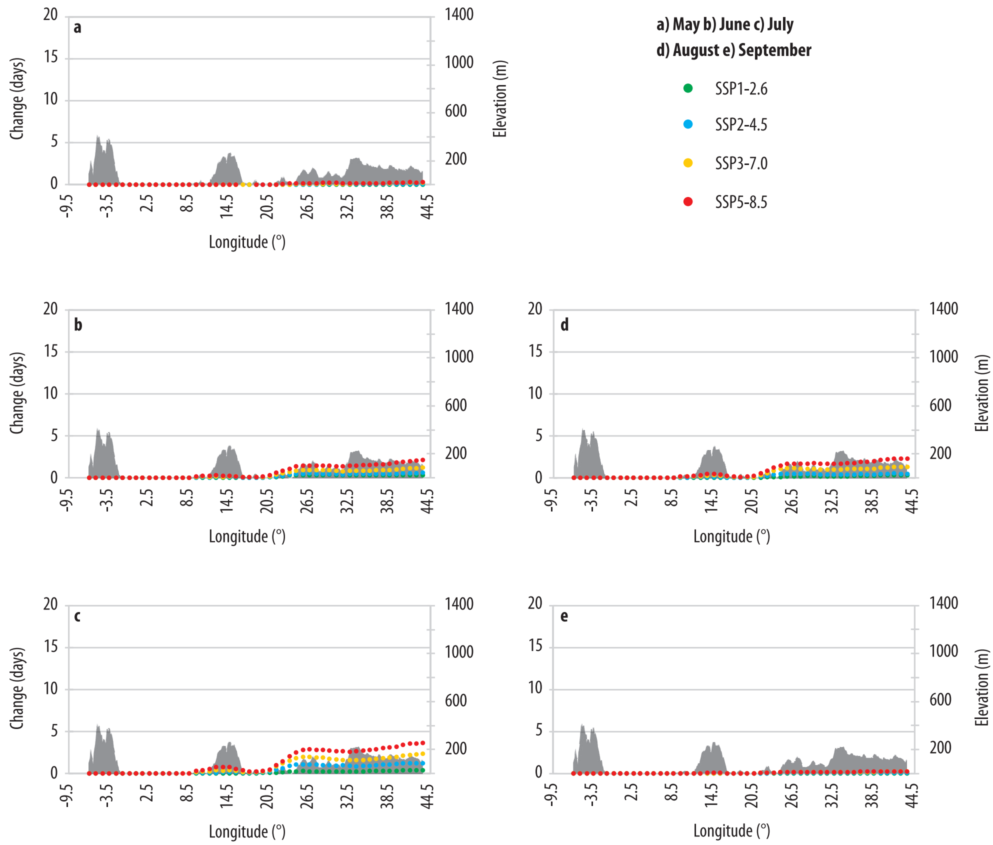

Fig. 14. Projected monthly changes of TX35 (2081–2100 vs. 1995–2014) for SSP1-2.6, SSP2-4.5, SSP3-7.0, SSP5-8.5 and elevation along the zonal segment of 57.5°N. *Source:* Authors' own elaboration.

overall smaller change compared to the driving CMIP5 simulations, however, CMIP6 simulations result in higher increase than CMIP5 simulations. This can be partly due to the coarser horizontal resolution of CMIP5 simulations (2°). Certainly, regional climate models with 0.11° horizontal resolution better represent orography, and, thus, more precise differences are simulated in temperature-related extremes, compared to the global models. Nevertheless, the overall spatial pattern of the projected changes of temperature extremes (including TX35) is similar in regional and global models. All these allow providing information on the basis of CMIP6 simulations before downscaled regional climate model simulations are available.

Suarez-Gutierrez, L. *et al.* (2023) also used a similar methodology as e.g. Wobus, C. *et al.* (2018), but instead of a temperature-threshold, the main results highlight the time by which never-seen-before heat waves and multi-year successive extremes in temperature will become common in the European continent. For this purpose, compound heat and drought metrics were used instead of selecting a particular temperature threshold and analysing the frequency changes of its exceedances over time. Despite the different approach, their results are similar to our findings as they also highlight that even a slight warming may cause huge consequences in Europe.

Overall, the future projections of CMIP6 simulations across the entirety of Europe have not been analysed in a systematic way before, so we aimed to fill this gap with visual and qualitative assessments. Most studies focus mainly on the Mediterranean region; however, our findings show that a substantial increase is projected even as north as the Baltic Sea. The results presented here contain four SSP scenarios providing the widest range of potential future climate compared to other studies carried out earlier. Furthermore, the usage of the TX35 index is not as widespread as other indices, even though it is an important threshold when analysing extreme temperature events with high heat stress. The projected occurrence of the daily maximum temperature above 35 °C is a clear warning signal in the northern parts of Europe as well, since the spatial extent of such extreme temperatures towards the polar region was much smaller in the reference period (*Figure S1*). Finally, the use of zonal segments to study the effects of sea cover, continentality or elevation is a unique and novel approach to make systematic inter-comparisons between segments or even grid points.

The main underlying causes of extreme heat occurrences in Europe are discussed in details by Andrade, C. *et al.* (2012), and Sousa, P.M. *et al.* (2018). They both analysed large-scale circulation patterns focusing on blocking and ridges over the continent. Overall, changes in the meridional pressure gradient play a major role in extreme hot conditions over Europe.

We note that there are some limitations of the present study. (i) The inter-model variability or the uncertainty from the simulations' ensemble cannot be assessed, as only the multi-model mean was available in the IPCC IA, which is the basis of the present analysis. (ii) The horizontal resolution of global climate models is quite coarse, so detailed regional specifics cannot always be properly represented. (iii) This study analysed only one specific climate index indicating the frequency of heat conditions above a fixed threshold. Even though these heat-related climate indices are interrelated they certainly have their unique approach, e.g. duration of consecutive heat conditions, intensity of heat, which are clearly not addressed by TX35. (iv) The underlying meteorological and climatological processes require further detailed analysis of large-scale circulation using pressure and wind data from CMIP6 simulations. This is beyond the aims of the current study.

Conclusions

In this study, future extreme temperature projections are analysed over Europe using the CMIP6 simulations included in the IPCC's AR6 report (i.e. in the IA) for a specific heat-related climate index, the TX35. Based on the presented analysis, the main research questions can be answered as follows.

(i) On the basis of the ensemble mean of historical simulations, the TX35 index had a distinct spatial distribution in the reference period of 1995–2014. It was an important climatic feature in the Mediterranean Region even in the recent years, with a mean monthly number of days above 35 °C reaching almost 14 in August. On the other hand, in the northern parts of Europe, there were only 1–2 days in a year on average, when the daily maximum temperature reached the 35 °C threshold.

(ii) Climate change is expected to further accentuate the spatial patterns already observed. The highest increases are projected for the southern segments (around 18 days for the 42.5°N), whereas at the most northern 57.5°N segment, very slight changes are projected (maximum of +4 days in August). This can be expected because the 35 °C threshold of daily maximum temperature is so extreme at this segment, that even the temperature increase projected by the SSP5-8.5 scenario is not high enough to reach it. Regarding the scenarios, the results clearly imply that the projections for the highest radiative forcing changes, SSP5-8.5, will lead to the greatest increases, and therefore the greatest spatial differences between the different parts of the continent. Meanwhile, the projected changes for the lowest radiative forcing changes, the SSP1-2.6 scenario, show the smallest increases, potentially creating much smaller spatial differences than the SSP5-8.5. For instance, at the maximal increase grid point (42.5°N, 22.5°E), the projections range between +4 days (SSP1-2.6) to +18 days (SSP5-8.5). The difference of the TX35 projections is a quite straightforward consequence of the difference of global and regional warming originating from the direct link between the radiative forcing and temperature changes.

(iii) There are also several geographical effects that influence the patterns of the TX35. For instance, a greater increase is projected for the more continental (eastern) parts of the 47.5°N, 52.5°N and 57.5°N segments, which creates greater intra-zonal differences than in the reference period. For instance, at the 47.5°N, the difference in the increase of TX35 in August between the most western and eastern parts based on the SSP5-8.5 scenario is 9 days. In the southern segments, namely along 37.5°N and 42.5°N, the most important influence is the sea cover, as the increase of TX35 is much lower above the water surfaces than above the land areas (e.g. at the 42.5°N, the greatest difference is 15 days for the SSP5-8.5 scenario in August) due to the moderating climate effect of large water bodies. Finally, the height above sea level can also be an important factor, especially along the 47.5°N segment, as much lower increase is projected by the ensemble mean of the CMIP6 simulations for any scenario in the higher elevation regions than in the lower elevations. For instance, the differences can reach 12 days in August based on the SSP5-8.5 scenario. The Alps is especially important in this segment as the results show that there is a great difference in the increase of the TX35 between the sub-segments to the east and to the west from the mountainous area (except the Carpathians, which area has similar characteristics to the western part of the segment due to its higher elevation).

The potential increase of heat stress certainly is one of the major future challenges, especially in case of the more pessimistic scenarios. Therefore, in addition to mitigation efforts, adaptation is also essential in the next decades. In order to develop reliable adaptation strategies, interdisciplinary studies are necessary, which take into account not only climatological aspects, but other key factors (e.g. population, financial demand, environmental constrains) as well.

Acknowledgements: This work has been implemented by the National Multidisciplinary Laboratory for Climate Change (RRF-2.3.1-21-2022-00014) project within the framework of Hungary's National Recovery and Resilience Plan supported by the Recovery and Resilience Facility of the European Union.

REFERENCES

Alvarez, I., Diaz-Poso, A., Lorenzo, M.N. and Roye, D. 2024. Heat index historical trends and projections due to climate change in the Mediterranean basin based on CMIP6. *Atmospheric Research* 308. 107512. https://doi.org/10.1016/j.atmosres.2024.107512

Andrade, C., Leite, S.M. and Santos, J.A. 2012. Temperature extremes in Europe: Overview of their driving atmospheric patterns. *Natural Hazards and Earth System Sciences* 12. 1671–1691. https://doi.org/10.5194/nhess-12-1671-2012

Cardil, A., Molina, D.M. and Kobziar, L.N. 2014. Extreme temperature days and their potential impacts on southern Europe. *Natural Hazards and Earth System Sciences* 14. 3005–3014. https://doi.org/10.5194/nhess-14-3005-2014

Cogato, A., Meggio, F., de Antoni Migliorati, M. and Marinello, F. 2019. Extreme weather events in agriculture: A systematic review. *Sustainability* 11. (9): 2547. https://doi.org/10.3390/su11092547

C3S 2025. *The 2024 Annual Climate Summary: Global Climate Highlights 2024.* Copernicus Climate Change Services (C3S). Available at https://climate.copernicus.eu/global-climate-highlights-2024

Coppola, E., Nogherotto, R., Ciarlo, J.M., Giorgi, F., van Meijgaard, E., Kadygrov, N., Iles, C., Corre, L., Sandstad, M., Somot, S., Nabat, P., Vautard, R., Levavasseur, G., Schwingschackl, C., Sillmann, J., Kjellström, E., Nikulin, G., Aalbers, E., Lenderink, G., Christensen, O.B., Boberg, F., Sorland, S.L., Demory, M-E., Bülow, K., Teichmann, C., Warrach-Sagi, K. and Wulfmeyer, V. 2021. Assessment of the European climate projections as simulated by the large EURO-CORDEX regional and global climate model ensemble. *Journal of Geophysical Research: Atmospheres* 126. (4): e2019JD032356. https://doi.org/10.1029/2019JD032356

Engdaw, M.M., Steiner, A.K., Hegerl, G.C. and Ballinger, A.P. 2023. Attribution of observed changes in extreme temperatures to anthropogenic forcing using CMIP6 models. *Weather and Climate Extremes* 39. 100548. https://doi.org/10.1016/j.wace.2023.100548

Eyring, V., Bony, S., Meehl, G.A., Senior, C.A., Stevens, B., Stouffer, R.J. and Taylor, K.E. 2016. Overview of the Coupled Model Intercomparison Project Phase 6 (CMIP6) experimental design and organization. *Geoscientific Model Development* 9. 1937–1958. https://doi.org/10.5194/gmd-9-1937-2016

Eyring, V., Gentine, P., Camps-Valls, G., Lawrence, D.M. and Reichstein, M. 2024. AI-empowered next-generation multiscale climate modelling for mitigation and adaptation. *Nature Geoscience* 17. 963–971. https://doi.org/10.1038/s41561-024-01527-w

Fan, X., Duan, Q., Shen, C., Wu, Y. and Xing, C. 2020. Global surface air temperatures in CMIP6: Historical performance and future changes. *Environmental Research Letters* 15. (10): 104056. https://doi.org/10.1088/1748-9326/abb051

Gallo, E., Quijal-Zamorano, M., Méndez Turrubiates, R.F., Tonne, C., Basagaña, X., Achebak, H. and Ballester, J. 2024. Heat-related mortality in Europe during 2023 and the role of adaptation in protecting health. *Nature Medicine* 30. 3101–3105. https://doi.org/10.1038/s41591-024-03186-1

Gutiérrez, J.M., Jones, R.G., Narisma, G.T., Alves, L.M., Amjad, M., Gorodetskaya, I.V., Grose, M., Klutse, N.A.B., Krakovska, S., Li, J., Martínez-Castro, D., Mearns, L.O., Mernild, S.H., Ngo-Duc, T., van den Hurk, B. and Yoon, J.-H. 2021. Atlas. In *Climate Change 2021: The Physical Science Basis. Contribution of Working Group I to the Sixth Assessment Report of the Intergovernmental Panel on Climate Change.* Eds.: Masson-Delmotte, V., Zhai, P., Pirani, A., Connors, S.L., Péan, C., Chen, Y., Goldfarb, L., Gomis, M.I., Matthews, J.B.R., Berger, S., Huang, M., Yelekçi, O., Yu, R., Zhou, B., Lonnoy, E., Maycock, T.K., Waterfield, T., Leitzell, K. and Caud, N., Cambridge, UK and New York, NY, USA, Cambridge University Press, 1927–2058. https://doi.org/10.1017/9781009157896.021. Interactive Atlas available from IPCC WGI Interactive Atlas

IPCC 2021. *Climate Change 2021: The Physical Science Basis. Contribution of Working Group I to the Sixth Assessment Report of the Intergovernmental Panel on Climate Change*. Eds.: Masson-Delmotte, V., Zhai, P., Pirani, A., Connors, S.L., Péan, C., Berger, S., Caud, N., Chen, Y., Goldfarb, L., Gomis, M.I., Huang, M., Leitzell, K., Lonnoy, E., Matthews, J.B.R., Maycock, T.K., Waterfield, T., Yelekçi, O., Yu, R. and Zhou, B., Cambridge, UK and New York, NY, USA, Cambridge University Press. https://doi.org/10.1017/9781009157896

King, A.D., Knutti, R., Uhe, P., Mitchell, D.M., Lewis, S.C., Arblaster, J.M. and Freychet, N. 2018. On the linearity of local and regional temperature changes from 1.5 °C to 2 °C of global warming. *Journal of Climate* 31. 7495–7514. https://doi.org/10.1175/JCLI-D-17-0649.1

Lorenz, R., Stalhandske, Z. and Fischer, E.M. 2019. Detection of a climate change signal in extreme heat, heat stress, and cold in Europe from observations. *Geophysical Research Letters* 46. (14): 8363–8374. https://doi.org/10.1029/2019GL082062

Lüthi, S., Fairless, C., Fischer, E.M., Scovronick, N., Armstrong, B., de Sousa Zanotti Stagliorio Coelho, M., Guo, Y.L., Guo, Y., Honda, Y., Huber, V., Kyselý, J., Lavigne, E., Royé, D., Ryti, N., Silva, S., Urban, A., Gasparrini, A., Bresch, D.N., Vicedo-Cabrera, A.M. and Multi-Country Multi-City (MCC) Collaborative Research Network 2023. Rapid increase in the risk of heat-related mortality. *Nature Communications 14.* (1): 4894. https://doi.org/10.1038/s41467-023-40599-x

O'Neill, B.C., Kriegler, E., Ebi, K.L., Kemp-Benedict, E., Riahi, K., Rothman, D.S., van Ruijven, B.J., van Vuuren, D.P., Birkmann, J., Kok, K., Levy, M. and Solecki, W. 2017. The roads ahead: Narratives for shared socioeconomic pathways describing world futures in the 21st century. *Global Environmental Change* 42. 169–180. https://doi.org/10.1016/j.gloenvcha.2015.01.004

Rojas-Downing, M.M., Nejadhashemi, A.P., Harrigan, T. and Woznicki, S.A. 2017. Climate change and livestock: Impacts, adaptation, and mitigation. *Climate Risk Management* 16. 145–163. https://doi.org/10.1016/j.crm.2017.02.001

Schaeffer, R., Szklo, A.S., de Lucena, A.F.P., Borba, B.S.M.C., Nogueira, L.P.P., Fleming, F.P., Troccoli, A., Harrison, M. and Boulahya, M.S. 2012. Energy sector vulnerability to climate change: A review. *Energy* 38. (1): 1–12. https://doi.org/10.1016/j.energy.2011.11.056

Sousa, P.M., Trigo, R.M., Barriopedro, D., Soares, P.M. and Santos J.A. 2018. European temperature responses to blocking and ridge regional patterns. *Climate Dynamics* 50. 457–477. https://doi.org/10.1007/s00382-017-3620-2

Srivastava, A.K., Wehner, M., Bonfils, C., Ullrich, P.A. and Risser, M. 2024. Local hydro-climate drives differential warming rates between regular summer days and extreme hot days in the Northern Hemisphere. *Weather and Climate Extremes* 45. 100709. https://doi.org/10.1016/j.wace.2024.100709

Suarez-Gutierrez, L., Müller, W.A. and Marotzke, J. 2023. Extreme heat and drought typical of an end-of-century climate could occur over Europe soon and repeatedly. *Communications Earth and Environment* 4. (1): 415. https://doi.org/10.1038/s43247-023-01075-y

Sulikowska, A. and Wypych, A. 2021. Seasonal variability of trends in regional hot and warm temperature extremes in Europe. *Atmosphere* 12. (5): 612. https://doi.org/10.3390/atmos12050612

Taylor, K.E., Stouffer, R.J. and Meehl, G.A. 2012. An overview of CMIP5 and the experiment design. *Bulletin of the American Meteorological Society* 93. 485–498. https://doi.org/10.1175/BAMS-D-11-00094.1

Tebaldi, C. and Knutti, R. 2018. Evaluating the accuracy of climate change pattern emulation for low warming targets. *Environmental Research Letters* 13. (5): 055006. https://doi.org/10.1088/1748-9326/aabef2

van Vuuren, D.P., Edmonds, J., Kainuma, M., Riahi, K., Thomson, A., Hibbard, K., Hurtt, G.C., Kram, T., Krey, V., Lamarque, J-F., Masui, T., Meinshausen, M., Nakicenovic, N., Smith, S.J. and Rose, S.K. 2011. The representative concentration pathways: An overview. *Climatic Change* 109. 5–31. https://doi.org/10.1007/s10584-011-0148-z

Wilks, D.S. 2006. *Statistical Methods in the Atmospheric Sciences*. 2nd edition. London, Academic Press.

WMO 2025. *State of the Global Climate in 2024*. WMO-No. 1368. Geneva, WMO.

Wobus, C., Zarakas, C., Malek, P., Sanderson, B., Crimmins, A., Kolian, M., Sarofim, M. and Weaver, C.P. 2018. Reframing future risks of extreme heat in the United States. *Earth's Future* 6. (9): 1323–1335. https://doi.org/10.1029/2018EF000943

Supplementary section

*Table S1. The list of simulations included in the multi-model ensemble of the IA for the different scenarios**

Models	SSP1-2.6	SSP2-4.5	SSP3-7.0	SSP5-8.5
ACCESS-CM2_r1i1p1f1	✓	✓	✓	✓
ACCESS-ESM1-5_r1i1p1f1	✓	✓	✓	✓
AWI-CM-1-1-MR_r1i1p1f1	✓	✓	✓	✓
BCC-CSM2-MR_r1i1p1f1	✓	✓	✓	✓
CanESM5_r1i1p1f1	✓	✓	✓	✓
CNRM-CM6-1_r1i1p1f2	✓	✓	✓	✓
CNRM-CM6-1-HR_r1i1p1f2	✓	–	–	✓
CNRM-ESM2-1_r1i1p1f2	✓	✓	✓	✓
EC-Earth3_r1i1p1f1	✓	✓	✓	✓
EC-Earth3-Veg_r1i1p1f1	✓	✓	✓	✓
EC-Earth3-Veg-LR_r1i1p1f1	–	✓	✓	–
FGOALS-g3_r1i1p1f1	✓	✓	✓	✓
GFDL-CM4_r1i1p1f1	–	✓	–	✓
GFDL-ESM4_r1i1p1f1	✓	✓	✓	✓
HadGEM3-GC31-LL_r1i1p1f3	✓	✓	–	✓
INM-CM4-8_r1i1p1f1	✓	✓	✓	✓
INM-CM5-0_r1i1p1f1	✓	✓	✓	✓
IPSL-CM6A-LR_r1i1p1f1	✓	✓	✓	✓
KACE-1-0-G_r2i1p1f1	✓	✓	✓	✓
KIOST-ESM_r1i1p1f1	✓	✓	–	✓
MIROC-ES2L_r1i1p1f2	✓	✓	✓	✓
MIROC6_r1i1p1f1	✓	✓	✓	✓
MPI-ESM1-2-HR_r1i1p1f1	✓	✓	✓	✓
MPI-ESM1-2-LR_r1i1p1f1	✓	✓	✓	✓
MRI-ESM2-0_r1i1p1f1	✓	✓	✓	✓
NESM3_r1i1p1f1	✓	✓	–	✓
NorESM2-MM_r1i1p1f1	✓	✓	✓	✓
UKESM1-0-LL_r1i1p1f2	✓	✓	✓	✓

*Note that the most simulations (27) are available for the SSP2-4.5 and SSP5-8.5 scenarios, whereas the least for the SSP3-7.0 (23).

Table S2. Correlation coefficients of the projected monthly changes along the different zonal segments between SSP1-2.6 and the other three scenarios, SSP2-4.5, SSP3-7.0, and SSP5-8.5.

Zone	SSP2-4.5				
Segments	May	June	July	August	September
37.5°N	0.91	0.99	0.97	0.97	0.99
42.5°N	0.91	0.97	0.97	0.98	0.92
47.5°N	0.97	0.97	0.99	0.99	0.98
52.5°N	0.93	0.99	0.99	0.99	0.84
57.5°N	0.83	0.98	0.97	0.87	0.74
SSP3-7.0					
Segments	May	June	July	August	September
37.5°N	0.95	0.97	0.80	0.80	0.95
42.5°N	0.91	0.94	0.93	0.93	0.87
47.5°N	0.96	0.98	0.96	0.93	0.97
52.5°N	0.93	0.99	0.98	0.96	0.80
57.5°N	0.89	0.97	0.98	0.90	0.71
SSP5-8.5					
Segments	May	June	July	August	September
37.5°N	0.93	0.97	0.75	0.70	0.96
42.5°N	0.83	0.94	0.88	0.87	0.82
47.5°N	0.96	0.98	0.96	0.96	0.85
52.5°N	0.98	0.98	0.96	0.96	0.85
57.5°N	0.82	0.95	0.98	0.94	0.65

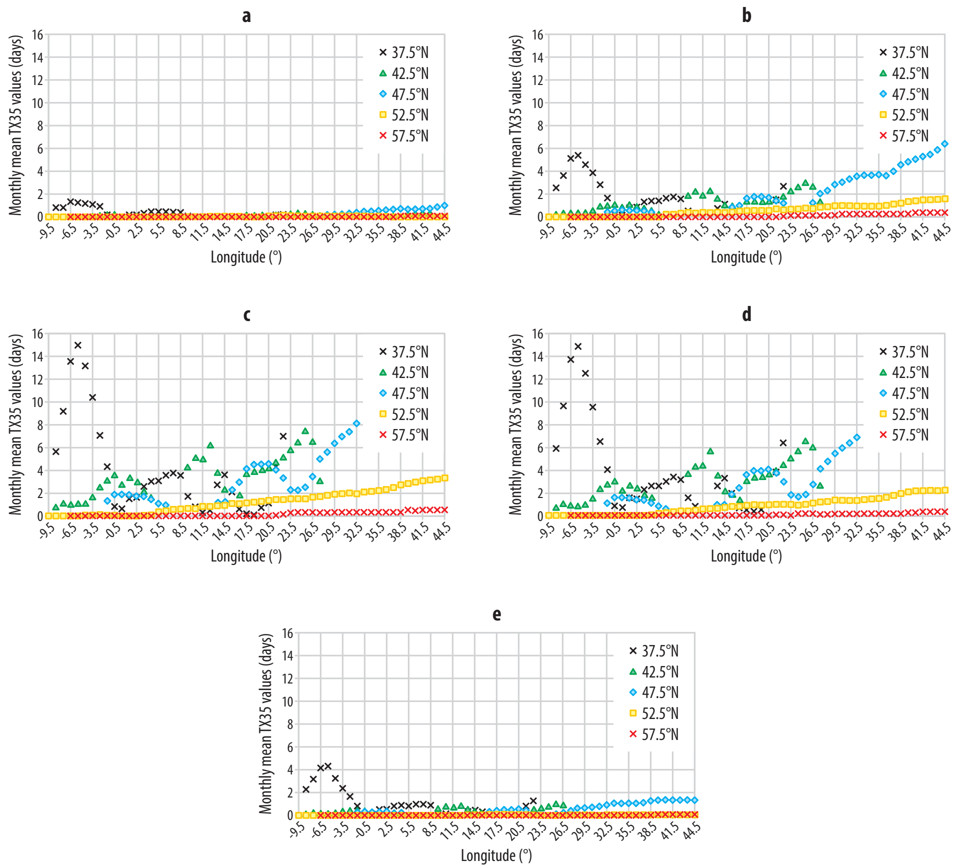

Fig. S1. Average monthly values of TX35 in the reference period 1995–2014 based on the historical CMIP6 simulations ensemble: a) May, b) June, c) July, d) August, e) September. *Source:* Authors' own elaboration.

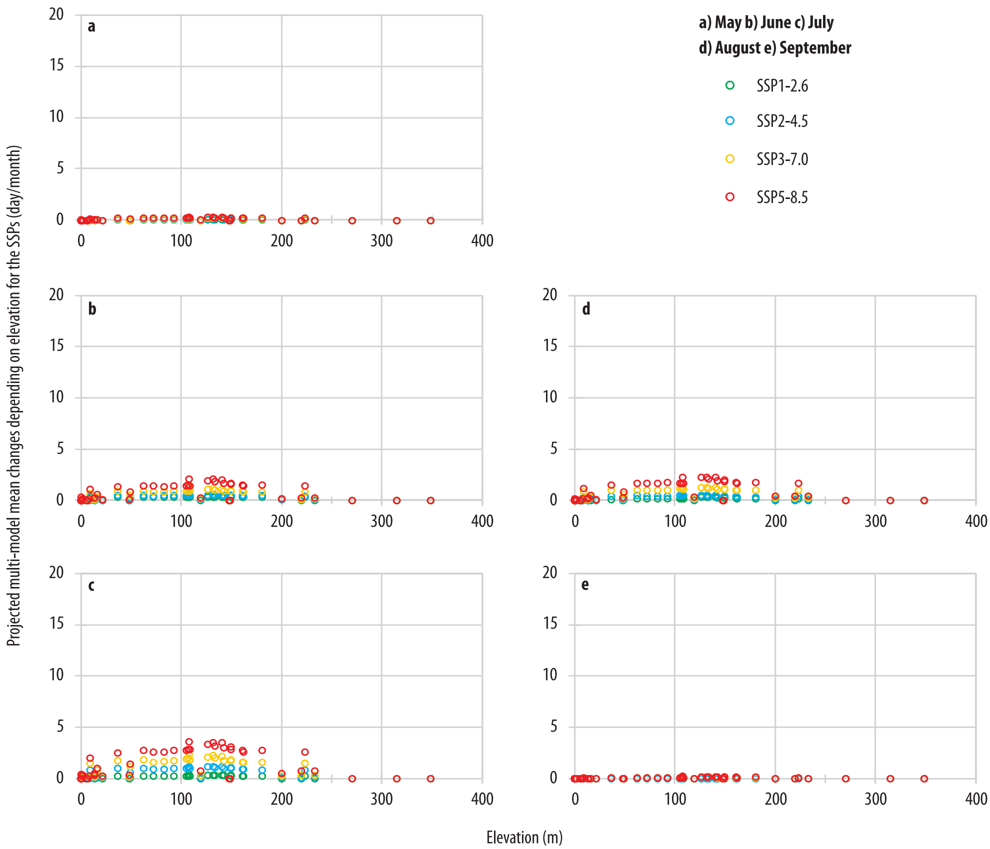

Fig. S2. Projected monthly changes of TX35 depending on elevation at 57.5°N for SSP1-2.6, SSP2-4.5, SSP3-7.0 and SSP5-8.5. *Source:* Authors' own elaboration.

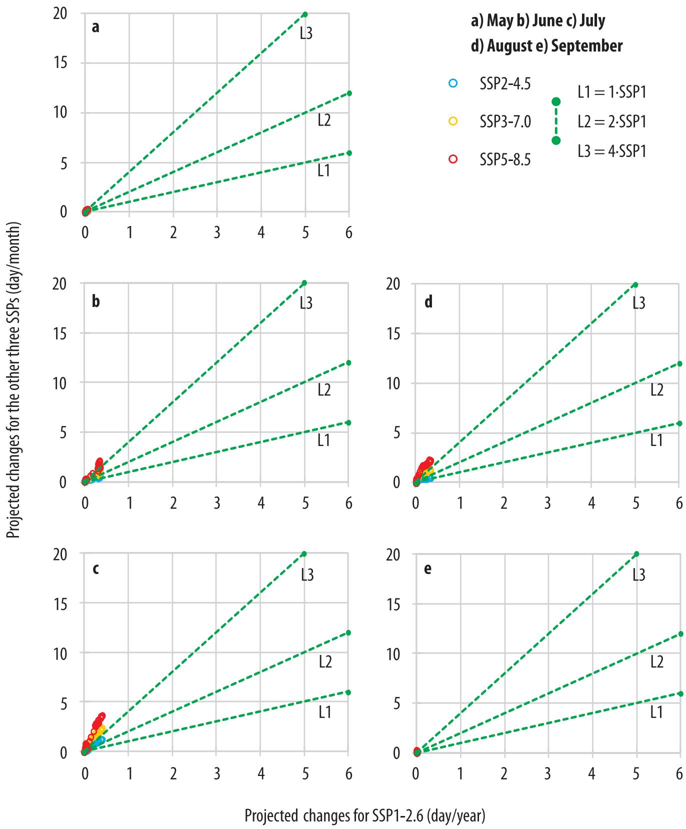

Fig. S3. Projected monthly changes of TX35 for SSP2-4.5, SSP3-7.0, and SSP5-8.5 compared to SSP1-2.6 at 57.5°N. *Source:* Authors' own elaboration.

DOI: 10.15201/hungeobull.75.1.2 Hungarian Geographical Bulletin **75** 2026 (1) 31–51.

Evaluation of the applicability of potential evapotranspiration models in Hungary

Marcell IMRE[1], Noémi SARKADI[1], Ervin PIRKHOFFER[2] and Szabolcs CZIGÁNY[3]

Abstract

One of the most challenging problems in hydrometeorology is the quantification of potential evapotranspiration (PET) rates. The aim of this study was to identify PET models that can reliably approximate the FAO Penman–Monteith reference evapotranspiration or available PET data provided by the Hungarian Meteorological Service (HungaroMet) for Hungary while requiring fewer meteorological input variables. Nevertheless, an understanding of PET values and trends can offer invaluable insights into the drought sensitivity of an area. We analysed the performance of 18 PET models for Hungary based on meteorological data from 2010 to 2022 and identified and ranked the most relevant ones. The PET values were calculated at 16 meteorological stations using different models and subsequently ranked according to six distinct statistical indicators. As a basis for comparison, data from the nearest pan-evaporation measuring station and FAO Penman-Monteith (FAO-PM) values were calculated. PET provided by HungaroMet was used as the reference potential evaporation value. Model performances were ranked on a 1–120 scale. Our results showed that the temperature-based Oudin model had the most accurate performance, but in general, the radiation-based models were the most reliable. The spatial distribution of the data indicates that the performance of the PET models is somewhat inferior in the eastern and western regions of the country in comparison to that observed in the central areas. Our results are likely applicable to the temperate zone of similar subhumid climates.

Keywords: potential evapotranspiration (PET), model performance, pan-evaporation, Hungary

Received November 2024, accepted March 2026.

Introduction

Concepts for describing the rate of evaporation and evapotranspiration

Evapotranspiration (ET) is the combined process of evaporation from soil and open water surfaces, and transpiration from plants and other organisms. As such, ET represents a key link between the water and energy cycles and plays a central role in the hydrological balance. To describe ET more precisely, different terms have been introduced. Reference evapotranspiration (ET_0) refers to the evapotranspiration from a standardized reference surface and is widely used in hydrological, agricultural, and environmental studies. The Food and Agriculture Organization (FAO) Penman–Monteith equation (FAO-PM) is recommended as the standard method for estimating ET_0 under different climatic conditions. Potential evapotranspiration (PET) expresses the maximum evapotranspiration under the assumption of an unlimited water supply, independent of soil water storage. In contrast, actual evapotranspiration (AET) refers to the real amount

[1] Department of Geology and Meteorology, Institute of Geography and Earth Sciences, Faculty of Sciences, University of Pécs. Ifjúság útja 6, H-7624 Pécs, Hungary. Corresponding author's e-mail: sarkadin@gamma.ttk.pte.hu
[2] Department of Cartography and Geoinformatics, Institute of Geography and Earth Sciences, Faculty of Sciences, University of Pécs. Ifjúság útja 6, H-7624 Pécs, Hungary.
[3] Department of Physical and Environmental Geography, Institute of Geography and Earth Sciences, Faculty of Sciences, University of Pécs. Ifjúság útja 6, H-7624 Pécs, Hungary.

of water evaporated and transpired under existing soil moisture conditions, which is generally less than or equal to PET.

Quantifying ET using both measurements and numerical models is a complex and arduous task and is regarded as one of the greatest challenges in hydrometeorology. This difficulty arises because ET is not a single physical quantity, but the result of a constantly changing interaction between the atmosphere, soil, water availability, vegetation, and meteorological drivers such as vapour pressure deficit. For instance, Breuer, H. and Ács, F. (2010) demonstrated that crop surface resistance strongly influences ET rates, with the highest variability observed in summer months in Hungary.

The models utilized for PET estimation can be classified into four categories: aerodynamic, temperature-based, radiation-based, and combination models. The distinction between these models is based on the type of input data required. Aerodynamic models consider mass transfer; nonetheless, their margins of error are rather high. Temperature-based models, such as Thornthwaite's method (Thornthwaite, C.W. 1931) are relatively straightforward to parameterize and are widely utilized in literature (Blaney, H.F. and Criddle, W.D. 1950; Baier, W. and Robertson, G.W. 1965; Kharrufa, N.S. 1985; Oudin, L. *et al.* 2005). Radiative models integrate empirical data and the radiative equation, which may result in varying degrees of applicability across different regions. Combination models use multiple meteorological parameters, with the FAO-PM equation being the most widely accepted method (Allen, R.G. *et al.* 1998). However, FAO-PM has a relatively high data demand, which often restricts its use in areas with limited observations.

PET models are validated using several approaches, such as lysimeters, scintillation methods (Xu, Z. *et al.* 2013), Bowen ratio method (Douglas, E.M. *et al.* 2009), or pan evaporation (Brouwer, C. and Heibloem, M. 1986). Yet, evaporation pans and evaporimeters reflect only site-specific conditions and are often scarce. Consequently, PET models based on meteorological inputs are required to ensure applicability across different climatic zones and land use types

Climate and environmental conditions in Hungary

In general, continental climates are prone to weather extremes, which may be further intensified by climate change. The climate of Hungary has also shown noticeable changes during the 20th century (Breuer, H. *et al.* 2017). The unwanted impacts of climate change, especially under continental and semi-arid climates, are further exacerbated by increasing evaporation due to increased temperatures. It is indicated by the decreasing length of winters and the increasing length of summer days. Winters in the Northern Hemisphere have shortened by an average of 20 days between 1976 and 2012, while summers were extended by 13 days (Kutta, E. and Hubbart, J.A. 2016).

Recent research confirms that seasonal dynamics across Europe are undergoing substantial shifts. In Central and Northern Europe, the thermal growing season has lengthened mainly due to earlier onset and only secondarily to later termination (Miś, F. and Tomczyk, A.M. 2025). At the same time, regional climate model projections indicate a marked prolongation of compound dry–hot seasons throughout Europe, primarily driven by rising temperatures and, thus, higher evaporative demand, while precipitation changes exert regionally opposing effects by amplifying the signal in the south and moderating it in the north (Lhotka, O. *et al.* 2023). Working within a climatic water balance (P−PET) framework and using the Oudin PET model, Lhotka, O. *et al.* (2023) emphasize that temperature- and radiation-based PET formulations are particularly relevant for assessing evaporative demand trends in mid-latitude continental climates. Collectively, these findings justify a detailed evaluation of low-input PET models under the data-limited but hydroclimatically sensitive conditions characteristic of Hungary.

Continental climates also pose a variety of challenges for agriculture, as droughts caused by periods of water deficit can alternate with large riverine floods and flash floods of increasing frequency. These two dichotomous abiotic hazards have the highest probability of occurrence in Hungary (Pirkhoffer, E. *et al.* 2009; Lóczy, D. 2010). To highlight these extremes, in Hungary, the years of 2010 and 2011 were the wettest (959 mm), and the driest (407.4 mm), respectively, between 1901 and 2014 (Schmeller, G. *et al.* 2022).

According to the data published in the UNCCD National Report (2022), ten years were affected by some level of drought between 2006 and 2021, in which at least 30 percent of Hungary was impacted. The total area affected by extreme drought was the highest in the years 2000, 2003, 2011, and 2022 (UNCCD, 2022). The increasing trend of annual evapotranspiration and drought in Hungary has been revealed by many authors (e.g. Blanka, V. *et al.* 2013; Mezősi, G. *et al.* 2016; Szabó, Sz. *et al.* 2019).

Numerous studies have evaluated PET models worldwide, e.g. for Germany and China (e.g. Bormann, H. 2011; Yang, Y. *et al.* 2021; Li, Z. *et al.* 2024), but, to our knowledge, no study has systematically compared models representing all four methodological categories for Hungary.

Anda, A. and co-authors investigated evaporation processes in shallow aquatic environments in the Lake Balaton and Kis-Balaton regions, with particular focus on the effects of littoral sediments and submerged macrophytes. Their studies demonstrated that these factors could enhance evaporation compared to standard Class A pan measurements and should be considered when estimating evaporation and evapotranspiration in shallow lakes and wetlands (Anda, A. *et al.* 2015, 2016, 2018a, b).

The current study aims at analysing the performance of 18 PET models for Hungary, not only in aquatic environments, but also to identify the most applicable models for Hungary.

The specific objectives of the current research were the following:

1. Ranking the accuracy of 18 PET models by statistical methods using pan-evaporation and FAO-PM, and reference PET calculated by the Hungarian Meteorological Service (hereafter HungaroMet) as reference.

2. Research for regularities in the spatial distribution of the top-three models.

3. Examination of the potential for replacing high-input models with lower-input models.

Material and methods

Study area

The topography of Hungary is mainly dominated by alluvial plains (the Little and Great Hungarian Plain) with low mountain areas in the west and the north. Hungary is dominated by a subhumid continental climate with marked Mediterranean influence from the south and oceanic influences from the west. Climatic conditions are far from homogeneous over the country with considerable differences in an east-west direction and between the mountainous and lowland areas. Recent studies of the Carpathian Region, including Hungary, identify distinct climatic zones and spatial gradients shaped by topography and regional position, reflecting differences between lowland plains and mountainous areas as well as east–west climatic variation (Szelepcsényi, Z. *et al.* 2014; Szabó, A.I. *et al.* 2021).

The 30-year mean annual precipitation totals range between 500 and 800 mm, with a maximum in May and June and a minimum from February to April. The mean annual temperature is around 9–13 °C with 13+ °C over the past years from 2018 on, similar to the global climatic trends. The prevailing wind direction is from the west and northwest in the majority of the country (Bihari, Z. *et al.* 2018).

Sources of meteorological and pan-evaporation data used in the research

Meteorological data for 16 stations (*Figure 1*) were obtained from the database of HungaroMet Zrt. Class A evaporation pan data series

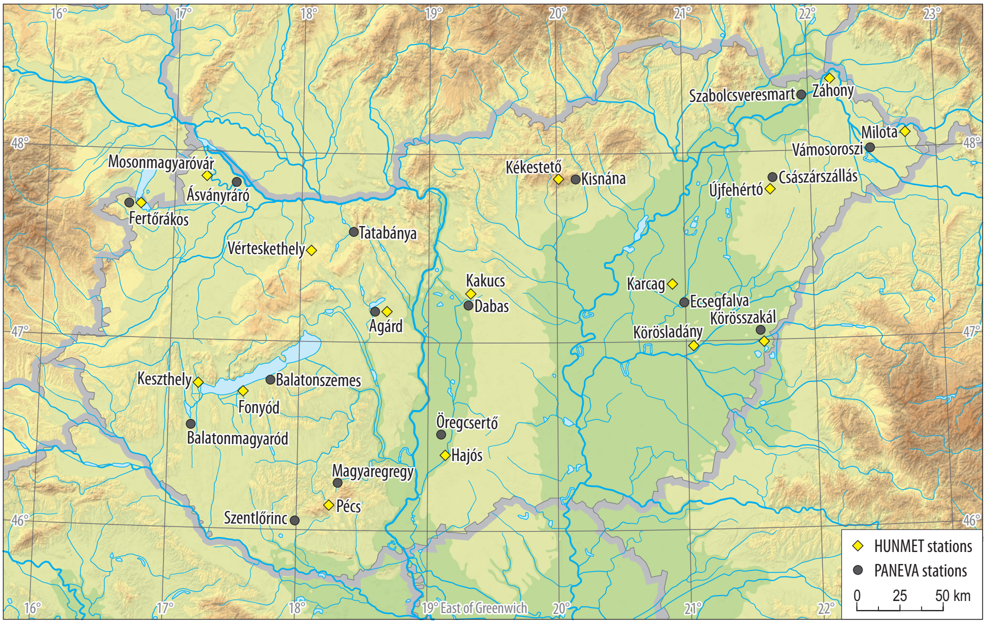

Fig. 1. Geographical location of the meteorological and pan-evaporation stations used.
Source: Authors' own elaboration.

(PANEVA) for 15 stations, used as a reference, were provided by the Hungarian General Directorate for Water Management for the period of 2010 to 2022. A total of 18 PET models (aerodynamic, temperature-based, radiation-based, and combination) were used for the calculation of PET (*Table 1*). The reference PET dataset is calculated by HungaroMet Zrt. (HUNMET) was used as a control data set.

Comparability of pan-evaporation data and PET

Pan-evaporation and PET are closely related, as both measure atmospheric demand for water loss, but they are not directly equivalent. Despite the high correlations between the two values, systematic biases exist. Pan evaporation often overestimates or underestimates PET depending on climate, season, and environmental conditions. The need for site-specific evaporation coefficients (K_p) and regular recalibration is emphasized to correct these biases and improve comparability (Mekoya, A. 2021).

The estimation of the K_p value is determined primarily by surface cover and micro-environmental factors (Allen, R.G. *et al.* 1998). To this end, GIS tools were utilised to estimate the K_p value for each pan evaporation station. Land cover information was derived from the CORINE Land Cover 2018 database (vector format, Europe-wide, version 2020_20u1, released in May 2020), provided by the European Environment Agency (EEA, 2020). For the present study, only the Hungarian subset was used (*Table 2*). To identify any potential differences, analyses were conducted using both raw pan-evaporation data and data adjusted with a K_p value (PANEVA_K).

Model ranking

To validate the numeric models, their results were compared with pan-evaporation data.

*Table 1. Potential evapotranspiration models used to calculate daily PET**

Type	Name of the PET model	Equation	Reference	Climate zone according to Köppen
Aerodynamic	Albrecht (ALBRCT)	$PET = (0.1005 + 0.297u_2) \times (e_s - e_a)$	Albrecht, F. 1950; Bormann, H. 2011.	Cfb, Cfa
	Brockamp-Wenner (BRWENR)	$PET = (0.543u_2^{0.456}) \times (e_s - e_a)$	Brockamp, B. and Wenner, H. 1963; Bormann, H. 2011.	Cfb
	Harbeck (HARBEC)	$PET = (0.0578u_8) \times (e_s - e_a) \times 25.4$	Harbeck, G.E. 1966; Singh, V.P. and Xu, C-Y. 1997.	Cfb, Dfb
	Rohwer (ROHWER)	$PET = 0.44 \times (1 + 0.27u_2) \times (e_s - e_a)$	Rohwer, C. 1931; Xu, C.Y. and Singh, V.P. 2002.	BSk, Dfa
Temperature-based	Baier-Robertson (BAROBR)	$PET = 0.157T_x + 0.158(T_x - T_n) + 0.109R_a - 5.39$	Baier, W. and Robertson, G.V. 1965.	Dfb, Cfb
	Hamon (HAMON)	$PET = \left(\frac{N}{12}\right)^2 \times \exp\left(\frac{T_a}{16}\right)$	Hamon, W.R. 1961; Oudin, L. *et al.* 2005.	Cfa, Cfb
	Romanenko (ROMANE)	$PET = 4.5 \times \left(1 + \frac{T_a}{25}\right)^2 \times \left(1 - \frac{e_a}{e_s}\right)$	Romanenko, V.A. 1961.	Dfb, Dfa
	Schendel (SCHEND)	$PET = 16\frac{T_a}{RH}$	Schendel, U. 1967; Bormann, H. 2011.	Cfb, Dfb
	Oudin (OUDIN)	$\begin{cases} PET = (\lambda\rho)^{-1} \times R_a\left(\frac{T_a + 5}{100}\right) & T_a > -5°C \\ PET = 0 & T_a \leq -5°C \end{cases}$	Oudin, L. *et al.* 2005.	Cfb, Dfb, Dfc
	Reference PET (HUNMET)	$PET = 0.74 \times (e_s - e_a)^{0.7} + \left(1 + \frac{T_a}{273}\right)^{4.8}$	Antal, E. 1968; Antal, E. and Kozmáné T.E. 1968.	PET-based on climatology of Hungary

Table 1. Continued

Type	Name of the PET model	Equation	Reference	Climate zone according to Köppen
Radiation-based	Turc (TURC)	$\begin{cases} PET = 0.013 \times \left(\frac{T_a}{T_a+15}\right) \times (R_s+50) \times \left(1+\frac{50-RH}{70}\right) & RH < 50\% \\ PET = 0.013 \times \left(\frac{T_a}{T_a+15}\right) \times (R_s+50) & RH \geq 50\% \end{cases}$	Turc, L. 1955, 1961; Lu, J. *et al.* 2005.	Cfb, Cfa
	Jensen-Haise (JENHAI)	$PET = 25.4 \times (0.014T_a - 0.37) \times (0.000673R_s)$	Jensen, M.E. and Haise, H.R. 1963; Zheng, H. *et al.* 2017.	BSk, BSh
	Stephens-Stewart (STESTW)	$PET = 25.4 \times (0.0082T_a - 0.19) \times \left(\frac{R_s}{1500}\right)$	Stephens, J.C. and Stewart, E.H. 1963; Zheng, H. *et al.* 2017.	BSk
	Hargreaves (HARGRE)	$PET = 0.0135R_s \times \frac{T_a+17.8}{\lambda}$	Hargreaves, G.H. 1975.	BWh, BSh, BSk
	Milly-Dunne (MILDUN)	$PET = \frac{0.8 \times (R_n - G)}{\lambda}$	Milly, P.C.D. and Dunne, K.A. 2016.	All climates
	Priestley-Taylor (PRITAY)	$PET = \alpha \times \frac{\Delta}{\Delta+\gamma} \times \frac{(R_n - G)}{\lambda}$	Priestley, C.H.B. and Taylor, R.J. 1972.	Af, Cfa, Cfb
Combination	Rijtema (RIJTEM)	$PET = \frac{\frac{\Delta(R_n - G)}{\lambda} + \gamma r u_2^{0.75} \times (e_s - e_a)}{\Delta+\gamma}$	Rijtema, P.E. 1965; Bormann, H. 2011.	Cfb, Cfa
	Wright-Jensen (WRIJEN)	$PET = \frac{\Delta(R_n - G)}{\lambda(\Delta+\gamma)} + \frac{\gamma}{\Delta+\gamma} \times 2.63 \times (0.75 + 0.993u_2) \times (e_s - e_a)$	Jensen, M.E. and Wright, J.L. 1978; Allen, R.G. and Pruitt, W.O. 1986.	BSk, BSh
	Penman (PENMAN)	$PET = \frac{\Delta(R_n - G)}{\lambda(\Delta+\gamma)} + \frac{\gamma}{\Delta+\gamma} \times \frac{6.43(1 + 0.536u_2) \times (e_s - e_a)}{\lambda}$	Penman, H.L. 1948; Shuttleworth, W.J. 1992.	All climates

Table 1. Continued

PET	Potential evapotranspiration	mm/day	–
u_2, u_8	Wind speed at 2 m and 8 m, respectively	m/s	–
e_s, e_a	Sturation and actual vapour pressure, respectively	kPa	hPa for Albrecht, F., and for Brockamp, B. and Wenner, H. inch Hg for Harbeck, G.E. mm Hg for Rohwer, C.
T_a	Average daily air temperature	°C	°F for Jensen, M.E. and Haise, H.R., and for Stephens, J.C. and Stewart, E.H.
T_n, T_x	Daily minimum and maximum air temperature, respectively	°C	–
R_a	Extraterrestrial radiation	$MJ/m^2/day$	–
N	Hours of sunshine	h	–
RH	Relative humidity	%	–
λ	Latent heat of vaporisation	MJ/kg	2.45
ϱ	Water density	kg/m^3	–
R_s	Incident solar radiation	$MJ/m^2/day$	$cal/cm^2/day$ for Turc, L., for Jensen, M.E. and Haise, H.R., and for Stephens, J.C. and Stewart, E.H.
R_n	Net radiation	$MJ/m^2/day$	–
G	Soil heat flux density	$MJ/m^2/day$	can be considered as 0 in daily time steps
α	Priestley-Taylor parameter	–	1.26
Δ	Slope vapour pressure curve	kPa/°C	–
γ	Psychrometric constant	kPa/°C	–

*After Yang, Y. *et al.* 2021.

Potential Evapotranspiration (PET) and pan evaporation are two different concepts, although they are closely related and often used together to estimate water loss. Generally, PET represents the maximum water loss from the surface with *abundant water*, combining both evaporation from soil and transpiration from plants. Pan evaporation does not include plant transpiration. It is purely physical evaporation, which is highly affected by the heat storage and thermal properties of the metal pan, making it behave differently from natural water bodies or vegetation. Nevertheless, Class A pan measurements are widely used to estimate the evaporation of natural water bodies, providing a practical approach when direct measurements of reference evapotranspiration (ET_0) are not available. For example, Anda, A. *et al.* (2018a) applied Class A pans to quantify evaporation from a natural water body in the Keszthely region of Hungary, accounting for factors such as vegetation and sediment cover. Their results were compared with FAO-56 PM-based ET_0 estimates, demonstrating that pan-derived measurements, when properly adjusted, can provide reliable site-specific evaporation estimates. This highlights the continued relevance of pan-evaporation-based approaches for assessing water balance in natural environments, particularly where standard meteorological data may be limited.

Pan-evaporation stations are approximately evenly distributed across Hungary. The Körösszakál pan-evaporation dataset was used for both the Körösszakál and Körösladány modelled PET data, evaporation data from only 16 pan evaporation stations were used for analysis. For validation purposes, the geographically nearest weather station was selected for each pan evaporation station (see *Table 2*). Pan evaporation data was only available for the period of 1 April to 31 October each year, hereafter denoted as $PET_{A\text{-}O}$. Hence, weather data was only used for the same period of each year.

Calculated data was mapped with QGIS 3.38.0 software environment. Statistical data was processed using MS Excel, and MATLAB R2024b. The statistical indicators employed for the evaluation of the 18 PET models were as follows:

Table 2. Meteorological stations with the corresponding pan-evaporation stations used and the CORINE Land Cover classes with the K_p values

Pan-evaporation measurement station	Nearest HungaroMet weather station	CORINE class	K_p value
Agárd	Agárd	Intertidal flats	0.55
Fertőrákos	Fertőrákos	Road and rail networks and associated land	0.60
Balatonszemes	Fonyód		0.60
Öregcsertő	Hajós		0.65
Dabas	Kakucs		0.65
Ecsegfalva	Karcag		0.65
Kisnána	Kékestető		0.65
Balatonmagyaród	Keszthely, Tanyakereszt	Discontinuous urban fabric	0.70
Körösszakál	Körösladány		0.70
Körösszakál	Körösszakál	Vineyards	0.72
Vámosoroszi	Milota	Road and rail networks and associated land	0.65
Ásványráró	Mosonmagyaróvár		0.65
Magyaregregy/Szentlőrinc	Pécs, Egyetem	Salt marshes	0.55
Császárszállás	Újfehértó	Intertidal flats	0.55
Tatabánya	Vérteskethely	Industrial and commercial units	0.70
Szabolcsveresmart	Záhony	Road and rail networks and associated land	0.65

1. Mean Absolute Error (MAE) in mm/day;
2. Mean Percentage Error (MPE), dimensionless;
3. Mean Bias Deviation (MBD) in mm/day;
4. Mean Bias Error (MBE) in mm/day;
5. Nash-Sutcliffe Model Efficiency Coefficient (NSE), dimensionless;
6. Coefficient of Determination (R^2), dimensionless.

All statistics are calculated using daily PET estimates, and annual aggregations are derived from these daily values when needed. A cumulative scoring system has been applied, for PET model evaluation and show that comparing models with reference PET/ET_0 data is a common, established methodology in hydrological literature (see references: Bormann, H. 2011; Yang, Y. *et al.* 2021; Li, Z. *et al.* 2024, and Toušková, J. *et al.* 2025). All models were ranked according to each statistical method at each station. The maximum score for each statistical indicator was, thus, 19. The models that scored most frequently in positions 1-3, 4-6, and 7-9 at each station received an additional 6, 3, and 1 correction points, respectively. The correction points are representative of the range of use of the models. This gives a higher score to models that are applicable to a larger geographic area of the country. The maximum score a model could obtain was 120. Always, the results of comparisons with the PANEVA_K dataset were used in the ranking system; the HUNMET dataset was only used as a reference (e.g. for R^2 values).

Results

Model comparison without the K_p coefficient

The average calculated $PET_{A\text{-}O}$ values of the 18 PET models range between 285 and 1516 mm over the period of 2010 to 2022 (*Figure 2*). The lowest value was calculated for the Harbeck method, while the highest value was obtained for the Jensen-Haise model. The overall average value was 805.5 mm, whereas the median value was 766.7 mm. The temperature- and radiation-based methods demonstrated the most optimal performance, and the aerodynamic models exhibited the least favourable model performance. For Hungarian conditions, particularly in the Cfb, Cfa, Dfb, and Dfa Köppen climate zones (see *Table 1*), several PET models are considered suitable, including Albrecht, Brockamp-Wenner, Harbeck, Baier-Robertson, Hamon, Romanenko, Schendel, Oudin, Turc, Rijtema, Milly-Dunne, Priestley-Taylor, and Penman. Models such as Rohwer, Jensen-Haise, and Wright-Jensen may be partially applicable under specific conditions, while Stephens-Stewart and Hargreaves should be used with caution due to their limited suitability for the region. The mean annual PANEVA value was 682.67 mm/year, whereas the mean annual PANEVA_K value was 436.06 mm/year.

The MAE values were more favourable in the central two-thirds of the country, particularly for data calculated with radiation-based models. The temperature-based Oudin and the combination-type Rijtema models yielded favourable MAE values. With regard to MAE, the most optimal fit was yielded at Vérteskethely station, calculated by the Oudin model (MAE = 0.571 mm/day). As the country approached the eastern and western extremes, the MAE values of the models exhibited a general deterioration. Given the intrinsic nature of MAE as an indicator, it does not indicate the direction of deviations, thus, under- or overestimation cannot be determined from it.

Due to its ability to detect under- and overestimation, MPE values are also plotted on a map for the top-three ranked PET models (compared with PANEVA and PANEVA_K, too) (*Figure 3*). The MPE results showed substantial variability among the evaluated methods and stations. Several models produced large positive MPE values, indicating systematic overestimation of evapotranspiration. In particular, the Jensen-Haise model frequently exhibited the largest positive MPE values across many stations, suggesting a consistent tendency to overestimate evapotranspiration. Similarly, Rijtema, Wright-Jensen were mostly overestimators. Of the models, the Harbeck

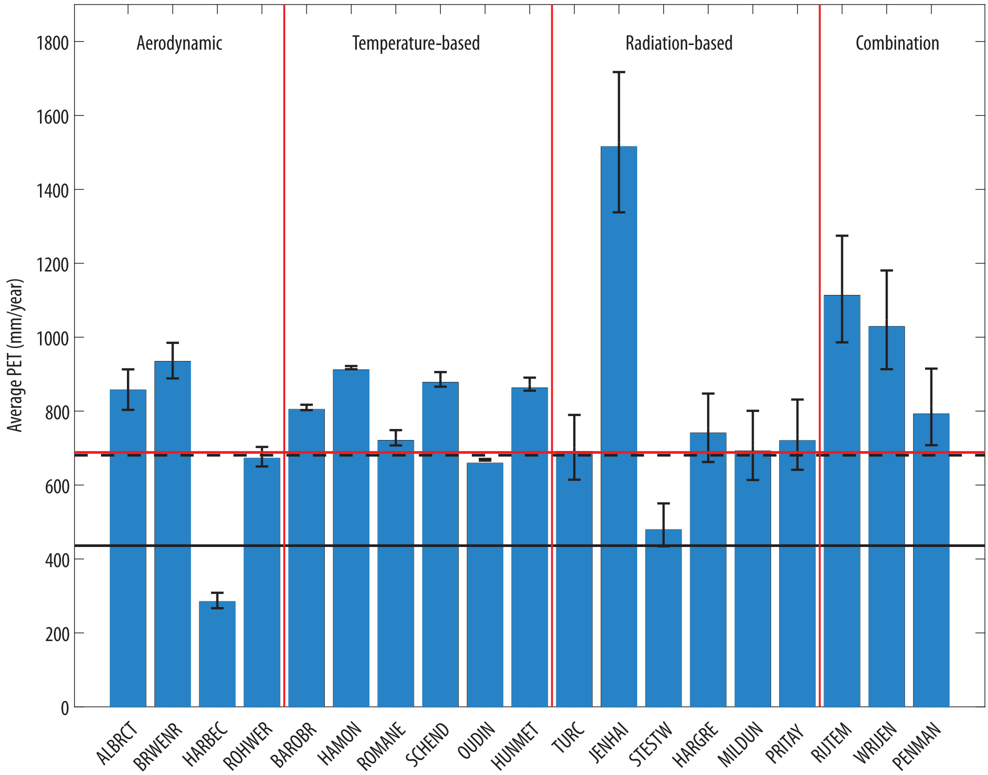

Fig. 2. The mean country-averaged $PET_{A\text{-}O}$ values (columns) for the 18 models and HUNMET reference PET (2010–2022 data). The black error bars show the total annual standard deviation for the different methods. The black dashed line marks the average annual PANEVA values (overlapped with FAO-PM reference ET_0), the continuous black line marks the average annual PANEVA_K values and red line represents FAO-PM reference ET_0 between April and October for the same years. *Source:* Authors' own elaboration.

and at some stations Stephens-Stewart models were shown to be net underestimators. Radiation-based models also showed elevated positive MPE values at several locations. In contrast, certain temperature-based approaches, including the Oudin and Turc models, often yielded lower MPE magnitudes, indicating a more balanced estimation behaviour at multiple stations. Among the spatial specificities, it is notable that the Baier-Robertson, Harbeck, Stephens-Stewart, Romanenko and Rohwer models underestimated the $PET_{A\text{-}O}$ values (columns) for the most elevated Kékestető station, while all other stations showed overestimated values. Oudin, in both cases, slightly or generally overestimated the PET values. The Stephens-Stewart (MPE = 2.8%) model showed the smallest percentage point deviations. In the case of STESTW model underestimation only occurred in Vérteskethely and Kékestető stations. On the other hand HARBEC estimated well PANEVA_K, generally with lower values, except for Mosonmagyaróvár and Fonyód stations. Of the models, Jensen-Haise has the worst error of 244.2 percent. It was examined whether there is any correlation between the best performing models at each station and the Péczely climate class at the station location, but no evidence of a relationship was found.

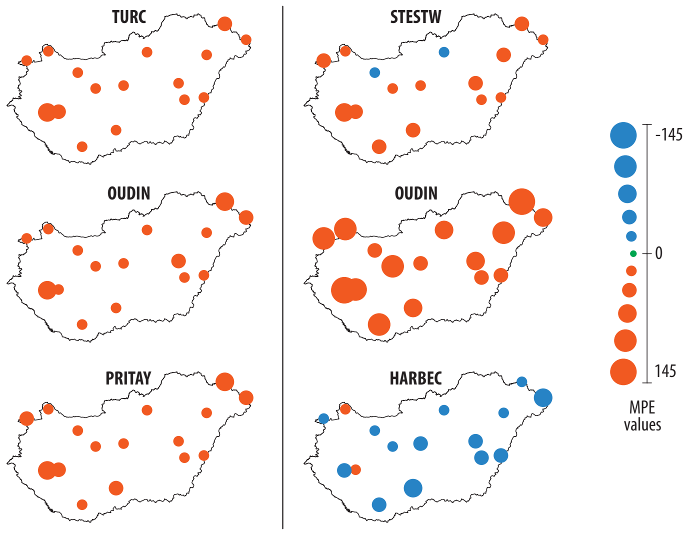

Fig. 3. Mean percentage error (MPE) of the top three PET models relative to pan-evaporation, without the pan coefficient applied (left) and with the K_pan coefficient applied (right), for each station.
Source: Authors' own elaboration.

The MBD and MBE values confirmed the under- and overestimation trends indicated by the MPE. In the analysed dataset, the results of these two indicators showed very similar patterns across the evaluated stations and models. Several methods exhibited positive bias values, indicating a general tendency toward overestimation of evapotranspiration. In particular, the Jensen-Haise model frequently produced relatively large positive MBD and MBE values at multiple stations, reflecting consistent overestimation. Radiation-based methods also displayed positive bias at several locations, although the magnitude of these deviations varied among stations. In contrast, some models occasionally produced negative MBD and MBE values, indicating underestimation of evapotranspiration under certain climatic conditions. The underestimation of the Harbeck and Stephens-Stewart models also emerged for these indicators. In contrast, the Oudin model exhibited both positive and negative deviations, although the magnitude of the bias remained relatively small, with MBD values ranging between -15 and +15.

The NSE indicator is a commonly calculated indicator in hydrological model calculations, which is why it was used in this study. Most models produced NSE values in the range of approximately 0.3–0.7, indicating acceptable but variable agreement with the reference dataset. The highest NSE values were typically obtained for several temperature-based and combination-type models, including Oudin, Turc, and Rijtema at multiple stations. In contrast, lower NSE values were frequently observed for models with strong systematic bias, particularly the Jensen-Haise method.. Furthermore, negative NSE values were also observed with considerable frequency in this latter group, which serves as an indicator of particularly high inaccuracy.

When plotting the data by station on boxplot diagrams (*Figure 4*), it is visible that the median of the PANEVA and HUNMET data series differed only slightly at the highest Pécs and Záhony. Moderate differences are noticed in stations: Keszthely and Fonyód. The range of the PET models analysed is also narrower at these stations, which are considered to be the extremes, than the coun-

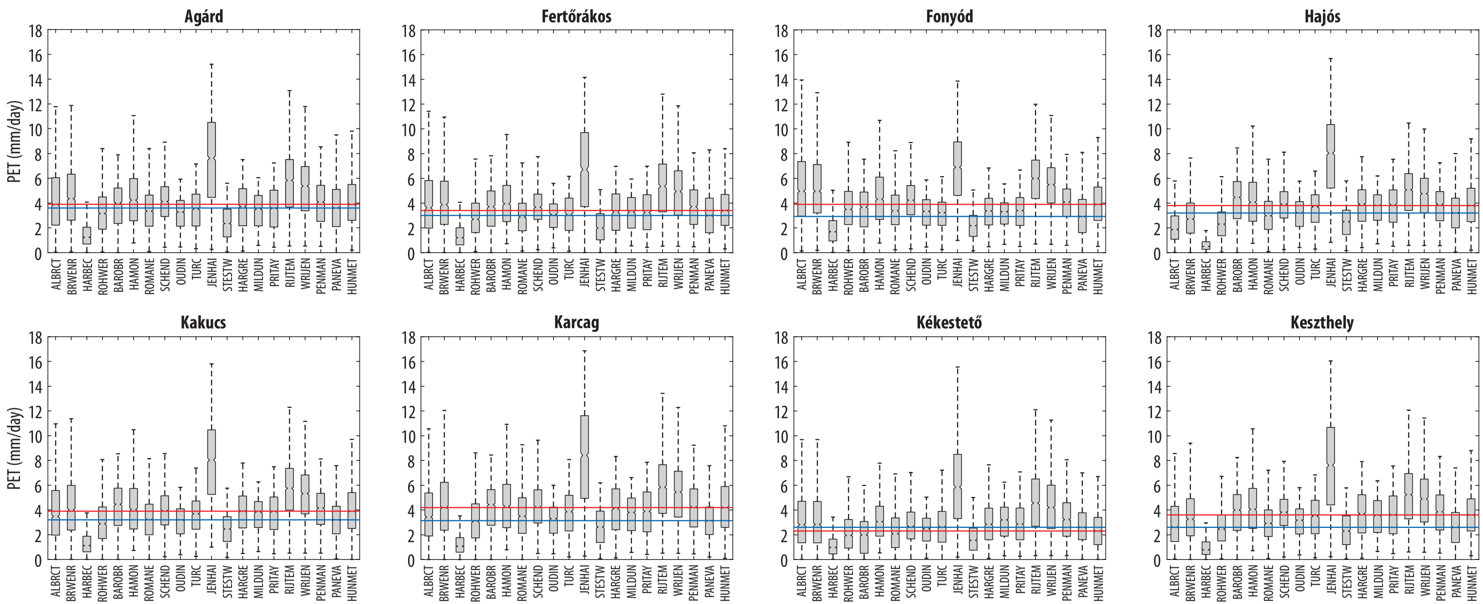

Fig. 4. Daily modelled $PET_{A\text{-}O}$ values for for the years between 2010 and 2022. The purple line represents the median of the PANEVA dataset and the orange line the median of the HUNMET dataset. *Source:* Authors' own elaboration.

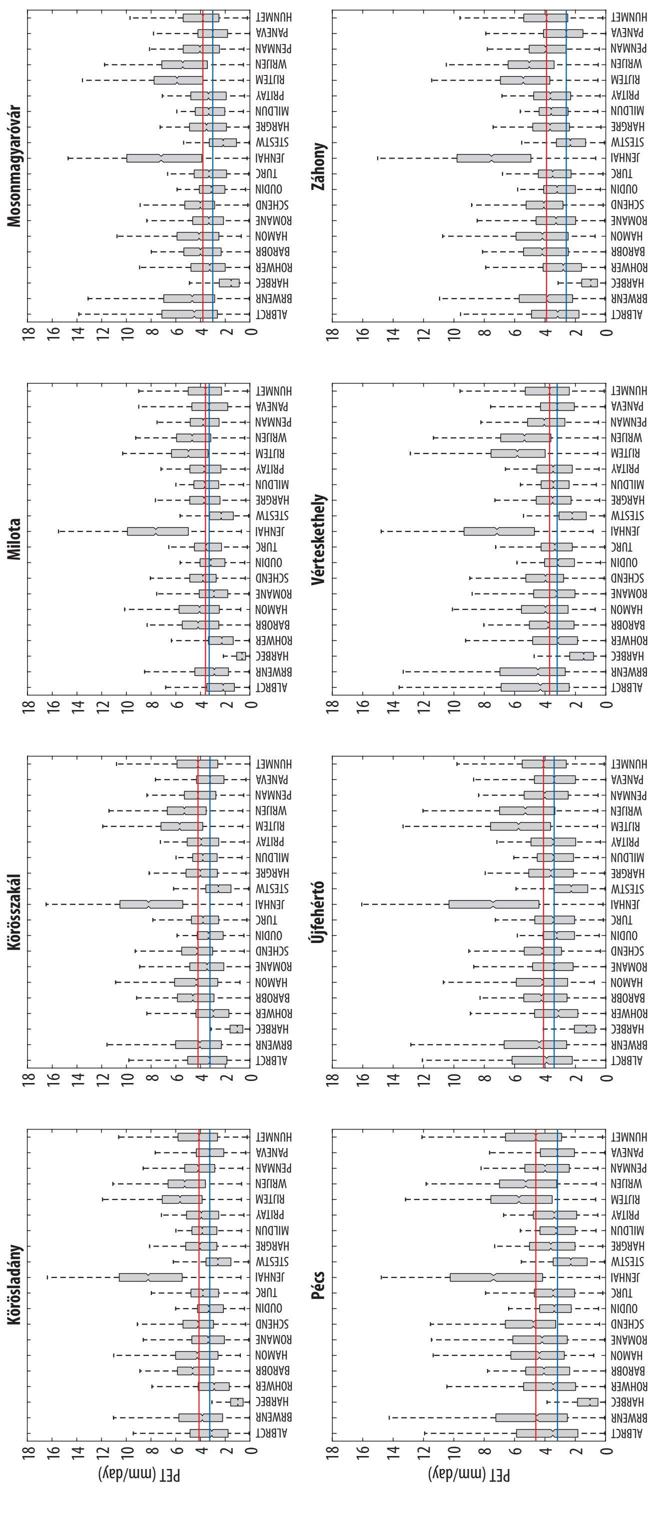

Fig. 4. Continued.

try average. The HARBEC and STESTW model consistently produced the smallest range across the stations, but also consistently behaved as a strong underestimator. Temperature-based models (e.g. Oudin, Hargreaves) generally show narrower IQRs and more stable distributions, with medians often close to the HUNMET reference PET and occasionally the pan evaporation reference. In contrast, several radiation-based and combination models display wider IQRs and longer whiskers, indicating greater variability and more frequent extreme values. The Jensen-Haise model frequently exhibits higher medians and extended upper whiskers, suggesting a tendency to overestimate PET. Overall, temperature-based models tend to produce more balanced estimates, while some radiation-based approaches show greater spread and uncertainty.

Most models achieved moderate correlations with the reference data (PANEVA), generally ranging between approximately 0.3 and 0.75 depending on the station and method. Higher R^2 values were commonly associated with models that also demonstrated higher NSE values, indicating stronger linear agreement with observed evapotranspiration. However, even models with relatively high R^2 values occasionally exhibited noticeable bias, highlighting the importance of evaluating multiple statistical indicators simultaneously when assessing model performance.

Country aggregated ranking

The 18 PET models were ranked according to the six statistical methods (MAE, MPE, MBD, MBE, NSE, R^2). When the country aggregated statistical data, the four PET methods were ranked: the temperature-based models performed the best, and the aerodynamic models performed the most poorly. In terms of the individual PET models the highest scores were achieved by the Turc (110 points), Oudin (109 points), and Priestley-Taylor (94 points) models (*Figure 5,* left). For the MAE, NSE and R^2 indicators, the temperature-based models scored highest (except for Jensen-Haise), and for the MBD and MBE indicators, the radiation-based models achieved the highest scores. The aerodynamic models had the lowest scores for all statistical indicators (except ROHWER). The group with the highest number of correction points was the radiation-based models, suggesting that this type of model gives valid $PET_{A\text{-}O}$ values over the widest area. Although the combination models did not perform well on average, the Penman model was ranked in sixth place. The aerodynamic models showed the lowest accuracy, with the Albrecht model being the most inaccurate.

Overall, the results demonstrate that the performance of empirical evapotranspiration estimation models varies substantially across both stations and model types. Temperature-based and combination-type approaches frequently provided balanced performance across several evaluation metrics, whereas some radiation-based models tended to produce larger systematic deviations at certain locations. These findings emphasize the importance of regional calibration and careful model selection when applying empirical evapotranspiration estimation methods under varying climatic conditions.

In the analysis using the PANEVA_K data set (*Figure 5,* right), significant changes can also be seen in the ranking. The average scores of the temperature-based, radiation-based, and aerodynamic models decreased slightly, while the combined models scored below median points. In both cases, radiation-based models dominate the top eight places. The average performance of the aerodynamic models is mainly due to the HARBEC and ROHWER model's rise in the rankings.

In the event that a potential substitution of the most optimal PET model is warranted, for instance, due to the absence of required data, alternative models must be selected. For the majority of Hungary, HUNMET reference PET can be optimally substituted by OUDIN, SCHEND, TURC, BAROBR, and HAMON models.

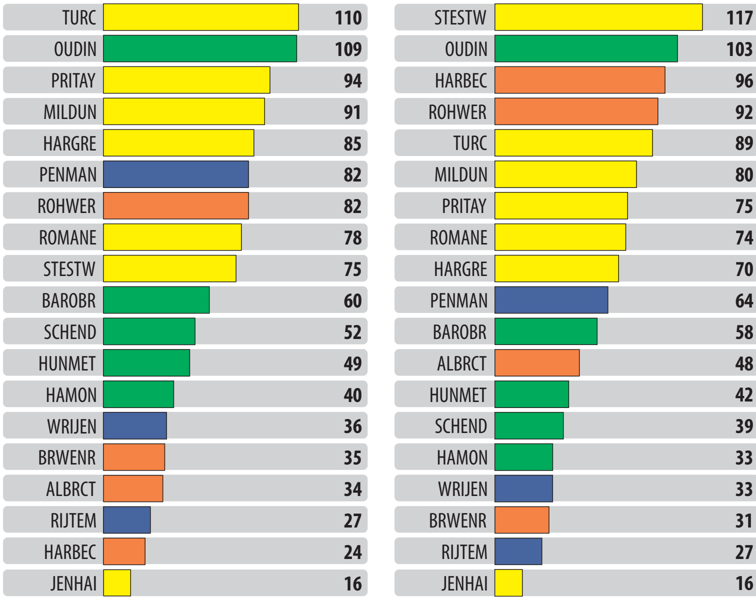

Fig. 5. Scores of each PET model based on the ranking system of this study (left: PANEVA, right: PANEVA_K). Yellow colours represent radiation-based methods, green for temperature-based methods, orange denote aerodynamic models and blue used to present combination methods. *Source:* Authors' own elaboration.

Changes in results using the K_p value

The results of the analysis show differences depending on whether the PANEVA or PANEVA_K data series is used for comparison. When using the PANEVA_K data series, the performance of the RIJTEM, STESTW, and PRITAY models also shows a statistically significant ($p < 0.05$) improvement. When using the PANEVA data set, the OUDIN model, which shows high performance, also improves, but in this case, we cannot observe a significant improvement ($p = 0.423$). At the same time, the PENMAN, WRIJEN, and TURC models show significantly worse reliability when using PANEVA_K.

A spatial analysis of the models reveals that the smallest differences in MPE values occur at the Kékestető, Vérteskethely, Hajós, Pécs, and Agárd stations when using the two bases. The largest differences are found at the Záhony, Mosonmagyaróvár, Keszthely, and Fonyód stations.The use of the pan-coefficient worsened the MPE values by an average of +38 percentage points in the annual aggregate results. It was also observed that the reliability of the model improved in proportion to the increase in altitude above sea level compared to the PANEVA_K data series.

The pan-coefficient recommended by the FAO reduced accuracy in nearly 80 percent of cases. Most of the models examined show a more accurate fit without K_p. The introduction of the correction caused a general overestimation and systematic biases.

Discussion

Varga, Gy. *et al.* (2018) have demonstrated that, on average, the amount of actual evapotranspiration in the annual water balance of Hungary is 85.9 percent of the annual precipitation sum. The dominant period of precipitation in the country occurs between May and October, which coincides with the period of pan-evaporation (Anda, A. *et al.* 2018b). This precipitation accounts for 68–70 percent of the 500–800 mm annual precipitation (Bihari, Z. *et al.* 2018).

A similar study was conducted in China by Li, Z. *et al.* (2024). Due to its vast geographic extent, China is represented by a multitude of climatic zones. In the temperate continental zone, the Penman model was found to be the most optimal, while the aerodynamic-based Rohwer and temperature-based Romanenko models also demonstrated satisfactory performance. In general, the combination models yielded the most precise results. In the case of Hungary, the radiation-based Turc model showed the best accuracy, followed by the temperature-based Oudin model in matching the pan-evaporation data series in most of the 16 meteorological stations, while the radiation-based Stephens-Stewart model showed the best fit with the pan-evaporation data series. This discrepancy between China and Hungary may be attributed to the fact that the climatic conditions in continental China tend to be more arid than those in Hungary, particularly in terms of relative humidity. The discrepancy between the models that demonstrate optimal performance in Hungary and those that exhibit superior results in the Chinese temperate continental zone may be attributed to the contrasting conditions of vapour pressure deficit and relative humidity. Therefore, vapour pressure deficit exerts a considerable influence on all models that function effectively in Hungary.

Yang, Y. *et al.* (2021) calculated PET with eighteen different empirical models for the major climatic regions of China, and they concluded that the combination models performed the best followed by the radiation-based models, whereas the temperature-based models obtained the worst performance.

The current study compares calculated $PET_{A\text{-}O}$ with the data of the closest pan-evaporation stations. However, PET is influenced by multiple parameters, hence the closest station may be inappropriate for direct comparison of calculated and measured data. For example, when a pan-evaporation station is located in a downwind direction from the weather station of interest, then it may be more adequate to compare it to the closest meteorological station in an upwind direction. It is also noteworthy that, as previously stated, the calculation of PET with models represents one of the most challenging tasks in meteorology, given the diverse range of inputs required. Evaporation is the result of a multitude of interacting effects. It can be posited that the meteorological and environmental influences that result in PET form a complex system that is not amenable to analysis using a single statistical indicator. It is recommended that as many statistical parameters as possible be examined, which is why a complex scoring system was used for the evaluation in this study. If only the R^2 and MPE values were considered, the performance of some PET models in our study would appear to be rather inaccurate. However, the MAE, MBD, and MBE values demonstrated high accuracy even for the worst-performing models in the point system.

Bormann, H. (2011) also studied the efficacy of the four main PET methods on the data obtained from six weather stations of distinctly different climates in Germany. The results demonstrated that models validated for the same climatological and geographical conditions should be selected when determining the appropriate PET model. Moreover, it has been verified that in regions where the effects of climate change and warming are more pronounced, the reliability of PET models is diminished, necessitating their correction.

Seiller, G. and Anctil, F. (2016) also confirmed that the selection of the right PET model is key in the simulated climate scenarios, as PET has a strong impact on each of the simulated global climate change outputs.

The selection of relevant meteorological stations for pan-evaporation stations has also been a pivotal issue in the present study. Although the nearest station might initially appear to be a suitable option, this approach neglects the influence of orographic characteristics, along with microclimatic (e.g.

prevailing wind direction) and microenvironmental (e.g. land use, aspect, and relief) variables. Similarly, the spatial linear interpolation and the Kriging method should be used with caution, as the numerous variables that influence the PET value make it challenging to obtain precise results through these methods.

Conclusions

The quantification of PET represents one of the most challenging problems in hydrometeorology. The majority of the models are only accurate under specific meteorological and microenvironmental conditions and are only valid for relatively small areas. It is, thus, necessary to employ PET models that have been previously validated for the specific geographic and micro- and mesoclimatic conditions. The aim of this study was to select the most appropriate model for Hungary. In order to achieve this, the applicability of 18 PET models in Hungary was investigated. The HungaroMet reference PET is calculated based on Antal, E. (1968) (cited in Antal, E. and Kozmáné Tóth, E. 1980), and it has been used as a reference potential evaporation method. Investigating already known formulae formerly used for the Carpathian Basin was not the goal of the present study. On the other hand, some may argue that omitting the already validated Carpathian Basin-specific models could be seen as a limitation. We also consider that future research should aim to integrate these models into the continuation of the present study.

Our results also demonstrate that models with high input requirements can be replaced by models with lower input requirements under appropriate conditions. This also means that monitoring points where the quality and availability of sensors are limited can be included in the countrywide monitoring network. The PM equation currently used is internationally recognised as a reliable and accurate model, but its input requirements are very high and its calculation is complicated. Most of the standard meteorological variables, such as air temperature, relative humidity, solar radiation, and wind speed, are generally available. However, the FAO Penman–Monteith equation also requires additional parameters (for instance, soil heat flux, surface resistance, psychrometric constant, etc.), which may not be readily obtained at all sites, particularly in complex environments such as forested areas, highlighting the continued relevance of simplified, site-specific PET models. On the other hand, lower-input models remain useful for historical analyses or simplified computations.

The accuracy of the Turc and Oudin model, which has been repeatedly positively evaluated in our study, is similar to that of the PM method, although it only requires daily mean temperature and extraterrestrial radiation as inputs. The measurement of temperature is cost-effective and can be measured at basically any meteorological station, while radiation can be calculated mathematically based on the geographic location of the measurement location. Models that have been calculated to produce accurate overall values may be appropriately parameterised by the application of numerical methods. These methods shall then be adapted to reflect the geographically specific climatic, orographic, and other environmental-meteorological characteristics of the site in which they are to be examined.

The key findings of the study:

– Countrywide, the radiation-based models were the most accurate, but in our ranking, the temperature-based Oudin model has also scored high. This may be due to the inclusion of extraterrestrial radiation as a coefficient in the Oudin equation. Presumably, in the continental climate of Hungary, temperature alone is not a sufficient proxy for the calculation of $PET_{A\text{-}O}$.
– The combination models demonstrated the least effective performance in this study. This does not imply that these models are inherently unsuitable for estimating PET; however, it is evident that they are not consistently applicable for tracking climate dynamics in Hungary, which is not free of extremes.

– The spatial distribution demonstrates that PET models are less effective in the easternmost and westernmost regions of the country. One potential explanation for this phenomenon is the uneven distribution of rainfall across the country. The western and eastern edges of the country exhibit higher mean annual rainfall totals than the central region.
– Our study has demonstrated that, due to its high reliability, the widely used but very high-input PM equation can be replaced by lower-input models (e.g. Oudin, Turc) in input-deficient cases without a notable loss of accuracy in the PET calculation. Pan-evaporation is not always the most appropriate reference because of frequent measurement errors, and it is not necessarily measurable at all periods of the year. The correlation was also more pronounced when comparing the models with PM values calculated by HungaroMet than when comparing with pan-evaporation. Nevertheless, this can be attributed to the fact that, as with the models under examination, PM is also a mathematical method, which evidently exhibits a stronger correlation with other mathematical methods than with a method based on observation and measurement. It is anticipated that this study will provide a valuable basis for the agricultural sector and meteorological research in the quantification of potential evapotranspiration as an indicator of drought risk. It should be emphasized that our results are well applicable in sub-humid continental climates similar to Hungary, during the period April to October.
– The HUNMET reference PET values showed a correlation of 0.87 with the reference evapotranspiration (FAO-PM) when annual sums were considered. In comparison, some empirical models, such as Turc and Stephens–Stewart, yielded higher coefficients of determination (R^2 = 0.94 and 0.96, respectively) at the annual scale. This suggests that certain investigated PET models may provide comparable or even closer agreement with the reference evapotranspiration than the currently applied HUNMET reference PET in terms of annual totals. However, it should be emphasized that long-term analyses were not performed in this study, and the daily structure and variability of PET were not examined in detail. Therefore, it is possible that under specific conditions, the HUNMET approach may perform better at finer temporal resolutions. Consequently, further investigations, particularly focusing on long-term behaviour and daily variability, would be necessary before drawing definitive conclusions regarding the replacement of the current operational method.
– The application and evaluation of different PET calculation methods may become increasingly relevant under changing climatic conditions. Although Hungary currently falls under the Dfa/Dfb climate categories, Beck, H.E. *et al.* (2018) showed that by the end of the century, it is likely to shift toward Cfa/Cfb conditions. Consequently, PET calculations may not be fully applicable at present, but they could gain significance for future climate assessments and become a valuable tool in climatological studies.
– The application of the pan coefficient in the complex evaluation system systematically rearranges the ranking. Radiation- and temperature-based models remain powerful in both cases. When using raw pan-evaporation (PANEVA) data, the OUDIN, TURC, and PRITAY models are the most reliable, while when using K_p-corrected data series (PANEVA_K), the STESTW, OUDIN, and HARBEC models offer greater reliability.

***Acknowledgement*:** We are grateful to László Balatonyi for his help in obtaining the pan-evaporation data.

REFERENCES

Albrecht, F. 1950. Die Methoden zur Bestimmung der Verdunstung der natürlichen Erdoberfläche. *Archiv für Meteorologie, Geophysik und Bioklimatologie, Serie B* 2. (1–2): 1–38. https://doi.org/10.1007/BF02242718
Allen, R.G. and Pruitt, W.O. 1986. Rational use of the FAO Blaney-Criddle formula. *Journal of Irrigation*

and Drainage Engineering 112. (2): 139–155. https://doi.org/10.1061/(ASCE)0733-9437(1986)112:2(139)

Allen, R.G., Pereira, L.S., Raes, D. and Smith, M. 1998. *Crop Evapotranspiration – Guidelines for Computing Crop Water Requirements.* FAO Irrigation and Drainage Paper 56. Rome, FAO.

Anda, A., Nagy, K. Soós, G., Kucserka, T. 2015. Analysing long-term evapotranspiration of Lake Fenéki wetland (Kis-Balaton, Hungary) between 1970 and 2012. *Időjárás / Quarterly Journal of the Hungarian Meteorological Service* 119. 91–109.

Anda, A., Simon, B., Soós, G., Teixeira da Silva, J.A., Kucserka, T. 2016. Effect of submerged, freshwater aquatic macrophytes and littoral sediments on pan evaporation in the Lake Balaton region, Hungary. *Journal of Hydrology* 542. 615–626. https://doi.org/10.1016/j.jhydrol.2016.09.034

Anda, A., Simon, B., Soós, G., Menyhárt, L., Teixeira da Silva, J.A. and Kucserka, T. 2018a. Extending Class A pan evaporation for a shallow lake to simulate the impact of littoral sediment and submerged macrophytes: A case study for Keszthely Bay (Lake Balaton, Hungary). *Agricultural and Forest Meteorology* 250. 277–289. https://doi.org/10.1016/j.agrformet.2018.01.001

Anda, A., Simon, B., Soós, G. and Kucserka. T. 2018b. Estimation of natural water body's evaporation based on Class A pan measurements in comparison to reference evapotranspiration. *Időjárás / Quarterly Journal of the Hungarian Meteorological Service* 122. 41–58. https://doi.org/10.28974/idojaras.2018.1.4

Antal, E. 1968. Új módszer a potenciális evapotranspiráció számítására. Beszámolók az 1967-ben végzett kutatásokról (New method for the calculation of potential evapotranspiration. Reports on research in 1967). Országos Meteorológiai Intézet Hivatalos Kiadványa, 34. 414–423. Budapest, OMI. (Cited in Antal, E. and Kozmáné Tóth, E. 1980.)

Antal, E. and Kozmáné Tóth, E. 1980. Klimatológiai módszer a területi párolgás számítására (Climatological method for the calculation of territorial evaporation). *Időjárás* 84. (2): 55–65.

Baier, W. and Robertson, G.W. 1965. Estimation of latent evaporation from simple weather observations. *Canadian Journal of Plant Science* 45. (3): 276–284. https://doi.org/10.4141/cjps65-051

Beck, H.E., Zimmermann, N.E., McVicar, T.R., Vergopolan, N., Berg, A. and Wood, E.F. 2018. Present and future Köppen-Geiger climate classification maps at 1-km resolution. *Scientific Data* 5. 180214. https://doi.org/10.1038/sdata.2018.214

Bihari, Z., Babolcsai, Gy., Bartholy, J., Ferenczi, Z., Gerhátné Kerényi, J., Haszpra, L., Homokiné Ujváry, K., Kovács, T., Lakatos, M., Németh, Á., Pongrácz, R., Putsay, M., Szabó, P. and Szépszó, G. 2018. Climate. In *National Atlas of Hungary, Vol 2. Natural Environment.* Editor-in-Chief: Kocsis, K., Budapest, MTA CSFK Geographical Institute, 58–69.

Blaney, H.F. and Criddle, W.D. 1950. *Determining Requirements Water in Irrigated Areas from Climatological and Irrigation Data.* USDA Soil Conservation Service Tech Paper 96. Washington D.C., USDA.

Blanka, V., Mezősi, G. and Meyer, B. 2013. Projected changes in the drought hazard in Hungary due to climate change. *Időjárás* 117. 219–237.

Bormann, H. 2011. Sensitivity analysis of 18 different potential evapotranspiration models to observed climatic change at German climate stations. *Climatic Change* 104. (3–4): 729–753. https://doi.org/10.1007/s10584-010-9869-7

Breuer, H. and Ács, F. 2010. Surface resistance estimation of some crops using different climate, soil-, and vegetation-specific data. *Időjárás* 114. (3): 203–215.

Breuer, H., Ács, F. and Skarbit, N. 2017. Climate change in Hungary during the twentieth century according to Feddema. *Theoretical and Applied Climatology* 127. 853–863. https://doi.org/10.1007/s00704-014-1103-5

Brockamp, B. and Wenner, H. 1963. Verdunstungsmessungen auf den Steiner See bei Munster. *Deutsche gewässerkundliche Mitteilungen* 7. 149–154.

Brouwer, C. and Heibloem, M. 1986. *Irrigation Water Management: Irrigation Water Needs*. Rome, FAO.

Douglas, E.M., Jacobs, J.M., Sumner, D.M. and Ray, R.L. 2009. A comparison of models for estimating potential evapotranspiration for Florida land cover types. *Journal of Hydrology* 373. (3–4): 366–376. https://doi.org/10.1016/j.jhydrol.2009.04.029

Hamon, W.R. 1961. Estimating potential evapotranspiration. *Journal of the Hydraulics Division* 87. (3): 107–120. https://doi.org/10.1061/JYCEAJ.0000599

Harbeck, G.E. 1966. Annual variability in lake evaporation. *International Association of Scientific Hydrology Publication* 70. 294–303.

Hargreaves, G.H. 1975. Moisture availability and crop production. *Transactions of the ASAE* 18. (5): 980–984. https://doi.org/10.13031/2013.36722

Jensen, M.E. and Haise, H.R. 1963. Estimating evapotranspiration from solar radiation. *Journal of the Irrigation and Drainage Division* 89. (4): 15–41. https://doi.org/10.1061/JRCEA4.0000287

Jensen, M.E. and Wright, J.L. 1978. The role of evapotranspiration models in irrigation scheduling. *Transactions of the ASAE* 21. (1): 82–87. https://doi.org/10.13031/2013.35254

Kharrufa, N.S. 1985. Simplified equation for evapotranspiration in arid region. *Beiträge zur Hydrologie* 5. (1): 39–47.

Kutta, E. and Hubbart, J.A. 2016. Reconsidering meteorological seasons in a changing climate. *Climatic Change* 137. (3–4): 511–524. https://doi.org/10.1007/s10584-016-1704-3

Lhotka, O., Beštáková, Z. and Kyselý, J. 2023. Prolongation of compound dry-hot seasons over Europe under climate change scenarios. *Earth's Future* 11. (9): 3557. https://doi.org/10.1029/2023EF003557

Li, Z., Li, Y., Yu, X., Jia, G., Chen, P., Zheng, P., Wang, Y. and Ding, B. 2024. Applicability and improvement of different potential evapotranspiration models in different climate zones of China. *Ecological Processes* 13. (1): 1–21. https://doi.org/10.1186/s13717-024-00488-7

Lóczy, D. 2010. Flood hazard in Hungary: A re-assessment. *Central European Journal of Geosciences* 2. 537–547. https://doi.org/10.2478/v10085-010-0029-0

Lu, J., Sun, G., McNulty, S.G. and Amatya, D.M. 2005. A comparison of six potential evapotranspiration methods for regional use in the southeastern United States. *Journal of the American Water Resources Association* 41. (3): 621–633. https://doi.org/10.1111/j.1752-1688.2005.tb03759.x

Mekoya, A. 2021. Comparison of evaporation schemes and methods of estimation of Class A pan coefficient at Tharandt, Germany. *Water Conservation Science and Engineering* 6. (1): 25–35. https://doi.org/10.1007/s41101-020-00099-1

Mezősi, G., Blanka, V., Ladányi, Z., Bata, T., Urdea, P., Frank, A. and Meyer, B.C. 2016. Expected mid- and long-term changes in drought hazard for the South-Eastern Carpathian Basin. *Carpathian Journal of Earth and Environmental Sciences* 11. 355–366.

Milly, P.C.D. and Dunne, K.A. 2016. Potential evapotranspiration and continental drying. *Nature Climate Change* 6. (10): 946–949. https://doi.org/10.1038/nclimate3046

Miś, F. and Tomczyk, A.M. 2025. Spatial and temporal differentiation of the thermal growing season in central and Northern Europe. *Theoretical and Applied Climatology* 156. (2): 137. https://doi.org/10.1007/s00704-025-05382-6

Oudin, L., Michel, C. and Anctil, F. 2005. Which potential evapotranspiration input for a lumped rainfall-runoff model? *Journal of Hydrology* 303. (1–4): 275–289. https://doi.org/10.1016/j.jhydrol.2004.08.025

Penman, H.L. 1948. Natural evaporation from open water, bare soil and grass. *Proceedings of the Royal Society of London. Series A. Mathematical and Physical Sciences* 193. (1032): 120–145. https://doi.org/10.1098/rspa.1948.0037

Pirkhoffer, E., Czigány, Sz. and Geresdi, I. 2009. Impact of rainfall pattern on the occurrence of flash floods in Hungary. *Zeitschrift für Geomorphologie* 53. (2): 139–157. https://doi.org/10.1127/0372-8854/2009/0053S3-0139

Priestley, C.H.B. and Taylor, R.J. 1972. On the assessment of surface heat flux and evaporation using large-scale parameters. *Monthly Weather Review* 100. (2): 81–92. https://doi.org/10.1175/1520-0493(1972)100<0081:OTAOSH>2.3.CO;2

Rijtema, P.E. 1965. *An Analysis of Actual Evapotranspiration*. Agricultural Research Reports 659. Wageningen, NL, Centre for Agricultural Publications and Documentation.

Rohwer, C. 1931. Evaporation from free water surfaces. *Technical Bulletin* 271. 1–96.

Romanenko, V.A. 1961. Computation of the autumn soil moisture using a universal relationship for a large area. *Proceedings of Ukrainian Hydrometeorological Research Institute,* No 3. Kiev, Ukrainian Hydrometeorological Research Institute.

Schendel, U. 1967. *Vegetationswasserverbrauch und -wasserbedarf*. Kiel, PhD Habilitation.

Schmeller, G., Nagy, G., Sarkadi, N., Cséplő, A., Pirkhoffer, E., Geresdi, I., Balogh, R., Ronczyk, L. and Czigány, Sz. 2022. Trends in extreme precipitation events (SW Hungary) based on a high-density monitoring network. *Hungarian Geographical Bulletin* 2009. 71. (3): 231–247. https://doi.org/10.15201/hungeobull.71.3.2

Seiller, G. and Anctil, F. 2016. How do potential evapotranspiration formulas influence hydrological projections? *Hydrological Sciences Journal* 61. (12): 2249–2266. https://doi.org/10.1080/02626667.2015.1100302

Shuttleworth, W.J. 1992. Evaporation. In *Handbook of Hydrology*. Ed.: Maidment, D.R., New York, McGraw Hill, 4.1–4.53.

Singh, V.P. and Xu, C. 1997. Evaluation and generalization of 13 mass-transfer equations for determining free water evaporation. *Hydrological Processes* 11. (3): 311–323. https://doi.org/10.1002/(SICI)1099-1085(19970315)11:3<311::AID-HYP446>3.3.CO;2-P

Stephens, J.C. and Stewart, E.H. 1963. A comparison of procedures for computing evaporation and evapotranspiration. *Publication 62, International Association of Scientific Hydrology, International Union of Geodynamics and Geophysics*. Berkeley, CA, IASH–IUGG, 123–133.

Szabó, A.I., Ács, F. and Breuer, H. 2021. Larger Carpathian region climate according to Köppen, Feddema and the Worldwide Bioclimatic Classification System methods. *International Journal of Climatology* 41. Supplement 1. 2482–2496. https://doi.org/10.1002/joc.6859

Szabó, Sz., Szopos, N.M., Bertalan-Balázs, B., László, E., Milošević, D.D., Conoscenti, C. and Lázár, I. 2019. Geospatial analysis of drought tendencies in the Carpathians as reflected in a 50-year time series. *Hungarian Geographical Bulletin* 68. (3): 269–282. https://doi.org/10.15201/hungeobull.68.3.5

Szelepcsényi, Z., Breuer, H. and Sümegi, P. 2014. The climate of the Carpathian Region in the 20th century based on the original and modified Holdridge life zone system. *Central European Journal of Geosciences* 6. (3): 293–307. https://doi.org/10.2478/s13533-012-0189-5

Toušková, J., Falatkova, K. and and Šípek, V. 2025. Estimating potential and reference evapotranspiration in the Central European region: The challenge of model selection. *Water Resource Management* 39. 5911–5927. https://doi.org/10.1007/s11269-025-04233-3

Thornthwaite, C.W. 1931. The climates of North America: According to a new classification. *Geographical Review* 21. (4): 633–655. https://doi.org/10.2307/209372

Turc, L. 1955. Le bilan d'eau des sols: relations entre les précipitations, l'évaporation et l'écoulement. *Journées de l'hydraulique* 3. (1): 36–44.

Turc, L. 1961. Water requirements assessment of irrigation, potential evapotranspiration: Simplified and updated climatic formula. *Annales Agronomiques* 12. 13–49.

UNCCD, 2022. *Report from Hungary*. United Nations Convention to Combat Desertification. UN publication.

Varga, Gy., Alföldi, L., Gábris, Gy., Horváth, G., Kocsis, K., Lázár, I., Maginecz, J., Szalai, J. and Szalay, M. 2018. Waters. In *National Atlas of Hungary, Vol 2. Natural Environment.* Editor-in-Chief: Kocsis, K., Budapest, MTA CSFK Geographical Institute, 70.

Xu, C.Y. and Singh, V.P. 2002. Cross comparison of empirical equations for calculating potential evapotranspiration with data from Switzerland. *Water Resources Management* 16. 197–219. https://doi.org/10.1023/A:1020282515975

Xu, Z., Liu, S., Li, X., Shi, S., Wang, J., Zhu, Z., Xu, T., Wang, W. and Ma, M. 2013. Intercomparison of surface energy flux measurement systems used during the HiWATER-MUSOEXE. *Journal of Geophysical Research: Atmospheres* 118. (23): 13.140–13.157. https://doi.org/10.1002/2013JD020260

Yang, Y., Chen, R., Han, C. and Liu, Z. 2021. Evaluation of 18 models for calculating potential evapotranspiration in different climatic zones of China. *Agricultural Water Management* 244. 2–19. https://doi.org/10.1016/j.agwat.2020.106545

Zheng, H., Yu, G., Wang, Q., Zhu, X., Yan, J., Wang, H., Shi, P., Zhao, F., Li, Y., Zhao, L., Zhang, J. and Wang,Y. 2017. Assessing the ability of potential evapotranspiration models in capturing dynamics of evaporative demand across various biomes and climatic regimes with ChinaFLUX measurements. *Journal of Hydrology* 551. 70–80. https://doi.org/10.1016/j.jhydrol.2017.05.056

DOI: 10.15201/hungeobull.75.1.3 Hungarian Geographical Bulletin **75** 2026 (1) 53–90.

Specifying organic fertilizer composition in process-based models: overview of available data and sensitivity analysis with Biome-BGCMuSo

Klára POKOVAI[1], Zoltán BARCZA[2,3], Marianna MAGYAR[1], Erzsébet KRISTÓF[2], Nándor ZRINYI[2,4], Vivien PACSKÓ[4,5], Tamás ÁRENDÁS[6], Dóra HIDY[2], Márton DENCSŐ[1], Thomas GRÜNWALD[7], Tünde TAKÁCS[1] and Nándor FODOR[6]

Abstract

Organic fertilizers are widely used around the world, because they support the circular economy, sustainable agriculture, and improved soil quality, as well as carbon sequestration. State-of-the-art, process-based models can simulate the environmental impacts of organic fertilizer use and can address issues like the effect of fertilizer amount and type on crop production, soil fertility, soil organic matter accumulation, nitrate leaching, and greenhouse gas emission. However, the lack of information on the proper attribute settings for fertilizer inputs in the models hampers their application. In this study, the main goal was to support the setting of organic fertilizer attributes for process-based model applications. A comprehensive data collection was performed to gather organic fertilizer attributes that are relevant for the carbon and nitrogen cycle-related simulations. Based on the literature search, representative values are presented that can be instantly used in the models as generalized settings for several farmyard manure and slurry types. We also addressed the question of how fertilizer attribute-setting-related uncertainties propagate to the simulation outputs. We used the Biome-BGCMuSo biogeochemical model for that purpose with a maize monoculture simulation. The results indicate that manure type specific attribute setting is crucial for the nitrogen balance related model variables. For soil nitrous oxide efflux, improper composition settings can severely distort the simulation results. Sensitivity analysis suggested that dry matter content and organic nitrogen content are the two most important manure attributes that modellers must properly adjust. For slurry, the dry matter and ammonium content must be constrained for proper simulation results. The study supports crop and biogeochemical model setup with ready-to-use pragmatic information.

Received October 2025, accepted March 2026.

Keywords: Biome-BGCMuSo, farmyard manure, slurry, parameterization, model uncertainty

Introduction

The field application of animal manure is currently experiencing a revival, as it can support the circular economy and sustainable agriculture, improve soil quality, and promote resource-use efficiency (Verma, G. *et al.* 2012; Wang, Y. *et al.* 2018; Chojnacka, K. *et al.* 2020). Manure application can stimulate soil microbial activity, soil organic mat-

[1] Centre for Agricultural Research HUN-REN, Institute for Soil Sciences, Fehérvári út 132-144., H-1116, Budapest, Hungary. Corresponding author's e-mail: pokovai.klara@atk.hun-ren.hu
[2] ELTE Eötvös Loránd University, Faculty of Science, Department of Meteorology, Pázmány Péter sétány 1/A., H-1117, Budapest, Hungary.
[3] Czech Academy of Sciences, Global Change Research Institute, Bělidla 986/4a., 603 00 Brno, Czech Republic.
[4] ELTE Eötvös Loránd University, Doctoral School of Earth Sciences, Pázmány Péter sétány 1/A., H-1117, Budapest, Hungary.
[5] Lechner Non-profit Ltd., Earth Observation Operations Center, Budafoki út 59., H-1111, Budapest, Hungary.
[6] Centre for Agricultural Research HUN-REN, Agricultural Institute, Brunszvik u. 2., H-2462, Martonvásár, Hungary.
[7] Technische Universität Dresden, Institute of Hydrology and Meteorology, 01737. Tharandt, Germany.

ter (SOM) stabilization, thus, increasing soil organic carbon (SOC) content, potentially mitigating global climate change (Yang, R. *et al.* 2016; Li, H. *et al.* 2017; Menšík, L. *et al.* 2019). Organic manure and slurry are widely used in many regions worldwide (FAO, 2018; FAOSTAT, 2021a). According to FAOSTAT (2021b), the global farmyard manure (FYM) use increased by 35 percent in the past 50 years. Today, around 7.5 Gt FYM is applied worldwide annually, amounting to approximately 800, 27, 13 and 35 Mt carbon, nitrogen, phosphorus and potassium input to soils, respectively (not mentioning additional important micronutrients).

Among other factors, manure composition greatly affects the nutrient release from organic fertilizers, thus, its effect on plant growth and SOM dynamics. The composition of animal manure varies greatly among source materials (Brown, C. 2013). The animal's diet, the use and type of bedding material, manure age, and the technology used for storage are the main factors that affect manure nutrient level (Chastain, J.P. and Camberato, J.J. 2003; Pettygrove, G.S. *et al.* 2009). These factors can vary substantially at local or at larger spatial scales. Some manure composition attributes can be found in incubation studies (e.g. Morvan, T. *et al.* 2006), agronomic reviews (e.g. Webb, J. *et al.* 2013), National Inventory Report (NIR) literature (e.g. Finzi, A. *et al.* 2015), and modelling studies (e.g. Levavasseur, F. *et al.* 2021). However, comprehensive summary of the manure composition attributes is not available from the scientific literature which is a major drawback if proper data is needed for practical applications such as modelling.

Crop models and generic biogeochemical models are widely used to quantify crop yield, net primary production, nutrient requirements, SOC content, and greenhouse gas (GHG) emissions of croplands (Rosenzweig, C. *et al.* 2013; Fodor, N. *et al.* 2014; Hidy, D. *et al.* 2021). These models are driven by environmental data (most of all meteorological data and soil properties), while quantification of management also plays a major role in the simulations (Potter, P. *et al.* 2010; Li, C. *et al.* 2012; Dobor, L. *et al.* 2016; Mohanty, S. *et al.* 2020). Since fertilization greatly affects crop growth and yield, also modulating GHG emission, manure decomposition and nutrient release have to be simulated well.

In biogeochemical models, a wide variety of methods are used to simulate the effects of manure application on plant- and soil-related processes. For example, the grazing module of LPJmL 5.0 uses specific equations to quantify N and C in animal feces and urine. Feces-derived C and N and urine-derived C are added into aboveground litter pools of the model, while urine-derived N is associated with the NH_4 pool (Heinke, J. *et al.* 2023). ORCHIDEE has dedicated modules for manure application (housing, yard, storage), considering important parameters like pH and timing of application, but the manure is not directly coupled with the biomass productivity (Beaudor, M. *et al.* 2023). The JULES model considers manure as a N input, and N cycling is included, but the model does not distinguish between manure and inorganic fertilizers (Wiltshire, A.J. *et al.* 2021; Mathison, C. *et al.* 2023). The AquaCrop model has no dedicated manure modules; it rather models soil fertility stress through user-calibrated coefficients and does not simulate nutrient balances or fertilizer effects directly (Gijsman, A.J. *et al.* 2002; Van Gaelen, H. *et al.* 2015). Manure-DNDC model handles manure with a microbe-mediated decomposition with linear and differential equations, urea hydrolysis, nitrification, denitrification, ammonia volatilization and fermentation modules with several sub-pools to calculate GHG and NH_3 emissions (Zhao, S. *et al.* 2025). Other models also handle manure and slurry applications like DSSAT and others (Zhao, S. *et al.* 2025). Obviously, for proper simulation of net biome production (NBP; see Chapin, F.S. *et al.* [2006] for definition of NBP) and GHG emission, the dry matter (DM), carbon and organic/mineral nitrogen content of manure must be prescribed accurately. This poses a challenge to the research community.

In this study, we present the results of a major data-collection initiative to develop generic manure composition parameters for a wide range of process-based models. Using the Biome-BGCMuSo biogeochemical-crop model (Hidy, D. *et al.* 2016, 2021) we demonstrate the effect of manure type attribute settings on the model results (note that in this study we distinguish between *model parameters* that are adjustable plant and soil characteristic, and *attributes* that are considered as known and have to be set by the user including management timing, amount and type of fertilizer and other human-induced activity; using this convention we call the properties of the manure and slurry as attributes or manure composition settings). Additionally, as the manure composition attributes are always associated with uncertainty, by performing sensitivity analysis, we highlight the manure composition attributes that have a determining role on the simulation for two sites in Hungary with contrasting soil composition parameters.

We aimed to answer the following questions: 1) What is the range of the most important animal manure composition parameters that are available in the literature and in other diverse information sources? 2) Based on the newly constructed, generic manure/slurry attribute setting, what is the effect of the manure/slurry composition settings on the biogeochemical model results? 3) Using the results of the sensitivity analysis, which manure attributes have to be quantified precisely to achieve adequate simulation results? Answering these research questions provides a pragmatic solution for setting the manure-related attributes.

The study fills a major scientific gap, as, to the best knowledge of the authors, no similar study exists that presents such a comprehensive dataset for animal manure composition-related attributes. The presented results provide solutions for the modeller community, independent from the Biome-BGCMuSo model. The results can be used to design targeted laboratory analysis to support modelling and proper estimation of the full GHG balance of the croplands to support country reporting.

Materials and methods

Organic fertilizer attributes

Crop models and process-based biogeochemical models need information (among others) on the C and N input of the simulated ecosystem in order to quantify plant production and the complete C and N cycle of the plant-soil system including SOC content. For the present study, we focus on the Biome-BGCMuSo model that has a large application history, thorough validation, and good documentation (Thornton, P.E. *et al.* 2002; Hidy, D. *et al.* 2012, 2016, 2021). The required parameters for the model's fertilizer input file are the following (Hidy, D. *et al.* 2021): date and depth of the fertilization, DM content of the fertilizer (%), nitrate (NO_3) fraction of DM (%), ammonium (NH_4) fraction of DM (%), organic nitrogen (ON) content of DM (%), organic carbon (OC) content of DM (%), labile (LAB) fraction of the organic carbon content (%) and cellulose (CEL) fraction of the organic carbon content (%). As the focus of this study is the composition of the organic fertilizers, application-related attributes, such as application date, depth, and amount, were not addressed here.

As it is suggested by Chambers, B. *et al.* (2001), to assess the fertilization value of livestock manure, the laboratory analyses should include the determination of DM, total N, P, K, and NH_4-N (crop available N). Additionally, for well-composted FYM, NO_3-N should be measured, and for poultry manure, uric acid-N should also be included. This list of prescribed attributes corresponds well with the list of organic fertilizer specific input data of the Biome-BGCMuSo model, which means that the model is suitable for studying the effect of organic fertilizer attribute setting on the simulated ecosystem. However, some of the above-mentioned attributes were (at least partially) excluded from the study due to two main reasons. First, at the moment, Biome-BGCMuSo does not have a routine for urea-related calculations. Second, only a very limited amount of data was found for the LAB and CEL fractions.

Our literature review, the keywords used, the selection of databases, and inclusion/exclusion criteria followed a predefined protocol *(Figure 1)*. According to previous works (ASAE, 2005; Pain, B. and Menzi, H. 2011), in this study, liquid manure and slurry are not handled separately, as their physical and chemical behaviours (i.e. how they flow and release nitrogen) are similar. Hits from Google Scholar, ScienceDirect and Web of Science were collected and completed with some additional references from the Land Application and Manure Storage and Handling database (ISU, 2025).

In our approach, animal-specific data contain all available data irrespective of the age and gender of the animals. For example, the cattle group contains data of dairy cattle and beef, as well; the pig group contains data of sow, nursery, feeder, and farrow. More detailed analysis of manure content based on the animal sub-groups would be relevant, but is out of scope of the present study. A summary of the compiled manure database can be found in *Table 1*.

We paid particular attention to ensure that data from different sources were comparable. Data relating to wet weight was converted to dry weight, and the units of measurement were standardized.

One-way ANOVA was used to test if there is a significant difference between the composition of the manure and slurry of different animals. This analysis was carried out in R programming language (R Core Team, 2021). Given that the data were compiled from multiple studies with varying methodologies and geographic regions, the assumptions of classical ANOVA may not be fully satisfied. Consequently, p-values were interpreted with caution. To account for the hierarchical structure of the data, the calculated mean and median values are presented as practical benchmarks for crop and/or environmental modelling rather than absolute inferential thresholds.

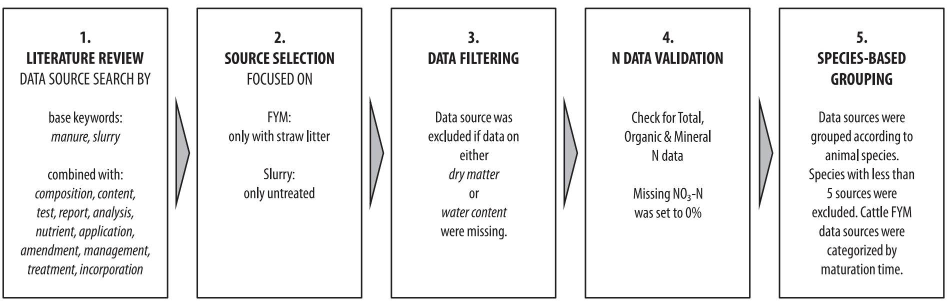

Fig. 1. Summarizing flow chart of the data source search. *Source:* Authors' own elaboration.

*Table 1. The number of FYM- and slurry-related data sources**

Period of publication	Total number of	FYM-related	Slurry-related	Country of origin
	data sources			
1961–1980	5	4	1	Hungary, Russia, USA
1981–2000	7	5	5	Italy, Moldova, UK
2001–2019	25	13	20	Austria, Canada, Chile, Denmark, Hungary, Ireland, Italy, Sweden, Switzerland, UK, USA

*As well as the period in which they were published, and the country from which the data originated.

Biome-BGCMuSo biogeochemical model

Biome-BGCMuSo model was used in this study to quantify the effect of manure type selection and attribute setting on the simulated plant production, GHG balance and soil related variables. Biome-BGCMuSo is a general-purpose biogeochemical model that simulates the storage and fluxes of carbon, nitrogen and water of terrestrial ecosystems (Hidy, D. *et al.* 2012, 2016). It can quantify the full GHG budget of the ecosystem including CO_2 and N_2O fluxes.

Biome-BGCMuSo was developed from the widely used Biome-BGC model (Running, S.W. and Hunt, E.R.J. 1993; Thornton, P.E. 1998; Thornton, P.E. *et al.* 2002; Churkina, G. *et al.* 2009). During the development, the original Biome-BGC was significantly extended and re-formulated in terms of soil processes, possible management options, disturbance effects on plant physiology, and many other processes not addressed in the original model. The major milestones of the model development were the construction of a 10-layer soil submodule with sophisticated soil water balance routine, the layer-by-layer representation of C and N dynamics within the soil, the implementation of detailed nitrification/denitrification routine including separate handling of soil NH_4-N and NO_3-N pools, the implementation of a submodel for soil N_2O and CH_4 emission, the improvement of handling of stomatal response due to soil water stress and increasing atmospheric CO_2 mixing ratio, the separation of soil related and plant related parameters in the input structure, the implementation of the option for phenophase dependent allocation patterns using a maximum of 7 phenophases (including option for varying specific leaf area), and the implementation of root growth dynamics including a nonlinear vertical root distribution function. New, detailed disturbance handler logic was also implemented that supports the simulation of major generic management events such as planting, fertilization, harvest, ploughing, forest thinning, grass mowing and grazing. The current version of Biome-BGCMuSo (v6.1; also some of the earlier versions, like v4.1) is capable of simulating cropland carbon and nitrogen balance with the estimation of the final crop yield. In cropland simulations, the timing, the amount, and the composition of the applied fertilizer are essential input information that is needed for the calculation of the total C and N balance of the ecosystem (Hidy, D. *et al.* 2021, 2022). The performance of Biome-BGCMuSo in simulating soil mineral N and soil N_2O efflux was validated by Hidy, D. *et al.* (2022) using experimental data collected in a fertilization experiment.

The fertilization submodel of Biome-BGCMuSo

In Biome-BGCMuSo, inorganic or organic fertilization affects the litter and soil turnover processes and, thus, directly affects the C and N stocks and fluxes, including SOC accumulation and N mineralization. Inorganic fertilizers directly increase the soil NH_4-N and NO_3-N pools. Organic fertilizers are handled as organic matter input in an alternative way (besides, e.g. litterfall or fine root mortality). The simulation of soil organic and inorganic matter turnover is a complex process in Biome-BGCMuSo v6.1 (Hidy, D. *et al.* 2021). A new feature of this model version is the separation of carbon and nitrogen pools for each soil layer defined in the form of litter and soil organic matter (see *Figure 1*). Biome-BGCMuSo uses the concept proposed by Thomas, R.Q. *et al.* (2013) which assumes that plants have access only to a part of the given inorganic nitrogen pool, and the rest is bounded in the soil aggregates. The plant available NH_4-N and NO_3-N pools are assumed to be 10 and 100 percent of the actual pools, respectively (Gerber, S. *et al.* 2010, and Thomas, R.Q. *et al.* 2013), but the mobile proportion of NH_4 can be set by the modeller.

Application of fertilizers directly interacts with the nitrogen, and in the case of FYM, also with the carbon cycle-related calculations of the model (for details see Hidy, D. *et al*. 2022). Fertilizer input indirectly affects many additional processes due to the model logic that handles the carbon, nitrogen and water cycle jointly. The most important simulated, nitrogen-related processes are N-fixation (N flux from atmosphere to the root zone layers by microorganisms), N-deposition (N input from the atmosphere to the top soil layers by gravitation (dry) and precipitation (wet)), plant uptake (mineral N absorption from the soil layers in the root zone by plants), mineralization (release of plant-available nitrogen from SOM to inorganic nitrogen), immobilization (the consumption of mineralized nitrogen by microorganisms), nitrification (NO_3-production of nitrifying bacteria by biological oxidation of NH_4), denitrification (NO_3-reduction and conversion to nitrogen gas through microbial process), leaching (downward movement of water-soluble mineral nitrogen below the root zone), litterfall (transfer of plant material, including N, from plant reservoir to litter) and decomposition (transfer of litter carbon and nitrogen to soil pools and between soil pools) (see *Figure 1*). Input fluxes of soil organic matter pools are planting (carbon and nitrogen content of seeds), decomposition of litter pools and fertilizing (organic fertilizer). Output fluxes are mineralization and leaching from the lowermost soil layer. Input fluxes of soil inorganic nitrogen (NO_3-N and NH_4-N) pools are N-deposition, N-fixation, fertilizing (inorganic fertilizer), and mineralization. Output fluxes are leaching, immobilization (for NO_3 and NH_4), mineralization (for NO_3 and NH_4), denitrification (for NO_3), nitrification (for NH_4), and plant uptake.

Mass fluxes between different source (arrow head) and target (arrow tip) soil and litter pools are calculated based on the converging cascade scheme (Thornton, P.E. 1998; *Figure 2*). The C/N ratio of the source and target pools is the key factor in the direction of the processes, which determines whether mineralization or immobilization occurs: nitrogen leaves or enters the corresponding litter or SOM pools (Thornton, P.E. 1998).

In case of fertilization, the carbon and nitrogen content of the fertilizer is distributed across the litter pools of the soil layers that fall within the fertilizer depth (which is a model input) (see *Figure 2*).

Using the dry matter content percent, the water content of the fertilizer is also calculated which is added to the water content of affected soil layers (proportionally to thickness of the soil layer). The nitrate, ammonium and organic fractions of the fertilizer are added to the nitrate, ammonium and organic nitrogen and carbon content of litter pools of the model. The amount of C and N originated from the fertilizer is distributed across the different litter (LITTER1, LITTER2, LITTER3, LITTER4 – see *Figure 2*) pools based on the labile and cellulose content required to be set by the User. In this way, the organic part of the fertilizer enters the cascade scheme of the model presented in *Figure 2*. As organic matter increases, the amount of inorganic N also increases through mineralization, which reduces the N stress of the plant. Nutrients (organic C and N, inorganic N) are leached out in parallel with plant uptake and mineralization-immobilization, so the amount of precipitation can significantly influence the availability of nutrients from fertilizer.

Model calibration

The effect of organic fertilizer-related input data (or as we call it here, fertilizer attribute setting) on the model results was studied through maize monoculture simulations performed with the Biome-BGCMuSo model (v6.1). Biome-BGCMuSo maize parameterization was evaluated previously at multiple sites (among others at Klingenberg in Germany, Martonvásár and Kartal in Hungary, Mead and Bushland in the USA, Polkovice and Kresin in the Czech Republic; Hollós, R. *et al.* 2022; Kimball, B.A. *et al.* 2023, 2024; Nand, V. *et al.* 2025). Generally, Biome-BGCMuSo performed well at the sites based on diverse observational data (LAI, ET, GPP, biomass, yield), and it was among the best models in the multimodel intercomparison study performed by Kimball, B.A. *et al.* (2023). The

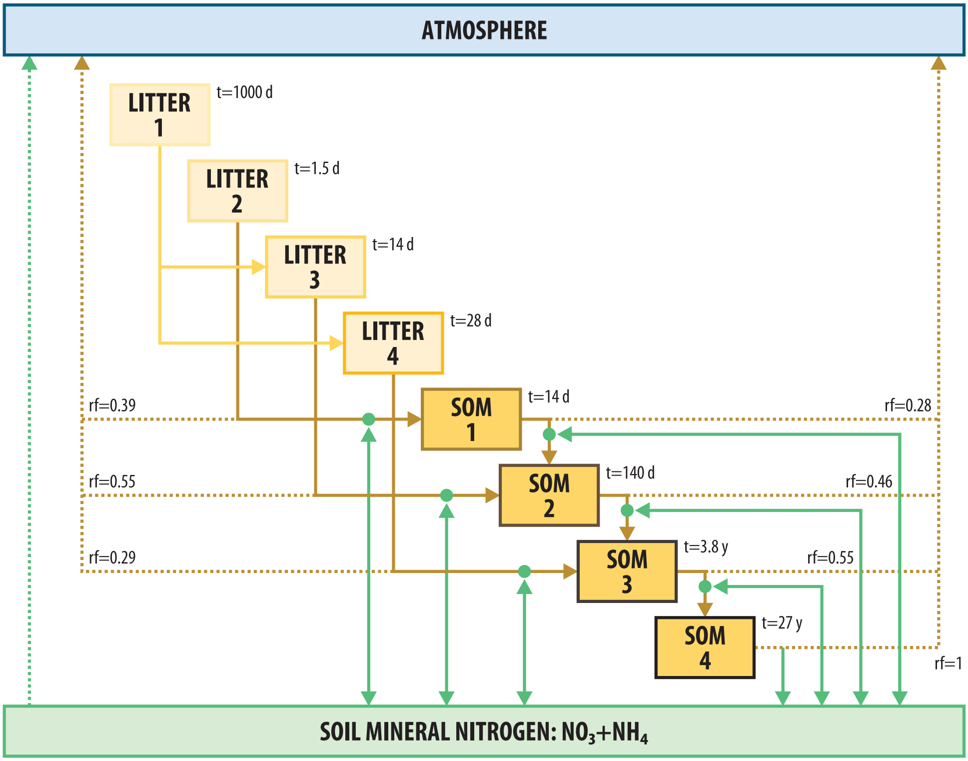

Fig. 2. The converging cascade model of litter and soil organic matter of Biome-BGCMuSo v6.1 model. rf is the respiration fraction of the different transformation fluxes; t is the residence time (reciprocal of the rate constants that is the turnover rate); brown solid arrows show mass fluxes of decomposing organic matter; brown dotted arrows show heterotrophic respiration (CO_2 emission) related to decomposition; solid green arrows show immobilization/mineralization fluxes. The subpools of litter and soil organic matter pools are defined based on their turnover are: coarse woody debris (LITTER1), labile litter (LITTER2), unshielded and shielded cellulose (LITTER3), lignin (LITTER4), labile SOM(1), medium decomposition rate SOM(2), slow decomposition rate SOM(3), passive/recalcitrant SOM(4). The subpools of inorganic (mineralized) nitrogen pool: NO_3 and NH_4. The dotted green arrow represents N loss via denitrification. *Source:* Authors' own elaboration.

maize parameterization that was used in the study is based on Hollós, R. *et al.* (2022, Supplement), where the parameterization was created using the Martonvásár long-term experiments (LTE), which is one target site for the present study.

In Biome-BGCMuSo v6.1, nitrogen cycle-related parameters can be adjusted in the soil file of the model (Hidy, D. *et al.* 2021). Observations were used to adjust the N cycle parameters based on data from one of the LTE with FYM treatments at Martonvásár (Hungary, 47.327° N, 18.789° E). Topsoil NH_4-N and NO_3-N content from 2017 was available for parameter adjustment. Additionally, dynamic chamber-based soil N_2O efflux observations were available from 2020. The N_2O efflux measurements with a gas incubation time of 10 minutes were performed by the Picarro G2508 cavity ring-down spectrometer (Christiansen, J.R. *et al.* 2015; Zhen, M. *et al.* 2021). Five soil parameters were adjusted during the optimization (denitrification rate per gC respiration of SOM, nitrification-related parameters, coefficient of N_2O emission for nitrification and

N_2/N_2O ratio multiplier for denitrification-related N gas flux; see corresponding equations in Del Grosso, S.J. *et al.* (2000), Parton, W.J. *et al.* (2001), and Thomas, R.Q. *et al.* (2013). Owing to the parameter adjustment, the model provided NH_4-N/NO_3-N content and N_2O emission that were consistent with the observations; however, the model somewhat overestimated the topsoil NH_4-N content.

Modelling strategy

Two sites in Hungary with contrasting soil characteristics were selected for model simulations. The Martonvásár experimental site, which is run by the Centre for Agricultural Research, HUN-REN, is located in the Mezőföld region of the Transdanubia macroregion on endocalcic chernozem soil. This region is characterised by intensive agricultural operations and commercial farms. In contrast, the Kiskunhalas site is located in the Danube-Tisza Interfluve plain, which is the second largest sandy region in the EU after the Landes of Gascony in France. This area is characterized mainly by small- to medium-sized farms, and the focus is on the importance of adaptive farming and land protection. The main climatic parameters and topsoil characteristics of these sites are presented in *Table 2*. The water management properties and organic matter content of the soils are important factors in crop production. In this respect, the two selected soil types differ significantly from each other. Soil selection is relevant because approximately 30 percent of Hungary's arable land is chernozem soils, which are characterised by a deep, humus-rich layer, excellent water and air management and a good nutrient supply. In contrast, around 8 percent of the cultivated land consists of light-textured sandy soils with low colloid content, unfavourable water management properties, and low water holding capacity (Tóth, E. *et al*. 2025).

For the presented modelling exercise, the Biome-BGCMuSo model was run from 1961 to 2018 with maize monoculture. The CarpatClim database was used to provide meteorological data for the simulations (Spinoni, J. *et al.* 2015). Soil-specific input data were retrieved from the DOSoReMi database (Pásztor, L. *et al.* 2020). The other settings followed the method from earlier Biome-BGC related studies (Barcza, Z. *et al.* 2010). Simulation results were analysed for the 2001–2010 years. Slurry or FYM were applied at 40 t ha^{-1} on a fresh weight basis in every 3rd year in the simulations. Organic fertilizer was added on 1st of October and was incorporated in 0.15 m depth. The fertilization composition attributes were set based on the results of the data collection. No irrigation was set in the simulations.

Selected model output variables were analysed at daily and annual time scale. Final crop yield and LAI were used to characterize plant production. LAI and yield were assessed in daily and annual time steps, respectively. Daily NEE and topsoil (0–30 cm) SOC were used to represent carbon cycle dynamics. Topsoil available NH_4-N and NO_3-N content, and daily N_2O soil efflux were studied to represent nitrogen cycle dynamics. N_2O flux was selected since it is a strong GHG with high relevance in terms of climate change.

*Table 2. Main climatic and topsoil characteristics of the two selected sites**

Parameters	Martonvásár	Kiskunhalas
Average temperature, °C	11.2	11.5
Average annual precipitation, mm	547	577
Soil bulk density, kg m^{-3}	1340	1390
Soil Organic Matter, %	3.05	0.78
Sand fraction, %	18	89
Clay fraction, %	17	4

* Climate data was derived from the CarpatClim database, while soil data was retrieved from the DOSoReMi database.

Model simulations were performed with the proposed organic fertilizer attribute values that are derived as the median of all collected data per attribute per manure type (*Table 3* and *4*). Model output data was filtered for the growing seasons only. The Wilcoxon rank sum test was performed to check whether the manure attribute setting (manure type selection) had a significant effect on the simulation results. The statistical test compared the medians of the daily data aggregated for the growing season (DOY: 120–243).

*Table 3. Minimum, maximum and median of the cattle, pig and poultry FYM composition values**

Farmyard manure (FYM) composition values		Cattle Fr	Cattle 3mo	Cattle 6mo	Pig	Poultry
DM, %	minimum	17.5	18.4	20.0	19.3	35.0
	maximum	28.0	31.4	39.0	36.0	65.2
	median	21.1	25.0	32.0	25.0	48.4
ON (DM %)	minimum	1.00	1.40	1.32	1.62	1.60
	maximum	2.33	3.28	2.95	3.28	4.20
	median	1.88	2.13	2.04	2.35	2.99
NH_4-N (DM %)	minimum	0.368	0.008	0.009	0.210	0.787
	maximum	0.620	0.652	0.350	1.661	1.800
	median	0.556	0.243	0.155	0.720	1.250
NO_3-N (DM %)	minimum	0	0.08	0.001	0	0
	maximum	0	0.08	0.063	0	0
	median	0	0.08	0.013**	0	0
OC (DM %)	minimum	38.20	31.20	26.00	28.00	21.32
	maximum	40.10	39.36	35.60	37.67	40.54
	median	39.15	36.40	28.50	37.13	36.60

*See more details in *Figure S1* (Supplementary section). **Although very small but non-zero values were also found in the literature, zero values were used and proposed for model parameterization according to Chadwick, D.R. *et al.* (2011).

*Table 4. Minimum, maximum and median of the cattle and pig slurry composition values**

Composition values		Cattle	Pig
DM, %	minimum	3.10	2.27
	maximum	14.80	7.95
	median	6.50	5.00
ON (DM %)	minimum	0.26	0.36
	maximum	4.50	5.54
	median	2.16	2.89
NH_4-N (DM %)	minimum	0.001	0.722
	maximum	3.973	10.310
	median	2.000	5.870
NO_3-N (DM %)	minimum	0	0
	maximum	0.005	0
	median	0	0
OC (DM %)	minimum	31.46	17.93
	maximum	46.30	33.10
	median	37.83	31.96

*See more details in *Figure S2* (Supplementary section). DM % abbreviation means that the parameters are expressed as percent of DM content.

Sensitivity analysis

A sensitivity analysis was performed to pinpoint the important fertilizer-related model input data. We used the so-called least squares linearization (LSL) method (Verbeeck, H. *et al.* 2006) for this purpose. The LSL method is a computationally efficient numerical approximation technique used to estimate variance-based Sobol sensitivity indices (Saltelli, A. *et al.* 2004). Rather than requiring an unfeasibly large number of full model runs, LSL approximates the model's response surface at the Monte Carlo sampling points using multidimensional planes.

The aim of the analysis is to highlight the importance of the fertilizer-related input data uncertainty in terms of output variability. The advantage of the technique against the one-at-a-time approaches is that the LSL method varies all input data simultaneously.

The analysis was carried out in two different ways. First, the attributes were changing within uniform ranges (±10% around the medians). Second, the attributes were allowed to change within the full range defined by the minimum and maximum of the selected manure input data based on the presented literature review (see Results). The first option shows the relative model sensitivity to the selected input data, while the second option shows an overall, effective sensitivity that includes the uncertainty of the input data, represented by the magnitude of the data ranges found in the literature.

In both cases, uniform distribution was assumed within the input attribute intervals because a preliminary analysis indicated that the distribution of the parameters is not Gaussian in many cases, but rather it is closer to a uniform distribution. Fertilization-related input data sensitivity was quantified by the variance observed in the model outputs. The relative sensitivity to every input data (manure parameter) for every investigated model output was scored. If the relative sensitivity was between 0–20, 20–40, 40–60, 60–80 or 80–100 percent, a score of 1, 2, 3, 4, or 5 was given, respectively. The final score, which is a metric of overall model sensitivity to a given manure parameter, was calculated by cumulating the given scores across the model outputs. The mean or the median of the relative sensitivity values could also be used, but these metrics are greatly affected by extreme relative sensitivity values and can suggest disproportionately high or low overall relative sensitivity. The higher the final score, the more important the input data in terms of model result uncertainty. We present the scores in color-coded figures suggested by Olesen, J.E. *et al.* (2011).

The sensitivity analysis was performed separately for all FYM and slurry types addressed in this study. For cattle FYM a categorization was used according to the stabilization time (Fr, 3mo and 6mo old), cf. the data collection method presented above (see subsection *Organic fertilizer attributes*). Note that sensitivity analysis was performed for manure composition attributes with sufficient data availability. For this reason, LAB and CEL fractions were excluded from the analysis, and their values were fixed based on the limited available data (see Results). For each fertilizer type, 10,000 simulations were performed.

Results

Organic fertilizer composition: DM content

Figure S1 (Supplementary section) shows the distribution of DM content values based on the collected data. *Table 3* shows the summary of the data collection, presenting the median, the minimum, and the maximum of all collected data for each manure type. The range of the medians is somewhat broader than that of the means *(Table S1)* (Supplementary section).

Comparison of the DM values per manure type is presented in *Table S1*. The mean DM content values of the five investigated manure groups are significantly different, except for the Fr vs. 3mo group. The ranges (defined by the difference between the maximum and the minimum) of the cattle and pig manure DM content data are similar but differ considerably from the poultry FYM characteristics (*Figure S1*, *Table S1*). The corresponding p-values of the ANOVA tests are presented in *Table S2* (Supplementary section).

Figure S2 (Supplementary section) shows the distribution of DM content values of the collected slurry data. *Table 4* shows the summary for slurry in terms of minimum, maximum, and median of all collected DM data for each slurry type. The average DM content of cattle slurry is significantly higher than that of the pig slurry, and their data ranges are also quite different *(Figure S2)* based on the published studies investigated *(Table S1)*. The corresponding p-values of the ANOVA tests can be found in *Table S2*.

There is additional information in the animal-specific DM contents. According to age, piglets' slurry contained less DM than that of sows (2.27 vs 7.95% – Csaba, L. *et al.* 1978). According to breeding goal, DM content of laying hens manure was less than that of broilers (40.6 vs. 60.3% – Menzi, H. 2002; Webb, J. *et al.* 2010). More detailed analysis of the results is out of scope of the present study.

Organic fertilizer parameters: Nitrogen

Figure S1 shows the distribution of nitrogen-related parameters based on the data collection. The median and mean ON values of cattle FYM (see *Table 3*), and also *Table S3* (Supplementary section) show an increasing tendency because of the maturation process (Levi-Minzi, R. *et al.* 1986). The resulting differences are significant between the fresh and the older FYMs *(Table S2)*. ON content is significantly higher in pig FYM, though only in comparison with the Fr cattle manure. Poultry FYM has the highest ON content, significantly higher than any of the other types *(Table S3)*. Pig slurry ON is significantly higher than cattle slurry ON, although their data ranges are similar *(Figure S2)*.

Considering inorganic N forms, FYM NH_4-N means *(Table S4)* (Supplementary section) differ significantly for any pair of manure groups except for the Fr cattle and pig manure type comparison *(Table S2)*, though even those are significantly different at $p = 0.1$ level. In general, slurry tends to have much higher NH_4-N than manure, which is especially true for pig slurry.

Regarding NO_3-N, there are only scarce data (in fact, only one data source) for Fr and 3mo cattle manures (see *Table 3*), and also *Table S5* (Supplementary section), as NO_3-N is not present in fresh manure unless active mixing is present in the animal house (Chadwick, D.R. *et al.* 2011). The only zero value found in this data source was used as an input parameter for modelling (see *Table 3*). In contrast, the well-composted 6mo cattle FYM has significant NO_3 content. Note that *Table 3* indicates lower maximum for 6mo cattle FYM NO_3-N than for Fr and 3mo but this is compensated by the high number of zero values found in the literature.

Hardly any data has been published for pig and poultry manure as practically no NO_3-N is present in these FYM types *(Table S5)*. Scarce NO_3-N data was found for slurries *(Table S5)*.

Organic fertilizer parameters: Carbon

Synthesis of the collected OC data is presented in *Figure S1* and *Table 3*. According to *Table S6* (Supplementary section) OC data are less available than nutrient content data for manures. According to the statistical analysis presented in *Table S2*, all manure types show significant differences regarding cattle FYM OC. Owing to the low number and the scatter of poultry data, its mean value does not show a significant difference in comparison with other manure types, though, for example, the difference between the means of the Fr and 3mo cattle FYM types is actually smaller than that of the Fr cattle and poultry FYM types.

The average cellulose and lignin data used in this study are calculated from the limited number of references (Chadwick, D.R. *et al.* 2000; Li, Y. *et al.* 2013; Li, K. *et al.* 2015; Rehman, K.U. *et al.* 2017; Li, R. *et al.* 2019; Shen, J. *et al.* 2019). The average cellulose and lignin content for cattle FYM is 44.6 and 29.3 percent, for pig FYM 46.8 and 15.4 percent, for poultry FYM 46.5 and 21.3 percent, for cattle slurry 40.9 and 22.1 percent, and for pig slurry 43.1 and 19.2 percent, respectively. Labile fraction was calculated as a residual based on the above numbers for each organic fertilizer type separately.

Simulations with the proposed parameterization using median values

Figure 3 shows the simulated time series of LAI, final crop yield, NEE, SOC, soil N_2O flux, topsoil NO_3-N and NH_4-N concentration for the 10 simulated years for Martonvásár, based on the proposed FYM parameterizations (see *Table 3*) for 5 different manure

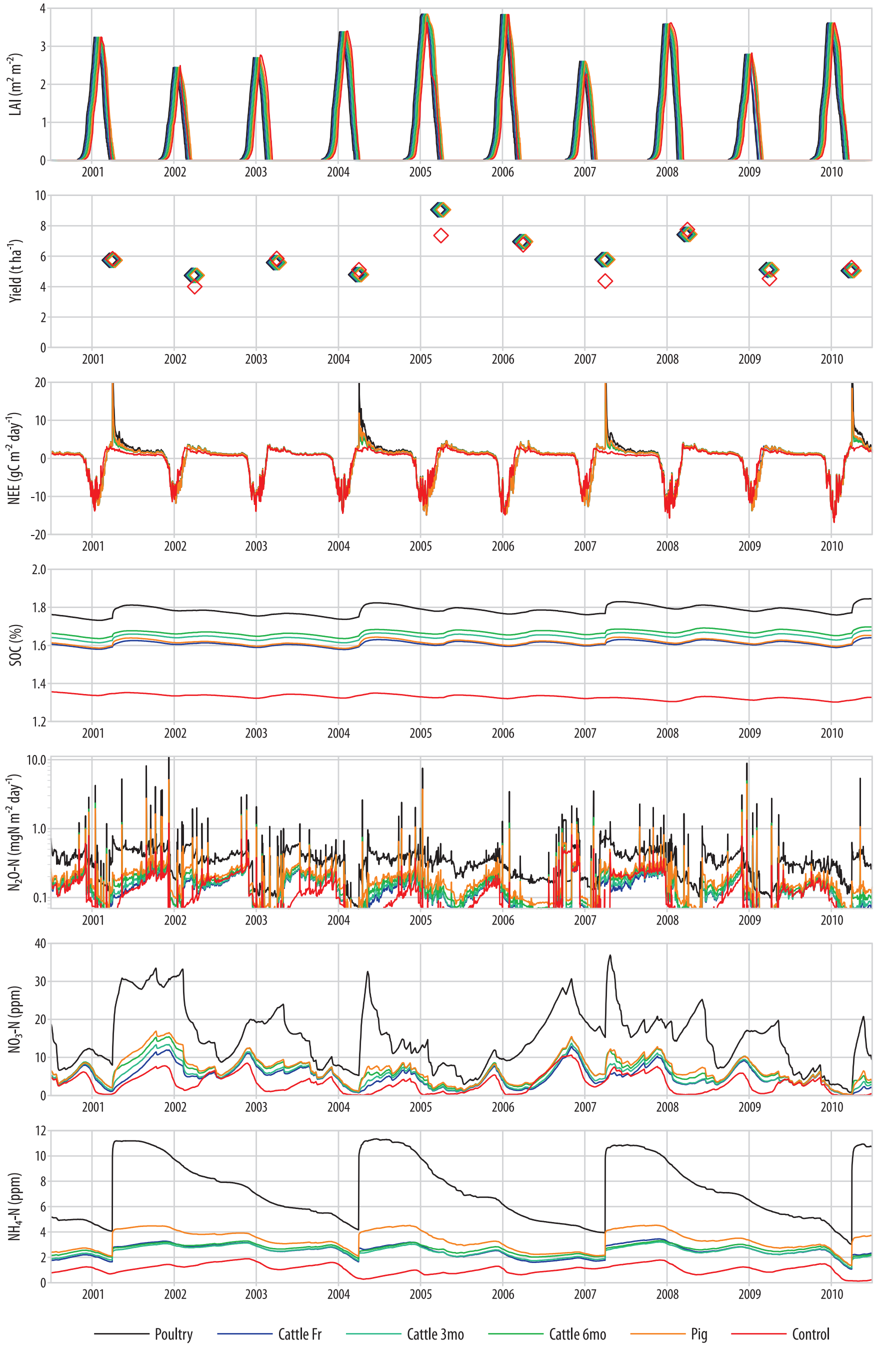

Fig. 3. Biome-BGCMuSo simulation results for Martonvásár using the median parameter values (proposed parameterization; see *Table 2*) for the different FYM types. For N_2O efflux logarithmic scale is used for clarity. Note that in some cases, the lines/symbols overlap. Black, blue, light blue, light green, yellow and red lines represent poultry, cattle Fr, cattle 3mo, cattle 6mo, pig FYM and control treatments, respectively. NO_3-N and NH_4-N refer to the simulated topsoil N content. *Source:* Authors' own elaboration.

types and for the non-fertilized control. The Kiskunhalas simulations show a similar pattern *(Figure S3)* (Supplementary section).

The figures show that manure application affects all simulated quantities to some extent relative to the control. The LAI for the non-fertilized simulation differs from the fertilized LAI dynamics in some (but not all) years. LAI, final crop yield, and NEE time series are very similar for all manure types. In contrast, SOC and soil nitrogen-related variables show considerable dependency on manure type selection. Similar conclusions can be drawn from slurry-related simulations (*Figure S4* and *S5*) (Supplementary section).

The Wilcoxon rank sum test was performed separately for the two study sites, for the two manure types (FYM and slurry), and for the selected output variables individually. We discuss the existence or lack of significant differences in the following subsections for the major output variable groups. Manure type dependent simulations were compared against each other, plus we compared the organic fertilizer driven simulations with the control as well, and searched for significant differences between the time series.

LAI and yield

In the case of LAI, the control simulation significantly differed from the fertilized simulations ($p < 0.001$) for both sites and for both organic fertilizer types (FYM and slurry). Fertilizer type selection caused non-significant differences between the LAI simulations, both for FYM and slurry, which is well demonstrated by the overlap of the LAI curves representing the fertilized simulations in *Figure 3*.

Mean crop yield for the control simulations was 5.7 t ha^{-1} at Martonvásár and 4.4 t ha^{-1} at Kiskunhalas. For the five FYM simulations, the yield was 6 t ha^{-1} for Martonvásár, and 5.4 t ha^{-1} for Kiskunhalas, in accordance with the fact that the soil at Kiskunhalas is less fertile. Slurry driven yields were slightly lower at both sites than that of the FYM driven yields (not shown). In spite of the increase of the final yield, there was no significant difference between the control simulation time series and any of the organic fertilizer driven simulations. The exception is the five FYM simulations at Kiskunhalas where the control simulation was different from all of the FYM related simulations, but the differences were significant only at the $p = 0.1$ level. No significant differences were found between the yield simulations made with the different organic fertilizer types for both the Martonvásár and the Kiskunhalas site.

NEE and SOC

Simulation results indicated that NEE is not affected significantly by the FYM/slurry type selection either at Martonvásár or at Kiskunhalas. One exception is the pig slurry-related simulation that differs from the control at Kiskunhalas, but the difference is significant only at $p = 0.1$ level. The control simulation did not differ significantly from the organic fertilizer-driven ones, considering all possible combinations at both sites.

In contrast, SOC was found to be affected by the choice of the organic fertilizer type (and the associated parameterization) at both sites (see *Figure 3*). All differences (control vs. FYM, control vs. slurry, and also FYM vs. another FYM, slurry vs. the other slurry) were significant ($p = 0.001$).

Nitrogen balance

Considering NH_4-N and NO_3-N content in the topsoil and soil N_2O efflux, almost all simulation results differed significantly, at both sites and for both organic fertilizer types ($p = 0.001$). For NO_3, 6mo cattle and pig FYM-related simulations did not differ significantly at Martonvásár. For NH_4-N and N_2O-N emission, Fr and 3mo cattle FYM driven simulations did not differ significantly at both sites; however, in the case of N_2O flux, they differed significantly at $p = 0.1$ for the Kiskunhalas site.

Given the importance of soil N_2O efflux in the global warming context, the related simulation results were further analysed. The long-term mean daily N_2O flux is 1.2-3.4 times larger in the fertilized simulations at Martonvásár, and 1.9-9.5 times larger at Kiskunhalas relative to the control (the high end was obtained with poultry FYM).

Results of the sensitivity analysis

The presentation of the results of the LSL-based sensitivity analysis follows the same logic as in previous subsection (*Simulations with the proposed parameterization using median values*). Namely, the output variables are grouped, and the importance of the organic fertilizer parameters is discussed for the target sites together. The results are expressed as a contribution to the overall variability of the selected output variable (in %), and scores are associated with the sensitivity values for a more generalized view. In the following subsections, output variable specific assessment of the effective sensitivity was in focus (relative model sensitivity is also presented but not discussed in detail).

Yield and LAI

Tables S7–S10 (Supplementary section) show the detailed results of the sensitivity analysis for the simulated LAI and final yield for both demonstration sites and for all fertilizer types. OC has an insignificant effect on the plant growth-related output variance for most of the manure types. The same holds for NH_4-N, but only for FYM types. For the investigated slurry types, especially when the full range of the input parameter variance was taken into account, NH_4-N may account for up to 58.2 percent of the variance of the growth-related outputs. ON is an important parameter in the case of cattle FYMs, especially on the chernozem soil. For slurry types, ON has a very low share in determining the output variance. DM is the most determinative FYM parameter in terms of output uncertainty only for the sandy soil. For the chernozem soil, ON was found to be the main source of output uncertainty except for poultry FYM. The comparison of the results for pig and poultry FYMs *(Table S7)* shows that the model is sensitive to the DM parameter when considering LAI and yield results, but the effective sensitivity is very different for the two FYM types. It is likely because the mean and standard deviation of DM of poultry FYM are almost two and three times larger than those of pig FYM, respectively.

If the contributions are averaged for both sites and for both output variables, DM content is found to be the most relevant for FYMs (with 49.1% overall contribution), followed by ON (35.4%) and NH_4-N (10.3%). For slurries, NH_4-N is the main source of output variability (45.8%), followed by DM (36.9%) and ON (17.3%).

NEE and SOC

According to *Tables S7–S10* NH_4-N has an insignificant effect on the carbon balance-related output variance in the case of FYM types. For slurries, NH_4-N has a more significant contribution to the output variability, but only in the case of NEE. SOC seems to be insensitive to the manure NH_4 content. ON has an insignificant effect on the output variance with only one exception. For fresh cattle FYM, only for the chernozem soil and only for the NEE output ON accounts for almost 95 percent of the variability. With the exception of poultry FYM, manure OC is not responsible for the large variability in carbon-related outputs. For poultry FYM, the wide range of the literature-based OC values looks to be the main reason for its importance, causing large variability when considering NEE and SOC outputs. Regarding SOC the DM content has a prominent role which is reasonable given that soil C input is determined by the DM content of the manure. Regarding NEE, for slurries and for fresh cattle FYM, this determinative role is not so pronounced. The contribution of DM to output variability varies between 1.4 and 21.2 percent. The sandy soil is an extreme exception here, showing 93.4 percent contribution.

If the contributions are averaged for both sites and for all output variables, DM content is found to be the most relevant for FYMs (with 67.9% overall contribution), which is followed by OC (21.1%) and ON (10.0%). For slurries DM and NH_4-N content is equally important (with 41.4 and 41.2% overall contribution) followed by ON (15.7%).

Nitrogen balance

Tables S7–S10 show the detailed results of the sensitivity analysis for the simulated soil N_2O emission, and topsoil NO_3 and NH_4 contents for both demonstration sites and for all fertilizer types. The uncertainty of the OC input parameter has practically zero effect on the nitrogen balance-related outputs, irrespective of the fertilizer type and the soil type. It is consistent with the fact that OC ranges are relatively smaller than those of the ON and NH_4-N ranges. DM is the second most important input parameter determining the variance of the outputs, showing the minimum and maximum relative contribution for 3mo cattle FYM and poultry FYM, respectively. For slurries, pig and poultry FYMs ON has a relatively low contribution to the output variability, while for cattle FYMs the contribution is large, varying between 32 and 74 percent. Practically the opposite can be stated for NH_4-N as it is marginally determinative in case of cattle FYMs but very important for slurries and pig FYM. In terms of the soil types, no sharp differences were found in the contribution characteristics.

If the contributions are averaged for the two sites and for the three output variables, ON content is found to be the most relevant for FYMs (41.8% overall contribution), which is followed by DM (35.5%) and NH_4-N (22.6%). For slurries, NH_4-N content contributes the most to the output variance (45.2%) followed by DM (41.1%) and ON (13.7%).

Overall scores

In *Table 5*, the relative contribution of the investigated input attributes to the variance of the selected outputs is presented, averaged for the fertilizer types and for the two sites. Here, we discuss relative and effective sensitivity together. Both for FYM and slurry, DM content is the parameter the model is most sensitive to (*Table 5*; SCORE2). If we consider the effective sensitivity, when the literature-based uncertainty of the input parameters is taken into account, FYM DM is still the most determinative. However, for slurry, NH_4-N content seems to be the most important input (see *Table 5*) due to the one order of magnitude larger range of NH_4-N values found in the literature (*Figure S2*). The effective sensitivity to the nitrogen-related inputs is usually larger than the corresponding model sensitivity caused by the fact that the minimum values for these input parameters are close to zero for many manure types. Consequently, effective sensitivity to DM and OC is usually smaller than the corresponding model sensitivity.

Discussion

Organic fertilizer composition

Animal manure is traditionally considered to be a mixture of faeces and urine. It contains DM, such as several nutrients, plant residues, indigestible food, and other wastes. DM is comprised of ash and organic matter. During composting, ash content remains the same, while organic matter is decreasing due to decomposition and stabilization processes. DM loss could be up to 40 percent of the initial content (Eghball, B. *et al.* 1997; Tiquia, S.M. *et al.* 2002). At the same time, water content also decreases until the end of the composting, thus, the DM content of the mature manure could be higher than that of the fresh one (Tiquia, S.M. *et al.* 1998). Results of the comprehensive data collection presented in this study indicate that during the maturation process, the DM content increases, which is consistent with the expectations (see *Table 3*).

Nitrogen is present in manures in different forms. Our results indicated that glob-

*Table 5. Relative contribution of the investigated input parameters (in columns) to the variance of the selected outputs (in rows) and the SCORE for each input showing their overall importance in terms of output uncertainty**

FYM full range					FYM ±10% range				
Parameter	DM	NH_4-N	ON	OC	Parameter	DM	NH_4-N	ON	OC
LAI	45.7	10.8	38.8	4.7	LAI	62.0	2.9	20.3	14.9
YIELD	52.5	9.6	32.1	5.9	YIELD	62.7	2.9	19.3	15.1
NEE	58.9	1.6	16.5	23.1	NEE	41.8	0.5	5.8	51.9
SOC	77.0	0.4	3.5	19.1	SOC	55.9	0.1	1.0	43.0
N_2O	34.6	24.1	41.2	0.2	N_2O	57.8	8.4	32.9	0.9
SNO_3	35.7	12.2	51.9	0.1	SNO_3	54.5	4.1	40.5	0.9
SNH_4	36.2	31.6	32.2	0.0	SNH_4	63.6	11.0	25.3	0.3
SCORE1	*19*	*9*	*14*	*8*	*SCORE2*	*24*	*7*	*12*	*11*

Slurry full range					Slurry ±10% range				
Parameter	DM	NH_4-N	ON	OC	Parameter	DM	NH_4-N	ON	OC
LAI	35.3	47.4	17.3	0.0	LAI	61.7	25.4	12.1	1.0
YIELD	38.5	44.2	17.2	0.2	YIELD	51.7	24.5	10.4	13.5
NEE	16.4	59.6	22.7	1.3	NEE	30.7	25.7	12.1	31.4
SOC	66.4	22.8	8.7	2.2	SOC	72.1	7.2	5.6	15.1
N_2O	40.8	46.7	12.6	0.0	N_2O	59.5	29.5	10.7	0.3
SNO_3	44.3	36.8	19.0	0.0	SNO_3	63.1	23.7	13.2	0.1
SNH_4	38.4	52.3	9.4	0.0	SNH_4	60.3	31.7	7.6	0.3
SCORE1	*17*	*19*	*8*	*7*	*SCORE2*	*24*	*13*	*7*	*8*

*DM, NH_4-N, ON and OC denote the DM, NH_4, organic nitrogen and organic carbon content of the fertilizer, respectively. LAI, YIELD, NEE, SOC, N_2O, SNO_3 and SNH_4 denote the simulated leaf area index, final yield, net ecosystem exchange, SOC content, soil N_2O emission, and topsoil NO_3 and NH_4 content, respectively.

ally, the most abundant mineral N pool in manures is NH_4. NO_3 content is very low and can be considered to be virtually zero for all studied organic fertilizer types (see *Tables 3* and *4*). Our results might support simple estimations for practical considerations. If missing, total N can be estimated from the presented DM content, and NH_4-N can be approximated from total N content.

As OC is not considered as a nutrient, its measurement is not included in a typical routine laboratory analysis of manures. Consequently, there is much less information available on carbon content than on nitrogen content. It should be mentioned that carbon is present in proteins, fatty acids, lipids, carbohydrates, cellulose, and lignin, but the detailed investigation of the fractions of these components is beyond the scope of the study. The maturity process is responsible for the significant decrease of OC that can be observed in the presented cattle FYM data (Levi-Minzi, R. *et al.* 1986). The total C content can be estimated from the organic matter content (Navarro, A.F. *et al.* 1993; Hao, X. *et al.* 2004; Larney, F.J. *et al.* 2004). According to the literature, the mean OM/TC ratio for pig slurries is 1.83 (Hao, X. *et al.* 2004), and in the case of organic wastes, including livestock manure, it is 1.94 (1.71–2.19) (Navarro, A.F. *et al.* 1993). For beef FYM it is 1.917 (1.51–2.60) according to Larney, F.J. *et al.* (2004).

Fractions of hemicelluloses, cellulose and lignin in organic carbon are important parameters of the carbon cycle and required during the Biome-BGCMuSo model simulations. The manure carbon fractions depend on the type of animal and its feeding, but some useful ranges are available in the literature, providing an overview (FAO, 1987). Besides, our mean values provide guidance for practical applications.

Proposed parameterization for manure composition

Application of the proposed, median-based organic fertilizer attribute setting is a relevant next step considering the practical use of our results. Biome-BGCMuSo provided insight into the effect of the end-users' input data choice on the simulated variables of interest. The results indicated that for LAI and final crop yield, organic fertilizer type selection and its related input data setting are not relevant. In contrast, manure type selection (in terms of the proposed parameterization of FYM and slurry) has a major role in SOC dynamics simulation. This finding is relevant if the long-term SOC dynamics are the focus of the study. The results highlighted that nitrogen balance-related simulation results are substantially affected by the selected manure attribute setting. This indicates that setting the proper input values is essential in the N_2O efflux estimations in any kind of organic fertilizer management.

Previous multi-model intercomparison studies found that model calibration might result in biased internal model parameter estimation (Martre, P. *et al.* 2015) with acceptable relevant output variables (like final yield or NPP). Our study is a major step forward in the sense that it also focuses on the internal model parameters (NH_4-N and NO_3-N in the topsoil) that are useful if the model is supposed to be parameterized properly.

Sensitivity analysis

Sensitivity analysis might support the selection of relevant input values, leaving the other attributes at their default value. This kind of logic simplifies the simulation procedure if the results have a general message. The study used the Biome-BGCMuSo biogeochemical model, which was first parameterized at one of the target sites (Martonvásár) with data from treatments including FYM application. As all biogeochemical models are associated with parameter and input data uncertainty, possible interactions can be present. One limitation of the study is the static parameterization of the soil module that affects the organic fertilizer utilization. Nevertheless, as we kept the decomposition and nitrification/denitrification, etc. parameters constant, and also as the model provided feasible results during the optimization, the results indicate the effect of the manure application. Interactions between calibration uncertainty and fertilizer attribute uncertainty are inevitable, which means that further studies might be needed to address this issue.

The presented results highlighted the determinant role of DM and ON in the FYM-related simulations when production-related output variables were considered. Sensitivity to DM and ON settings is consistent with our knowledge about the long-term, slow mineralization of organic manure after field application (Archontoulis, S.V. *et al.* 2014; Wang, Y. *et al.* 2018). For some organic fertilizer types (e.g. pig slurry), the proper setting of NH_4 content is also crucial for reliable simulations.

The results indicate that soil type and selection of simulation output variable strongly determine the set of most important organic fertilizer attribute settings. The fertilizer type can also have a strong effect on the rank of input data sensitivity, so no general pattern can be highlighted.

Due to the lack of obvious and simplified findings, our recommendation is that the modellers should perform a preliminary analysis for their model, for the selected manure type, which can be easily done following the presented method. The results of the modelling exercise are expected to support the selection of the input values (organic fertilizer attributes) that require accurate adjustment. If a given attribute has a major influence on the overall variability of a selected output variable, then the end-user is supposed to focus on the proper setting of the attribute, based on locally available data, information from experts, or based on targeted laboratory analysis.

Scope of validity of the results

The results are restricted to two sites representing two different soil types and similar climatic conditions, and to the Biome-BGCMuSo biogeochemical model. Within the European Union, 3.6 percent of soils are classified as sandy soils (arenosols), whereas only 2 percent are classified as chernozems (Tóth, G. *et al*. 2008). These soil types are uncommon in western European regions but are characteristic of Central Europe. (FAO, 2022). According to Tóth, G. *et al*. (2020), Hungary is situated in the Carpathian Basin and belongs to the southern subcontinental pedoclimatic zone. Therefore, our findings regarding C and N cycling and GHG emissions on arenosols and chernozems can only be extended to similar regions in Europe, which occupy an estimated total area of 12 million hectares. Nevertheless, as the model can be considered as a typical, process-based model, and as the results are consistent with our general knowledge about the functioning of the plant-soil system, the findings might be generalized to other sites and models as well.

The current version of Biome-BGCMuSo does not have the capacity to simulate the effect of dry matter (e.g., crop residue) on infiltration. Since both simulated soils have a high infiltration capacity, no runoff was observed in the simulation results. Therefore, considering the positive effect of accumulated surface biomass on infiltration would not significantly alter the results.

Conclusions

Manure storage and management is a major emission source of GHGs, mostly in the form of CH_4 and N_2O (Amon, B. *et al.* 2006; Kupper, T. *et al.* 2020). There is a large literature focusing on the quantification of GHG emission of manure and slurry storage, but relatively few studies address the GHG emission-related consequences of field application of organic fertilizers (e.g. Sommer, S.G. and Olesen, J.E. 1991).

In this study, we focused on the synthesis and direct application of available organic fertilizer composition data that supports the usage of crop models simulating the effects of FYM and slurry application. The results can support improved estimation of crop production and GHG balance of agro-ecosystems based on process-oriented models.

We addressed the question of whether generic manure-related input data settings per manure type are expected to affect the simulation results significantly. The results suggest that the manure type choice matters mostly for the internal model parameters (e.g. topsoil NO_3 content, SOC), thus, no single generic FYM or slurry input data set can be constructed. We also highlighted that N_2O emission is largely affected by the manure type selection, which is relevant in the estimation of the GHG balance of croplands. Mitigation-related model simulations have to be careful in the manure attribute setting in order to avoid biased estimations.

The results of the sensitivity analysis highlighted that site conditions, manure type, and selection of simulated output variables jointly affect the most important organic fertilizer attribute that needs to be constrained for a proper modelling exercise. In any case, careful estimation of the most relevant fertilizer attributes is always recommended (most of all DM and ON for FYM; DM and NH_4-N for slurry). Given the large variability of some of the organic fertilizer composition values, this task might be challenging.

Probably the most important added value of the study is the comprehensive, quantitative summary of available data on the manure-related C and N attributes. The presented results are unique to the knowledge of the authors, since no similar synthesis study is available in the literature that is easily accessible and that can be directly used by the modelling community for adjusting the organic fertilizer-related inputs. In other biogeochemical models or crop models, different input requirements can be present. For that purpose, some additional calculations can be done (e.g. if organic N content is expected to be provided relative to total manure weight), but this can be easily accomplished using the presented tables. The complete dataset is available from the lead author upon request.

***Acknowledgements*:** This work has been supported by the National Multidisciplinary Laboratory for Climate Change (RRF-2.3.1-21-2022-00014) project within the framework of Hungary's National Recovery and Resilience Plan supported by the Recovery and Resilience Facility of the European Union; by the "Advanced methods of greenhouse gases emission reduction and sequestration in agriculture and forest landscape for climate change mitigation" (CZ.02.01.01/00/22_008/0004635) project; and also by the PlantAId (150795 NKKP-ADVANCED_24) project, financed by the National Research, Development and Innovation Office, Hungary. Also supported by the French-Hungarian bilateral partnership through the BALATON (No 44703TF)/TéT (2019-2.1.11-TÉT-2019-00031) program.

REFERENCES

Amon, B., Kryvoruchko, V., Amon, T. and Zechmeister-Boltenstern, S. 2006. Methane, nitrous oxide and ammonia emissions during storage and after application of dairy cattle slurry and influence of slurry treatment. *Agriculture, Ecosystems & Environment* 112. (2–3): 153–162. https://doi.org/10.1016/j.agee.2005.08.030

Archontoulis, S.V., Miguez, F.E. and Moore, K.J. 2014. Evaluating APSIM maize, soil water, soil nitrogen, manure, and soil temperature modules in the Midwestern United States. *Agronomy Journal* 106. 1025–1040. https://doi.org/10.2134/agronj2013.0421

ASAE 2005. *ASAE D384.2 MAR2005: Manure Production and Characteristics*. St. Joseph, MI, American Society of Agricultural Engineers.

Barcza, Z., Bondeau, A., Churkina, G., Ciais, Ph., Czóbel, Sz., Gelybó, Gy., Grosz, B., Haszpra, L., Hidy, D., Horváth, L., Machon, A., Pásztor, L., Somogyi, Z. and van Oost, K. 2010. Modelling of biosphere-atmosphere exchange of greenhouse gases – Model based biospheric greenhouse gas balance of Hungary. In *Atmospheric Greenhouse Gases: The Hungarian Perspective.* Ed.: Haszpra, L., Dordrecht–Heidelberg–London–New York, Springer, 295–330. https://doi.org/10.1007/978-90-481-9950-1

Beaudor, M., Vuichard, N., Lathière, J., Evangeliou, N., van Damme, M., Clarisse, L. and Hauglustaine, D. 2023. Global agricultural ammonia emissions simulated with the ORCHIDEE land surface model. *Geoscientific Model Development* 16. (3): 1053–1081. https://doi.org/10.5194/gmd-16-1053-2023

Brown, C. 2013. *Available Nutrients and Value for Manure from Various Livestock Types.* Guelph, ON, Canada, Ministry of Agriculture, Food and Rural Affairs. https://files.ontario.ca/omafra-available-nutrients-and-value-for-manure-from-various-livestock-types-21-077-en-2022-11-24.pdf (accessed 26 September 2025).

Chadwick, D.R., John, F., Pain, B.F., Chambers, B. and Williams, J.R. 2000. Plant uptake of nitrogen from the organic nitrogen fraction of animal manures: a laboratory experiment. *The Journal of Agricultural Science* 134. 159–168. https://doi.org/10.1017/S0021859699007510

Chadwick, D.R., Sommer, S., Thorman, R., Fangueiro, D., Cardenas, L., Amon, B. and Misselbrook, T.H. 2011. Manure management: Implications for greenhouse gas emissions. *Animal Feed Science and Technology* 166–167. 514–531. https://doi.org/10.1016/j.anifeedsci.2011.04.036

Chambers, B., Nicholson, N., Smith, K., Pain, B., Cumby, T. and Scotford, I. 2001. *Managing Livestock Manures Booklet 1. Making Better Use of Manures on Arable Land.* 2nd Edition. Mansfield, UK, ADAS Gleadthorpe Research Centre. https://www.triedandtested.org.uk/media/nwsmt3he/managing-livestock-manures-1-making-better-use-of-livestock-manures-on-arable-land.pdf

Chapin, F.S., Woodwell, G.M., Randerson, J.T., Rastetter, E.B., Lovett, G.M., Baldocchi, D.D., Clark, D.A., Harmon, M.E., Schimel, D.S., Valentini, R., Wirth, C., Aber, J.D., Cole, J.J., Goulden, M.L., Harden, J.W., Heimann, M.R., Howarth, W., Matson, P.A., McGuire, A.D., Melillo, J.M., Mooney, H.A., Neff, J.C., Houghton, R.A., Pace, M.L., Ryan, M.G., Running, S.W., Sala, O.E., Schlesinger, W.H. and Schulze, E.D. 2006. Reconciling carbon-cycle concepts, terminology, and methods. *Ecosystems* 9. 1041–1050. https://doi.org/10.1007/s10021-005-0105-7

Chastain, J.P. and Camberato, J.J. 2003. Dairy manure production and nutrient content. In *Confined Animal Manure Managers Certification Program Dairy Training Manual.* Clemson, SC, US, Clemson University Cooperative Extension Service, Chapter 3a, 1–16. https://www.clemson.edu/extension/camm/manuals/dairy/dch3a_04.pdf

Chojnacka, K., Moustakas, K. and Witek-Krowiak, A. 2020. Bio-based fertilizers: A practical approach towards circular economy. *Bioresource Technology*

295. January, 122223. https://doi.org/10.1016/j.biortech.2019.122223

Christiansen, J.R., Outhwaite, J. and Smukler, S.M. 2015. Comparison of CO_2, CH_4 and N_2O soil-atmosphere exchange measured in static chambers with cavity ring-down spectroscopy and gas chromatography. *Agricultural and Forest Meteorology* 211–212. 48–57. https://doi.org/10.1016/j.agrformet.2015.06.004

Churkina, G., Brovkin, V., von Bloh, W., Trusilova, K., Jung, M. and Dentener, F. 2009. Synergy of rising nitrogen depositions and atmospheric CO_2 on land carbon uptake moderately offsets global warming. *Global Biogeochemical Cycles* 23. GB4027. https://doi.org/10.1029/2008GB003291

Csaba, L., Kiss, O., Szinay, M. and Vermes, L. 1978. *Hígtrágya-hasznosítás* (Slurry utilization). Budapest, Hungary, Mezőgazdasági Kiadó.

Del Grosso, S.J., Parton, W.J., Mosier, A.R., Ojima, D.S., Kulmala, A.E. and Phongpan, S. 2000. General model for N_2O and N_2 gas emissions from soils due to denitrification, *Global Biogeochemical Cycles* 14. 1045–1060. https://doi.org/10.1029/1999GB001225

Dobor, L., Barcza, Z., Hlásny, T., Árendás, T., Spitkó, T. and Fodor, N. 2016. Crop planting date matters: Estimation methods and effect on future yields. *Agricultural and Forest Meteorology* 223. 103–115. https://doi.org/10.1016/j.agrformet.2016.03.023

Eghball, B., Power, J.F., Gilley, J.E. and Doran, J.W. 1997. Nutrient, carbon, and mass loss during composting of beef cattle feedlot manure. *Journal of Environmental Quality* 26. 189–192. https://doi.org/10.2134/jeq1997.00472425002600010027x

FAO, 1987. *Soil Management: Compost Production and Use in Tropical and Subtropical Environments. Soils Bulletin 56.* Rome, Italy, FAO. https://www.fao.org/4/s8930e/s8930e.pdf (accessed 26 September 2025).

FAO, 2018. *Nitrogen Inputs to Agricultural Soils from Livestock Manure. New Statistics. Integrated Crop Management 24.* Rome, Italy, FAO. https://www.fao.org/4/s8930e/s8930e.pdf (accessed 26 September 2025).

FAO, 2022. *Global Map of Black Soils*. Rome, Italy, FAO. https://doi.org/10.4060/cc3124en

FAOSTAT, 2021a. *Manure Applied to Soils (N content), World* + (Total). http://www.fao.org/faostat/en/#data/EMN/visualize (accessed 12 Feb 2021).

FAOSTAT, 2021b. *Manure Applied to Soils (N content) by All Animals* + (Total). http://www.fao.org/faostat/en/#data/EMN/visualize (accessed 12 Feb 2021).

Finzi, A., Oberti, R., Negri, A.S., Perazzolo, F., Cocolo, G., Tambone, F., Cabassi, G. and Provolo, G. 2015. Effects of measurement technique and sample preparation on NIR spectroscopy analysis of livestock slurry and digestates. *Biosystems Engineering* 134. 42–54. https://doi.org/10.1016/j.biosystemseng.2015.03.015

Fodor, N., Pásztor, L. and Németh, T. 2014. Coupling the 4M crop model with national geo-databases for assessing the effects of climate change. *International Journal of Digital Earth* 7. 391–410. https://doi.org/10.1080/17538947.2012.689998

Gerber, S., Hedin, L.O., Oppenheimer, M., Pacala, S.W. and Shevliakova, E. 2010. Nitrogen cycling and feedbacks in a global dynamic land model. *Global Biogeochemical Cycles* 24. (1): GB1001. https://doi.org/10.1029/2008GB003336

Gijsman, A.J., Hoogenboom, G., Parton, W.J. and Kerridge, P.C. 2002. Modifying DSSAT crop models for low-input agricultural systems using a soil organic matter–residue module from CENTURY. *Agronomy Journal* 94. (3): 462–474. https://doi.org/10.2134/agronj2002.4620

Hao, X., Chang, C. and Larney, F.J. 2004. Carbon, nitrogen balances and greenhouse gas emission during cattle feedlot manure composting. *Journal of Environmental Quality* 33. 37–44. https://doi.org/10.2134/jeq2004.3700

Heinke, J., Rolinski, S. and Müller, C. 2023. Modelling the role of livestock grazing in C and N cycling in grasslands with LPJmL5.0-grazing. *Geoscientific Model Development* 16. (9): 2455–2475. https://doi.org/10.5194/gmd-16-2455-2023

Hidy, D., Barcza, Z., Haszpra, L., Churkina, G., Pintér, K. and Nagy, Z. 2012. Development of the Biome-BGC model for simulation of managed herbaceous ecosystems. *Ecological Modelling* 226. 99–119. https://doi.org/10.1016/j.ecolmodel.2011.11.008

Hidy, D., Barcza, Z., Marjanović, H., Ostrogović Sever, M.Z., Dobor, L., Gelybó, G., Fodor, N., Pintér, K., Churkina, G., Running, S.W., Thornton, P., Bellocchi, G., Haszpra, L., Horváth, F., Suyker, A. and Nagy, Z. 2016. Terrestrial ecosystem process model Biome-BGCMuSo v4.0: Summary of improvements and new modelling possibilities. *Geoscientific Model Development* 9. 4405–4437. https://doi.org/10.5194/gmd-9-4405-2016

Hidy, D., Barcza, Z., Thornton, P., Running, S.W. and Fodor, N. 2021. *User's Guide for Biome-BGC MuSo 6.1.* Budapest, Hungary, ELTE Eötvös Loránd University. Available at nimbus.elte.hu/bbgc/files/Manual_BBGC_MuSo_v6.1.pdf

Hidy, D., Barcza, Z., Hollós, R., Dobor, L., Ács, T., Zacháry, D., Filep, T., Pásztor, L., Incze, D., Dencső, M., Tóth, E., Merganičová, K., Thornton, P., Running, S. and Fodor, N. 2022. Soil-related developments of the Biome-BGCMuSo v6.2 terrestrial ecosystem model. *Geoscientific Model Development* 15. 2157–2181. https://doi.org/10.5194/gmd-15-2157-2022

Hollós, R., Fodor, N., Merganičová, K., Hidy, D., Árendás, T., Grünwald, T. and Barcza, Z. 2022. Conditional interval reduction method: A possible new direction for the optimization of process based models. *Environmental Modelling and Software* 158. 105556. https://doi.org/10.1016/j.envsoft.2022.105556

ISU, 2025. *Literature Database*. Ames, Iowa, US, Iowa State University. https://www.extension.iastate.edu/ampat/literature-database

Kimball, B.A., Thorp, K.R., Boote, K.J., Stockle, C., Suyker, A.E., Evett, S.R., Brauer, D.K., Coyle, G.G., Copeland, K.S., Marek, G.W., Colaizzi, P.D., Acutis, M., Alimagham, S., Archontoulis, S., Babacar, F., Barcza, Z., Basso, B., Bertuzzi, P., Constantin, J., de Antoni Migliorati, M., Dumont, B., Durand, J.L., Fodor, N., Gaiser, T., Garofalo, P., Gayler, S., Giglio, L., Grant, R., Guan, K., Hoogenboom, G., Jiang, Q., Kim, S.H., Kisekka, I., Lizaso, J., Masia, S., Meng, H., Mereu, V., Mukhtar, A., Perego, A., Peng, B., Priesack, E., Qi, Z., Shelia, V., Snyder, R., Soltani, A., Spano, D., Srivastava, A., Thomson, A., Timlin, D., Trabucco, A., Webber, H., Weber, T., Willaume, M., Williams, K., van der Laan, M., Ventrella, D., Viswanathan, M., Xu, X. and Zhou, W. 2023. Simulation of evapotranspiration and yield of maize: An inter-comparison among 41 maize models. *Agricultural and Forest Meteorology* 333. 109396. https://doi.org/10.1016/j.agrformet.2023.109396

Kimball, B.A., Thorp, K.R., Boote, K.J., Stockle, C., Suyker, A.E., Evett, S.R., Brauer, D.K., Coyle, G.G., Copeland, K.S., Marek, G.W., Colaizzi, P.D., Acutis, M., Archontoulis, S., Babacar, F., Barcza, Z., Basso, B., Bertuzzi, P., Migliorati, M.D.A., Dumont, B., Durand, J.L., Fodor, N., Gaiser, T., Gayler, S., Grant, R., Guan, K., Hoogenboom, G., Jiang, Q., Kim, S.H., Kisekka, I., Lizaso, J., Perego, A., Peng, B., Priesack, E., Qi, Z., Shelia, V., Srivastava, A.K., Timlin, D., Webber, H., Weber, T., Williams, K., Viswanathan, M. and Zhou, W. 2024. Simulation of soil temperature under maize: An inter-comparison among 33 maize models. *Agricultural and Forest Meteorology* 351. 110003. https://doi.org/10.1016/j.agrformet.2024.110003

Kupper, T., Häni, C., Neftel, A., Kincaid, C., Bühler, M., Amon, B. and van der Zaag, A. 2020. Ammonia and greenhouse gas emissions from slurry storage – A review. *Agriculture, Ecosystems & Environment* 300. 106963. https://doi.org/10.1016/j.agee.2020.106963

Larney, F.J., Ellert, B.H. and Olson, A.F. 2004. Carbon, ash and organic matter relationships for feedlot manures and composts. *Canadian Journal of Soil Science* 85. 261–264. https://doi.org/10.4141/S04-060

Levavasseur, F., Lashermes, G., Mary, B., Morvan, T., Nicolardot, B., Parnaudeau, V., Thuriès, L. and Houot, S. 2021. Quantifying and simulating carbon and nitrogen mineralization from diverse exogenous organic matters. *Soil Use and Management* 38. (1): 411–425. https://doi.org/10.1111/sum.12745

Levi-Minzi, R., Riffaldit, R. and Saviozzi, A. 1986. Organic matter and nutrients in fresh and mature farmyard manure. *Agricultural Wastes* 16. 225–236. https://doi.org/10.1016/0141-4607(86)90068-5

Li, C., Salas, W., Zhang, R., Krauter, C., Rotz, A. and Mitloehner, F. 2012. Manure-DNDC – a biogeochemical process model for quantifying greenhouse gas and ammonia emissions from livestock manure systems. *Nutrient Cycling in Agroecosystems* 93. 163–200. https://doi.org/10.1007/s10705-012-9507-z

Li, H., Feng, W., He, X., Zhu, P., Gao, H., Sun, N. and Xu, M. 2017. Chemical fertilizers could be completely replaced by manure to maintain high maize yield and soil organic carbon (SOC) when SOC reaches a threshold in the Northeast China Plain. *Journal of Integrative Agriculture* 16. 937–946. https://doi.org/10.1016/S2095-3119(16)61559-9

Li, K., Liu, R. and Sun, C. 2015. Comparison of anaerobic digestion characteristics and kinetics of four livestock manures with different substrate concentrations. *Bioresource Technology* 198. 133–140. https://doi.org/10.1016/j.biortech.2015.08.151

Li, R., Tan, W., Zhao, X., Dang, Q., Song, Q., Xi, B. and Zhang, X. 2019. Evaluation on the methane production potential of wood waste pre-treated with NaOH and co-digested with pig manure. *Catalysts* 9. 539. https://doi.org/10.3390/catal9060539

Li, Y., Zhang, R., Chen, C., Liu, G., He, Y. and Liu, X. 2013. Biogas production from co-digestion of corn stover and chicken manure under anaerobic wet, hemi-solid, and solid state conditions. *Bioresource Technology* 149. 406–412. https://doi.org/10.1016/j.biortech.2013.09.091

Martre, P., Wallach, D., Asseng, S., Ewert, F., Jones, J.W., Rotter, R.P., Boote, K.J., Ruane, A.C., Thorburn, P.J., Cammarano, D., Hatfield, J.L., Rosenzweig, C., Aggarwal, P.K., Angulo, C., Basso, B., Bertuzzi, P., Biernath, C., Brisson, N., Challinor, A.J., Doltra, J., Gayler, S., Goldberg, R., Grant, R.F., Heng, L., Hooker, J., Hunt, L.A., Ingwersen, J., Izaurralde, R.C., Kersebaum, K.C., Müller, C., Kumar, S.N., Nendel, C., O'leary, G., Olesen, J.E., Osborne, T.M., Palosuo, T., Priesack, E., Ripoche, D., Semenov, M.A., Shcherback, I., Steduto, P., Stöckle, C.O., Stratonovitch, P., Streck, T., Supit, I., Tao, F., Travasso, M., Waha, K., White, J.W. and Wolf, J. 2015. Multi-model ensembles of wheat growth: Many models are better than one. *Global Change Biology* 21. 911–925. https://doi.org/10.1111/gcb.12768

Mathison, C., Burke, E., Hartley, A.J., Kelley, D.I., Burton, C., Robertson, E., Gedney, N., Williams, K., Wiltshire, A., Ellis, R.J., Sellar, A.A. and Jones, C.D. 2023. Description and evaluation of the JULES-ES set-up for ISIMIP2b. *Geoscientific Model Development* 16. (14): 4249–4264. https://doi.org/10.5194/gmd-16-4249-2023

Menšík, L., Hlisnikovský, L. and Kunzová, E. 2019. The state of the soil organic matter and nutrients in the long-term field experiments with application of organic and mineral fertilizers in different soil-climate conditions in the view of expecting climate change. In *Organic Fertilizers – History, Production and Applications*. Eds.: Larramendy, M. and Soloneski, S., London, UK, IntechOpen Ltd., 23–42. https://doi.org/10.5772/intechopen.77847

Menzi, H. 2002. Manure management in Europe. In *10th FAO Ramiran Conference on Recycling of Organic Residues in Agriculture.* Eds.: Venglovsky. J. and Greserova, G., Strebske Pleso, Slovakia, University of Veterinary Medicine in Kosice, 93–102.

Mohanty, S., Nayak, A.K., Swain, C.K., Dhal, B.R., Kumar, A., Kumar, U., Tripathi, R., Shahid, M. and Behera, K.K. 2020. Impact of integrated nutrient management options on GHG emission, N loss and N use efficiency of low land rice. *Soil and Tillage Research* 200. 104616. https://doi.org/10.1016/j.still.2020.104616

Morvan, T., Nicolardot, B. and Péan, L. 2006. Biochemical composition and kinetics of C and N mineralization of animal wastes: a typological approach. *Biology and Fertility of Soils* 42. 513–522. https://doi.org/10.1007/s00374-005-0045-6

Nand, V., Qi, Z., Ma, L., Helmers, M.J., Madramootoo, C.A., Smith, W.N., Zhang, T., Weber, T.K.D., Pattey, E., Li, Z., Wang, J., Jin, V.L., Jiang, Q., Tenuta, M., Trout, T.J., Cheng, H., Harmel, R.D., Kimball, B.A., Thorp, K.R., Boote, K.J., Stockle, C., Suyker, A.E., Evett, S.R., Brauer, D.K., Coyle, G.G., Copeland, K.S., Marek, G.W., Colaizzi, P.D., Acutis, M., Alimagham, S.M., Archontoulis, S., Babacar, F., Barcza, Z., Basso, B., Bertuzzi, P., Constantin, J., De Antoni Migliorati, M., Dumont, B., Durand, J.L., Fodor, N., Gaiser, T., Garofalo, P., Gayler, S., Giglio, L., Grant, R., Guan, K., Hoogenboom, G., Kim, S.H., Kisekka, I., Lizaso, J., Masia, S., Meng, H., Mereu, V., Mukhtar, A., Perego, A., Peng, B., Priesack, E., Shelia, V., Snyder, R., Soltani, A., Spano, D., Srivastava, A., Thomson, A., Timlin, D., Trabucco, A., Webber, H., Willaume, M., Williams, K., van der Laan, M., Ventrella, D., Viswanathan, M., Xu, X. and Zhou, W. 2025. Evaluation of multi-model averaging approaches for ensembling evapotranspiration and yield simulations from maize models. *Journal of Hydrology* 661. 133631. https://doi.org/10.1016/j.jhydrol.2025.133631

Navarro, A.F., Cegarra, J., Roig, A. and Garcia, D. 1993. Relationships between organic matter and carbon contents of organic wastes. *Bioresource Technology* 44. 203–207. https://doi.org/10.1016/0960-8524(93)90153-3

Olesen, J.E., Trnka, M., Kersebaum, K.C., Skjelvåg, A.O., Seguin, B., Peltonen-Sainio, P., Rossi, F., Kozyra, J. and Micale, F. 2011. Impacts and adaptation of European crop production systems to climate change. *European Journal of Agronomy* 34. 96–112. https://doi.org/10.1016/j.eja.2010.11.003

Pain, B. and Menzi, H. (eds.) 2011. *RAMIRAN Glossary of Terms on Livestock and Manure Management*. Second Edition. Darmstadt, Kuratorium für Technik und Bauwesen in der Landwirtschaft (KTBL).

Parton, W.J., Holland, E.A., Del Grosso, S.J., Hartman, M.D., Martin, R.E., Mosier, A.R., Ojima, D.S. and Schimel, D.S. 2001. Generalized model for NO_x and N_2O emissions from soils. *Journal of Geophysical Research Atmospheres* 106. 17403–17419. https://doi.org/10.1029/2001JD900101

Pásztor, L., Laborczi, A., Takács, K., Illés, G., Szabó, J. and Szatmári. G. 2020. Progress in the elaboration of GSM conform DSM products and their functional utilization in Hungary. *Geoderma Regional* 21. e00269. https://doi.org/10.1016/j.geodrs.2020.e00269

Pettygrove, G.S., Heinrich, A.L. and Eagle, A.J. 2009. *Dairy Manure Nutrient Content and Forms.* University of California Cooperative Extension Manure Technical Bulletin Series.

Potter, P., Ramankutty, N., Bennett, E.M. and Donner, S.D. 2010. Characterizing the spatial patterns of global fertilizer application and manure production. *Earth Interactions* 14. 1–22. https://doi.org/10.1175/2009EI288.1

R Core Team 2021. *R: A Language and Environment for Statistical Computing.* Vienna, Austria, R Foundation for Statistical Computing. http://www.R-project.org/

Rehman, K.U., Cai, M., Xiao, X., Zheng, L., Wang, H., Soomro, A.A., Zhou, Y., Li, W., Yu, Z. and Zhang, J. 2017. Cellulose decomposition and larval biomass production from the co-digestion of dairy manure and chicken manure by mini-livestock (*Hermetia illucens L.*). *Journal of Environ Management* 196. 458–465. https://doi.org/10.1016/j.jenvman.2017.03.047

Rosenzweig, C., Jones, J.W., Hatfield, J.L., Ruane, A.C., Boote, K.J., Thorburn, P., Antle, J.M., Nelson, G.C., Porter, C., Janssen, S., Asseng, S., Basso, B., Ewert, F., Wallach, D., Baigorria, G. and Winter, J.M. 2013. The Agricultural Model Intercomparison and Improvement Project (AgMIP): Protocols and pilot studies. *Agricultural and Forest Meteorology* 170. 166–182. https://doi.org/10.1016/j.agrformet.2012.09.011

Running, S.W. and Hunt, E.R.J. 1993. Generalization of a forest ecosystem process model for other biomes, BIOME-BGC, and an application for global-scale models. In *Scaling Physiological Processes: Leaf to Globe.* Eds.: Ehleringer, J.R. and Field, C., San Diego, CA, US, Academic Press, 141–158. https://doi.org/10.1016/B978-0-12-233440-5.50014-2

Saltelli, A., Tarantola, S., Campolongo, F. and Ratto, M. 2004. *Sensitivity Analysis in Practice: A Guide to Assessing Scientific Models*. Chichester, John Wiley & Sons. https://doi.org/10.1002/0470870958

Shen, J., Zhao, C., Liu, Y., Zhang, R., Liu, G. and Chen, C. 2019. Biogas production from anaerobic co-digestion of durian shell with chicken, dairy, and pig manures. *Energy Conversion and Management* 198. 110535. https://doi.org/10.1016/j.enconman.2018.06.099

Sommer, S.G. and Olesen, J.E. 1991. Effects of dry matter content and temperature on ammonia loss from surface-applied cattle slurry. *Journal of Environmental Quality* 20. 679–683. https://doi.org/10.2134/jeq1991.00472425002000030029x

Spinoni, J., Szalai, S., Szentimrey, T., Lakatos, M., Bihari, Z., Nagy, A., Németh, Á., Kovács, T., Mihic, D., Dacic, M., Petrovic, P., Kržič, A., Hiebl, J., Auer, I., Milkovic, J., Štepánek, P., Zahradnícek, P., Kilar, P., Limanowka, D., Pyrc, R., Cheval, S., Birsan, M.-V., Dumitrescu, A., Deak, G., Matei, M., Antolovic, I., Nejedlík, P., Štastný, P., Kajaba, P., Bochnícek, O., Galo, D., Mikulová, K., Nabyvanets, Y., Skrynyk, O., Krakovska, S., Gnatiuk, N., Tolasz, R., Antofie, T. and Vogt, J. 2015. Climate of the Carpathian region in the period 1961–2010: Climatologies and trends of 10 variables. *International Journal of Climatology* 35. 1322–1341. https://doi.org/10.1002/joc.4059

Thomas, R.Q., Bonan, G.B. and Goodale, C.L. 2013. Insights into mechanisms governing forest carbon response to nitrogen deposition: a model-data comparison using observed responses to nitrogen addition. *Biogeosciences* 10. 3869–3887. https://doi.org/10.5194/bg-10-3869-2013

Thornton, P.E. 1998. *Regional ecosystem simulation: Combining surface- and satellite-based observations to study linkages between terrestrial energy and mass budgets.* Doctoral dissertation. Billings, MT, US, The University of Montana. https://scholarworks.umt.edu/etd/10519/ (accessed 26 September 2025).

Thornton, P.E., Law, B., Gholz, H.L., Clark, K.L., Falge, E., Ellsworth, D., Goldstein, A., Monson, R., Hollinger, D., Falk, M., Chen, J. and Sparks, J. 2002. Modelling and measuring the effects of disturbance history and climate on carbon and water budgets in evergreen needle-leaf forests. *Agricultural and Forest Meteorology* 113. 185–222. https://doi.org/10.1016/S0168-1923(02)00108-9

Tiquia, S.M., Tam, N.F.Y. and Hodgkiss, I.J. 1998. Changes in chemical properties during composting of spent pig litter at different moisture contents. *Agriculture, Ecosystems & Environment* 67. 79–89. https://doi.org/10.1016/S0167-8809(97)00132-1

Tiquia, S.M., Richard, T.L. and Honeyman, M.S. 2002. Carbon, nutrient and mass loss during composting. *Nutrient Cycling in Agroecosystems* 62. 15–24. https://doi.org/10.1023/A:1015137922816

Tóth, E., Magyar, M., Cseresnyés, I., Dencső, M., Laborczi, A., Szatmári, G. and Koós, S. 2025. Climate-smart agricultural practices – Strategies to conserve and increase soil carbon in Hungary. *Land* 14. 1206. https://doi.org/10.3390/land14061206

Tóth, G., Montanarella, L., Stolbovoy, V., Máté, F., Bódis, K., Jones, A., Panagos, P. and van Liedekerke, M. 2008. *Soils of the European Union.* Brussels, European Commission Joint Research Centre, Institute for Environment and Sustainability. https://doi.org/10.2788/87029

Tóth, G., Kismányoky, T., Kassai, P., Hermann, T., Fernandez-Ugalde, O. and Szabó, B. 2020. Farming by soil in Europe: Status and outlook of cropping systems under different pedoclimatic conditions. *PeerJ* 8:e8984 http://doi.org/10.7717/peerj.8984

Van Gaelen, H., Tsegay., Delbecque, N., Shrestha, N., Garcia, M., Fajadro, H., Miranda, R., Vanuytrecht, E., Abrha, B., Diels, J. and Raes, D. 2015. A semi-quantitative approach for modelling crop response to soil fertility: Evaluation of the AquaCrop procedure. *The Journal of Agricultural Science* 153. (7): 1218–1233. https://doi.org/10.1017/S0021859614000872

Verbeeck, H., Samson, R., Verdonck, F. and Lemeur, R. 2006. Parameter sensitivity and uncertainty of the forest carbon flux model FORUG: A Monte Carlo analysis. *Tree Physiology* 26. 807–817. https://doi.org/10.1093/treephys/26.6.807

Verma, G., Sharma, R.P., Sharma, S.P., Subehia, S.K. and Shambhavi, S. 2012. Changes in soil fertility status of maize-wheat system due to long-term use of chemical fertilizers and amendments in an alfisol. *Plant, Soil and Environment* 58. 529–533. https://doi.org/10.17221/133/2012-PSE

Wang, Y., Zhu, Y., Zhang, S. and Wang, Y. 2018. What could promote farmers to replace chemical fertilizers with organic fertilizers? *Journal of Cleaner Production* 199. 882–890. https://doi.org/10.1016/j.jclepro.2018.07.222

Webb, J., Sørensen, P., Velthof, G.L., Amon, B., Pinto, M., Rodhe, L., Salomon, E., Hutchings, N., Burczyk, J. and Reid, J.E. 2010. *Study on Variation of Manure N Efficiency throughout Europe*. Didcot, UK, AEA Technology Plc.

Webb, J., Sørensen, P., Velthof, G., Amon, B., Pinto, M., Rodhe, L., Salomon, E., Hutchings, N., Burczyk, P., Reid, J. 2013. Chapter seven – An assessment of the variation of manure nitrogen efficiency throughout Europe and an appraisal of means to increase manure-N efficiency. In *Advances in Agronomy 119*. Ed.: Sparks, D.L., Newark, DE, US, Academic Press, 371–442. https://doi.org/10.1016/B978-0-12-407247-3.00007-X

Wiltshire, A.J., Burke, E.J., Chadburn, S.E., Jones, C.D., Cox, P.M., Davies-Barnard, T., Friedlingstein, P., Harper, A.B., Liddicoat, S., Sitch, S. and Zaehle, S. 2021. JULES-CN: A coupled terrestrial carbon–nitrogen scheme (JULES vn5.1). *Geoscientific Model Development* 14. (4): 2161–2186. https://doi.org/10.5194/gmd-14-2161-2021

Yang, R., Su, Y., Wang, T. and Yang, Q. 2016. Effect of chemical and organic fertilization on soil carbon and nitrogen accumulation in a newly cultivated farmland. *Journal of Integrative Agriculture* 15. 658–666. https://doi.org/10.1016/S2095-3119(15)61107-8

Zhao, S., Schmidt, S., Ciais, P., Benoît, G., Guenet, B., Smith, P., Fang, Y., Yan, X., Zhang, W. and Zhou, F. 2025. A meta-analysis reveals large potential of substituting synthetic nitrogen fertilizer with solid organic fertilizer for climate mitigation in China. *Journal of Cleaner Production* 525. 146615. https://doi.org/10.1016/j.jclepro.2025.146615

Zhen, M., Tang, J., Li, C. and Sun, H. 2021. Rhamnolipid-modified biochar-enhanced bioremediation of crude oil-contaminated soil and mediated regulation of greenhouse gas emission in soil. *Journal of Soils and Sediments* 21. 123–133. https://doi.org/10.1007/s11368-020-02746-5

Supplementary section

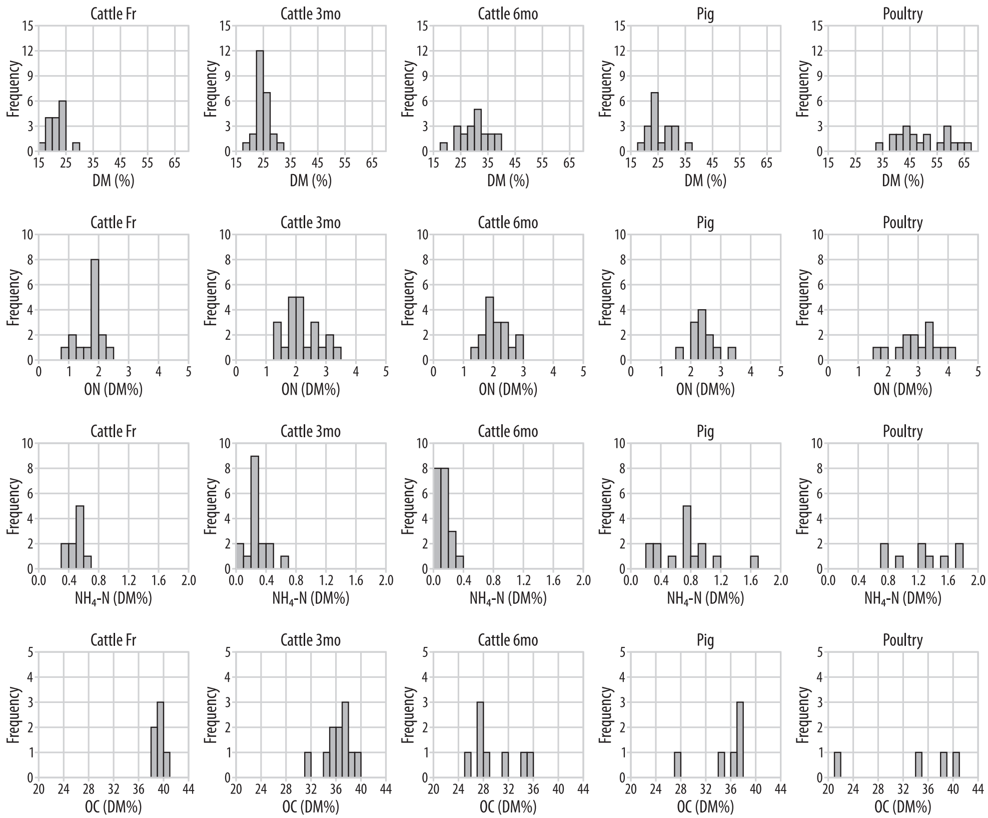

Fig. S1. Results of data collection presented as histograms for the different FYM types. DM denotes DM content; ON, NH_4-N and OC denote the organic nitrogen, NH_4-N and organic carbon content of DM, respectively. *Source:* Authors' own elaboration.

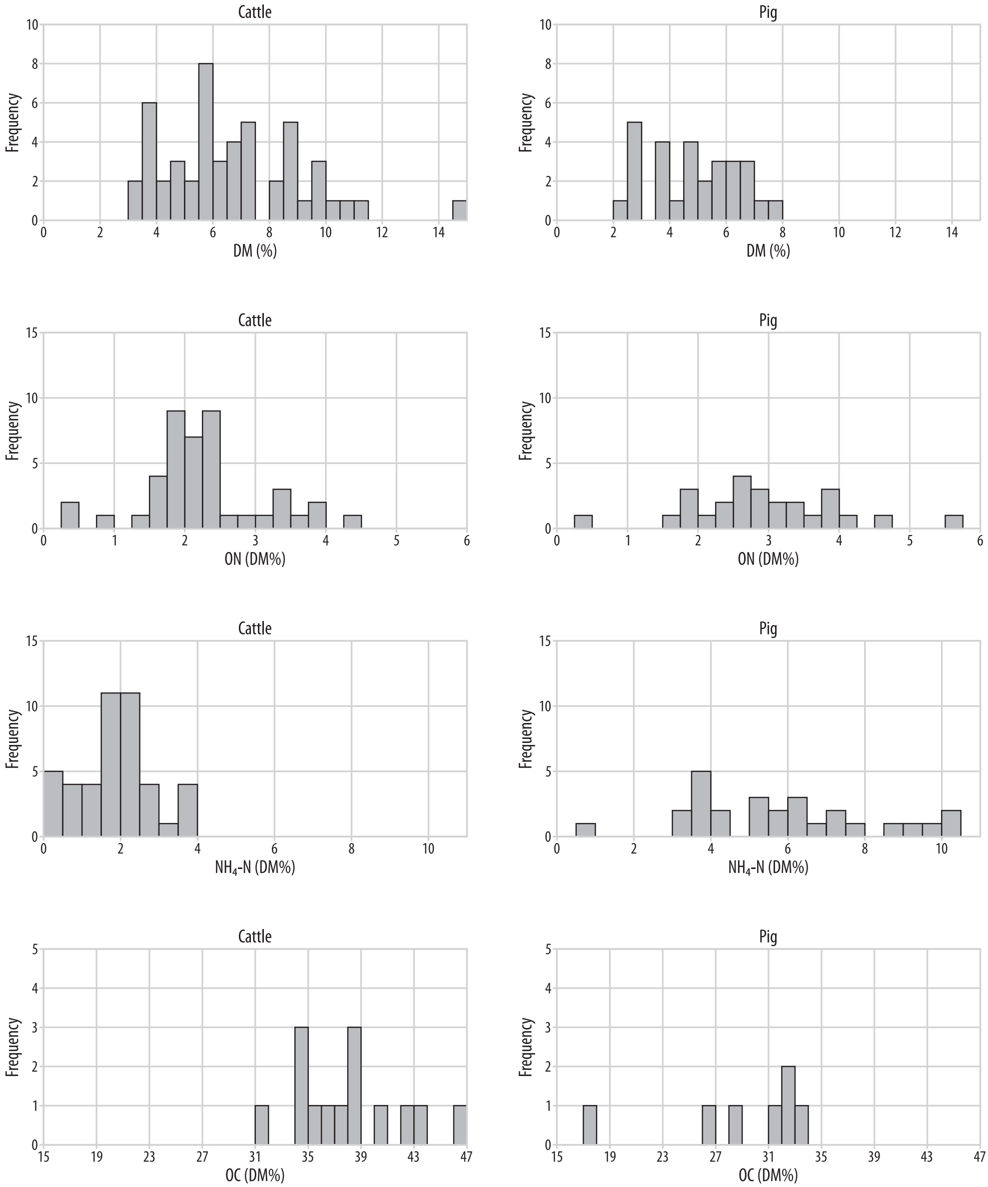

Fig. S2. Results of the data collection for slurry related organic fertilizer parameters. The abbreviations are the same as in *Fig. S1. Source:* Authors' own elaboration.

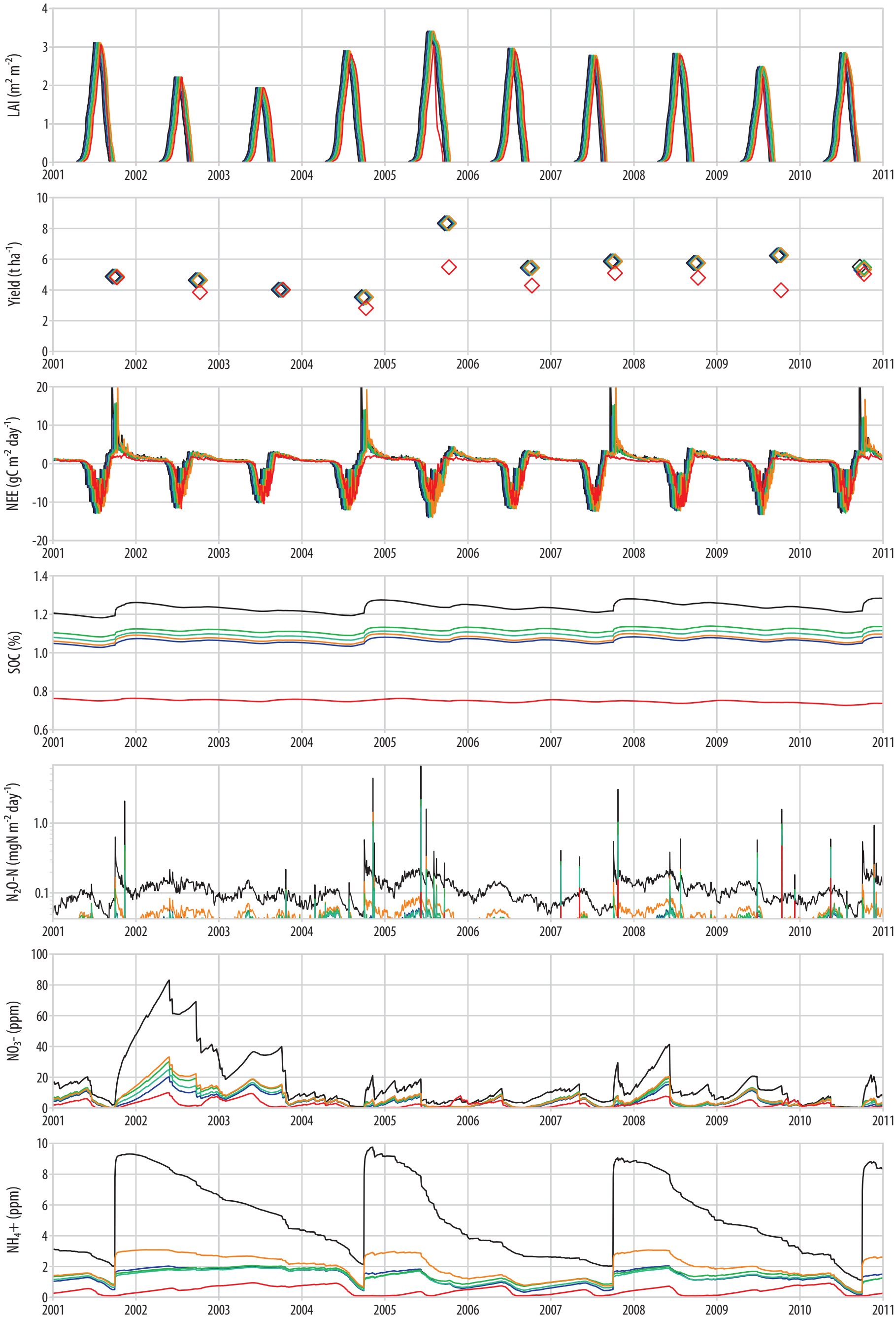

Fig. S3. Biome-BGCMuSo simulation results for Kishunhalas (sandy soil) using the median (proposed) parameterization for the different FYM types. For N_2O efflux logarithmic scale is used for clarity. Note that in some cases the lines/symbols overlap. The different colors represent simulation results driven by different FYM types. Black line represents poultry, blue line represents cattle Fr, light blue represents cattle 3mo, light green represents cattle 6mo, yellow represents pig, red represents control treatment. *Source:* Authors' own elaboration.

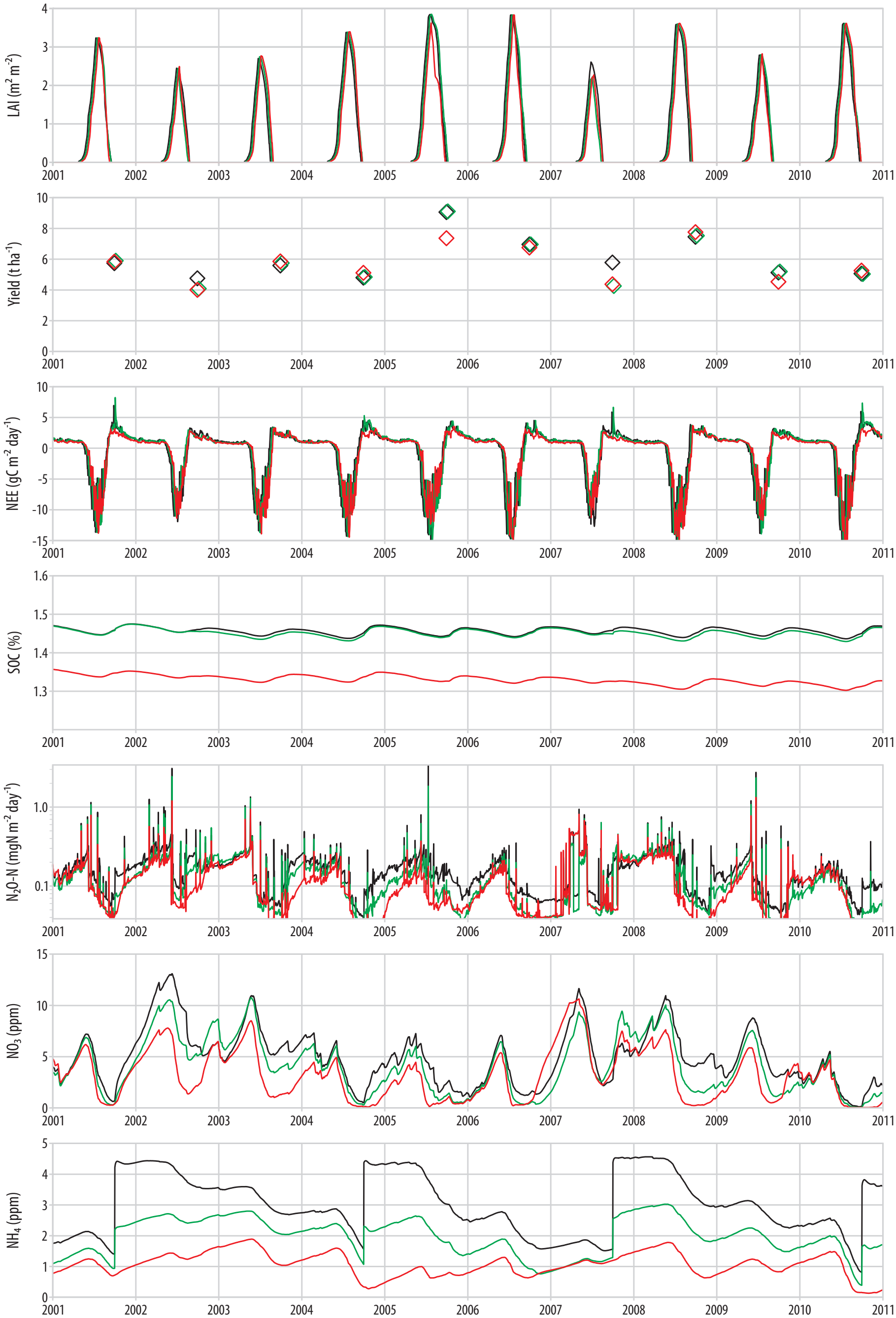

Fig. S4. Biome-BGCMuSo simulation results for Martonvásár (chernozem soil) using the median (proposed) parameterization for the different slurry types. For N_2O efflux logarithmic scale is used for clarity. Note that in some cases the lines/symbols overlap. The different colors represent simulation results driven by different slurry types. Black line represents pig, light green represents cattle, red represents control treatment. *Source:* Authors' own elaboration.

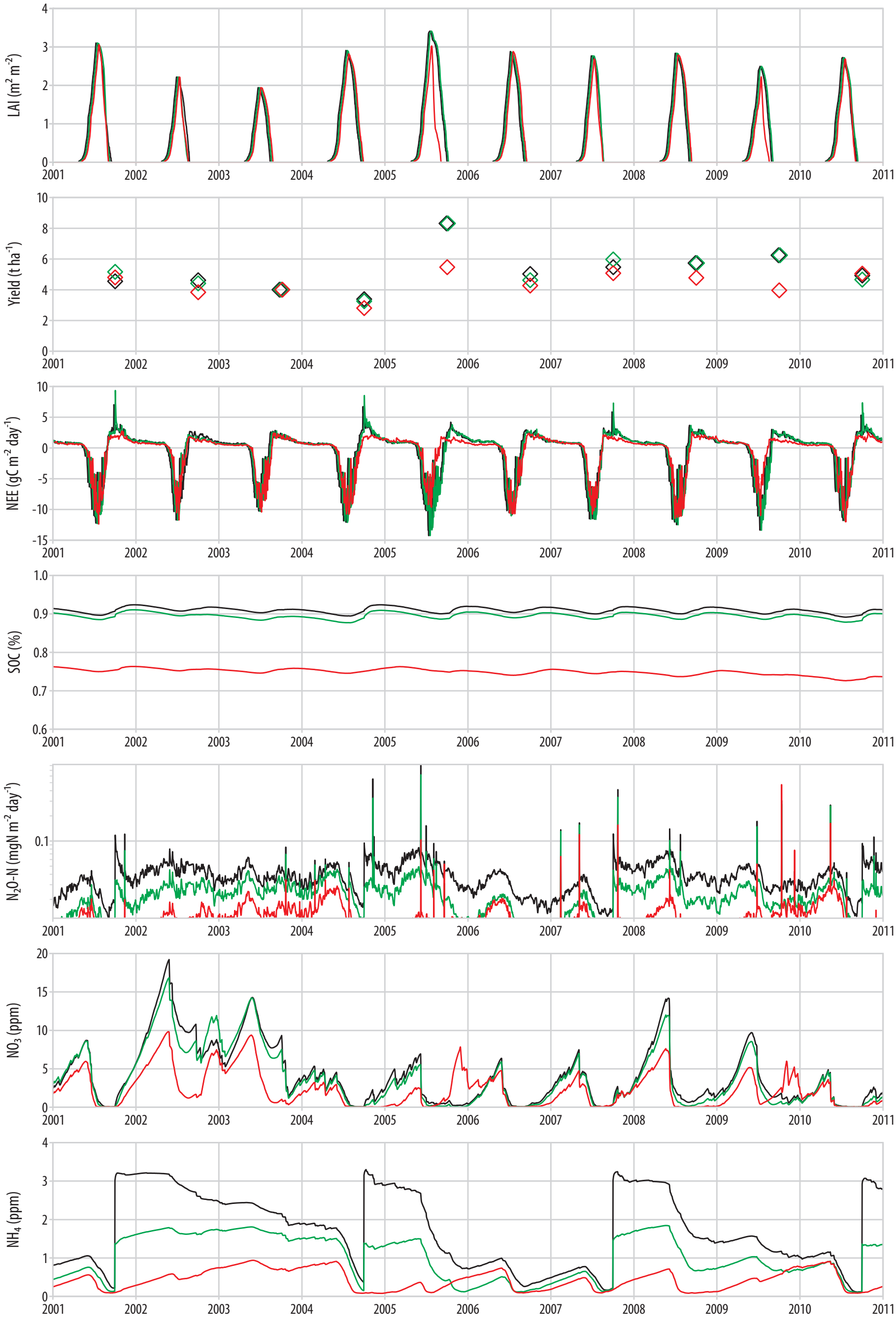

Fig. S5. Biome-BGCMuSo simulation results for Kiskunhalas (sandy soil) using the median (proposed) parameterization for the different slurry types. For N_2O efflux logarithmic scale is used for clarity. Note that in some cases the lines/symbols overlap. The different colors represent simulation results driven by different slurry types. Black line represents pig, light green represents cattle, red represents control treatment. *Source:* Authors' own elaboration.

Table S1. Dry matter content of manure, %

Animal	Manure	Number of data	Mean and SD	References
Cattle	FYM Fr	16	22.0 ± 3.13	Stefanovits, P. 1964; Szpravocsnik, 1964; Levi-Minzi, R. *et al.* 1986; Chambers, B.J. *et al.* 1999; Misselbrook, T.H. *et al.* 2005b; DEFRA, 2010; Chadwick, D.R. *et al.* 2011; Richner, W. *et al.* 2017.
Cattle	FYM 3mo	25	25.2 ± 2.62	Stefanovits, P. 1964; Szpravocsnik, 1964; Levi-Minzi, R. *et al.* 1986; Chambers, B.J. *et al.* 1999; Chadwick, D.R. *et al.* 2000a, 2000b, 2011; Misselbrook, T.H. *et al.* 2005a; Properties of manure, 2005; DEFRA, 2010; Brown, C. 2013.
Cattle	FYM 6mo	20	30.1 ± 5.1	Stefanovits, P. 1964; Szpravocsnik, 1964; McGinn, S.M. and Sommer, S.G. 2007; Pettygrove, G.S. *et al.* 2009; Árendás, T. 2019.
Pig	FYM	20	26.3 ± 3.83	Benne, E.J. *et al.* 1961; Szpravocsnik, 1964; Chambers, B.J. *et al.* 1999; Chadwick, D.R. *et al.* 2000a, 2000b, 2011; Misselbrook, T.H. *et al.* 2005b; DEFRA, 2010; Hartman, M. 2010; Rajendran, K. *et al.* 2012; Brown, C. 2013; Richner, W. *et al.* 2017.
Poultry	FYM	20	50.0 ± 9.37	Benne, E.J. *et al.* 1961; Sesztakov, K.A. 1961; Curkan, M.A. 1985; Chadwick, D.R. *et al.* 2000b, 2011; Menzi, H. 2002; Rao, J.R. *et al.* 2007; DEFRA, 2010; Hartman, M. 2010; Brown, C. 2013; Richner, W. *et al.* 2017.
Cattle	slurry	50	6.81 ± 2.46	Csaba, L. *et al.* 1978; Thompson, R.B. *et al.* 1990; Chambers, B.J. *et al.* 1999; Chadwick, D.R. *et al.* 2000a, 2000b, 2011; Smith, K.A. *et al.* 2000; Menzi, H. 2002; Thompson, R.B. and Meisinger, J.J. 2002; Bol, R. *et al.* 2003; Chastain, J.P. and Camberato, J.J. 2003; Misselbrook, T.H. *et al.* 2005a, 2005b; Properties of manure, 2005; Amon, B. *et al.* 2006; Fangueiro, D. *et al.* 2008; Bhandral, R. *et al.* 2009; DEFRA, 2010; Brown, C. 2013; Cavalli, D. *et al.* 2016; Nguyen, Q.V. *et al.* 2017; Richner, W. *et al.* 2017; Alfaro, M. *et al.* 2018.
Pig	slurry	28	4.92 ± 1.60	Csaba, L. *et al.* 1978; Chambers, B.J. *et al.* 1999; Chadwick, D.R. *et al.* 2000a, 2000b, 2011; Menzi, H. 2002; Misselbrook, T.H. *et al.* 2005b; Properties of manure, 2005; Bertora, C. *et al.* 2008; DEFRA, 2010; Brown, C. 2013; Richner, W. *et al.* 2017.

Table S2. P-values of ANOVA test for cattle Fr, 3mo and 6mo, pig and poultry FYM and for cattle and pig slurry comparison

FYM	DM	ON	NH_4-N	OC
Cattle Fr – 3mo	0.001036**	0.01148*	0.000116***	0.01444*
Cattle Fr – 6mo	$< 10^{-5}$ ***	0.02338*	$< 10^{-5}$ ***	$< 10^{-5}$ ***
Cattle 3mo – 6mo	$< 10^{-5}$ ***	0.5992	0.001132 **	0.000227***
Cattle Fr – Pig	0.00131**	0.00054***	0.08379	0.03399*
Cattle 3mo – Pig	0.2847	0.3736	$< 10^{-5}$ ***	0.455
Cattle 6mo – Pig	0.00599**	0.1299	$< 10^{-5}$ ***	0.02268*
Cattle Fr – Poultry	$< 10^{-5}$ ***	$< 10^{-5}$ ***	$< 10^{-5}$ ***	0.155
Cattle 3mo – Poultry	$< 10^{-5}$ ***	0.00073***	$< 10^{-5}$ ***	0.3366
Cattle 6mo – Poultry	$< 10^{-5}$ ***	0.00024***	$< 10^{-5}$ ***	0.3209
Pig – Poultry	$< 10^{-5}$ ***	0.01382 *	0.002492 **	0.6985
SLURRY				
Cattle – Pig	0.0004722***	0.003736**	$< 10^{-5}$ ***	0.0004148***

***, **, and *: Denote significant differences at 0.001, 0.01, and 0.05 confidence level, respectively.

Table S3. ON content of manure, DM %

Animal	Manure	Number of data	Mean and SD	References
Cattle	FYM Fr	16	1.8 ± 0.38	Stefanovits, P. 1964; Szpravocsnik, 1964; Levi-Minzi, R. *et al.* 1986; Chambers, B.J. *et al.* 1999; Misselbrook, T.H. *et al.* 2005b; DEFRA, 2010; Chadwick, D.R. *et al.* 2011; Richner, W. *et al.* 2017.
Cattle	FYM 3mo	22	2.2 ± 0.56	Stefanovits, P. 1964; Szpravocsnik, 1964; Levi-Minzi, R. *et al.* 1986; Chambers, B.J. *et al.* 1999; Chadwick, D.R. *et al.* 2000b; 2011; Misselbrook, T.H. *et al.* 2005a.
Cattle	FYM 6mo	17	2.1 ± 0.44	Stefanovits, P. 1964; Szpravocsnik, 1964; McGinn, S.M. and Sommer, S.G. 2007; Pettygrove, G.S. *et al.* 2009; Árendás, T. 2019.
Pig	FYM	12	2.37 ± 0.42	Chambers, B.J. *et al.* 1999; Chadwick, D.R. *et al.* 2000b, 2011; DEFRA, 2010; Richner, W. *et al.* 2017.
Poultry	FYM	14	2.99 ± 0.72	Curkan, M.A. 1985; Chadwick, D.R. *et al.* 2000b, 2011; Menzi, H. 2002; Rao, J.R. *et al.* 2007; Richner, W. *et al.* 2017.
Cattle	slurry	43	2.27 ± 0.85	Thompson, R.B. *et al.* 1990; Chambers, B.J. *et al.* 1999; Chadwick, D.R. *et al.* 2000a, 2000b; 2011; Smith, K.A. *et al.* 2000; Menzi, H. 2002; Thompson, R.B. and Meisinger, J.J. 2002; Chastain, J.P. and Camberato, J.J. 2003; Misselbrook, T.H. *et al.* 2005a, 2005b; Properties of manure, 2005; Amon, B. *et al.* 2006; Fangueiro, D. *et al.* 2008; Bhandral, R. *et al.* 2009; DEFRA, 2010; Brown, C. 2013; Cavalli, D. *et al.* 2016; Nguyen, Q.V. *et al.* 2017; Richner, W. *et al.* 2017; Alfaro, M. *et al.* 2018.
Pig	slurry	26	2.96 ± 1.05	Csaba, L. *et al.* 1978; Chambers, B.J. *et al.* 1999; Chadwick, D.R. *et al.* 2000b, 2011; Menzi, H. 2002; Misselbrook, T.H. *et al.* 2005b; Properties of manure, 2005; Bertora, C. *et al.* 2008; DEFRA, 2010; Brown, C. 2013; Richner, W. *et al.* 2017.

Table S4. NH_4-N content of manure, DM %

Animal	Manure	Number of data	Mean and SD	References
Cattle	FYM Fr	10	0.53 ± 0.09	Stefanovits, P. 1964; Szpravocsnik, 1964; Levi-Minzi, R. *et al.* 1986; Chambers, B.J. *et al.* 1999; Misselbrook, T.H. *et al.* 2005b; DEFRA, 2010; Chadwick, D.R. *et al.* 2011; Richner, W. *et al.* 2017.
Cattle	FYM 3mo	17	0.28 ± 0.15	Stefanovits, P. 1964; Szpravocsnik, 1964; Chambers, B.J. *et al.* 1999; Chadwick, D.R. *et al.* 2000a, 2000b, 2011; Misselbrook, T.H. *et al.* 2005a.
Cattle	FYM 6mo	20	0.132 ± 0.10	Stefanovits, P. 1964; Szpravocsnik, 1964; McGinn, S.M. and Sommer, S.G. 2007; Pettygrove, G.S. *et al.* 2009; Árendás, T. 2019.
Pig	FYM	15	0.742 ± 0.37	Szpravocsnik, 1964; Chambers, B.J. *et al.* 1999; Chadwick, D.R. *et al.* 2000a, 2000b, 2011; Misselbrook, T.H. *et al.* 2005b; Richner, W. *et al.* 2017.
Poultry	FYM	9	1.279 ± 0.38	Chadwick, D.R. *et al.* 2000b, 2011; DEFRA, 2010; Richner, W. *et al.* 2017.
Cattle	slurry	44	1.896 ± 1.00	Thompson, R.B. *et al.* 1990; Chambers, B.J. *et al.* 1999; Chadwick, D.R. *et al.* 2000b, 2011; Smith, K.A. *et al.* 2000; Thompson, R.B. and Meisinger, J.J. 2002; Chastain, J.P. and Camberato, J.J. 2003; Misselbrook, T.H. *et al.* 2005a, 2005b; Properties of manure, 2005; Amon, B. *et al.* 2006; Fangueiro, D. *et al.* 2008; Bhandral, R. *et al.* 2009; DEFRA, 2010; Brown, C. 2013; Cavalli, D. *et al.* 2016; Nguyen, Q.V. *et al.* 2017; Richner, W. *et al.* 2017; Alfaro, M. *et al.* 2018.
Pig	slurry	27	5.864 ± 2.41	Csaba, L. *et al.* 1978; Chambers, B.J. *et al.* 1999; Chadwick, D.R. *et al.* 2000a, 2000b, 2011; Misselbrook, T.H. *et al.* 2005b; Properties of manure, 2005; Bertora, C. *et al.* 2008; DEFRA, 2010; Brown, C. 2013; Richner, W. *et al.* 2017.

Table S5. NO_3-N content of manure, DM %

Animal	Manure	Number of data	Mean and SD	References
Cattle	FYM Fr	1	0	Chadwick, D.R. *et al.* 2011.
Cattle	FYM 3mo	1	0.08	Chadwick, D.R. *et al.* 2000.
Cattle	FYM 6mo	16	0.017 ± 0.02	McGinn, S.M. and Sommer, S.G. 2007; Pettygrove, G.S. *et al.* 2009; Árendás, T. 2019.
Pig	FYM	2	0	Chadwick, D.R. *et al.* 2000a negligible; Chadwick, D.R. *et al.* 2011.
Poultry	FYM	1	0	Chadwick, D.R. *et al.* 2011.
Cattle	slurry	5	0.002 ± 0.003	Chadwick, D.R. *et al.* 2000a negligible; Fangueiro, D. *et al.* 2008; Chadwick, D.R. *et al.* 2011; Alfaro, M. *et al.* 2018.
Pig	slurry	3	0	Chadwick, D.R. *et al.* 2000a negligible; Chadwick, D.R. *et al.* 2011.

Table S6. OC content of manure, DM %

Animal	Manure	Number of data	Mean and SD	References
Cattle	FYM Fr	6	39.13 ± 0.65	Levi-Minzi, R. *et al.* 1986.
Cattle	FYM 3mo	11	36.45 ± 2.30	Levi-Minzi, R. *et al.* 1986; Chadwick, D.R. *et al.* 2000a, 2000b, 2011.
Cattle	FYM 6mo	8	30.20 ± 3.57	Pettygrove, G.S. *et al.* 2009; Árendás, T. 2019.
Pig	FYM	6	35.33 ± 3.74	Chadwick, D.R. *et al.* 2000a, 2000b, 2011.
Poultry	FYM	4	33.77 ± 8.60	Chadwick, D.R. *et al.* 2000b, 2011.
Cattle	slurry	14	38.02 ± 4.25	Chadwick, D.R. *et al.* 2000a, 2000b, 2011; Bol, R. *et al.* 2003; Amon, B. *et al.* 2006; Rodhe, L. *et al.* 2006; Fangueiro, D. *et al.* 2008; Cavalli, D. *et al.* 2016.
Pig	slurry	7	28.88 ± 5.35	Chadwick, D.R. *et al.* 2000a, 2000b, 2011; Bertora, C. *et al.* 2008.

*Table S7. Relative contribution of the investigated FYM input parameters (in columns) to the variance of the selected outputs (in rows) and the SCORE for each input showing their importance in terms of output uncertainty. Simulation results for chernozem soil at Martonvásár**

Parameter	DM	NH_4-N	ON	OC		Parameter	DM	NH_4-N	ON	OC
LAI	17.2	3.6	79.2	0.0	Fresh Cattle FYM	LAI	42.1	5.1	47.1	5.7
YIELD	13.5	3.0	83.4	0.0		YIELD	48.1	10.8	39.3	1.9
NEE	1.4	3.5	94.4	0.7		NEE	2.1	4.7	43.0	50.3
SOC	87.7	0.6	11.2	0.5		SOC	62.4	0.3	2.2	35.0
N_2O	28.0	4.6	67.4	0.0		N_2O	54.0	7.7	36.5	1.8
SNO_3	29.6	3.3	67.1	0.0		SNO_3	57.5	5.2	36.6	0.7
SNH_4	32.4	7.7	59.9	0.0		SNH_4	62.1	11.2	26.3	0.4
SCORE1	*14*	*7*	*26*	*7*		*SCORE2*	*21*	*7*	*15*	*10*
Parameter	DM	NH_4-N	ON	OC	3mo Cattle FYM	Parameter	DM	NH_4-N	ON	OC
LAI	17.7	16.9	65.0	0.4		LAI	36.7	1.0	56.7	5.7
YIELD	17.9	22.7	59.2	0.2		YIELD	22.0	0.2	68.0	9.8
NEE	32.7	9.2	38.5	19.6		NEE	16.7	0.2	14.3	68.9
SOC	83.5	0.8	3.3	12.3		SOC	60.6	0.1	2.2	37.1
N_2O	24.4	18.8	56.6	0.2		N_2O	47.9	2.0	48.1	2.0
SNO_3	27.2	13.4	59.3	0.1		SNO_3	49.7	1.3	48.0	1.0
SNH_4	27.7	40.7	31.6	0.0		SNH_4	63.1	4.6	32.3	0.0
SCORE1	*15*	*10*	*18*	*7*		*SCORE2*	*19*	*7*	*17*	*11*
Parameter	DM	NH_4-N	ON	OC	6mo Cattle FYM	Parameter	DM	NH_4-N	ON	OC
LAI	27.6	7.0	64.5	0.9		LAI	70.7	2.6	23.1	3.6
YIELD	31.7	7.9	59.8	0.6		YIELD	87.3	0.5	7.2	5.0
NEE	41.8	2.7	26.8	28.7		NEE	52.1	0.0	0.1	47.9
SOC	83.2	0.2	2.0	14.5		SOC	54.6	0.0	0.3	45.1
N_2O	33.0	6.4	60.0	0.7		N_2O	44.3	0.8	52.1	2.9
SNO_3	34.3	3.8	61.4	0.5		SNO_3	44.4	0.5	52.8	2.3
SNH_4	42.9	18.5	38.5	0.0		SNH_4	63.7	2.5	33.7	0.1
SCORE1	*19*	*7*	*20*	*8*		*SCORE2*	*25*	*7*	*13*	*11*
Parameter	DM	NH_4-N	ON	OC	Pig FYM	Parameter	DM	NH_4-N	ON	OC
LAI	19.5	39.9	39.8	0.7		LAI	96.0	0.0	0.0	4.0
YIELD	2.6	52.8	43.9	0.7		YIELD	95.9	0.0	0.0	4.1
NEE	80.0	0.1	0.1	19.9		NEE	50.1	0.0	0.0	49.9
SOC	81.6	0.0	0.0	18.4		SOC	49.9	0.0	0.0	50.1
N_2O	33.8	49.1	17.1	0.1		N_2O	60.6	9.4	29.4	0.6
SNO_3	39.4	43.5	17.2	0.0		SNO_3	65.7	7.5	26.7	0.0
SNH_4	30.8	62.7	6.5	0.0		SNH_4	69.4	15.6	14.8	0.2
SCORE1	*18*	*17*	*10*	*7*		*SCORE2*	*28*	*7*	*9*	*11*
Parameter	DM	NH_4-N	ON	OC	Poultry FYM	Parameter	DM	NH_4-N	ON	OC
LAI	98.5	0.0	0.0	1.5		LAI	96.9	0.0	0.2	2.8
YIELD	98.3	0.0	0.0	1.7		YIELD	97.1	0.0	0.1	2.8
NEE	48.8	0.0	0.0	51.2		NEE	48.9	0.0	0.0	51.1
SOC	49.0	0.0	0.0	51.0		SOC	49.1	0.0	0.0	50.9
N_2O	43.3	22.9	32.7	1.1		N_2O	59.5	17.8	21.6	1.1
SNO_3	47.6	19.9	32.2	0.2		SNO_3	64.1	15.1	20.6	0.1
SNH_4	52.3	32.6	15.0	0.1		SNH_4	67.5	23.4	8.9	0.2
SCORE1	*25*	*9*	*9*	*11*		*SCORE2*	*27*	*8*	*9*	*11*

*Left charts: full range; right charts: median±10% range.

*Table S8. Relative contribution of the investigated slurry input parameters (in columns) to the variance of the selected outputs (in rows) and the SCORE for each input showing their importance in terms of output uncertainty. Simulation results for chernozem soil at Martonvásár**

Parameter	DM	NH_4-N	ON	OC		Parameter	DM	NH_4-N	ON	OC
LAI	34.7	37.7	27.5	0.1	Cattle Slurry	LAI	65.4	16.1	17.4	1.1
YIELD	37.7	35.1	27.1	0.1		YIELD	57.0	25.7	15.0	2.3
NEE	8.0	52.1	37.3	2.6		NEE	36.1	18.5	22.4	23.0
SOC	79.7	10.3	7.7	2.2		SOC	74.8	8.1	7.0	10.0
N_2O	44.4	36.3	19.3	0.0		N_2O	56.8	25.4	17.6	0.2
SNO_3	47.2	32.3	20.5	0.0		SNO_3	63.1	18.9	17.9	0.1
SNH_4	41.3	46.1	12.6	0.0		SNH_4	62.5	27.0	10.3	0.2
SCORE1	*18*	*15*	*11*	*7*		*SCORE2*	*24*	*10*	*8*	*8*
Parameter	DM	NH_4-N	ON	OC	Pig Slurry	Parameter	DM	NH_4-N	ON	OC
LAI	31.8	55.6	12.6	0.0		LAI	48.2	39.6	12.2	0.1
YIELD	30.8	55.7	13.5	0.0		YIELD	51.6	39.1	9.3	0.0
NEE	20.6	64.8	13.5	1.1		NEE	5.1	25.7	8.0	61.2
SOC	59.2	30.8	6.9	3.1		SOC	68.3	5.1	1.1	25.5
N_2O	40.1	52.6	7.4	0.0		N_2O	60.5	34.5	4.9	0.1
SNO_3	40.8	51.1	8.1	0.0		SNO_3	62.0	33.0	5.0	0.0
SNH_4	36.3	59.4	4.3	0.0		SNH_4	59.5	37.5	3.0	0.0
SCORE1	*17*	*21*	*7*	*7*		*SCORE2*	*22*	*13*	*7*	*11*

*Left charts: full range; right charts: median±10% range.

*Table S9. Relative contribution of the investigated FYM input parameters (in columns) to the variance of the selected outputs (in rows) and the SCORE for each input showing their importance in terms of output uncertainty. Simulation results for sandy soil at Kiskunhalas**

Parameter	DM	NH_4-N	ON	OC		Parameter	DM	NH_4-N	ON	OC
LAI	47.7	3.7	48.6	0.0	Fresh Cattle FYM	LAI	66.0	1.8	8.2	24.0
YIELD	90.7	0.1	8.3	0.9		YIELD	67.4	0.1	4.2	28.4
NEE	93.4	0.3	4.7	1.6		NEE	46.9	0.0	0.1	53.0
SOC	87.1	0.6	11.8	0.5		SOC	60.3	0.2	1.3	38.2
N_2O	29.1	5.8	65.1	0.0		N_2O	58.4	8.7	32.1	0.9
SNO_3	24.8	1.6	73.6	0.0		SNO_3	50.3	2.5	45.8	1.4
SNH_4	27.9	6.9	65.2	0.0		SNH_4	56.9	10.2	31.5	1.5
SCORE1	*24*	*7*	*18*	*7*		*SCORE2*	*24*	*7*	*11*	*12*
Parameter	DM	NH_4-N	ON	OC	3mo Cattle FYM	Parameter	DM	NH_4-N	ON	OC
LAI	48.8	14.5	35.9	0.7		LAI	68.0	0.1	8.7	23.1
YIELD	70.0	0.3	25.0	4.7		YIELD	68.7	0.1	11.2	20.0
NEE	81.9	0.1	0.3	17.8		NEE	51.5	0.0	0.0	48.5
SOC	83.7	0.9	3.8	11.6		SOC	60.7	0.0	2.9	36.4
N_2O	28.6	33.9	37.5	0.0		N_2O	59.3	3.1	37.5	0.0
SNO_3	27.0	5.0	67.9	0.1		SNO_3	45.8	0.4	52.4	1.5
SNH_4	26.6	39.2	34.2	0.0		SNH_4	59.6	4.1	36.2	0.1
SCORE1	*23*	*9*	*14*	*7*		*SCORE2*	*24*	*7*	*11*	*12*
Parameter	DM	NH_4-N	ON	OC	6mo Cattle FYM	Parameter	DM	NH_4-N	ON	OC
LAI	55.6	6.2	37.8	0.3		LAI	69.2	0.0	14.8	16.1
YIELD	70.3	0.0	22.9	6.8		YIELD	68.1	0.0	14.7	17.2
NEE	80.0	0.0	0.0	19.9		NEE	51.1	0.0	0.0	48.8
SOC	83.3	0.2	2.4	14.1		SOC	57.1	0.0	1.0	41.9
N_2O	43.1	14.5	42.5	0.0		N_2O	61.0	2.0	37.0	0.1
SNO_3	34.8	1.3	63.5	0.3		SNO_3	43.3	0.2	54.8	1.7
SNH_4	41.2	18.1	40.7	0.0		SNH_4	60.8	2.5	36.7	0.0
SCORE1	*25*	*7*	*16*	*7*		*SCORE2*	*25*	*7*	*11*	*11*
Parameter	DM	NH_4-N	ON	OC	Pig FYM	Parameter	DM	NH_4-N	ON	OC
LAI	73.9	13.9	6.0	6.2		LAI	66.4	0.7	2.7	30.1
YIELD	80.7	6.7	5.5	7.1		YIELD	65.9	0.7	3.8	29.6
NEE	80.1	0.1	0.0	19.8		NEE	49.6	0.0	0.0	50.4
SOC	82.4	0.3	0.1	17.2		SOC	55.1	0.1	0.2	44.6
N_2O	32.4	57.3	10.3	0.0		N_2O	66.9	12.6	20.6	0.0
SNO_3	46.4	22.8	30.7	0.0		SNO_3	60.6	3.0	36.4	0.0
SNH_4	30.7	60.3	9.0	0.0		SNH_4	66.6	14.3	19.1	0.0
SCORE1	*26*	*13*	*8*	*7*		*SCORE2*	*26*	*7*	*9*	*13*
Parameter	DM	NH_4-N	ON	OC	Poultry FYM	Parameter	DM	NH_4-N	ON	OC
LAI	50.7	2.6	10.7	36.0		LAI	8.3	17.2	41.1	33.4
YIELD	48.8	2.5	12.9	35.8		YIELD	6.3	16.7	44.5	32.5
NEE	48.5	0.0	0.0	51.5		NEE	49.4	0.0	0.0	50.6
SOC	48.7	0.0	0.0	51.3		SOC	49.5	0.0	0.0	50.5
N_2O	50.1	27.3	22.6	0.0		N_2O	66.3	19.8	13.9	0.0
SNO_3	46.1	7.6	46.3	0.0		SNO_3	63.6	5.7	30.7	0.0
SNH_4	49.9	29.0	21.1	0.0		SNH_4	65.8	21.2	13.0	0.0
SCORE1	*21*	*9*	*11*	*13*		*SCORE2*	*20*	*8*	*12*	*13*

*Left charts: full range; right charts: median±10% range.

*Table S10. Relative contribution of the investigated slurry input parameters (in columns) to the variance of the selected outputs (in rows) and the SCORE for each input showing their importance in terms of output uncertainty. Simulation results for sandy soil at Kiskunhalas**

Parameter	DM	NH_4-N	ON	OC		Parameter	DM	NH_4-N	ON	OC
LAI	42.6	37.9	19.5	0.0	Cattle Slurry	LAI	66.1	17.5	14.9	1.6
YIELD	47.2	33.0	19.6	0.2		YIELD	68.4	15.0	14.5	2.2
NEE	15.7	54.6	28.6	1.1		NEE	74.1	13.2	12.0	0.6
SOC	74.8	12.7	10.9	1.7		SOC	73.9	8.3	12.2	5.7
N_2O	41.2	42.0	16.8	0.0		N_2O	60.4	22.9	15.8	0.9
SNO_3	45.9	21.6	32.4	0.0		SNO_3	63.0	14.9	21.6	0.4
SNH_4	39.3	45.8	14.9	0.0		SNH_4	59.7	25.9	13.4	1.0
SCORE1	*19*	*16*	*9*	*7*		*SCORE2*	*27*	*9*	*8*	*7*
Parameter	DM	NH_4-N	ON	OC	Pig Slurry	Parameter	DM	NH_4-N	ON	OC
LAI	32.1	58.2	9.6	0.0		LAI	67.0	28.2	3.7	1.1
YIELD	38.1	53.1	8.6	0.3		YIELD	29.6	18.0	2.9	49.5
NEE	21.2	67.0	11.3	0.5		NEE	7.6	45.5	6.0	40.9
SOC	52.0	37.3	9.1	1.6		SOC	71.2	7.3	2.2	19.3
N_2O	37.3	55.9	6.9	0.0		N_2O	60.2	35.1	4.6	0.1
SNO_3	43.1	42.0	14.9	0.0		SNO_3	64.1	27.8	8.1	0.0
SNH_4	36.5	57.8	5.7	0.0		SNH_4	59.6	36.4	3.8	0.1
SCORE1	*16*	*21*	*7*	*7*		*SCORE2*	*22*	*13*	*7*	*11*

*Left charts: full range; right charts: median±10% range.

SUPPLEMENTARY REFERENCES

Alfaro, M., Salazar, F., Hube, S., Ramírez, L. and Mora Ma, S. 2018. Ammonia and nitrous oxide emissions as affected by nitrification and urease inhibitors. *Journal of Plant Nutrition and Soil Science* 18. 479–486. https://doi.org/10.4067/S0718-95162018005001501

Amon, B., Kryvoruchko, V., Amon, T. and Zechmeister-Boltenstern, S. 2006. Methane, nitrous oxide and ammonia emissions during storage and after application of dairy cattle slurry and influence of slurry treatment. *Agriculture, Ecosystems & Environment* 112. (2–3): 153–62. https://doi.org/10.1016/j.agee.2005.08.030

Árendás, T. 2019. *Unpublished Manure Nutrient Data.* Martonvásár, Hungary, Department of Crop Production, Center for Agricultural Research (in Hungarian).

Benne, E.J, Hoglund, C.R., Longnecker, E.C. and Cook, R.L. 1961. Animal manures. In *Szennyvizek, iszapok, komposztok, szervestrágyák a talajtermékenység szolgálatában (*Wastewater, sludge, compost, and organic fertilizers in the service of soil fertility). Ed.: Kádár, I. 2013, Budapest, Hungary, Akaprint Nyomda Kft.

Bertora, C., Alluvione, F., Zavattaro, L., van Groenigen, J.W., Velthof, G. and Grignani, C. 2008. Pig slurry treatment modifies slurry composition, N_2O, and CO_2 emissions after soil incorporation. *Soil Biology & Biochemistry* 40. 1999–2006. https://doi.org/10.1016/j.soilbio.2008.03.021

Bhandral, R., Bittman, S., Kowalenko, G., Buckley, K., Chantigny, M.H., Hunt, D.E., Bounaix, F. and Friesen, A. 2009. Enhancing soil infiltration reduces gaseous emissions and improves N uptake from applied dairy slurry. *Journal of Environmental Quality* 38. 1372–1382. https://doi.org/10.2134/jeq2008.0287

Bol, R., Moering, J., Kuzyakov, Y. and Amelung, W. 2003. Quantification of priming and CO_2 respiration sources following slurry-C incorporation into two grassland soils with different C content. *Rapid Communications in Mass Spectrometry* 17. 2585–2590. https://doi.org/10.1002/rcm.1184

Brown, C. 2013. *Available Nutrients and Value for Manure from Various Livestock Types.* Guelph, ON, Canada, Ministry of Agriculture, Food and Rural Affairs. https://files.ontario.ca/omafra-available-nutrients-and-value-for-manure-from-various-livestock-types-21-077-en-2022-11-24.pdf

Cavalli, D., Cabassi, G., Borrelli, L., Geromel, G., Bechini, L., Degano, L. and Gallina, P.M. 2016. Nitrogen fertilizer replacement value of undigested liquid cattle manure and digestates. *European Journal of Agronomy* 73. 34–41. https://doi.org/10.1016/j.eja.2015.10.007

Chadwick, D.R., Pain, B.F. and Brookman, S.K.E. 2000a. Nitrous oxide and methane emissions following application of animal manures to grassland. *Journal of Environmental Quality* 29. 277–287. https://doi.org/10.2134/jeq2000.00472425002900010035x

Chadwick, D.R., John, F., Pain, B.F., Chambers, B. and Williams, J.R. 2000b. Plant uptake of nitrogen from the organic nitrogen fraction of animal manures: a laboratory experiment. *The Journal of Agricultural Science* 134. 159–168. https://doi.org/10.1017/S0021859699007510

Chadwick, D.R., Sommer, S., Thorman, R., Fangueiro, D., Cardenas, L., Amon, B. and Misselbrook, T.H. 2011. Manure management: Implications for greenhouse gas emissions. *Animal Feed Science and Technology* 166–167. 514–531. https://doi.org/10.1016/j.anifeedsci.2011.04.036

Chambers, B.J., Lord, E.I., Nicholson, F.A. and Smith, K.A. 1999. Predicting nitrogen availability and losses following arable land application of manures: MANNER. *Soil Use and Management* 15. 137–143. https://doi.org/10.1111/j.1475-2743.1999.tb00079.x

Chastain, J.P. and Camberato, J.J. 2003. Dairy manure production and nutrient content. In *Confined Animal Manure Managers Certification Program Dairy Training Manual.* Clemson, SC, US, Clemson University Cooperative Extension Service, Chapter 3a, 1–16. https://www.clemson.edu/extension/camm/manuals/dairy/dch3a_04.pdf

Csaba, L., Kiss, O., Szinay, M. and Vermes, L. 1978. *Hígtrágya-hasznosítás* (Slurry utilization). Budapest, Hungary, Mezőgazdasági Kiadó.

Curkan, M.A. 1985. Agrohimicseszkie osznovű primenenija organicseszkih udobrenij: Izd-vo „Stiinca." Kisinyov. (Agrochemical applications of organic fertilizers: Published by "Stiinca." Chisinau.) In *Szennyvizek, iszapok, komposztok, szervestrágyák a talajtermékenység szolgálatában* (Wastewater, sludge, compost, and organic fertilizers in the service of soil fertility). Ed.: Kádár, I. 2013, Budapest, Hungary, Akaprint Nyomda Kft.

DEFRA, 2010. *Fertiliser Manual (RB209).* 8th edition. London, UK, Food and Rural Affairs Great Britain, Department for Environment, Food & Rural Affairs.

Fangueiro, D., Senbayran, M., Trindade, H. and Chadwick, D. 2008. Cattle slurry treatment by screw press separation and chemically enhanced settling: Effect on greenhouse gas emissions after land spreading and grass yield. *Bioresource Technology* 99. 7132–7142. https://doi.org/10.1016/j.biortech.2007.12.069

Hartman, M. 2010. *Szervestrágyázás* (Organic fertilization). Budapest, Hungary, Nemzeti Szakképzési és Felnőttképzési Intézet. https://www.nive.hu/Downloads/Szakkepzesi_dokumentumok/Bemeneti_kompetenciak_meresi_ertekelesi_eszkozrendszerenek_kialakitasa/20_3112_005_101030.pdf

Levi-Minzi, R., Riffaldit, R. and Saviozzi, A. 1986. Organic Matter and Nutrients in Fresh and Mature Farmyard Manure. *Agricultural Wastes* 16. 225–236. doi:10.1016/0141-4607(86)90068-5

McGinn, S.M. and Sommer, S.G. 2007. Ammonia emissions from land-applied beef cattle manure. *Canadian Journal of Soil Science* 87. 345–352. https://doi.org/10.4141/S06-053

Menzi, H. 2002. Manure management in Europe. In *10th FAO Ramiran Conference on Recycling of Organic Residues in Agriculture.* Eds.: Venglovsky, J. and Greserova, G., Strebske Pleso, Slovakia, University of Veterinary Medicine in Kosice, 93–102.

Misselbrook, T.H., Nicholson, F., Chambers, B. and Johnson, R. 2005a. Measuring ammonia emissions from land applied manure: An intercomparison of commonly used samplers and techniques. *Environmental Pollution* 135. 389–397. https://doi.org/10.1016/j.envpol.2004.11.012

Misselbrook, T.H., Nicholson, F.A. and Chambers, B.J. 2005b. Predicting ammonia losses following the application of livestock manure to land. *Bioresource Technology* 96. 159–168. https://doi.org/10.1016/j.biortech.2004.05.004

Nguyen, Q.V., Wu, D., Kong, X., Bol, R., Petersen, S.O., Jensen, L.S. Liu, S., Brüggemann, N., Glud, R.N., Larsen, M. and Bruun, S. 2017. Effects of cattle slurry and nitrification inhibitor application on spatial soil O_2 dynamics and N_2O production pathways. *Soil Biology & Biochemistry* 114. 200–209. https://doi.org/10.1016/j.soilbio.2017.07.012

Pettygrove, G.S., Heinrich, A.L. and Eagle, A.J. 2009. *Dairy Manure Nutrient Content and Forms.* University of California Cooperative Extension Manure Technical Bulletin Series.

Properties of manure, 2005. Manitoba, CA, Manitoba Agriculture, Food and Rural Development. Available at https://www.gov.mb.ca/agriculture/environment/nutrient-management/pubs/properties-of-manure.pdf

Rajendran, K., Aslanzadeh, S. and Taherzadeh, M.J. 2012. Household biogas digesters – A review. *Energies* 5. 2911–2942. https://doi.org/10.3390/en5082911

Rao, J.R., Watabe, M., Stewart, T.A., Millar, B.C. and Moore, J.E. 2007. Pelleted organo-mineral fertilizers from composted pig slurry solids, animal wastes and spent mushroom compost for amenity grasslands. *Waste Management* 27. 1117–1128. https://doi.org/10.1016/j.wasman.2006.06.010

Richner, W., Flisch, R., Mayer, J., Schlegel, P., Zähner, M. and Menzi, H. 2017. Eigenschaften und Anwendung von Düngern. *Grundlagen für die Düngung landwirtschaftlicher Kulturen in der Schweiz (GRUD) Agrarforschung Schweiz* 8. (6): Spezialpublikation. 4. https://www.agrarforschungschweiz.ch/wp-content/uploads/2019/12/2017_06_2297.pdf (accessed 25 September 2025).

Rodhe, L., Pell, M. and Yamulki, S. 2006. Nitrous oxide, methane and ammonia emissions following slurry spreading on grassland. *Soil Use Management* 22. 229–237. https://doi.org/10.1111/j.1475-2743.2006.00043.x

Sesztakov, A.G. 1961. *Agrokémia* (Agrochemistry). Budapest, Hungary, Mezőgazdasági Kiadó. https://real.mtak.hu/95855/1/at_1961_10_4_575-576.pdf

Smith, K.A., Jackson, D.R., Misselbrook, T.H., Pain, B.F. and Johnson, R.A. 2000. Reduction of ammonia emission by slurry application techniques. *Journal of Agricultural Engineering Research* 77. 277–287. https://doi.org/10.1006/jaer.2000.0604

Stefanovits, P., Láng, G., Sipos, G., Sarkadi, J., Darab, K., Balla A., Krámer, M., Gléria, J., Klimes-Szmik, A., Kerpely, A. and Szekrényi, B. 1964. *Mezőgazdák talajismereti és trágyázási útmutatója* (Farmers' guide to soil science and fertilization management). Budapest, Hungary, Mezőgazdasági Kiadó.

Szpravocsnik, 1964. Szpravocsnik po Udobrenijam (Reference book on fertilizers). Moscow, Izd-vo „Kolosz". In *Szennyvizek, iszapok, komposztok, szervestrágyák a talajtermékenység szolgálatában* (Wastewater, sludge, compost, and organic fertilizers in the service of soil fertility). Ed.: Kádár, I. 2013, Budapest, Hungary, Akaprint Nyomda Kft.

Thompson, R.B., Pain, B.F. and Lockyer, D.R. 1990. Ammonia volatilization from cattle slurry following surface application to grassland. *Plant and Soil* 125. 119–128. https://doi.org/10.1007/BF00010751

Thompson, R.B. and Meisinger, J.J. 2002. Management factors affecting ammonia volatilization from land-applied cattle slurry in the Mid-Atlantic USA. *Journal of Environmental Quality* 31. 1329–1338. https://doi.org/10.2134/jeq2002.1329

DOI: 10.15201/hungeobull.75.1.4 Hungarian Geographical Bulletin **75** 2026 (1) 91–106.

Slope-driven edge analysis of high-resolution LiDAR data for automated detection of cultural terraces in Slovenia

Lenart ŠTAUT[1,2], Rok CIGLIČ[2] and Blaž REPE[1]

Abstract

Cultural terraces were often constructed to improve agriculture. Some terraces are still in use, while others have been abandoned. Knowledge of their locations is important for their preservation or potential reuse. There have been several attempts worldwide to create a register of terraces. In Slovenia, a suitable register has not yet been created due to heavy overgrowth and significant differences in cultural terrace types across different regions of the country. This research proposes detecting terraces using a LiDAR digital elevation model, geoinformation tools, and additional spatial data. The method detects sharp changes in slope data and creates polygons where such changes are detected in close proximity. The main advantage of the method is that it does not require any training samples yet still provides accurate results despite the diversity of terraced areas. We applied the method in Slovenia and achieved an accuracy of 91 percent, a precision of 76 percent, and a recognition value of 66 percent in one test area, and 92, 47, and 65 percent in another designated test area. To achieve higher accuracy, the input settings can be adapted to regional characteristics, which confirms earlier findings that terraces in Slovenia exhibit high diversity.

Keywords: terraced landscapes, feature detection, remote sensing, DEM, LiDAR, geomorphometry, Mediterranean, Slovenia

Received November 2025, accepted February 2026.

Introduction

A crop terrace consists of a flat or gently sloping area of varying width and length, which has been recently or historically cultivated, and terrace banks of varying heights. Terrace slopes can be made of different materials; they may be grassed over, paved, or stabilised with stones (Titl, J. 1965; Drobnjak, V. 1990; Ažman Momirski, L. and Kladnik, D. 2009; Kladnik, D. *et al.* 2016). Knowledge of the location of cultural terraces is important for their maintenance, conservation, and further studies, such as analysing soil degradation (Pijl, A. *et al.* 2021). Knowledge of their location and other geographical features would improve our understanding of the reasons for the construction of cultural terraces and their ecological, social, and economic roles in the landscape (Ferrarese, F. *et al.* 2019). In Slovenia, based on similar international initiatives, Berčič, T. (2016) proposed the establishment of a database on the distribution of cultural terraces, which could be continuously updated. There are various ways of recording the locations of terraced areas, but the approaches can be broadly categorised into field mapping and mapping using GIS (geographic information systems) tools. Field mapping of terraced areas is time-consuming and expensive for larger areas. Difficult access, overgrown areas, and

[1] University of Ljubljana, Faculty of Arts, Aškerčeva cesta 2, 1000 Ljubljana, Slovenia. Corresponding author's e-mail: lenart.staut@zrc-sazu.si

[2] Research Centre of the Slovenian Academy of Sciences and Arts, Anton Melik Geographical Institute, Novy trg 2, 1000 Ljubljana, Slovenia.

subjective recognition and interpretation of terrace areas are the main reasons why such field-based studies have only been conducted for smaller areas, either in Slovenia or abroad (e.g. Titl, J. 1965; Križaj Smrdel, H. 2010; Kladnik, D. *et al.* 2016; Zhang, Y. *et al.* 2017).

In addition to field surveys, terraces can also be recorded using computer techniques with various geodata. Different techniques for visualising the digital relief model can reveal cultural terraces in different ways. For visualisation, various methods can be used to represent the relief or surface, such as hillshade, sky-view factor (Zakšek, K. *et al.* 2011), surface curvature (Koenders, R. *et al.* 2014), visualisation for archaeological topography (VAT) (Verbovšek, T. *et al.* 2019), and other geomorphological algorithms. The digitisation of terraces is only possible on the basis of these visualisations, but it can be influenced by subjectivity. These limitations have led to the development of various remote sensing methods for the automatic detection of cultural terraces, which are more or less successful in recognising terraced areas.

Terraces can be identified using different approaches such as:

– Object-based image analysis: Diaz-Varela, R.A. *et al.* 2014; Capolupo, A. *et al.* 2018; Sun, W. *et al.* 2019; Zhao, F. *et al.* 2021; Yu, M. *et al.* 2022.
– Canny edge detection method: Dai, W. *et al.* 2019.
– Machine learning based on object-based image analysis: Pijl, A. *et al.* 2020.
– Manual mapping: Pijl, A. *et al.* 2021.
– Edge detection on slope data: Sofia, G. *et al.* 2016.

The first comprehensive survey of terraces in Slovenia was conducted by Kladnik, D. *et al.* (2016), who manually digitised terrace areas from digital orthophotos. Using convolutional neural networks and learning patterns from the research of Kladnik, D. *et al.* (2016), cultural terraces were later identified by Glušič, A. *et al.* (2021) in southwestern Slovenia and by Ciglič, R. *et al.* (2024) for the whole of Slovenia. For smaller areas, terrace areas were identified using various relief representations in the Vipava Valley (Berčič, T. and Ažman Momirski, L. 2023) and the Jeruzalem-Ormož Hills (Pipan, P. and Kokalj, Ž. 2017). Edge detection was used to identify terraces in the Vipava Hills by Štaut, L. 2025.

Databases covering larger areas, such as the entire country (e.g. Kladnik, D. *et al.* 2016), are rare and often incomplete, for example due to terraces that are missing because they are covered by forest and therefore not clearly visible on orthophotos. Suitable methods for identifying cultural terraces are still being developed and often depend on the subjective judgement of researchers or on trial and error to achieve optimal results. Methods based on deep learning have been somewhat more successful (Glušič, A. *et al.* 2021; Zhao, F. *et al.* 2021; Lu, Y. *et al.* 2023; Ciglič, R. *et al.* 2024). However, deep learning methods require precise, numerous, and diverse training examples (Glušič, A. *et al.* 2021). In Slovenia, the study by Ciglič, R. *et al.* (2024) used datasets from Kladnik, D. *et al.* (2016) for this purpose, which were created by manually digitising terraced areas from digital orthophotos.

Due to the great diversity of cultural terraces, terrace banks are often discontinuous on the digital elevation model, making it difficult to distinguish them correctly from other similar small features. The methods used so far in Slovenia to recognise cultural terraces have produced results with a low success rate (e.g. Jaccard-index 0.13 by Ciglič, R. *et al.* [2024]) and have been associated with various problems related to the training samples. To date, no such accurate detection of cultural terraces has been achieved in Slovenia, as examples from abroad demonstrate (e.g. Spano, A. *et al.* [2018] – 70% detection success rate; Lu, Y. *et al.* [2023] – 84% success rate). One of the most suitable and fastest data processing methods for extracting terraces is surface slope analysis. Slope analysis has been used by many authors for visual mapping of cultural terraces (Berčič, T. 2016; Sofia, G. *et al.* 2016; Capolupo, A. *et al.* 2018; Spanò, A. *et al.* 2018). If the resolution of the digital elevation model is sufficiently high, it is also possible to capture smaller or narrower terraces that may not be visible on low-resolution digital elevation models.

By developing a new slope edge detection method for recognising terraces, we aimed to address the shortcomings of established detection methods. The aim of this article is to present a new method for detecting cultural terraces based on slope-based edge detection that does not use training samples, and to evaluate the detection success rate using previous cultural terrace research in Slovenia.

Methods

We developed a new method for cultural terrace detection *(Figure 1)* based on the identification of strong relief changes in slope data, as part of broader research on terraces in Slovenia. All calculations were performed using ESRI ArcGIS Pro 3.2 software with ModelBuilder. Using data from the 0.5 m × 0.5 m digital elevation model (Triglav Čekada, M. and Bric, V. 2015), we calculated the slope and detected sharp changes using surface filters. LiDAR data were acquired for the Slovenian Environmental Agency for the entire country between 2011 and 2015, with at least 2 points per m² for the first return; some areas were scanned with higher point density, ellipsoid height accuracy of 15 cm, and positional accuracy of 30 cm. By adding barrier features, we considered only the changes that are part of the terrace banks. By merging the detected edges based on neighbourhood and barriers, we obtained the final layer of cultural terrace areas.

Slope-based identification of edges in the relief

The slope tool in ArcGIS Pro 3.2 is a procedure that uses a moving window of 3 x 3 cells and calculates, for each cell, the rate of change in the horizontal (east to west, *dz*/*dx*) and vertical (north to south, *dz*/*dy*) directions from the central cell to each neighbouring cell. The results are usually expressed in degrees, using the following equation (ESRI, 2025):

$$Slope = \tan^{-1}\left(\sqrt{\left(\left[\frac{dz}{dx}\right]^2 + \left[\frac{dz}{dy}\right]^2\right)}\right)$$

where *dz*/*dx* is the rate of change in the horizontal direction, and *dz*/*dy* in the vertical direction relative to the central cell. We used the Slope tool with default settings.

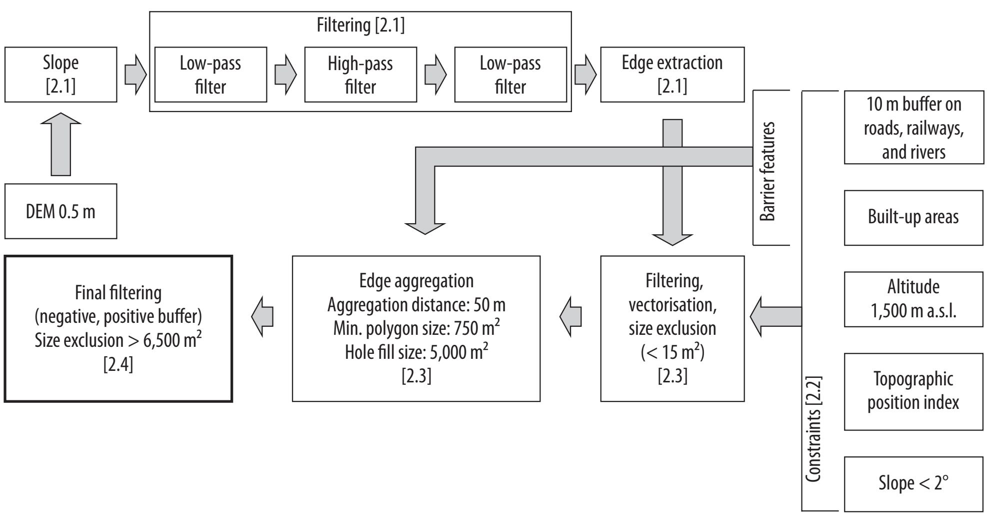

Fig. 1. Scheme of the research workflow. *Source:* Authors' own elaboration.

For further use, we require only data on the slopes, or the boundaries between the terrace bank and terrace platform. These are the locations where the slope changes significantly on the surface, but not on larger, non-flat areas with a uniform slope. Therefore, we applied a method combining low-pass and high-pass filters, which is also used in photography to remove blur (Susladkar, O. *et al.* 2022) and can be used to remove built-up areas from satellite images (Asal, F.F.F. 2019). A low-pass filter smooths the data by reducing local variance using a moving 3 × 3 cell window, thereby reducing noise. In this way, we smooth and eliminate minor changes on slopes that are not terraces, which appear to increase the range of steeper slopes around the terrace bank. By using a high-pass filter that emphasises the boundaries between objects, or where values change significantly between individual cells in a moving 3 × 3 cell window with a kernel sum of 0, we highlighted areas where the slope has changed. In areas where the slope is uniform, the raster values approach 0. The high-pass filter introduces more noise into the data. Surface irregularities too large to be eliminated in the initial smoothing process become visible again. Therefore, we reapplied a low-pass filter to the high-pass filter results to smooth these irregularities and apparently enlarge the area of detected slope change around the terrace banks *(Figure 2).*

Each terrace bank has two parts: an upper convex part and a lower concave part. After applying low-pass and high-pass filters, both parts were identified. Positive values indicate the convex part of the bank, while negative values indicate the concave part. The data obtained were visually inspected in five different areas: the Koper Hills, the Vipava Hills (Štaut, L. 2025), the Goriška Brda, the Jeruzalem-Ormož Hills, and the Posavje Hills,

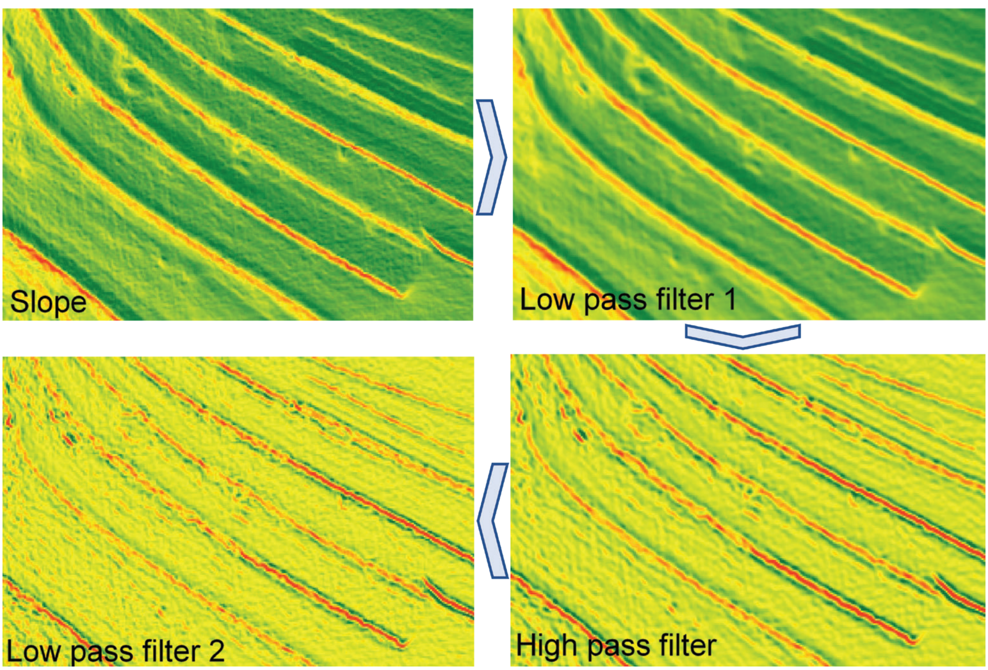

Fig. 2. Illustration of the individual steps of edge detection in the following order: calculation of the slope, application of a low-pass filter, application of a high-pass filter and re-application of the low-pass filter. *Source:* Authors' own elaboration.

to determine the threshold value distinguishing between edges on the convex and concave parts and to ensure that edges were detected on different types of terraces in various landscapes (Perko, D. *et al.* 2021). Values greater than 6 in the filtered slope data represented the areas of the convex part (edges), while all other cells (with negative values or values lower than 6) were assigned the value NODATA and were not used in further analysis.

Exclusion of areas based on additional data

At this point in the workflow, we have identified all edges that are sufficiently distinct on the surface. This includes edges that do not belong to terraces (e.g. road embankments, rocky outcrops, road ditches), which we excluded using constraints.

In this study, we focused solely on cultural terraces outside built-up areas, which is why we used the "built-up area and associated land" layer, the "roads and railways" layer, and the "watercourses" layer as constraints. For the Alpine hills area (Perko, D. *et al.* 2021), we also used the forest tracks layer as a constraint (Slovenia Forest Service. 2025). We applied a buffer of 10 m to the linear layers to capture strong changes in slope at the edges of roads or riverbanks.

According to Kladnik, D. *et al.* (2016), the highest terraces were found at altitudes up to 1400 m. The 2025 land use data from the Ministry of Agriculture, Forestry and Food indicate the highest marked arable land at about 1450 m. Therefore, we excluded all areas above 1500 m above sea level. Based on experience with remote sensing of cultural terraces (Zhao, F. *et al*. 2021; Ciglič, R. *et al*. 2024), we also excluded flat areas that do not exceed a slope of 2° on a 25 m digital elevation model (Ministry of Agriculture, Forestry and Food, 2026).

To eliminate pronounced slope changes in gullies and ridges, we used the topographic position index (TPI), which measures the elevation difference between the central point and the average elevation within a predefined range (*r*) (De Reu, J. *et al.* 2013). We used a radius of 60 cells (30 m) for *r*, which does not detect terrace banks up to a width of a few metres, but still detects other major changes on the surface. We categorised the TPI into three classes representing ridges, valleys, and flat surfaces or uniform slopes. TPI values between -1.1 and 1.5 (flat surfaces and uniform slopes), and less than -91.5 (floors of major valleys) were assigned the value NODATA and were not used as a constraint in further analyses. The remaining cells (with values from -91.5 to -1.1, representing gullies, and values above 1.5, representing ridges) were assigned the value 1 and used as one of the constraints. All input data, including the constraint and barrier features, are summarised in *Table 1*.

Table 1. Input and constraint features used in the research

Input data	Use	Resolution	Source
LiDAR	Edge detection, TPI	0.5 m	Slovenian Environmental Agency, 2015
TPI	Constraint feature	0.5 m	LiDAR (Slovenian Environmental Agency, 2015)
Roads	Constraint and barrier feature	Vector	Surveying and Mapping Authority of the Republic of Slovenia, 2025b
Railways	Constraint and barrier feature	Vector	Surveying and Mapping Authority of the Republic of Slovenia, 2025b
Rivers	Constraint and barrier feature	Vector	Surveying and Mapping Authority of the Republic of Slovenia, 2025b
Built-up area and related surfaces	Constraint and barrier feature	Vector	Ministry of Agriculture, Forestry and Food, 2025b
Forest tracks*	Constraint feature	Vector	Slovenia Forest Service, 2025
Slopes < 2°	Constraint feature	25 m	Surveying and Mapping Authority of the Republic of Slovenia, 2025a

*For Alpine hills only.

Edge merging

All constraint layers were rasterised at a resolution of 0.5 m and reclassified with the value 1 (constraint) and NODATA (no constraint), then aligned to the LiDAR data. The resulting layers were overlaid and summed with the layer of recognised edges. We retained all recognised edge cells where the value did not change. In the next step, the raster data were vectorised. Compared to the remaining noise in the data, terrace banks are relatively large linear spatial features that are close enough to each other to be merged based on proximity. We retained only polygons larger than 15 m². Smaller polygons usually represent noise in the data or minor relief changes that are not part of the cultural terraces. According to the literature (Titl, J. 1965; Drobnjak, V. 1990; Kladnik, D. *et al*. 2016), the vast majority of terraces in Slovenia are characterised by terrace platforms no wider than 50 m. The remaining edges were aggregated using the "Aggregate Polygons" tool, with barriers (see *Figure 1*) included to prevent polygons from merging across roads, railway lines, and built-up areas. The tool aggregated all detected edges closer than 50 m. During aggregation, it filled any holes smaller than 5000 m² and removed polygons smaller than 750 m².

Final filtering

The process of edge aggregation often produces narrow polygons that cannot be classified as terraced areas. Such errors, along with very small detected areas, were eliminated by applying a negative buffer of -10 m. The resulting layer was then assigned a 10 m buffer. In this way, polygons or parts of polygons narrower than 20 metres were removed. Based on the terrace platform width reported in the literature by Diaz-Varela, R.A. *et al.* (2014), the existing polygon sizes of terrace areas (Kladnik, D. *et al*. 2016), and a visual inspection of the test areas, all polygons with an area of less than 6,500 m² were also eliminated.

Analysis and evaluation of the terrace area identification

The obtained terrace area levels were used to calculate the areas and percentages of cultural terraces in Slovenian landscape types and administrative settlement areas. The results of the cultural terrace identification process were then analysed in two ways. The first, basic evaluation of the success of terrace area identification was carried out for two smaller areas *(Figure 3):*
– the area in the Vipava Valley, where terraced areas were mapped manually by examining the shaded relief (Berčič, T. 2016), and
– the Koper Hills area, using data from our own mapping of terraced areas, which we conducted by manually mapping terraced areas based on the analytical shaded relief of a 1 x 1 m digital elevation model.

The second evaluation of our results involved comparing them with the digitised terrace area data from Kladnik, D. *et al.* (2016). This evaluation was conducted for the entire country. We also repeated this comparison for the Koper Hills area, as we wanted to assess the accuracy of the only manually recorded terrace database for the whole of Slovenia.

For both the first (basic) and the second (comparison with Kladnik, D. *et al*. 2016) sets of terrace detection evaluation, we calculated quantitative indices: Jaccard-index, accuracy, precision, recall, and F1 score (Jaccard, P. 1912; Hicks, S.A. *et al.* 2022), which are commonly used to assess success rates in spatial analyses (e.g. Fisher, J.R.B. *et al*. 2018; Abdi, A.M. 2020; Kadyrov, R. *et al.* 2024). In this way, we were able to evaluate the accuracy of our method for detecting cultural terraces and to compare the results of our analysis with those of other studies.

Results

Characteristics of terraced areas and their distribution in Slovenia

Using the slope edge detection method, we identified 483.6 km² of terraced areas in Slo-

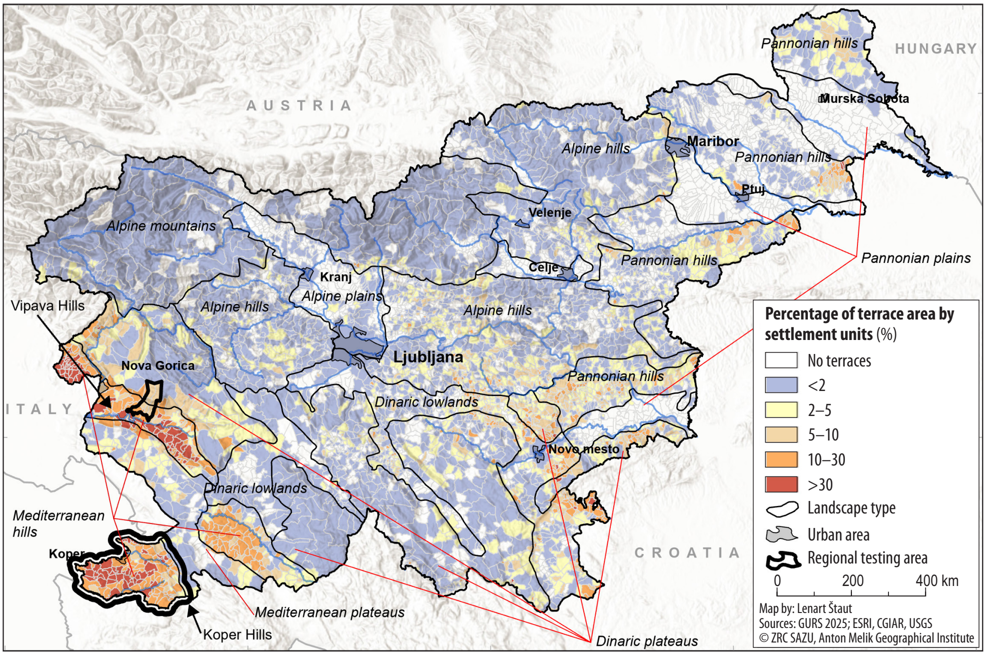

Fig. 3. Percentage of terraces by administrative settlement units. *Source:* Authors' own elaboration.

venia, representing 2.4 percent of the country (Štaut, L. 2025). The largest proportion of cultivated terraces is in the Mediterranean macro-region with 13.4 percent, followed by the Dinaric Alps with 2.2 percent, the Pannonian Basin with 1.4 percent, and the Alps with merely 0.7 percent.

The highest density of cultural terraces is found in the Mediterranean hills, with 0.26 km² of cultural terraces per km², while the lowest density occurs in the Pannonian plains. The Mediterranean hills account for as much as 45.1 percent of all cultural terraces, followed by the Dinaric plateaus with 16.4 percent, and the Pannonian hills with 12.3 percent. This distribution is also reflected in the proportion of terraced land within the administrative units of the settlements. In some units, more than 50 percent of the area is terraced. There are 40 such settlements in Slovenia, all but one of which are located in the Mediterranean hills. The settlement of Imenje in the Gorica Hills has the largest proportion of terraced land at 73.9 percent, followed by the settlement of Šmartno in the Gorica Hills with 70.5 percent, and Brdo in the Vipava Hills with 69.5 percent. Outside the Mediterranean hills, the proportion of terraced areas in the settlements is much lower. In the Mediterranean plateau type, the settlement of Tabor has the largest share (56.7%), while in the Pannonian low hills regional type, the settlement of Jeruzalem has the largest share (42.3%). In the Dinaric lowlands type, the settlement of Veliki Orehek near Novo Mesto has the largest share (39.5%), while in the Dinaric plateaus regional type, the settlements of Dolenje Nekovo (39.3%), Herinja Vas (35.8%), and Radovica (35.4%) have the largest shares of terraced land. In the Alpine hills landscape type, the highest proportion of terraced land is in the settlement of Straža pri Dolu (24.1%); in the Pannonian plain, it is in the settlement of

Norički Vrh (14%); in the Alpine mountains landscape type, in the settlement of Ravne (13.8%); and in the Alpine plain, in the settlement of Tunjice (4.2%).

The map (see *Figure 3*) shows six larger clusters where cultural terraces cover more than 20% of the settlement area. The largest proportion of such settlements is in the hinterland of Koper in the Koper Hills, the second in the area of the Vipava Valley and the Vipava Hills, and the third in the area of the Gorica Hills. In the south-east of the country, the areas under the Gorjanci Hills along the border with Croatia in White Carniola, as well as the areas of the Radulja Hills and the Krško Hills, stand out. In eastern Slovenia, the area of the Jeruzalem-Ormož Hills is notable. Within individual landscape types, there are significant differences in the density of cultural terraces. With the exception of the Mediterranean hills, these terraces occur locally in smaller areas and are not widespread across the entire landscape type.

Evaluation of the identification of cultural terraces

The basic evaluation was based on manually mapped terrace areas in the Koper Hills (own mapping) and the Vipava Hills (mapping according to Berčič, T. 2016) (*Table 2*). The highest overlap in terms of precision, recall, and F1 score was achieved in the Koper Hills, where the model correctly identified 66 percent of all manually mapped terrace surfaces. Similar results were obtained in the Vipava Hills, with 65 percent of areas correctly identified. The overall accuracy in both areas was just over 90 percent. The Jaccard-indices (see *Table 2*) were highest (0.54 out of 1) in the Koper Hills when comparing the terraces recognised by the slope edge detection method with the manually mapped terrace areas.

Table 2. Terrace identification performance in selected areas

Area	Koper Hills	Vipava Hills
Source of reference terraced areas	Own mapping	Mapping by Berčič, T. 2016
Accuracy	91%	92%
Precision	76%	47%
Recall	66%	65%
F1 score	0.71	0.55
Jaccard-index	0.54	0.38

As shown in *Table 3*, we calculated a confusion matrix for the area of the analysed settlements in the Vipava Valley. Using the slope edge detection method, we overestimated the areas of cultural terraces compared to the data from Berčič, T. (2016). We identified about 55 percent more areas than were mapped manually. We correctly identified 65.1 percent of terraced areas. The model did not recognise about 1 km² of the manually mapped terraces, which corresponds to almost one third of all manually mapped terraces.

We also presented a comparison of remote sensing and manual validation areas, with examples of common errors, for a smaller area in the Vipava Hills in *Figure 4* (see A, B and C inside). In the area marked with the letter A, the model overestimated the areas of cultural terraces. At this location, the sharp relief changes are due to the construction of

Table 3. Confusion matrices for terraced and non-terraced areas in the Vipava Hills

Vipava Hills		Slope edge detection, ha		*Total area*
		Terraced	Non-terraced	
Berčič's mapping	Terraced	186.29	99.86	*286.15*
	Non-terraced	208.14	3475.70	*3683.84*
Total area		*394.43*	*3475.56*	*3969.99*
		Slope edge detection, %		*Total percentage*
Berčič's mapping	Terraced	5	3	–
	Non-terraced	5	88	–
Total percentage		–	–	*100*

dry-stone walls. The situation is similar at site B, where a gully, which was not eliminated by the topographic position index, and traces of human alterations that are not cultural terraces are marked. At location C, the model did not recognise any cultural terraces, as the edges are not sufficiently pronounced. In the four settlements analysed, 10.7 percent of the settlement area is terraced according to the slope edge detection method, 7.8 percent according to Berčič, T. (2016), and 2.5 percent according to Kladnik, D. *et al.* (2016).

In the Koper Hills area, we detected 75.5 km² of cultural terraces *(Table 4)*, corresponding to 23.1 percent of the area. Manual terrace mapping, used as a reference for survey accuracy in this area, revealed 87.8 km² (26.9% of the area). Of the manually mapped cultural terraces, 57.6 km² (65.6%) match those identified by the slope detection method.

A visual comparison was made for a smaller section of the Koper Hills area shown in *Figure 5* (see D, E and F inside). In the area marked with the letter D, we identified cultural terraces that were not detected during manual mapping. This area contains anthropogenic structures in the form of dry-stone walls, which were recognised by the method. The area labelled with the letter E includes a gully that was not excluded by the TPI elimination process, or whose width is too small (less than 50 m), resulting in the merging of two polygons at the edges. In the area marked with the letter F, the model did not detect any terraces due to the proximity of the roads. The resulting polygon was too small or too narrow and was removed during the noise elimination process.

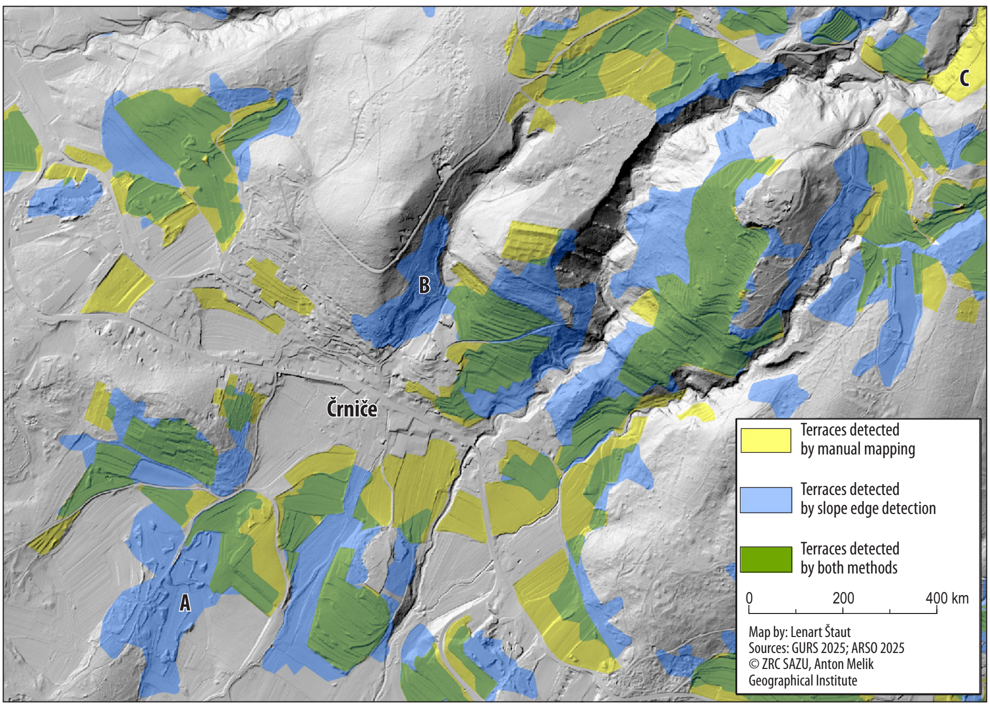

Fig. 4. Comparison of the results of manual mapping and the slope edge detection method in the Vipava Hills. *Source:* Authors' own elaboration.

Table 4. Confusion matrices for terraced and non-terraced areas in the Koper Hills

Koper Hills		Slope edge detection, ha		*Total area*
		Terraced	Non-terraced	
Manual mapping	Terraced	5,757.9	3,024.1	*8,782.0*
	Non-terraced	1,791.3	44,994.9	*46,786.1*
Total area		*7,549.1*	*48,019.0*	*55,568.1*
		Slope edge detection, %		*Total percentage*
Manual mapping	Terraced	10	5	–
	Non-terraced	3	81	–
Total percentage		–	–	*100*

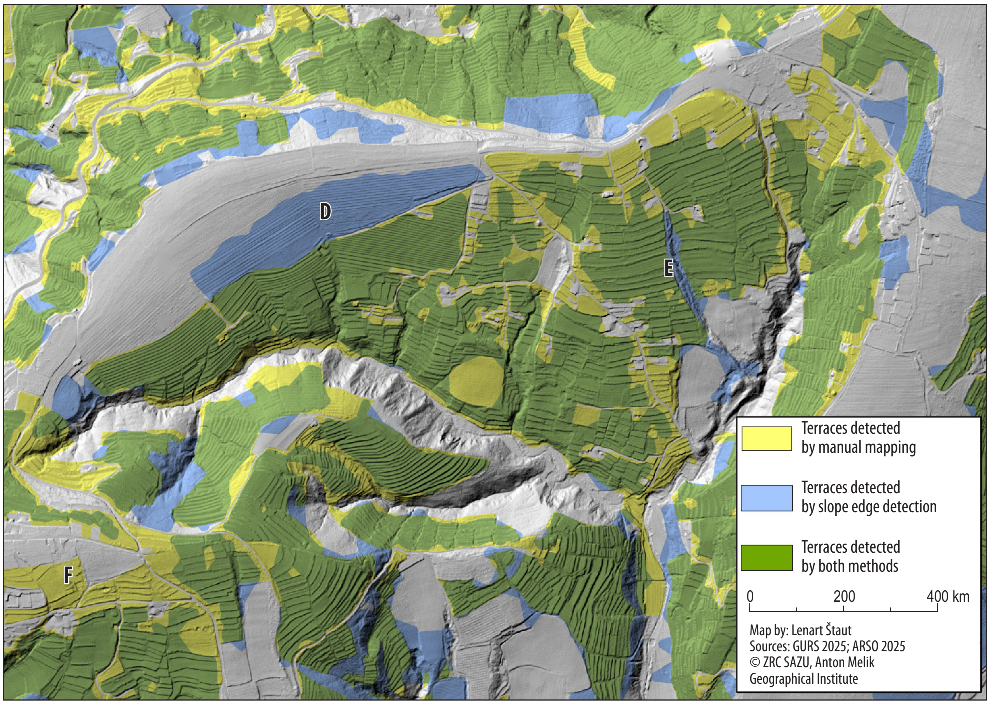

Fig. 5. Comparison of the results of manual mapping and the slope edge detection in the Koper Hills. *Source:* Authors' own elaboration.

Comparison with the existing terrace register

We compared the identified cultural terraces with the manually mapped terraces from the study by Kladnik, D. *et al.* (2016) for the entire territory of Slovenia. Despite some known shortcomings of this register, we aimed to assess the success rate *(Table 5)*, as it is the only nationwide database for terraces.

The relatively low overlap values in *Table 5* result from different approaches, particularly the disadvantage of the mapping of terraces

Table 5. Overlap of terraced areas according to the new method with the terraced areas for the entire territory of Slovenia*

Measure of accuracy	Value
Accuracy	97%
Precision	30%
Recall	45%
F1 score	0.36
Jaccard-index	0.22

*According to Kladnik, D. *et al.* 2016.

by Kladnik, D. *et al.* (2016), where, for example, areas under vegetation are missing.

To gain additional insights, we compared the manually recorded terraced areas on hillshade with those identified by Kladnik, D. *et al*. (2016) for the Koper Hills. Kladnik, D. *et al*. (2016) identified 58.2 km² of cultural terraces in this area, of which 44.5 km² (76.4%) overlap with our manually marked areas. Based on these data and the Jaccard-index (see *Table 2*), it is clear that the automatic detection method based on the digital elevation model was more successful in detecting cultural terraces than the manual mapping by Kladnik, D. *et al.* (2016), which relied only on orthophotos, topographic maps, and, in some cases, field observations, as we detected more cultural terraces. When comparing our manual mapping with the terraces identified by Kladnik, D. *et al*. (2016), the calculated Jaccard-index was 0.44, while the comparison between the slope detection method and Kladnik's mapping yielded an index value of 0.38. The highest overlap was found between the data obtained with the slope detection method and our own manually mapped terraces (0.54).

Discussion

Using the new slope detection method for recognising cultural terraces, which is based on edge detection on slope data, we identified 483.6 km² of terraces, or 2.4 percent of the area of Slovenia. Compared to the data on cultural terraces collected by Kladnik, D. *et al*. (2016) for the entire territory of Slovenia, we detected 161.9 km² more terraces. The difference in area is due to several factors. In our study, we used an automatic detection process sensitive to changes in relief. We detected smaller edges that may not belong to cultural terraces but can be falsely recognised as terraces when a large group of them is close together. Since we used the LiDAR DEM as input data, we were also able to detect cultural terraces beneath vegetation. Compared to Kladnik, D. *et al.* (2016), this is one of the main differences in the process of mapping cultural terraces.

Their data was based on manual mapping of cultural terraces using digital orthophotos and topographic map data. Therefore, their data mainly lacks cultural terraces under forest cover. Of the 483.6 km² of cultural terraces that we identified, 197.3 km² are under forest cover according to the land use data. This figure roughly corresponds to the difference between the areas of cultivated terraces determined by Kladnik, and the terraces defined in our research. The larger total area of cultural terraces that we detected with the slope detection method is also due to errors in automatic detection. Compared to the results of Ciglič, R. *et al*. (2024), we detected far fewer areas of cultural terraces with our method. They detected 1,397.2 km² of cultural terraces using machine learning, which is 913.6 km² more than we detected with our method. We conclude that the procedure according to Ciglič, R. *et al.* (2024) is too sensitive to small relief changes (drainage channels, arable land, minor surface irregularities), as the authors did not apply additional constraints to eliminate these shapes. A problem already highlighted by the authors (Ciglič, R. *et al.* 2024) is also the quality of the learning samples, which were based on Kladnik, D. *et al.* (2016) and therefore not sufficiently suitable for higher-quality machine learning.

The recognition performance of our method is comparable to the results of other approaches. Spanò, A. *et al.* (2018) recognised terraced areas at the regional level with a success rate of 70 percent, which is consistent with our success rates in the Koper Hills (65.6%) and the Vipava Hills (65.1%). Similar success rates (62.2% and 74.8%) were also obtained by Sun, W. *et al*. (2019) using object image analysis, while higher success rates of 87 and 90 percent were achieved using the U-net algorithm by Zhao, F. *et al*. (2021), and 96.9 and 98.4 percent by Lu, Y. *et al*. (2023). Ciglič, R. *et al*. (2024) calculated an accuracy of 89 percent on terraces, achieving a Jaccard-index of 0.68 for the area of Slovenia. Compared to our study, they achieved lower accuracy but a higher Jaccard-index. When comparing the results for smaller test areas (Glušič, A. *et al.* 2021; Ciglič, R. *et al*. 2024) and the Koper Hills area, which is comparable in terms of terrace density, the recognition results are similar *(Table 6).*

The newly developed method is not well suited to areas where the cultural terraces are not clearly visible (*Figure 6, e, f*). The slopes in such areas were excluded as noise due to their indistinctness, which could be improved in the future with settings adapted to the regional characteristics of the terraces. Forest tracks that are closer than 50 m on the slope and for which we did not obtain data on their location from the forest track register (2024) have a strong influence on the number of false-positive areas of the detected cultural terraces (*Figure 6, a, b, c)*. In areas where we had data on forest tracks and could therefore exclude them, there were far fewer false positives. Similar problems with forest tracks were also noted by Ciglič, R. *et al.* (2024). By using additional layers to delimit the areas where cultural terraces may occur, we were able to improve the quality of the data, similar to Spanò, A. *et al.* (2018). An additional problem can also be the quality of LiDAR data, where it shows relief changes caused by errors in data acquisition and preparation (Triglav Čekada, M. and Bric, V. 2015) (*Figure 6, d*).

Table 6. Basic success rates for the Koper Hills

Koper Hills	Slope edge detection	Testing area Ciglič, R. *et al.* 2024
Accuracy	91%	89%
Precision	76%	75%
Recall	66%	88%
F1 score	0.71	0.81
Jaccard-index	0.54	0.68

The terrace bank is typically a very small feature, usually no wider than a few metres (Berčič, T. 2016; Kladnik, D. *et al.* 2016). When the terrace bank consists of stones, its width on the digital relief model may be only one or two cells. The accuracy of the digital elevation model and the visibility of surface edges are also affected by vegetation (Triglav Čekada, M. and Bric, V. 2015). In our case, it appears as an interruption in the apparent line of the terrace slope.

The advantage of the slope edge detection method over other methods is that it does not require training samples and can be adapted to regional conditions with only minimal adjustments wherever LiDAR is available. In contrast, machine learning for terrace detection requires a large number of high-quality training samples (Zhao, F. *et al*. 2021; Lu, Y. *et al*. 2023; Ciglič, R. *et al*. 2024). The creation of training samples is also highly dependent on the accuracy of the person digitising, especially for a phenomenon as complex as cultural terraces, which do not have clearly defined boundaries (Van Coillie, F.M.B. *et al.* 2014; Berčič, T. 2016). Manual mapping of cultural terraces can be more accurate than other methods, but it is suitable only for smaller areas due to the time-consuming and potentially subjective nature of mapping cultural terraces (Kladnik, D. *et al.* 2016; Pijl, A. *et al.* 2021). Using the proposed method, we avoid these shortcomings by ensuring through initial method settings that it operates consistently in all areas, making the results independent of human influence. By using high-quality input data and appropriate constraint levels, we achieve similar accuracy more quickly. Cultural terraces in Slovenia, which are also highly diverse from a landscape perspective, vary greatly between regions (Kladnik, D. *et al.* 2016), and similar diversity is found worldwide (Diaz-Varela, R.A. *et al*. 2014; Sofia, G. *et al.* 2016; Kladnik, D. 2017; Yu, M. *et al*. 2022). By limiting the method to smaller homogeneous areas, we can adjust the sensitivity of the slope edge detection method. When applying the method to larger heterogeneous areas, as we did in our case, we adapted the

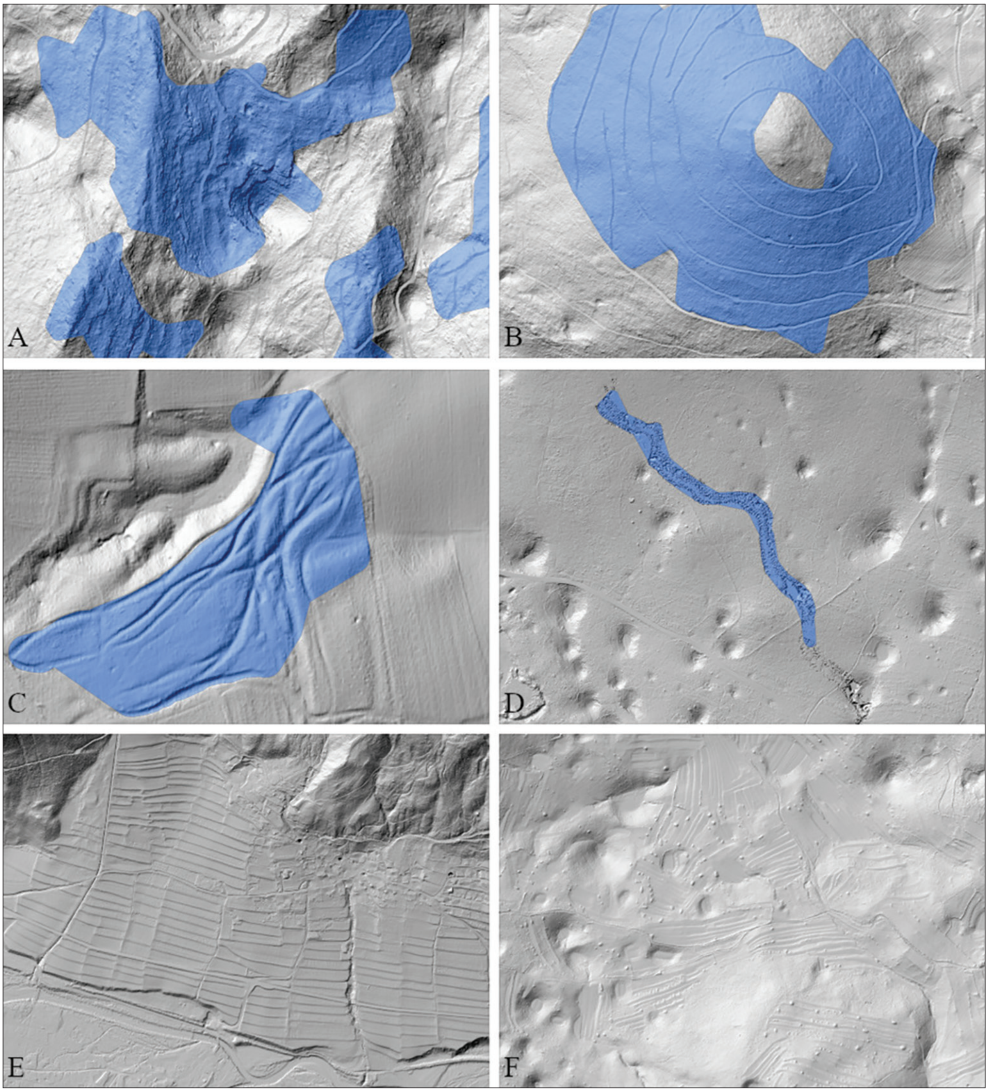

Fig. 6. Examples of false-positive (A–D) and false-negative (E–F) recognised terrace areas.
Source: Authors' own elaboration.

method to achieve the best average results, which can lead to overlooked or incorrectly identified terraced areas.

Conclusions

Terraced landscapes are found wherever humans have sought to increase land area for food production, reduce erosion, or enable mechanical cultivation of steep slopes. Many terraces have been abandoned for long periods and are now overgrown with vegetation. Therefore, accurate data on terrace distribution are important. In this paper, we demonstrate the performance of a new method for slope-based edge detection and aggregation on a LiDAR elevation model, without manual mapping or machine learning. We evaluated the detection of cultural terraces in selected areas. In the test areas of the Vipava Hills and the Koper Hills, we achieved overall accuracies of 91 and 92 percent, respectively, with recall values of 0.71 and 0.55. Compared to international studies (Spanò, A. *et al*. 2018; Lu, Y. *et al.* 2023), we achieved similar overall accuracy. Identification was most successful in areas where terraces were mechanically constructed at regular intervals (Pannonian hills) and in areas with well-defined, often stone-built banks (Mediterranean hills).

Outside these areas, there were more falsely recognised terraces despite the application of result filtering procedures. The analysis showed that, for more accurate recognition in all landscape types, the settings should be adjusted to regional characteristics and as many constraint layers as possible should be used. However, the results of the method, due to the speed of calculation and sufficient accuracy, can serve as a basis for collecting training samples in machine-learning recognition of cultural terraces.

***Acknowledgements*:** We would like to thank doc. dr. Tomaž Berčič for the data on terraces in Vipava Hills which helped us create better accuracy assessment. The authors acknowledge financial support from the Slovenian Research and Innovation Agency: Young researchers program (MR-56874), The Life and Death of Cultivated Terraces: Computer-Based Recognition and Spatial Analysis of Terraces (L6-60160) and research core funding program Geography of Slovenia (P6-0101). The study was also supported by the Slovenian Academy of Sciences and Arts (1/2026).

REFERENCES

Abdi, A.M. 2020. Land cover and land use classification performance of machine learning algorithms in a boreal landscape using Sentinel-2 data. *GIScience & Remote Sensing* 57. (1): 1–20. https://doi.org/10.1080/15481603.2019.1650447

Asal, F.F.F. 2019. Comparative analysis of the digital terrain models extracted from airborne LiDAR point clouds using different filtering approaches in residential landscapes. *Advances in Remote Sensing* 8. 51–75. https://doi.org/10.4236/ars.2019.82004

Ažman Momirski, L. and Kladnik, D. 2009. Terraced landscapes in Slovenia. *Acta geographica Slovenica* 49. (1): 7–37. https://doi.org/10.3986/AGS49101

Berčič, T. 2016. Discovering terraced areas in Slovenia: Reliable detection with LiDAR. *Annales. Series historia et sociologia* 26. (3): 449–468. https://doi.org/10.19233/ASHS.2016.35

Berčič, T. and Ažman Momirski, L. 2023. Inventory of dry-stone terraced landscape in the Vipava Valley. *Geodetski vestnik* 67. (4): 427–441. https://doi.org/10.15292/geodetski-vestnik.2023.04.427-441

Capolupo, A., Kooistra, L. and Boccia, L. 2018. A novel approach for detecting agricultural terraced landscapes from historical and contemporaneous photogrammetric aerial photos. *International Journal of Applied Earth Observation and Geoinformation* 73. 800–810. https://doi.org/10.1016/j.jag.2018.08.008

Ciglič, R., Glušič, A., Štaut, L. and Čehovin Zajc, L. 2024. Towards the deep learning recognition of cultivated terraces based on LiDAR data: The case of Slovenia. *Moravian Geographical Reports* 32. (1): 66–78. https://doi.org/10.2478/mgr-2024-0006

Dai, W., Hu, G., Huang, N., Zhang, P., Yan, X. and Tang, G. 2019. A contour-directional detection for deriving terrace ridge from open source images and digital elevation models. *IEEE Access* 7. 129215–129224. https://doi.org/10.1109/ACCESS.2019.2940437

De Reu, J., Bourgeois, J., Bats, M., Zwertvaegher, A., Gelorini, V., de Smedt, P., Chu, W., Antrop, M., de Maeyer, P., Finke, P., van Meirvenne, M., Verniers, J. and Crombe, P. 2013. Application of the topographic position index to heterogeneous landscapes. *Geomorphology* 186. 39–49. https://doi.org/10.1016/j.geomorph.2012.12.015

Diaz-Varela, R.A., Zarco-Tejada, P.J., Angileri, V. and Loudjani, P. 2014. Automatic identification of agricultural terraces through object-oriented analysis of very high resolution DSMs and multispectral imagery obtained from an unmanned aerial vehicle. *Journal of Environmental Management* 134. 117–126. https://doi.org/10.1016/j.jenvman.2014.01.006

Drobnjak, V. 1990. Fizičnogeografski pomen kulturnih teras (Physicalgeography significance of cultural terraces). In *Primorje – Zbornik 15. zborovanja slovenskih geografov*. Ed.: Orožen Adamič, M., Ljubljana, Zveza geografov Slovenije, 139–144.

ESRI 2025. *How Slope works*. ArcGIS Pro 3.4 by Environmental Systems Research Institute. Redlands, CA, USA, ESRI Inc. Available at https://pro.arcgis.com/en/pro-app/3.4/tool-reference/spatial-analyst/how-slope-works.htm

Ferrarese, F., Pappalardo, S.E., Cosner, A., Brugnaro, S., Alum, K., dal Pozzo, A. and de Marchi, M. 2019. Mapping agricultural terraces in Italy. Methodologies applied in the MAPTER project. *World Terraced Landscapes: History, Environment, Quality of Life* 9. 179–194. https://doi.org/10.1007/978-3-319-96815-5_11

Fisher, J.R.B., Acosta, E.A., Dennedy-Frank, P.J., Kroeger, T. and Boucher, T.M. 2018. Impact of satellite imagery spatial resolution on land use

classification accuracy and modelled water quality. *Remote Sensing in Ecology and Conservation* 4. (2): 137–149. https://doi.org/10.1002/rse2.61
Glušič, A., Ciglič, R. and Čehovin Zajc, L. 2021. Zaznavanje terasiranih pokrajin kot semantična segmentacija digitalnega modela višin (Detection of terraced landscapes as semantic segmentation of a digital elevation model). In *Zbornik mednarodne Elektrotehniške in računalniške conference.* Portorož, Slovenija, ERK'2021. 378–381. http://www.dlib.si/?URN=URN:NBN:SI:DOC-BMENDE0Q
Hicks, S.A., Strümke. I., Thambawita, V., Hammou, M., Riegler, M.A., Halvorsen, P. and Parasa, S. 2022. On evaluation metrics for medical applications of artificial intelligence. *Scientific Reports* 12. (1): 5979. https://doi.org/10.1038/s41598-022-09954-8
Jaccard, P. 1912. The distribution of the flora in the Alpine zone. *New Phytologist* 11. (2): 37–50. https://doi.org/10.1111/j.1469-8137.1912.tb05611.x
Kadyrov, R., Statsenko, E. and Nguyen, T.H. 2024. Integrating μCT imaging of core plugs and transfer learning for automated reservoir rock characterization and tomofacies identification. *Marine and Petroleum Geology* 168. 107014. https://doi.org/10.1016/j.marpetgeo.2024.107014
Kladnik, D., Ciglič, R., Geršič, M., Kokalj, Ž., Volk Bahun, M., Perko, D., Lenarčič, M., Kerbler, B.K., Orožen Adamič, M. and Vovk, A. 2016. *Terasirane pokrajine: Ob sedemdesetletnici Geografskega inštituta Antona Melika ZRC SAZU* (Terraced landscapes: On the occasion of the seventieth anniversary of the Anton Melik Geographical Institute ZRC SAZU). Ljubljana, Založba ZRC.
Kladnik, D. 2017. *Terraced Landscapes.* Ljubljana, Založba ZRC. https://doi.org/10.3986/9789610500193
Koenders, R., Lindenbergh, R.C., Storms, J.E.A. and Menent, M. 2014. Multiscale curvatures for identifying channel locations from DEMs. *Computers & Geosciences* 68. 11–21. https://doi.org/10.1016/j.cageo.2014.03.016
Križaj Smrdel, H. 2010. Kulturne terase v slovenskih pokrajinah (Cultural terraces in Slovenian landscapes). *Dela* 34. 39–60. https://doi.org/10.4312/dela.34.39-60
Lu, Y., Li, X., Xin, L., Song, H. and Wang, X. 2023. Mapping the terraces on the Loess Plateau based on a deep learning-based model at 1.89 m resolution. *Scientific Data* 10. (1): 115. https://doi.org/10.1038/s41597-023-02005-5
Ministry of Agriculture, Forestry and Food 2025. *Evidenca dejanske rabe kmetijskih in gozdnih zemljišč* (Records of actual use of agricultural and forest land). Ljubljana, MKGP.
Perko, D., Ciglič, R. and Hrvatin, M. 2021. Landscape macrotypologies and microtypologies of Slovenia. *Acta geographica Slovenica* 61. (3): 7–89. https://doi.org/10.3986/AGS.10384
Pijl, A., Reuter, L.E.H., Quarella, E., Vogel, T.A. and Tarolli, P. 2020. GIS-based soil erosion modelling under various steep-slope vineyard practices. *CATENA* 193. 104604. https://doi.org/10.1016/j.catena.2020.104604
Pijl, A., Quarella, E., Vogel, T.A., d'Agostino, V. and Tarolli, P. 2021. Remote sensing vs. field-based monitoring of agricultural terrace degradation. *International Soil and Water Conservation Research* 9. (1): 1–10. https://doi.org/10.1016/j.iswcr.2020.09.001
Pipan, P. and Kokalj, Ž. 2017. Transformation of the Jeruzalem Hills cultural landscape with modern vineyard terraces. *Acta geographica Slovenica* 57. (2): 149–162. https://doi.org/10.3986/AGS.4629
Slovenia Forest Service 2025. *Evidenca gozdnih vlak – interno delovno gradivo Zavoda za gozdove Slovenije* (Records of forest tracks – internal working material of the Slovenian Forest Service). Ljubljana, ZGS.
Slovenian Environmental Agency 2015. *Lasersko skeniranje Slovenije* (Laser scanning of Slovenia). Ljubljana, Agencija za Okolje, Republika Slovenija.
Sofia, G., Bailly, J.S., Chehata, N., Tarolli, P. and Levavasseur, F. 2016. Comparison of pleiades and LiDAR digital elevation models for terraces detection in farmlands. *IEEE Journal of Selected Topics in Applied Earth Observations and Remote Sensing* 9. (4): 1567–1576. https://doi.org/10.1109/JSTARS.2016.2516900
Spanò, A., Sammartano, G., Calcagno Tunin, F., Cerise, S. and Possi, G. 2018. GIS-based detection of terraced landscape heritage: Comparative tests using regional DEMs and UAV data. *Applied Geomatics* 10. (2): 77–97. https://doi.org/10.1007/s12518-018-0205-7
Štaut, L. 2025. Agricultural terraces in Slovenia. *Zenodo* 1 October. Online publication. https://doi.org/10.5281/zenodo.17242982
Sun, W., Zhang, Y., Mu, X., Li, J., Gao, P., Zhao, G., Dang, T. and Chiew, F. 2019. Identifying terraces in the hilly and gully regions of the Loess Plateau in China. *Land Degradation & Development* 30. (17): 2126-2138. https://doi.org/10.1002/ldr.3405
Surveying and Mapping Authority of the Republic of Slovenia 2025a. *Digitalni model reliefa* (Digital elevation model). Ljubljana, Geodetska Uprava, Republika Slovenija.
Surveying and Mapping Authority of the Republic of Slovenia 2025b. *Gospodarska javna infrastruktura* (Public infrastructure cadastre). Ljubljana, Geodetska Uprava, Republika Slovenija.
Susladkar, O., Deshmukh, G., Nag, S., Mantravadi, A., Makwana, D., Ravichandran, S., Chandra Teja, R.S., H Chavhan, G., Mohan, C.K. and Mittal, S. 2022. ClarifyNet: A high-pass and low-pass filtering based CNN for single image dehazing. *Journal of Systems Architecture* 132. 102736. https://doi.org/10.1016/j.sysarc.2022.102736
Titl, J. 1965. *Socialnogeografski problemi na koprskem podeželju* (Socio-geographical problems in the Koper countryside). Koper, Lipa.

Triglav Čekada, M. and Bric, V. 2015. Končan je projekt laserskega skeniranja Slovenije (The project of laser scanning of Slovenia is completed). *Geodetski vestnik* 59. (3): 586–592.

Van Coillie, F.M.B., Gardin, S., Anseel, F., Duyck, W., Verbeke, L.P.C. and de Wulf, R.R. 2014. Variability of operator performance in remote-sensing image interpretation: The importance of human and external factors. *International Journal of Remote Sensing* 35. (2): 754–778. https://doi.org/10.1080/01431161.2013.873152

Verbovšek, T., Popit, T. and Kokalj, Ž. 2019. VAT method for visualization of mass movement features: An alternative to hill-shaded DEM. *Remote Sensing* 11. (24): 2946. https://doi.org/10.3390/rs11242946

Yu, M., Rui, X., Xie, W., Xu, X. and Wei, W. 2022. Research on automatic identification method of terraces on the Loess Plateau based on deep transfer learning. *Remote Sensing* 14. (10): 2446. https://doi.org/10.3390/rs14102446

Zakšek, K., Oštir, K. and Kokalj, Ž. 2011. Sky-view factor as a relief visualization technique. *Remote Sensing* 3. (2): 398–415. https://doi.org/10.3390/rs3020398

Zhang, Y., Shi, M., Zhao, X., Wang, X., Luo, Z. and Zhao, Y. 2017. Methods for automatic identification and extraction of terraces from high spatial resolution satellite data (China-GF-1). *International Soil and Water Conservation Research* 5. (1): 17–25. https://doi.org/10.1016/j.iswcr.2017.02.002

Zhao, F., Xiong, L., Wang, C., Wang, H., Wei, H. and Tang, G. 2021. Terraces mapping by using deep learning approach from remote sensing images and digital elevation models. *Transactions in GIS* 25. (5): 2438–2454. https://doi.org/10.1111/tgis.12824

DOI: 10.15201/hungeobull.75.1.5 Hungarian Geographical Bulletin **75** 2026 (1) 107–129.

What sort of justice for what sort of urban development? A systematic review and content analysis of urban regeneration programmes

Ntombifuthi P. NZIMANDE[1] and Szabolcs FABULA[2]

Abstract

Urban regeneration interventions are known for attracting local and foreign investment in cities to improve neighbourhoods; however, the ongoing increase in these interventions has been associated with gentrification and the displacement of minority groups. With the growing scholarship on justice and urban transformation, this paper contributes to this literature by providing a systematic review and content analysis that examines how the concept of justice is conceptualised and operationalised across the global arena. Therefore, we offer a novel integrative theoretical framework of just urban regeneration that connects gentrification processes to broader debates on social justice in urban geography. Following the PRISMA method, the review examined 42 peer-reviewed articles that focus on urban regeneration (not urban governance, urban policy, or urban planning in general), and how justice is understood, interpreted, and reflected in urban regeneration, including justice typology (social, economic, environmental, spatial) and dimensions (distributive, procedural, recognition, etc.). The mixed-method approach revealed that the scholarship of urban regeneration is largely articulated through distributive, procedural, and recognition dimensions; issues of community displacement and gentrification emerge through distributive concerns, while procedural and recognition justice foreground the participation of marginalised communities. Finally, findings suggest that urban and spatial justice are linked to decision-making processes, highlighting how governance structures shape both the production and experience of injustice.

Keywords: Urban regeneration, content analysis, systematic review, justice

Received May 2025, accepted February 2026.

Introduction

The late 1980s and early 1990s saw the emergence of the concept of urban regeneration, which refers to the long-term strategic plans implemented in dilapidated areas to improve the city's environmental, social, and economic aspects. One of the most commonly accepted definitions of urban regeneration is by Roberts, P. (2000, 17), where urban regeneration is a "comprehensive and integrated vision and action which seeks to resolve urban problems and bring about a lasting improvement in the economic, physical, social and environmental condition of an area that has been subject to change or offers opportunities for improvement". In this paper, the term "urban regeneration" is interpreted broadly, covering a wide range of interventions, but still retaining some core characteristics. Urban regeneration activities are based on comprehensive, integrated policies and interventions that set multiple objectives and activities, depending on the area's problems and potential. They seek to foster economic competitiveness, enhance skills and capacities of the residents, and improve the nature and general appeal of the place

[1] University of KwaZulu-Natal, Department of Geography, Howard College, 4000 Durban, South Africa. E-mail: nzimanden2@ukzn.ac.za

[2] University of Szeged, Department of Human Geography, Egyetem u. 2. H-6722 Szeged, Hungary. E-mail: fabula.szabolcs@geo.u-szeged.hu

(economic, social/cultural, and physical/environmental dimensions of regeneration). In their governance, partnership and cooperation are key elements, involving the local community, private actors, and government agencies. Their scale of intervention varies from large-scale strategic to more local. In general, urban regeneration programmes use public, private, and voluntary funding, with the private sector increasingly dominant and government funding becoming more selective. They generally accept and embrace the sustainable development model (Roberts, P. 2000; Hall, T. 2006; Tallon, A. 2010). This broad interpretation is also reflected in the methodology we have employed, which ensures that studies using different terminologies for "urban regeneration" are taken into account *(Figure 1).*

Although urban regeneration is a global concept, its development trajectory, specific approaches, and emphasis vary by region. Early examples of this historical and geographical diversity include 19th-century efforts such as the renovation of Paris to address public health and infrastructure issues, efforts to address the negative impacts of industrialisation-driven urban growth in the UK, especially in London, and the City Beautiful movement in the US. From the mid-20th century onwards, the destruction caused by World War II was a significant catalyst for regeneration in many European cities, whereas in the US, urban renewal programs emerged for modernisation. However, the focus of interventions has changed significantly over the decades, from large-scale clearance and rebuilding to addressing the economic and environmental decline of inner cities, to sustainable urban regeneration as a response to environmental degradation and social inequality (Roberts, P. and Sykes, H. 2000; Hall, P. and Tewdwr-Jones, M. 2002). In other regions, such as Africa and Asia, rapid urbanisation in the second half of the 20th century led to a focus on large-scale redevelopment and infrastructure development to ensure that urban housing and public services kept pace with the growing population. Current approaches to urban regeneration often aim for a more integrated, comprehensive strategy that encompasses physical, economic, and social development, with an increasing emphasis on community involve-

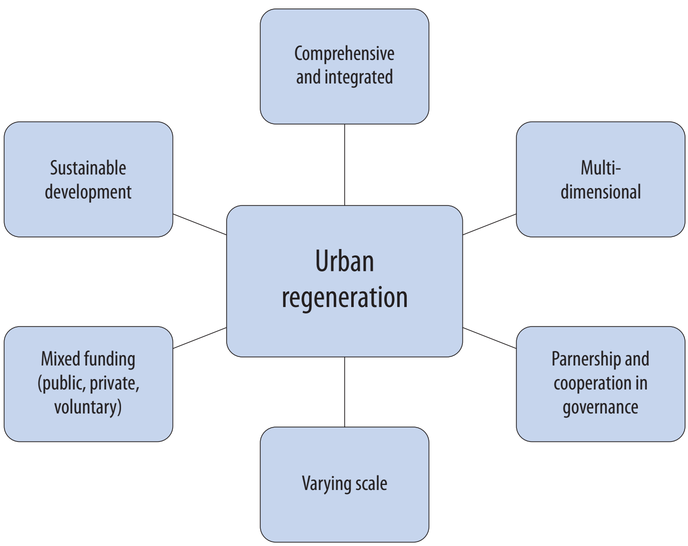

Fig. 1. Key dimensions of urban regeneration. *Source:* Authors' own elaboration.

ment. Nevertheless, urban regeneration initiatives have generally still not resolved the tensions between economic competitiveness and local social justice (Shaw, K. and Butler, T. 2019). Given that the application of the concept of urban regeneration shows geographical differences, yet, from the point of view of justice, different regions face many similar challenges, this article does not focus on a specific geographical region but examines the relationship between urban regeneration and justice in general, on a global scale.

Urban regeneration interventions are well known for attracting local and foreign investment in cities to improve neighbourhoods; however, the ongoing increase in these interventions has been linked to gentrification and the displacement of minority groups. Without meaning to be exhaustive, several authors have looked at these consequences: the increase in property value and, therefore, the cost of living (Granger, R. 2010), increase in traffic and air pollution (Egercioglu, Y. and Ozcan, N.S. 2016), segregation and inequality (Arbaci, S. and Tapada-Berteli, T. 2012), gentrification and displacement (Çaglar, A. and Glick Schiller, N. 2018; Hubbard, P. and Lees, L. 2018; Fitzgerald, T. and Maharaj, B. 2024), access to public services and infrastructure (Balzarini, J.E. and Shlay, A.B. 2016; Tsavdaroglou, C. 2020), environmental justice and urban sustainability (Anguelovski, I. and Connolly, J.J. 2024; McClintock, N. and Morris, G. 2024), homelessness (Langegger, S. and Koester, S. 2016), and need for social housing (Darcy, M. and Rogers, D. 2014). To eliminate such problems and improve urban regeneration, we believe that social justice is a concept that should be taken into account in such interventions.

The concept of justice discussed in this article has been in several pieces of literature, each presenting different dimensions of justice. As a theoretical framework, this study is grounded in what can be termed 'just urban regeneration', which argues that urban spaces should be inclusively, participatively, and equitably transformed in a manner that prioritises the voices of historically disadvantaged and marginalised societies to promote sustainable development. Though several dimensions of justice exist, we believe there are six key dimensions that provide a unique yet interconnected lens for understanding a *just urban regeneration*.

First, distributive justice is connected to the equity (i.e., not equal) and exchange principles, where people assess what they have received based on what they have contributed and compare this with others in similar situations (Lambert, E. 2003; Lucas, T. *et al*. 2016). The concept of distributive justice has also been extended to the discipline of geography and to urban studies as a whole. Though related to economic justice, when viewed through its spatial dimensions, distributive justice interrogates how space, opportunities and resources are distributed across urban landscapes.

Second, procedural justice refers to organisations' decision-making processes, which should be impartial and consistent to ensure unbiased outcomes that may reward or punish individuals (Folger, R.G. and Cropanzano, R. 1998). Communicative planning theories have argued that for urban regeneration projects to be socially just and democratically legitimate, emphasis must be placed on citizen participation and deliberate democracy (see Shahrad, A. *et al*. 2025).

Third, and linked to citizen participation, is recognition justice, which refers to the perceived injustice people experience based on their standpoint. As theorised by Nancy Fraser, Iris Marion Young, and Henri Lefebvre, recognition justice goes beyond the material redistribution of urban development and expands it to shed light on the power dynamics and residents' ability to be given a 'voice' or representation within their community. In this, Fraser, N. (1995) argues for both redistribution and recognition to ensure justice prevails, drawing attention to two types of injustice: socio-economic (such as economic marginalisation) and cultural (such as non-recognition and cultural domination). This is further supported by Taylor, C. (1992), who argued that recognition is a human need rather than a courtesy. Furthermore, misrecognition of an individual is not merely rude but deprives them of full access and participation that other recognised groups enjoy (Giladi, P. 2017). Misrecognition is intricately linked with epistemic injustice, whereby an individual is silenced, excluded, and misrepresented by others in their community (Fricker, M. 2007), and with testimonial injustice, where a social group is persistently assigned lower credibility due to their social identity (Díaz, R. and Almagro, M. 2019). Hermeneutical injustice occurs when a social group's experiences are misunderstood because no interpretive frameworks are in place to understand them (Carel, H. and Györffy, G. 2014). These injustices rob individuals of their self-esteem and power to become rational enquirers in their community. Therefore, recognition (in)justice includes the exclusion of certain groups from decision-making, the removal of cultural and indigenous heritage, the symbolic control over narratives and space, and spatial stigmatisation.

Urban justice, and subsequently spatial justice, especially within geography, has been a highly debated concept, with major points of contention including conflicts between static and dynamic views, between distributive and procedural approaches, and between normative and context-specific interpretations of urban justice. The concept of spatial justice can be derived from Henri Lefebvre's (1974 [1991]) "spatial triad," which holds that dominant representations of space do not oppress the poor. From the perspective of urban regeneration, Lefebvre's approach is especially important because for him, spatial justice is fundamentally about the right to the city, which latter concept includes two fundamental rights: the right to appropriation and the right to participation (Purcell, M. 2002). Based on Lefebvre's work, David Harvey (2008) postulates that, besides access to urban resources, the right to the city should involve the "democratic control over the production and utilisation of the surplus" (n. p.). With regards to the just city, Edward Soja also suggests that spatial (in)justice can be seen as both an outcome and a process, referring to the distributive and procedural dimensions of justice (Soja, E.W. 2009). According to Fainstein, S.S. (2014), justice, democracy, and diversity are the three guiding principles of urban justice, yet there is ongoing tension among them. Overall, there is no single definition of spatial justice, which makes it difficult to operationalise (Moroni, S. and De Franco, A. 2024). This is why research focused on the conceptual and analytical examination of spatial justice, for example, its relationship to other types of justice, is particularly important.

This draws attention to the concept of governance in relation to urban regeneration. The term 'governance' can have multiple meanings, depending on the context and approach, encompassing various forms of cooperation between the state and the private sector (Davies, J. 2001). Thus, understanding the governance mechanisms that drive successful urban regeneration is essential to achieving broader societal goals, such as sustainable development (Jones, P. and Evans, J. 2006). Therefore, spatial justice is intricately linked to planning sustainability. Although social sustainability is a contested phenomenon, in urban regeneration it "is seen as depending on social networks, community participation, a sense of place, and community stability and security" (Glasson, J. and Wood, G. 2009, 284). Overall, an essential part of spatial justice is an appropriate institutional and procedural base to ensure the greatest possible planning benefits for different individuals and groups. In this way, spatial justice refers to planning approaches such as advocacy planning, radical planning, equity planning, and communicative planning (Alfasi, N. and Fenster, T. 2014). Recent studies have also shown that other deliberative methods, such as collaborative planning, are gaining ground not only in liberal democratic systems but also in autocratic ones (Zhou, X. *et al.* 2024). The implication is therefore not only that institutional frameworks and processes should be taken into account when analysing the justice of urban regeneration, but also that geographical approaches are important in such research.

For this study, we define justice as a philosophical concept that refers to fair relations between the individual and society, enabling equal opportunities for people to participate in a sustainable social market economy, in general, and in urban regeneration, in particular. Specifically, as an theoretical framework, the just urban regeneration looks at the different forms of justice combined in that everyone has the right and opportunity to have an affordable, reasonable and decent home (distributional), residents can participate in neighbourhood planning processes (procedural), the law recognises the different disadvantages that various groups might experience (recognition), and finally, territorial exclusion may be prevented through the equitable access and distribution of opportunities and resources to the local neighbourhoods (urban and spatial justice).

We believe that a literature review article focusing on the relationship between urban regeneration and justice would have considerable added value. Although numerous articles have examined the relationship between urban regeneration and social justice (e.g. McCarthy, J. 2010; Gu, Z. and Zhang, X. 2021; Shen, L. *et al*. 2024; Jon, I. 2025), to our knowledge, no comprehensive analysis of the scientific literature has yet been undertaken. Therefore, this review aims to uncover the connection between urban regeneration and the concept of justice. More specifically, we examine scientific articles that focus on urban regeneration (not urban governance, urban policy, or urban planning in general), and how justice is understood, interpreted, and reflected with regards to urban regeneration, including justice typology (social, economic, environmental, spatial) and dimensions (distributive, procedural, recognition, etc.) *(Figure 2).* To understand this research gap, the following research question will guide our research: How are urban regeneration and the different types of justice connected in the international literature? We hope that this review and the content analysis will contribute to the slowly growing literature on understanding how the different forms of justice appear and are studied in urban regeneration literature. Furthermore, we aim to inspire new research focused solely on maximising the various forms of justice in urban regeneration, as this has significant implications for urban planners and other key urban stakeholders in these programmes.

Methodology

Research method

The research method incorporated two interlinked methods to answer the stated research question. First, a systematic literature review (SLR) was conducted to distil studies that addressed urban development (urban regeneration/renewal/rehabilitation) in relation to any type of justice. SLR is one of the standard processes used to collect specific information from a given topic in a rigorous, transparent, replicable, and scientific manner. Though commonly applied within healthcare, SLR has been found helpful in environmental management research (Maphosa, V. and Maphosa, M. 2020; Mengist, W. *et al*. 2020) and urban studies (e.g. Şahin, A. and Selçuk, S.A. 2025). The current SLR followed the Preferred Reporting Items for Systematic Reviews and Meta-Analyses (PRISMA) guidelines to ensure a transparent and trustworthy review is conducted (Page, M.J. *et al*. 2021).

Second, after the first method was completed, the selected literature underwent content analysis. Content analysis is a methodological tool focused on manifest and latent contents. In other words, this tool mainly focuses on using codes for the classification of key categories within the dataset; therefore, an inductive or deductive approach may be followed (Elo, S. and Kyngäs, H. 2008). Due to the selected literature having no prior analytical categories, the inductive logic was selected as information was extracted directly from the data (texts) through an iterative process.

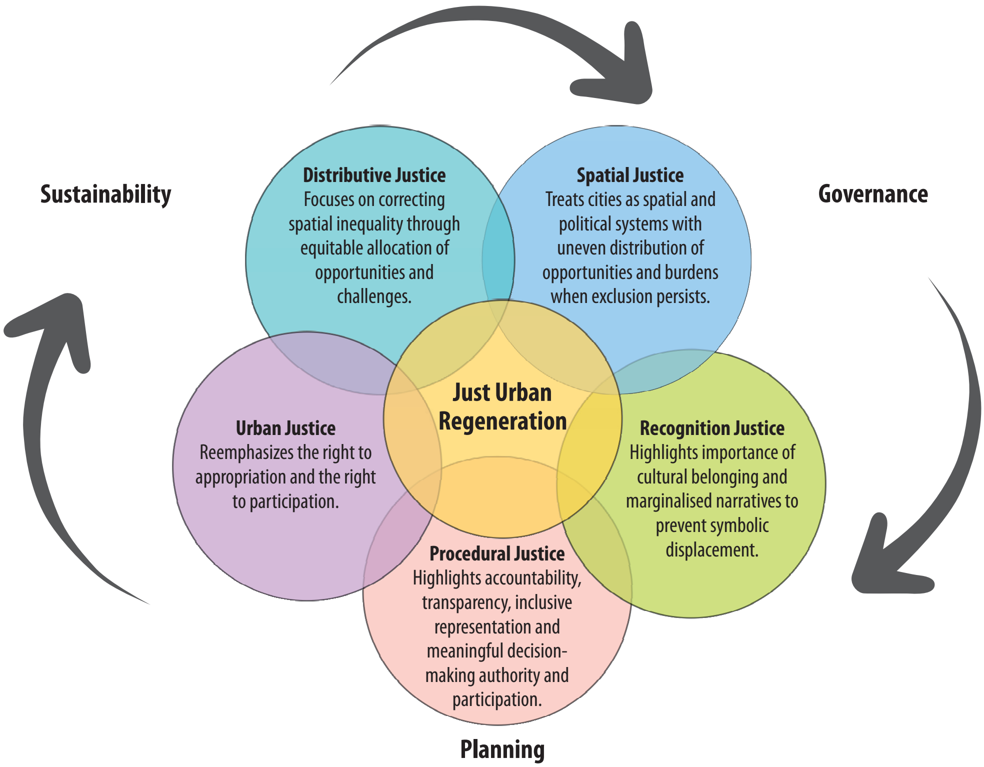

Fig. 2. Just urban regeneration theoretical framework. *Source*: Authors' own elaboration.

Literature search

The articles were retrieved from the Scopus database. The keywords searched were selected in relation to the research questions and were Title = (urban OR neighbourhood) AND Title = (renewal OR regeneration OR rehabilitation) AND Title = (justice OR distributive justice OR procedural justice OR recognition justice OR spatial justice OR social justice OR socio-spatial justice) AND (social sustainability OR collaborative planning OR urban governance). The search string yielded several publications within the urban development and justice field, with the first selection being targeted at the article's title, abstracts, and keywords. The specific inclusion and exclusion criteria that were applied in the SLR are available in *Table 1*.

As evidenced in *Figure 3*, the initial search resulted in 206 downloaded articles. 32 articles were removed due to duplicates and books, which reduced the total to 174, and these articles' titles and/or abstracts were then screened. After the exclusion and inclusion criteria were applied, 102 irrelevant articles were excluded. Next, a thorough review of the 72 articles was conducted. Initially, articles that did not directly address the (un)justices of urban development were removed from the inventory. However, during the course of the PRISMA protocol, we realised that some articles may include the term 'justice', but did not relate to any of the specific forms of justice in the manuscript, whether explicitly or suppressed. These articles were excluded from the analysis. We also found some articles that did not mention the term 'justice' but had suppressed

Table 1. The exclusion and inclusion criteria for the SLR

Inclusion criteria	Exclusion criteria
Articles published between 2011–2025 (November)	Articles published before 2011
Articles in English	Articles published in all other languages
Peer-reviewed articles	Books, non-peer-reviewed articles, conference proceedings and grey literature
A combination of keywords used in the title or abstract	–
Articles from all disciplines	None of the keywords are included in the title or abstract
Articles from all countries	–
Articles including any research method	–

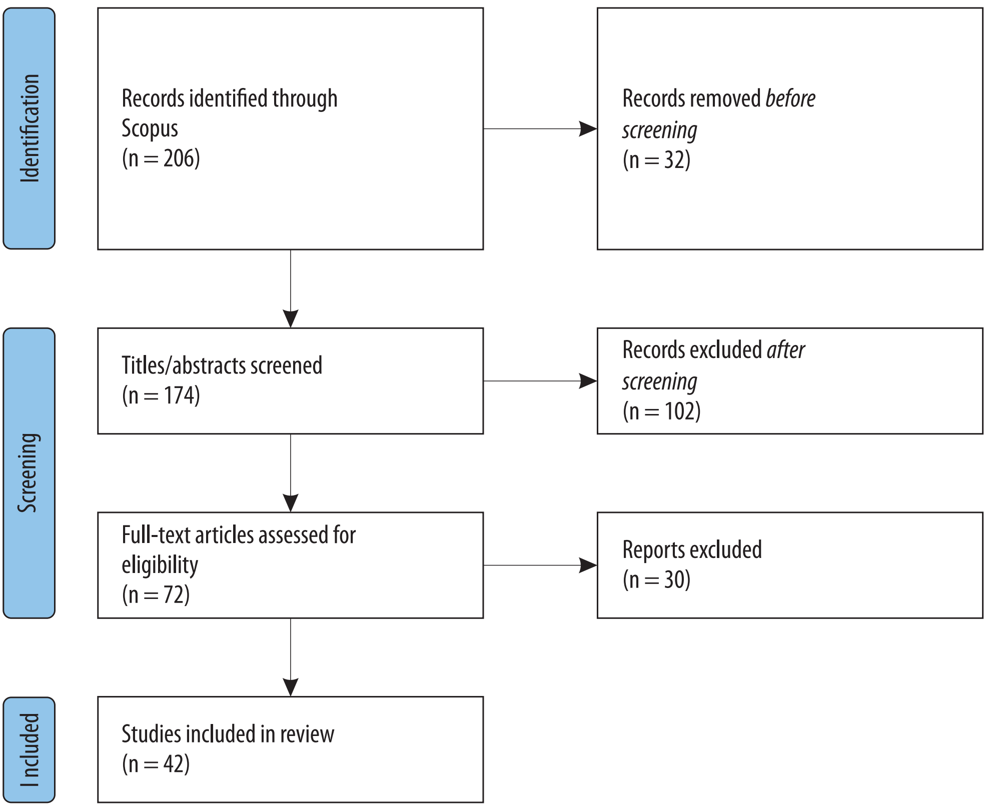

Fig. 3. Methodological flow based on the PRISMA protocol. *Source*: Authors' own elaboration.

(in)justices. These articles were read by the authors and then discussed several times to check if they fit or did not fit within the research. Only a selected few were included as they were also related to the other keywords. In doing so, we believe it is imperative that we mention that sometimes finding articles in which justice was implicitly present would be inconsistent, as this would then be subjective. However, we do recognise that this limits the scope of the research and our interpretation regarding the latent forms of justices. As such, articles that were initially placed on the 'maybe' folder were read and discussed in order to identify and integrate implicit indicators of (in)justice. It is hoped that this helped us better capture (mis)recognition dynamics, thus, aligning our research. After this stage, only 42 articles were included for the critical appraisal and, therefore, included in the final synthesis. The authors separately assessed the articles into different categories to reduce researcher subjectivity and bias. This was then reassessed by the next author, and when discrepancies existed, a discussion was held, and a consensus was reached.

Data analysis

The articles were initially analysed using research methods, year of publication, geographical jurisdiction, top citations received, and publication per journal. This information was then imported into Microsoft Excel for the completion of descriptive and manifest statistics. Moreover, for the content analysis, we examined (1) in what sense the term 'justice' appears in the articles, (2) what other terms and concepts are explicitly connected to justice in the text, and (3) whether another equivalent term was used instead of 'justice'. Based on these criteria, an Excel factsheet was created to encode the articles and extract the data. The factsheet contained the following coding categories: justice typology (e.g. social/economic/environmental justice); justice dimensions (e.g. distributive, procedural, recognition); geographic justice categories (e.g. spatial justice); understandings, definitions of justice; other terms and concepts mentioned in the interpretation and definition of justice. The second author of this study carried out coding. To increase reliability, the authors discussed the results and the work methods with each other and refined the analytical factsheet.

Delimitation and limitations

The combination of the SLR and content analysis was beneficial for uncovering both the latent and manifest content of the literature on urban development and urban justice. Moreover, these methods would allow for the identification of relevant literature and critical themes (and sub-themes) within the literature to derive valuable insights, together with the geographical scope of the studied phenomenon. The combined strengths of the SLR and content analysis, where the former summarises literature through maximising objectivity while minimising bias and the latter qualitatively and quantitatively analyses textual datasets, though beneficial to the current research, are not without drawbacks. The main strength of the SLR is also its main drawback: the former yields substantial publications, making the content analysis an extremely time-intensive process. This drawback was minimised by following the quality evaluation criteria proposed by Lincoln, Y.S. and Guba, E.G. (1985), namely credibility (truthfulness), transferability (applicability and replicability), dependability (level of consistency), and confirmability (positionality and objectivity). *Table 2* pro-

Table 2. Evaluation of quality

Evaluation criteria	Tactic
Credibility	Member checking Rich verbatim descriptions
Transferability	Providing detailed descriptions of procedures
Dependability	Verifying results with raw data
Confirmability	Individual verification of literature and documents

vides the protocol that was followed. This protocol ensured that the current research was reliable, valid, rigorous, and trustworthy, representing what it aimed to represent.

Results

Bibliometrics

The findings of the manifest data are first discussed. *Figure 4* presents the number of publications published between 2011 and 2025 (November) that are primarily focused on the (in)justices of urban development. The number of publications began to increase significantly in 2015, with four publications, followed by six in 2018 and 2021, and eight in 2024. Though research on urban development is not new, studies investigating socio-spatial justice in urban development have only begun to gain traction in 2015. Afterwards, with the exception of 2016, publications were recorded on an annual basis. This increase may have been attributed to the United Nations' adoption of the Sustainable Development Goals (SDGs) in 2015 and the rising production and circulation of knowledge within discipline developments.

Though no journal stood out for publishing numerous articles, three and four articles were published in Land Use Policy and Sustainability, respectively. Only two articles from HTS Teologiese Studies / Theological Studies and New Design Ideas appeared in special issues. With the exception of one journal, all the articles were published in journals ranked in the SJR, indicating that they met a certain standard. When analysing the journals, it is evident that the majority of publications were in journals focused on urban planning, research, and studies, while only one journal was in a separate field, i.e., HTS Teologiese Studies / Theological Studies *(Table 3).*

The distribution of the 42 articles reveal a striking difference in the geographical focus of urban research, with a strong emphasis on European contexts *(Figure 5).* Of the 42 articles reviewed, 18 focused on Europe, suggesting a regional bias that may be influenced by the continent's robust institutional frameworks and policy initiatives, such as the Urban Agenda for the European Union. These mechanisms have not only shaped urban development strategies and policies since the 2010s, but have also fostered a research environment that prioritises European urban issues.

In contrast, other regions are significantly underrepresented: Asia accounts for 10 publications, reflecting a moderate level of scholarly engagement, while Africa appears in only 5 articles – despite being home to

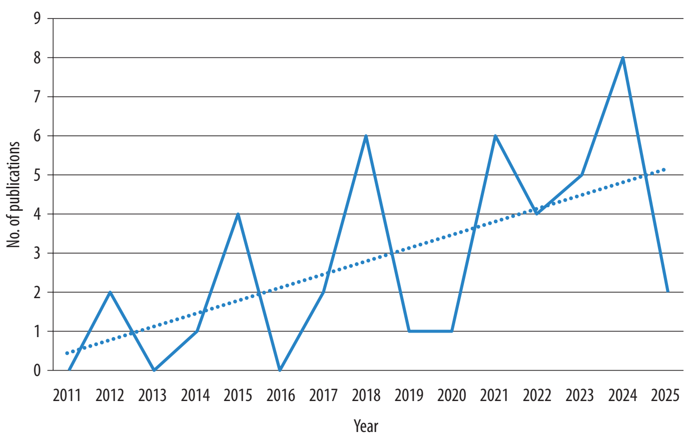

Fig. 4. The number of publications per year. *Source*: Authors' own elaboration.

Table 3. List of articles corresponding with journals

Journal	SJR (2023)	No. of publications
Buildings	0.575	2
Built Environment	0.408	1
Cities	1.733	2
Environmental Impact Assessment Review	2.681	1
Environment and Planning A: Economy and Space	2.084	1
Environment and Planning E: Nature and Space	1.285	1
Environmental Research Communications	0.797	1
Environmental Science and Policy	1.602	2
European Urban and Regional Studies	1.079	1
Frontiers in Sustainable Cities	0.799	1
Heritage	0.449	1
HTS Teologiese Studies / Theological Studies*	0.334	2
International Journal of Housing Policy	0.849	1
International Journal of Urban And Regional Research	1.636	1
Journal of Cleaner Production	2.085	1
Journal of Community Practice	0.488	1
Journal of Planning Literature	1.812	1
Journal of Sustainable Tourism	2.822	1
Land	3.200	2
Land Use Policy	1.847	3
Midwest Social Sciences Journal	..	1
New Design Ideas*	0.185	1
Planning Theory & Practice	0.953	1
Progress in Planning	1.963	1
Space and Culture	0.482	1
Sustainability	0.672	4
Town Planning Review	0.701	1
Transcultural Studies	0.101	1
Urban Affairs Review	1.130	2
Urban Research & Practice	0.757	1

*Articles were published under special issues.

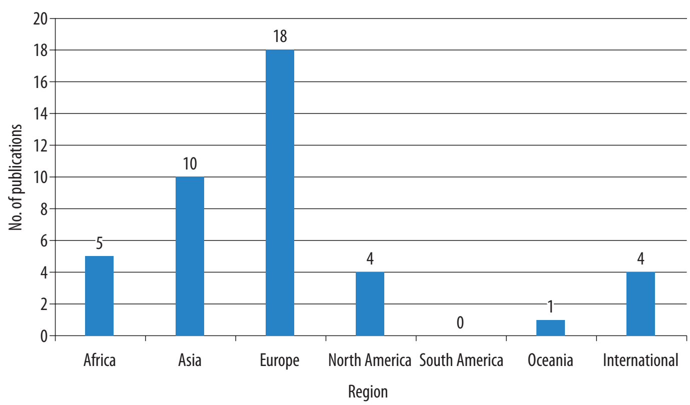

Fig. 5. Frequency of publications per region. *Source*: Authors' own elaboration.

some of the fastest-growing urban populations globally. Even more striking is the complete absence of studies focused on South America, with only one in Oceania, which raises important questions about the inclusivity of global urban research. Only four articles adopt a global perspective, further highlighting the tendency of urban scholarship to be geographically concentrated. This uneven representation is not merely an academic matter; it has real implications for how urban challenges are understood and addressed across contexts.

Finally, *Figure 6* depicts the frequency of the different research methods used per publication. Qualitative research methods, such as interviews and observations, were the most popular methods for data collection (n = 15), followed closely by review (n = 12), while quantitative and mixed-methods were used in 8 and 7 publications, respectively. Research within the field of urban development with a socio-spatial justice perspective is largely focused on marginalised, vulnerable communities, thereby requiring a multifaceted approach to investigating the effects of injustices arising from urban development. Hence, the popularity of qualitative research methods.

We also used VOSviewer to analyse the 42 articles to visualise how the keywords related to each other over time. As indicated in *Figure 7*, each node (circle) in the co-occurrence network represents a keyword, with its size indicating the frequency of occurrence, and the lines between the nodes representing the strength of the co-occurrence, with thicker lines indicating stronger relationships. The colour gradient reflects the temporal evolution of the research teams with blue-purple for earlier studies and yellow for recent studies. Additionally, the analysis produced four thematic clusters, with cluster 1, the largest, focusing on urban planning, urban development, urban regeneration, and social justice, indicating how regeneration processes intersect with equity. The second cluster focused on Chinese-specific case studies, reflecting the growing number of studies and attention to Chinese urban transformation. Topics related to governance, gentrification, planning, and brownfield redevelopment were included in the third cluster, with the final cluster focused on emerging concepts, such as environmental issues and sustainable urban development, geared towards sustainability-oriented urban policies.

Content analysis

We built the theoretical framework of our study around the concept of 'just urban regeneration'. Besides this concept, in the Introduction, we described different types of justice that we believe should be part of just urban regeneration. These include distributive justice, procedural justice, recognition justice, spatial justice, and urban justice. Finally, in addition to these types of justice,

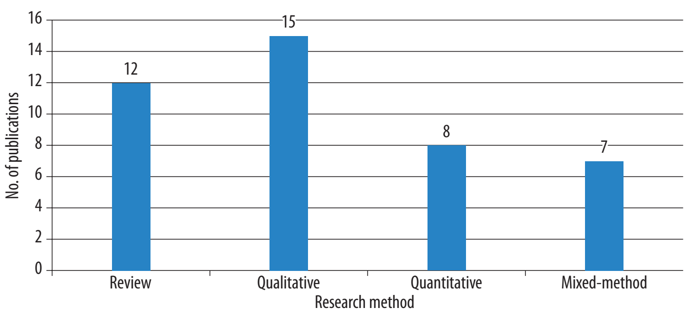

Fig. 6. Frequency of research methods per publication. *Source*: Authors' own elaboration.

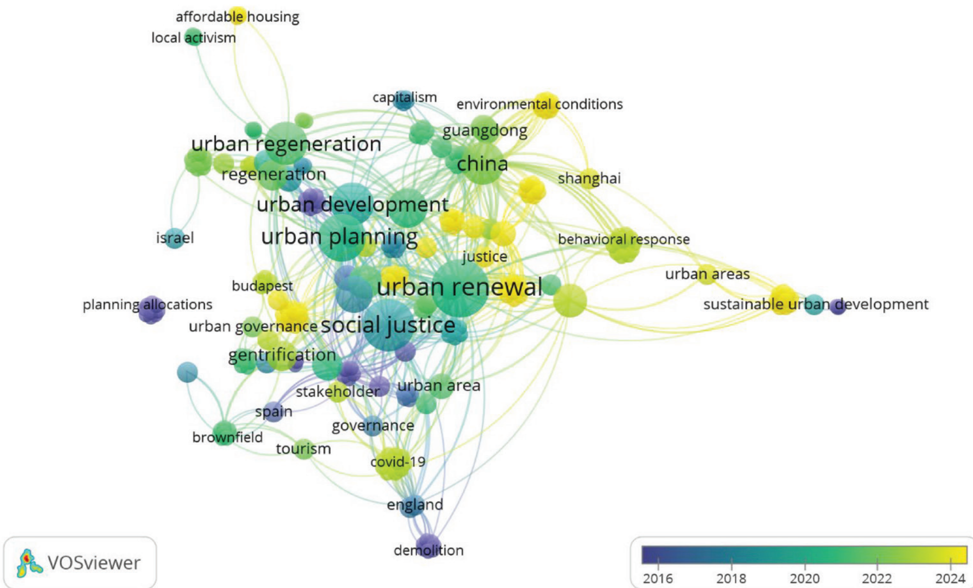

Fig. 7. The keyword co-occurrence network. *Source*: Authors' own elaboration.

we have also defined the concepts of governance, planning, and sustainability as part of just urban regeneration, which we discuss in relation to the types of justice listed above.

Based on the content analysis of the articles, several dimensions of justice can be distinguished within the above types of justice. The interpretations of justice in these papers can be divided into three major groups: social justice (social, socio-structural), economic justice (economic, socio-economic, justice of class), and environmental justice (environmental, ecological, socio-ecological, natural, energy, and climate justice). In addition to these three main categories, other justices are also used: tribal, legal, moral, political, historical, intersectional, and cultural justice/justice of difference. The above are not necessarily mutually exclusive categories, however, as they are intertwined in various ways in the analysed articles.

In the articles, the first justice type, *distributive justice* focuses on the distribution/allocation of benefits, goods, and resources on the one hand, and costs and detriments on the other. This shows, as is also explicitly stated in the articles, that the focus of distributive justice is on outcomes, but some articles also raise the issue of the power structures behind distribution (see below). Although this is not a quantitative analysis, it is worth noting that redistributive justice is mentioned explicitly in the articles more often than procedural or recognition justice: the term "re-/distributive justice" appears in 17 of 42 articles.

Among the different understandings of justice, re-/distributive justice, and within that, justice in the economic sense, plays a prominent role in the articles analysed. This interpretation of justice is generally referred to in the articles as "economic justice" (or socio-economic justice). Therefore, economic justice emphasises the distribution of economic outcomes, including the distribution of economic goods and benefits, as well as economic costs. Examples of this include housing and infrastructure (Margalit, T. and Vertes, E. 2015), property rights (Lai, L.W. *et al.* 2018), and the right of businesses (Siegenthaler, F. 2017) in the sampled articles. However, the concept of distributive justice refers not only to the allocation of economic outputs but also to broader issues. In the articles, it is mainly interpreted as the distribution of social goods, resources, and amenities (e.g. housing, infrastructure, green space) between less and more affluent urban areas or as the 'distribution of costs and benefits' in the society (Margalit, T. and Vertes, E. 2015; Puustinen, T. *et al.* 2018; Bosák, V. *et al*. 2024; Sun, X. and Liu, Z. 2024).

Distributive justice also appears in articles discussing the distribution of environmental goods, which is why the term "environmental justice" is used in some of them. Environmental justice is understood through the quality of environmental remediation and improvement in natural features. In this sense, environmental justice refers to the extent to which different social groups have access to environmental goods. For example, energy justice can refer to the fair distribution of energy benefits and resources, ensuring that all community members have access to affordable, sustainable, and reliable energy (Cui, D. *et al*. 2024). Other examples of such studies include investigations into how accessible an urban waterfront site is to urban inhabitants as in the case of Seattle, USA (Wessells, A.T. 2014), and how fair the distribution of energy benefits and resources is among individual social groups during urban renewal in the peri-urban area of Guangzhou, China (Shen, J. *et al*. 2024) or in the case of highway removal projects in the USA and Spain (Stehlin, J. 2023). The territorial dimension of distribution can also be observed in the analysed literature, that is, how environmental investments relate to each other in urban areas with different socio-economic status, i.e., in more and less affluent neighbourhoods.

Regarding the material, distributive justice, equity, and *equality* are also among the related concepts. In the analysed articles, equity is presented as a distribution issue, interpreted as equity of outcomes, socio-ecological equity, and environmental equity. It refers to both the (geographical) distribution of amenities and the provision of access to these resources. This understanding is exemplified by Freiburg (Germany), where the spatial concentration of old-age residents and the decline of community infrastructure and services have undermined community sustainability and social equity, spurring local authorities to introduce new residential design solutions (Hamiduddin, I. 2015). All in all, both (in)equity and (in)equality are used in a redistributive sense, but their content is relatively broad, ranging from economic disparity to the distribution of environmental goods.

Some studies focus not only on the fairness of the distribution of goods, but also on the fairness of processes (e.g. Ferrari, E. 2012; Avni, N. and Fischler, R. 2020; Hübscher, M. 2021). From this perspective, socio-spatial injustices are also the result of exclusionary decision-making processes (Paddison, B. and Hall, J. 2023). Participation in urban regeneration is therefore of particular importance in studies. The category of participation and inclusion is also very diverse, as it covers notions such as exclusion and inclusion, collaborative/inclusive/participatory planning (Wessells, A.T. 2014; Attia, S. and Ibrahim, A.A.A.M. 2018), radical inclusivity (De Beer, S.F. 2018), partnership and subsidiarity (Lai, L.W. *et al*. 2018), inclusive/participatory democracy or simply "democracy" (Sezer, C. and Maldonado, A.M.F. 2017; Larson, S.M. 2018; Kim, H. *et al*. 2019; Valli, C. and Hammami, F. 2021), fair democratic governance (Simic, I. *et al*. 2022), social emancipation (Van de Kamp, L. 2021). This draws attention to the need for theories and approaches that do not only address the normative distribution of resources but also emphasise the participation of marginalised people in urban regeneration.

The third type of justice, recognition justice, also appears in the articles included in the sample, but typically in connection with other concepts. One of them is *social difference* since social justice is intertwined with the recognition of groups and individuals across a range of markers, including race, ethnicity, gender, and class. This is shown, for example, by the (in)accessibility of waterfront sites for North American indigenous tribal people (Wessells, A.T. 2014). Also present in the articles, *social cohesion* "refers in this context to a combination of economic growth and policies aimed at accommodating social diversity and democracy", as in the case of Barcelona, where urban regeneration initiatives are combined with cultural strategies to enhance social cohesion (Degen, M. and García, M. 2012, 1024).

Last but not least, *spatial and urban justice* are often mixed with the types and dimensions of justice already described above. For example, using a broad definition of spatial justice, just urban regeneration results in socially just outcomes, which is a reference to distributive justice (Bissett-Scott, J. *et al*. 2015). It can be observed that several authors in the sample use the concept of urban justice in relation to urban regeneration from a critical social theory perspective (using Lefebvre, Harvey, Soja, Fainstein, Fincher and Iveson). For example, economic justice is interpreted as the uneven outcomes of urban development in people's relative access to capital (Wessells, A.T. 2014). Such studies show that socio-spatial injustices result from market and power relations (Haase, A. *et al*. 2022; Haase, A. 2024). Within the right to the city framework, justice is often discussed in relation to the basic rights of marginalised urban inhabitants. For example, topics such as housing (Ntakirutimana, E. 2018) or the (de)criminalisation of informal practices in urban areas are brought into focus (Siegenthaler, F. 2017). Further issues examined in the relationship between urban development and spatial justice are accessibility, public space, housing, environmental remediation (Avni, N. and Fischler, R. 2020), displacement and gentrification (Fitzgerald, T. and Maharaj, B. 2024). Scale is also an important topic in the articles, which refer to scales of governance (Bissett-Scott, J. *et al*. 2015) and the geographic scale at which justice may be produced (Hübscher, M. 2021). In the sampled articles, spatial and urban justice are commonly interpreted in complex ways, encompassing procedural and recognition forms of justice in addition to distributive justice. This is well illustrated by articles featuring, for example, Soja's idea that processes and outcomes are equally important in spatial justice (Soja, E.W. 2010; in Ferrari, E. 2012) or Fainstein's conceptual triad of distributional equity, diversity, and democracy (Fainstein, S.S. 2014 in Sezer, C. and Maldonado, A.M.F. 2017). As this paragraph shows, spatial justice is necessarily an integrative category in which the social, economic, and environmental aspects of justice are equally important, and, in the analysed articles, the "traditional" topics of critical urban research are mainly represented.

Finally, it should be noted that the term "justice" is not used explicitly in all of the analysed articles. There are two papers in which the term "fairness" is used instead. Notably, similar to the above-discussed typification of justice, in one article, there is a triple division of procedural, distributive, and interactional fairness (Wang, D. *et al*. 2022), whereas, in the other, fairness (together with equality and inclusion) is linked to social sustainability (Simic, I. *et al*. 2022). In two articles, neither the term "just/-ice" nor "fair/-ness" appears; instead, the authors use social and environmental sustainability and equity (Bianco, L. 2023; Zheng, S. *et al*., 2023).

Discussion

Urban social justice is a field that has a long tradition and is still relevant for research and policy. Improving urban living conditions is the subject of several international policies, such as the United Nations' SDG, of which SDG 11 aims at making cities and human settlements inclusive, safe, resilient and sustainable. As the share of the urban population increases globally, with worsening socio-economic inequalities, inadequacies of basic public services, and climate change risks, ensuring social justice becomes an increasingly urgent issue. However, recent research shows that the principles of justice are often neglected in urban renewal programmes, and such interventions can even violate justice and the right to the city (Fitzgerald, T. and Maharaj, B. 2024; Juhila, K. and Perälä, R. 2024).

Our findings demonstrate scientific discourse that touches on the concepts, methods and geography of research within the foci of urban regeneration and the forms of justice. We also found that, within the urban development discourse, the concept of justice is understood differently and holds different meanings to different scholars. These results are discussed in greater detail below, together with their implications.

We chose the concept of "just urban regeneration" as the conceptual basis for our study, implying that urban regeneration initiatives should be inclusive, participatory, equitable, and sustainable. In addition, we included several types of justice in our theoretical framework because we believe that they should play an important role in just urban regeneration. The main types are distributive, procedural, and recognition justice, as well as spatial justice and urban justice.

For interpretations of justice related to space, the term "spatial justice" is generally used in the content-analysed articles. Other relevant terms can also be detected, most commonly socio-spatial, territorial, or urban justice, whereas others, such as local, regional, and place-based justice, play a marginal role. One notable finding from these studies is that there is no uniform definition of spatial justice or a generally accepted set of its elements. Nevertheless, several approaches can be identified. One example is the broader definition of justice from a spatial perspective, suggesting that spatial justice is a spatial expression of social justice and that urban regeneration should result in socially just outcomes. Another broad interpretation is that of urban justice, referring to the scale at which justice is produced. In addition to these, a critical interpretation of spatial justice can also be observed in the articles. In this regard, the authors have essentially built on the works of Henri Lefebvre, David Harvey, and Edward Soja. In such studies, justice is typically viewed as a social product that is both a state and a process, and which is interrelated with space, depending on it but also influencing its production (see also Soja, E.W. 1983; Dikeç, M. 2001). Overall, the analysed articles show considerable variation in spatially informed interpretations of justice, necessitating further discourse among researchers with different perspectives.

A complex approach to spatial justice can also be observed as a result of content analysis. Authors representing this approach rely primarily on two sources. One is Susan Fainstein's concept of the just city, which considers equity, democracy, and diversity to be the fundamental elements of justice (Fainstein, S.S. 2014). The other main source is Ruth Fincher's and Kurt Iveson's social logics, according to which the basic elements of fair city planning are redistribution, recognition, and encounter (Fincher, R. and Iveson, K. 2008). Articles applying these theoretical foundations typically mix different types of justice within the framework of spatial justice, including distributive, procedural, and recognition justice. Combining different types of justice undoubtedly has certain analytical advantages, but it also has its limitations. As some scholars argue, just processes do not always lead to just outcomes. However, factors such as stakeholder involvement, leadership, intelligibility and transparency of the action, and inclusion of local knowledge reinforce success, i.e., fairness in planning (Schmitt, P. and Weck, S. 2024).

In the analysed articles, distributive justice is intertwined with the economic interpretation of justice, but it also encompasses other factors. These are, in general terms, various social goods, resources, and amenities, including examples such as housing, infrastructure, green space, and energy. Distributive justice is most often interpreted through the theoretical frameworks of equality and equity. In this way, the authors mainly advocate fair allocation and adequate access to goods for both less and more affluent social groups and urban areas. Furthermore, distributive justice mostly concerns outcomes, though not exclusively. The importance of power structures resulting in the just or unjust arrangement and (spatial) distribution of goods is also mentioned in some studies. For example, based on the right to the city concept, justice is often discussed in relation to the basic rights of (marginalised) urban inhabitants. This draws attention to the issue of [private] property rights and to how government-led urban regeneration in neighbourhoods may violate the rights of property owners. In fact, previous studies have noted the issues with private property rights as a dimension of social justice that urban regeneration has been viewed as a land-grabbing act by the state, instead of urban regeneration being for the people and making the people at the forefront (Hochstenbach, C. 2017; Shmaryahu-Yeshurun, Y. and Ben-Porat, G. 2021). Here, we can see urban renewal programmes being approved not necessarily because of a need to improve residents' quality of life and the overall neighbourhood, but rather for financial returns to investors, as seen in Hong Kong (Lai, L.W. *et al.* 2018). Thus, the term state-led gentrification. The private property owners are not the only ones at risk of being trumped over by the capitalist developers. However, property leasing from the state, despite its lease contracts, is affected by this (Lai, L.W.C. 1998). The denial of renters' rights to participate in a regeneration programme could be evident when the state uses its power to serve private interests, another form of justice denied.

The multiple interpretations of redistributive justice also highlight that we should not limit ourselves to a single concept of justice in our analyses. The distribution of benefits or resources can be justified on the basis of different theoretical assumptions and arguments, and it can be considered fair or unfair according to the criteria used to justify it (i.e., the principle of justice). However, as the criteria change, so does the assessment of justice in a given geographical area (Feitosa, F.O. *et al.* 2024). This is why some authors emphasise a dynamic interpretation of justice that helps navigate between plural concepts of justice in planning practice by articulating, connecting, and changing different elements of justice, such as the scope of justice or fundamental values, in discourses and institutions (Weghorst, M. *et al.* 2024).

It can be observed that some authors combine the distributive interpretation of justice with the procedural interpretation in the analysed articles. As the content analysis results show, procedural justice is also interpreted in various ways, but democratic participation and democratic representation are emphasised. This draws attention to the fact that, in addition to a static allocative interpretation of outcomes, it is necessary to analyse the decision-making processes that lead to the spatial configuration characterised by a given distribution. According to other authors, justice should be a central element of planning, i.e., the subject of planning rather than its object. Therefore, it is not enough to evaluate the outputs of urban planning in terms of whether they are just or not, but justice must be made the main goal of planning, and democratic engagement is also part of this (Lake, R.W. 2016). Consequently, instead of the normative and questionable allocative notion of just urban planning, the focus should be on how social institutions treat people (Moroni, S. 2023; Moroni, S. and De Franco, A. 2024).

Recognition justice is primarily associated with social difference and social diversity in the analysed articles. Previous research has shown that diversity is important for a just city, but it also makes planning problematic. This is because diverse social groups and perspectives also give rise to diverse expectations regarding planning and the just city. Multiple cultures entail multiple rationalities, and the institutional frameworks of each can contradict those of the others, leading to conflicts. It is therefore necessary to interpret justice in multiple ways and to understand how these conflicting rationalities can be reconciled in urban space (Hartmann, T. 2012; Hartmann, T. and Jehling, M. 2019).

Apart from the main categories of justices, i.e., distributive, procedural, and recognition justices, several concepts of justice were identified during the content analysis. They may not be mutually exclusive, as they are intertwined with the main categories of justice. These types of justice include tribal, legal, moral, political, historical, intersectional, and cultural justice/ justice of difference. Noteworthy, these articles seek to interpret justice from the perspective of indigenous communities, such as tribal justice among North American native peoples (Wessells, A.T. 2014 – see Appendix) or post-apartheid restorative justice in South African cities (De Beer, S.F. 2018). Nevertheless, there is a need for many more conceptual tools grounded in experiences from cities in the Global South to advance our understanding of contemporary urbanism in the Global South.

Finally, it is worth mentioning the concept of sustainability, which we believe is part of just urban regeneration. We would particularly like to highlight the importance of social sustainability, which appears in only a few of the articles analysed, although in these articles, justice is considered a fundamental indicator of sustainability. In the triple bottom line, little attention is given to the social dimension, despite it being an essential component of sustainable development (Nzimande, N.P. and Fabula, Sz. 2020). Thus, several scholars argue that the concept of social sustainability is underdeveloped and primarily reflects ideas from the Global North, thereby compromising its utility in the Global South (see Davidson, M. 2010; Vallance, S. *et al.* 2011). Apart from the theoretical challenges of social sustainability, Kohon's work has drawn attention to communities' contested challenges towards social sustainability (Kohon, J. 2018). In fact, concepts such as social integration, active participation and social capital have overlapped with social sustainability (Bramley, G. and Power, S. 2009). Instead of bemoaning the vast array of these definitions, the multi-faceted definitions of social sustainability have been accepted as a natural process of the sustainability agenda and, thus, social justice. For instance, in addition to social justice, Dempsey, N. *et al.* (2011) listed non-physical contributory factors such as participation, social capital, mixed tenure, quality of life, education, cultural traditions, place attachment, and fair distribution of income as indicators of social sustainability. Colantonio, A. (2009) argued that there has been a shift from traditional themes, such as social justice, to emerging themes, such as empowerment, which focus on the multidimensional issues faced by those experiencing urban regeneration programmes. Empowerment, as fostered by procedural justice, can encourage people to become agents in the social innovation of neighbourhood regeneration programmes (Queirós, M. 2010; Figueiredo, Y.D. *et al*. 2022). Although more research is needed to provide an in-depth analysis of active citizenship and empowerment roles in urban regeneration programmes, the current results indicate the complexities of understanding the different forms of justice within urban studies.

Despite the above implications of the study, practical limitations cannot be overlooked. First, this review included only 42 eligible papers that met the criteria; thus, it cannot and is not intended to be comprehensive. Specifically, the search engine was limited to Scopus, and non-English articles published were not considered. As a result, due to constraints such as limited resources, the study may not encompass all articles in the urban regeneration field related to forms of justice. Future research may consider including all types of documents and other languages to expand the SLR. Second, from a geographical perspective, most eligible articles focus on Europe, with limited international comparative studies among the analysed articles. This geographic context and the inherent bias in the selection criteria and content analysis may limit generalizability; thus, future studies can strengthen the validity of our findings by adopting enhanced, continuous, and rigorous selection criteria and content analysis. Lastly, empirical studies can employ in-depth interviews and questionnaires to investigate the 'presence' or lack of justice typologies in the different urban regeneration programmes in neighbourhoods.

Conclusions

This review examined how urban regeneration and justice interrelate in international scholarship, guided by the question: How are urban regeneration and the various forms of justice connected in the literature? Using the just urban regeneration analytical framework – which integrates distributive, procedural, recognition, spatial and urban justice and situates them within governance, planning, and sustainability – we mapped how studies conceptualise, operationalise, and assess justice across projects, programmes and places. Across the corpus, justice is engaged through three principal typologies – social, economic, and environmental – most often operationalised via distributive, procedural, and recognition dimensions, with spatial and urban justice serving as an integrative frame that explicitly links processes to outcomes. In practice, distributive concerns (frequently socio-economic) dominate; environmental justice appears through access to and burdens of environmental goods; and procedural debates foreground participation, deliberation, and voice; recognition justice exposes misrecognition and epistemic exclusion for marginalised groups. Together, these strands show justice in regeneration to be multi-scalar, context-dependent, and institutionally mediated.

We also see meta-trends in what, where and how knowledge regarding justice is created. The number of publications increases from the middle of the 2010s. Research is primarily conducted in Europe; however, there is an imbalance concerning the representation of research conducted in Africa, South America, and comparative international design. Moreover, qualitative research prevails over quantitative and mixed methodologies. These trends can be attributed to the importance of lived experience and the challenges of measuring justice. Important to note, the procedure of justice does not automatically equate to the results of justice – governance architecture, planning culture, and policy tools influence both who participates in the decision-making process and how the benefits and costs are distributed throughout space. By establishing the justice typologies and dimensions in urban regeneration and connecting them to governance, planning, and sustainability, we show that urban regeneration is practised through multiple interconnected lenses of justice, whose application varies by location and methodology. Spatial and urban justice serves as a unifying framework that connects the processes and outcomes of justice in urban regeneration. This directly addresses the objective of providing clarity regarding how justice is conceptualised, interpreted, and represented in urban regeneration studies, and provides a unified vocabulary and analytical structure to facilitate future empirical studies. However, it should be noted that this study has several limitations, including a limited scope due to language and time-frame constraints. Additionally, determining implied (in)justice required interpretation, and the varied levels of regional focus across the literature used in this study limit the broader applicability of this study's findings. Future research directions include developing empirically based evidence to support the framework, conducting comparative studies focused on underrepresented regions, and conducting a longitudinal study using a combination of methodologies to study all six types of justice at each stage of the urban regeneration process. This will allow the just urban regeneration framework to transform regeneration from a selective improvement mechanism into a viable means of achieving collective prosperity.

REFERENCES

Alfasi, N. and Fenster, T. 2014. Between socio-spatial and urban justice: Rawls' principles of justice in the 2011 Israeli Protest Movement. *Planning Theory* 13. (4): 407–427. https://doi.org/10.1177/1473095214521105

Anguelovski, I. and Connolly, J.J. 2024. Segregating by greening: What do we mean by green gentrification? *Journal of Planning Literature* 39. (3): 386–394. https://doi.org/10.1177/08854122241227804

Arbaci, S. and Tapada-Berteli, T. 2012. Social inequality and urban regeneration in Barcelona city centre: Reconsidering success. *European Urban and Regional Studies* 19. (3): 287–311. https://doi.org/10.1177/0969776412441110

Attia, S. and Ibrahim, A.A.A.M. 2018. Accessible and inclusive public space: The regeneration of waterfront in informal areas. *Urban Research & Practice* 11. (4): 314–337. https://doi.org/10.1080/17535069.2017.1340509

Avni, N. and Fischler, R. 2020. Social and environmental justice in waterfront redevelopment: The Anacostia river, Washington, D.C. *Urban Affairs Review* 56. (6): 1779–1810. https://doi.org/10.1177/1078087419835968

Balzarini, J.E. and Shlay, A.B. 2016. Gentrification and the right to the city: Community conflict and casinos. *Journal of Urban Affairs* 38. (4): 503–517. https://doi.org/10.1111/juaf.12226

Bianco, L. 2023. Adaptive re-use of historic covered markets: A review of selected cases in European capital cities. *Heritage* 6. (2): 1089–1102. https://doi.org/10.3390/heritage6020060

Bissett-Scott, J., Odeleye, D. and Frame, I. 2015. Spatial justice: Towards an ethics of spatial equity. In *UCUI '15: Proceedings of the ACM First International Workshop on Understanding the City with Urban Informatics*. 19 October 2015, Melbourne, Australia. New York, Association for Computing Machinery (ACM) publication, 31–34. https://doi.org/10.1145/2811271.2811277

Bosák, V., Slach, O., Ženková, K., Ženka, J. and Paszová, L. 2024. Developing social-ecological justice through a context-sensitive reuse of urban vacant spaces. *Environmental Science & Policy* 159. 103802. https://doi.org/10.1016/j.envsci.2024.103802

Bramley, G. and Power, S. 2009. Urban form and social sustainability: The role of density and housing type. *Environment and Planning B: Planning and Design* 36. (1): 30–48. https://doi.org/10.1068/b33129

Çaglar, A. and Glick Schiller, N. 2018. *Migrants and City-Making: Dispossession, Displacement, and Urban Regeneration*. Durham, Duke University Press. https://doi.org/10.1515/9781478091028

Carel, H. and Györffy, G. 2014. Seen but not heard: Children and epistemic injustice. *The Lancet* 384. (9950): 1256–1257. https://doi.org/10.1016/S0140-6736(14)61759-1

Colantonio, A. 2009. Social sustainability: A review and critique of traditional versus emerging themes and assessment methods. In *Sue-Mot Conference 2009: Second International Conference on Whole Life Urban Sustainability and its Assessment*. Eds.: Horner, M., Price, A., Bebbington, J. and Emmanuel, R., Loughborough, Loughborough University, 865–885.

Cui, D., Ditta, A.A. and Cao, S.J. 2024. Energy justice and sustainable urban renewal: A systematic review of low-income old town communities. *Journal of Cleaner Production* Online publication, No. 143470. https://doi.org/10.1016/j.jclepro.2024.143470

Darcy, M. and Rogers, D. 2014. Inhabitance, place-making and the right to the city: Public housing redevelopment in Sydney. *International Journal of Housing Policy* 14. (3): 236–256. https://doi.org/10.1080/14616718.2014.934157

Davidson, M. 2010. Social sustainability and the city. *Geography Compass* 4. (7): 872–880. https://doi.org/10.1111/j.1749-8198.2010.00339.x

Davies, J. 2001. *Partnerships and Regimes: The Politics of Urban Regeneration in the UK*. Aldershot, Ashgate.

De Beer, S.F. 2018. Faith-based action and urban regeneration. *HTS Teologiese Studies / Theological Studies* 74. (3): a5168. https://doi.org/10.4102/hts.v74i3.5168

Degen, M. and García, M. 2012. The transformation of the 'Barcelona model': An analysis of culture, urban regeneration and governance. *International Journal of Urban and Regional Research* 36. (5): 1022–1038. https://doi.org/10.1111/j.1468-2427.2012.01152.x

Dempsey, N., Bramley, G., Power, S. and Brown, C. 2011. The social dimension of sustainable development: Defining urban social sustainability. *Sustainable Development* 19. (5): 289–300. https://doi.org/10.1002/sd.417

Díaz, R. and Almagro, M. 2019. You are just being emotional! Testimonial injustice and folk-psychological attributions. *Synthese* 198. (6): 5709–5730. https://doi.org/10.1007/s11229-019-02429-w

Dikeç, M. 2001. Justice and the spatial imagination. *Environment and Planning A: Economy and Space* 33. (1): 1785–1805. https://doi.org/10.1068/a3467

Egercioglu, Y. and Ozcan, N.S. 2016. An assessment of the relationship between urban air quality and environmental urban factors in urban regeneration areas. *Environment-Behaviour Proceedings Journal* 1. (2): 171–177. https://doi.org/10.21834/e-bpj.v1i2.266

Elo, S. and Kyngäs, H. 2008. The qualitative content analysis process. *Journal of Advanced Nursing* 62. (1): 107–115. https://doi.org/10.1111/j.1365-2648.2007.04569.x

Fainstein, S.S. 2014. The just city. *International Journal of Urban Sciences* 18. (1): 1–18. https://doi.org/10.1080/12265934.2013.834643

Feitosa, F.O., Wolf, J.H. and Marques, J.L. 2024. Operationalising spatial justice in urban planning: Bridging theory with practice. *Urban Research & Practice* 17. (5): 720–736. https://doi.org/10.1080/17535069.2024.2341254

Ferrari, E. 2012. Competing ideas of social justice and space: Locating critiques of housing renewal in theory and in practice. *International Journal of Housing Policy* 12. (3): 263–280. https://doi.org/10.1080/14616718.2012.709668

Figueiredo, Y.D., Prim, M.A. and Dandolini, G.A. 2022. Urban regeneration in the light of social innovation: A systematic integrative literature review. *Land Use Policy* 113. (3): 105873. https://doi.org/10.1016/j.landusepol.2021.105873

Fincher, R. and Iveson, K. 2008. *Planning and Diversity in the City: Redistribution, Recognition and Encounter.* New York, Palgrave Macmillan. https://doi.org/10.1007/978-1-137-06960-3

Fitzgerald, T. and Maharaj, B. 2024. Displacement, social justice, and the right to the city: A review and critical reflections in the 21st century. *Midwest Social Sciences Journal* 26. (2): 8. https://doi.org/10.22543/2766-0796.1144

Folger, R.G. and Cropanzano, R. 1998. *Organisational Justice and Human Resource Management.* Vol. 7, London, Sage. https://doi.org/10.4135/9781452225777

Fraser, N. 1995. From redistribution to recognition? Dilemmas of justice in a 'post-socialist' age. *New Left Review* 212. (1): 68–93. https://doi.org/10.64590/4rl

Fricker, M. 2007. *Epistemic Injustice: Power and the Ethics of Knowing*. Oxford, Oxford University Press. https://doi.org/10.1093/acprof:oso/9780198237907.001.0001

Giladi, P. 2017. Epistemic injustice: A role for recognition? *Philosophy & Social Criticism* 44. (2): 141–158. https://doi.org/10.1177/0191453717707237

Glasson, J. and Wood, G. 2009. Urban regeneration and impact assessment for social sustainability. *Impact Assessment and Project Appraisal* 27. (4): 283–290. https://doi.org/10.3152/146155109X480358

Granger, R. 2010. What now for urban regeneration? *Proceedings of the Institution of Civil Engineers-Urban Design and Planning* 163. (1): 9–16. https://doi.org/10.1680/udap.2010.163.1.9

Gu, Z. and Zhang, X. 2021. Framing social sustainability and justice claims in urban regeneration: A comparative analysis of two cases in Guangzhou. *Land Use Policy*102. 105224. https://doi.org/10.1016/j.landusepol.2020.105224

Haase, A., Koprowska, K. and Borgström, S. 2022. Green regeneration for more justice? An analysis of the purpose, implementation, and impacts of greening policies from a justice perspective in Łódź Stare Polesie (Poland), and Leipzig's inner east (Germany). *Environmental Science & Policy* 136. 726–737. https://doi.org/10.1016/j.envsci.2022.08.001

Haase, A. 2024. Inequalities and injustices of urban green regeneration: Applying the conflict analysis perspective. *Land* 13. (3): 296. https://doi.org/10.3390/land13030296

Hall, P. and Tewdwr-Jones, M. 2002. *Urban and Regional Planning.* 5th edition. London, Routledge.

Hall, T. 2006. *Urban Geography.* 3rd edition. London and New York, Routledge.

Hamiduddin, I. 2015. Social sustainability, residential design and demographic balance: Neighbourhood planning strategies in Freiburg, Germany. *Town Planning Review* 86. (1): 29–52. https://doi.org/10.3828/tpr.2015.3

Hartmann, T. 2012. Wicked problems and clumsy solutions: Planning as expectation management. *Planning Theory* 11. (3): 242–256. https://doi.org/10.1177/1473095212440427

Hartmann, T. and Jehling, M. 2019. From diversity to justice – Unravelling pluralistic rationalities in urban design. *Cities* 91. 58–63. https://doi.org/10.1016/j.cities.2018.02.009

Harvey, D. 2008. The right to the city. *New Left Review* 53. 23–40. https://doi.org/10.64590/fmh

Hochstenbach, C. 2017. State-led gentrification and the changing geography of market-oriented housing policies. *Housing, Theory and Society* 34. (4): 399–419. https://doi.org/10.1080/14036096.2016.1271825

Hubbard, P. and Lees, L. 2018. The right to community? Legal geographies of resistance on London's gentrification frontiers. *City* 22. (1): 8–25. https://doi.org/10.1080/13604813.2018.1432178

Hübscher, M. 2021. Megaprojects, gentrification, and tourism. A systematic review on intertwined phenomena. *Sustainability* 13. (22): 1–22. https://doi.org/10.3390/su132212827

Jon, I. 2025. Temporalising "justice" in urban regeneration: thinking with Lockleaze. *Urban Geography.* In press. https://doi.org/10.1080/02723638.2025.2517872

Jones, P. and Evans, J. 2006. Urban regeneration, governance and the state: Exploring notions of distance and proximity. *Urban Studies* 43. (9): 1491–1509. https://doi.org/10.1080/00420980600749951

Juhila, K. and Perälä, R. 2024. Displacement and everyday resistance: Seeking spatial justice in urban renewal processes. *Social Inclusion* 12. 8329. https://doi.org/10.17645/si.8329

Kim, H., Marcouiller, D.W. and Choi, Y. 2019. Urban redevelopment with justice implications: The role of social justice and social capital in residential relocation decisions. *Urban Affairs Review* 55. (1): 288–320. https://doi.org/10.1177/1078087418759605

Kohon, J. 2018. Social inclusion in the sustainable neighbourhood? Idealism of urban social sustainability theory complicated by realities of community planning practice. *City, Culture and Society* 15. 14–22. https://doi.org/10.1016/j.ccs.2018.08.005

Lai, L.W.C. 1998. The leasehold system as a means of planning by contract: The case of Hong Kong. *Town Planning Review* 69. (3): 249. https://doi.org/10.3828/tpr.69.3.j621u418210j5481

Lai, L.W., Chau, K.W. and Cheung, P.A.C. 2018. Urban renewal and redevelopment: Social justice and property rights with reference to Hong Kong's constitutional capitalism. *Cities* 74. 240–248. https://doi.org/10.1016/j.cities.2017.12.010

Lake, R.W. 2016. Justice as subject and object of planning. *International Journal of Urban and Regional Research* 40. (6): 1205–1220. https://doi.org/10.1111/1468-2427.12442

Lambert, E. 2003. The impact of organisational justice on correctional staff. *Journal of Criminal Justice* 31. (2): 155–168. https://doi.org/10.1016/S0047-2352(02)00222-2

Langegger, S. and Koester, S. 2016. Invisible homelessness: Anonymity, exposure, and the right to the city. *Urban Geography* 37. (7): 1030–1048. https://doi.org/10.1080/02723638.2016.1147755

Larson, S.M. 2018. Imagining social justice and the false promise of urban park design. *Environment and Planning A: Economy and Space* 50. (2): 391–406. https://doi.org/10.1177/0308518X17742156

Lefebvre, H. 1996. *Writings on Cities* (translated by Kofman, E. and Lebas, E.), Cambridge, MA, Blackwell.

Lincoln, Y.S. and Guba, E.G. 1985. *Naturalistic Inquiry*. Newbury Park. CA, Sage. https://doi.org/10.1016/0147-1767(85)90062-8

Lucas, T., Kamble, S.V., Wu, M.S., Zhdanova, L. and Wendorf, C.A. 2016. Distributive and procedural justice for self and others: Measurement invariance and links to life satisfaction in four cultures. *Journal of Cross-Cultural Psychology* 47. (2): 234–248. https://doi.org/10.1177/0022022115615962

Maphosa, V. and Maphosa, M. 2020. E-waste management in Sub-Saharan Africa: A systematic literature review. *Cogent Business & Management* 7. (1): 1–19. https://doi.org/10.1080/23311975.2020.1814503

Margalit, T. and Vertes, E. 2015. Planning allocations and the stubborn north–south divide in Tel Aviv-Jaffa. *Planning Theory & Practice* 16. (2): 226–247. https://doi.org/10.1080/14649357.2015.1026925

McCarthy, J. 2010. Social justice and urban regeneration policy in Scotland. *Urban Research & Practice* 3. (3): 241–256. https://doi.org/10.1080/17535069.2010.524416

McClintock, N. and Morris, G. 2024. Urban geographies of waste. *Urban Geography* 45. (4): 518–527. https://doi.org/10.1080/02723638.2024.2319437

Mengist, W., Soromessa, T. and Legese, G. 2020. Method for conducting systematic literature review and meta-analysis for environmental science research. *MethodsX* 7. 100777. https://doi.org/10.1016/j.mex.2019.100777

Moroni, S. 2023. What can urban policies and planning really learn from John Rawls? A multi-strata view of institutional action and a canvas conception of the just city. *Planning Theory* 22. (4): 404–425. https://doi.org/10.1177/14730952231163274

Moroni, S. and De Franco, A. 2024. Spatial justice: A fundamental or derivative notion? *City, Culture and Society* 38. (1): 100593. https://doi.org/10.1016/j.ccs.2024.100593

Ntakirutimana, E. 2018. Housing challenge and urban regeneration: A contribution of faith-based action with special reference to a case study from the city of Tshwane. *HTS Teologiese Studies / Theological Studies* 74. (3): a5151. https://doi.org/10.4102/hts.v74i3.5151

Nzimande, N.P. and Fabula, Sz. 2020. Socially sustainable urban renewal in emerging economies: A comparison of Magdolna Quarter, Budapest, Hungary and Albert Park, Durban, South Africa. *Hungarian Geographical Bulletin* 69. (4): 383–400. https://doi.org/10.15201/hungeobull.69.4.4

Paddison, B. and Hall, J. 2023. Tourism policy, spatial justice and COVID-19: Lessons from a tourist-historic city. *Journal of Sustainable Tourism* 31. (12): 2809–2824. https://doi.org/10.1080/09669582.2022.2095391

Page, M.J., Moher, D., Bossuyt, P.M., Boutron, I., Hoffmann, T.C., Mulrow, C.D., Shamseer, L., Tetzlaff, J.M., Akl, E.A., Brennan, S.E. and Chou, R. 2021. PRISMA 2020 explanation and elaboration: Updated guidance and exemplars for reporting systematic reviews. *BMJ* 372. n160. https://doi.org/10.1136/bmj.n160

Purcell, M. 2002. Excavating Lefebvre: The right to the city and its urban politics of the inhabitant. *GeoJournal* 58. (2–3): 99–108. https://doi.org/10.1023/B:GEJO.0000010829.62237.8f

Puustinen, T., Pennanen, K., Falkenbach, H. and Viitanen, K. 2018. The distribution of perceived advantages and disadvantages of infill development among owners of a commonhold and its' implications. *Land Use Policy* 75. 303–313. https://doi.org/10.1016/j.landusepol.2018.03.051

Queirós, M. 2010. Integrated urban revitalisation in Montreal. Lessons from local development initiatives. *Finisterra: Revista Portuguesa de Geografia* 45. (89): 47–77.

Roberts, P. 2000. The evolution, definition and purpose of urban regeneration. In *Urban Regeneration: A Handbook*. Eds.: Roberts, P., Sykes, H. and Granger, R., London, Sage, 9–36. https://doi.org/10.4135/9781446219980.n2

Roberts, P. and Sykes, H. 2000. *Urban Regeneration. A Handbook*. London, Sage.

Şahin, A. and Selçuk, S.A. 2025. How does urban regeneration affect urban morphology? A systematic review and bibliometric analysis. *International Review for Spatial Planning and Sustainable Development* 13. (3): 79–98. https://doi.org/10.14246/irspsd.13.3_79

Schmitt, P. and Weck, S. 2024. Towards just planning: On the relationship between procedural and distributive justice in local development actions. *Planning Practice & Research* 39. (5): 753–771. https://doi.org/10.1080/02697459.2024.2359221

Sezer, C. and Maldonado, A.M.F. 2017. Cultural visibility and urban justice in immigrant neighbourhoods of Amsterdam. *Built Environment* 43. (2): 193–213. https://doi.org/10.2148/benv.43.2.193

Shahrad, A., Stålhammar, S. and Gulsrud, N.M. 2025. Procedural justice for whom? A case study of a densification project. *Local Environment* 30. (4): 546–566. https://doi.org/10.1080/13549839.2024.2447757

Shaw, K. and Butler, T. 2019. Urban regeneration. In *International Encyclopaedia of Human Geography.* Ed.: Kobayashi, A., Amsterdam, Elsevier, 97–103. https://doi.org/10.1016/B978-0-08-102295-5.10349-X

Shen, J., Wang, S. and Wang, Y. 2024. Environmental inequality in peri-urban areas: A case study of Huangpu district, Guangzhou city. *Land* 13. (5): 703. https://doi.org/10.3390/land13050703

Shen, L., Liu, Y., Ren, Y. and Wong, S.W. 2024. A methodological framework for analysing the justice phenomenon embedded in urban regeneration: A Chinese perspective based at the project level. *Land Use Policy* 145. 107287. https://doi.org/10.1016/j.landusepol.2024.107287

Shmaryahu-Yeshurun, Y. and Ben-Porat, G. 2021. For the benefit of all? State-led gentrification in a contested city. *Urban Studies* 58. (13): 2605–2622. https://doi.org/10.1177/0042098020953077

Siegenthaler, F. 2017. To embrace or to contest urban regeneration? Ambiguities of artistic and social practice in contemporary Johannesburg. *The Journal of Transcultural Studies* 8. (2): 7–39. https://doi.org/10.17885/heiup.ts.2017.2.23653

Simic, I., Stupar, A., Grujicic, A., Mihajlov, V. and Cvetkovic, M. 2022. The transformation of Dorćol Power Plant: Triggering a sustainable urban regeneration or selling the heritage? *Sustainability* 14. (1): 523. https://doi.org/10.3390/su14010523

Soja, E.W. 1983. The socio-spatial dialectic. *Annals of the Association of American Geographers* 70. (2): 207–225. https://doi.org/10.1111/j.1467-8306.1980.tb01308.x

Soja, E.W. 2009. *The city and spatial justice*. Paper prepared for presentation at the conference Spatial Justice, Nanterre, Paris, 12–14 March, 2008.

Soja, E.W. 2010. *Seeking Spatial Justice*. Minnesota, University of Minnesota Press. https://doi.org/10.5749/minnesota/9780816666676.001.0001

Stehlin, J. 2023. "Freeways without futures": Urban highway removal in the United States and Spain as socio-ecological fix? *Environment and Planning E: Nature and Space* 7. (3): 1391–1417. https://doi.org/10.1177/25148486231215179

Sun, X. and Liu, Z. 2024. Public green space injustice in high-density post-colonial areas: A case study of the Macau Peninsula, China. *Sustainability* 16. (9): 3774. https://doi.org/10.3390/su16093774

Tallon, A. 2010. *Urban Regeneration in the UK*. London and New York, Routledge. https://doi.org/10.4324/9780203872598

Taylor, C. 1992. Multiculturalism and the politics of recognition`. In *Multiculturalism and the Politics of Recognition*. Ed.: Guttman, A., Princeton, Princeton University Press, 25–73.

Tsavdaroglou, C. 2020. The refugees' right to the center of the city and spatial justice: Gentrification vs commoning practices in Tarlabaşı-Istanbul. *Urban Planning* 5. (3): 230–240. https://doi.org/10.17645/up.v5i3.3098

Vallance, S., Perkins, H.C. and Dixon, J.E. 2011. What is social sustainability? A clarification of concepts. *Geoforum* 42. (3): 342–348. https://doi.org/10.1016/j.geoforum.2011.01.002

Valli, C. and Hammami, F. 2021. Introducing business improvement districts (BIDs) in Sweden: A social justice appraisal. *European Urban and Regional Studies* 28. (2): 155–172. https://doi.org/10.1177/0969776420925525

Van de Kamp, L. 2021. Housing, personhood and affect in gentrifying garden villages of Amsterdam. *Space and Culture* 24. (3): 437–450. https://doi.org/10.1177/1206331221997697

Wang, D., Jiang, S., Liu, B., Li, X. and Yuan, X. 2022. Research on antecedents of residents' willingness to cooperate in urban regeneration projects: Based on an extended theory of planned behaviour (TPB) model. *Buildings* 12. (8): 1251. https://doi.org/10.3390/buildings12081251

Weghorst, M., Buitelaar, E. and Pelzer, P. 2024. A dynamic justice framework for analysing conceptions of justice: The case of urban development projects. *Planning Theory* 24. (3): 242–264. https://doi.org/10.1177/14730952241280523

Wessells, A.T. 2014. Urban blue space and "the project of the century": Doing justice on the Seattle waterfront and for local residents. *Buildings* 4. (4): 764–784. https://doi.org/10.3390/buildings4040764

Zheng, S., Fu, X., Zhuang, T. and Wu, W. 2023. Exit, voice, loyalty, and neglect framework of residents' responses to urban neighbourhood regeneration: The case of Shanghai, China. *Environmental Impact Assessment Review* 100. 107087. https://doi.org/10.1016/j.eiar.2023.107087

Zhou, X., Lin, Y., Monstadt, J., Hooimeijer, P., Wang, S. and Liu, Z. 2024. Examining collaborative planning processes and outcomes in urban regeneration: A deliberative turn in China? *Urban Studies* 62. (4): 682–699. https://doi.org/10.1177/00420980241259985

Appendix

Article	(In)justice typology	(In)justice dimensions	Geographical (in) justice categories	Understanding(s) of justice	Other related concepts
Wessells, A.T. 2014	Distributive	Economic Environmental Social Tribal	Local Regional	*Economic justice:* uneven urban development outcomes in people's relative access to capital. *Environmental justice:* accessibility of the waterfront site to different populations; the relationship between the central waterfront and public investment in shoreline sites; the quality of the environmental remediation. *Social justice:* indicates a concern with social difference and with inclusive democracy, beyond questions of economic distribution. *Tribal justice:* disparity between indigenous peoples and the settler society that displaced them.	Socio-ecological equity. Environmental equity. Income inequality. Right to the city. Sustainable development. Inclusive/ collaborative planning.

BOOK REVIEW SECTION

Geels, F.W.: Advanced Introduction to Sustainability Transitions. Cheltenham–Northampton, Edward Elgar, 2024. 145 p.

Since the publication of *The Limits to Growth* (Meadows, D.H. *et al.* 1972) and its global impact, concerns over biodiversity loss, resource scarcity, natural disasters, and climate change have intensified. These challenges suggest that modern civilization is on an unsustainable trajectory in its pursuit of socioeconomic prosperity, a concern foreshadowed by Malthus, who emphasized the finite nature of resources relative to population growth (Malthus, T. 1798). Today, there is a broad consensus on the unprecedented impact of human activity. From resource exploitation and pollutant emissions to disruptions of climate and biogeochemical cycles, evidence increasingly underscores the unsustainability of current practices (Richardson, K. *et al.* 2023).

Amid this growing unsustainability and the need for new socio-economic models, the field of sustainability transitions has emerged, focusing on pathways toward more resilient societal systems. This field argues that sustainability cannot be achieved through incremental reforms to existing socio-technical structures. Instead, it explores how profound systemic transformations can be achieved in energy, mobility, food, and industrial sectors.

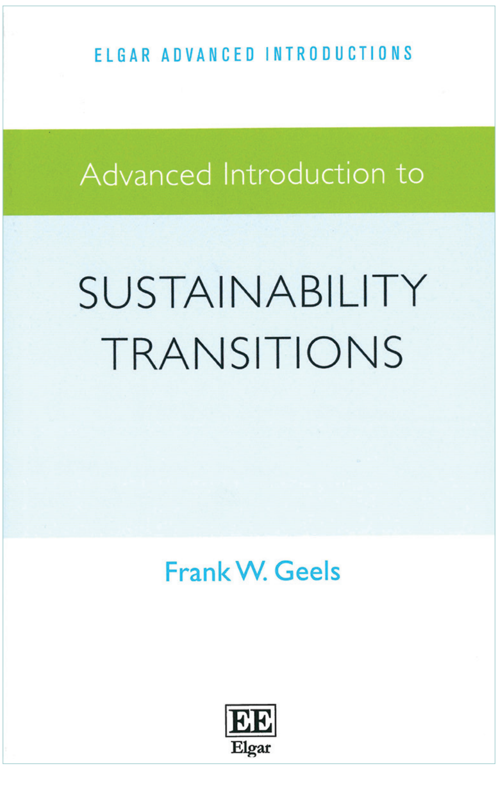

The book under review offers a rigorous yet accessible introduction to this field. The volume contains five regular chapters, while Chapter 6 provides concluding comments on the entire book. The book explores the evolution of sustainability transitions from early conceptual models through mid-2010s consolidation, to current debates about acceleration, destabilization, and justice. By doing so, it establishes important bridges between environmental studies, innovation studies, and political economy.

Authored by Frank W. Geels, Professor of System Innovation and Sustainability at the University of Manchester and chairman of the International Sustainability Transitions Research Network, the volume reflects his two decades of experience shaping the field. Published in 2024 with Edward Elgar, it draws on insights from evolutionary economics, sociology, institutional theory, and political science to guide readers through the complex and expanding landscape of sustainability transitions.

This review situates the book within the wider field, summarizes its core arguments, and evaluates its contributions and limitations. It concludes that the book succeeds as an authoritative introduction, though its emphasis on middle-range frameworks and reconfiguration pathways risks underplaying the urgency of the radical alternatives advocated by many environmental movements.

To contextualize the volume, it is useful to review the origins and growth of sustainability transitions as a field of study. Sustainability transitions emerged in the early 2000s in response to increasing evidence that climate change, biodiversity loss, and resource scarcity could not be addressed through incremental adjustments to existing socio-technical systems. Instead, systemic shifts driven by radical innovations in energy, food, mobility, housing, and manufacturing were recognized to be central. The field expanded rapidly in the 2010s, stimulated by the escalating climate crisis, the diffusion of renewable technologies, and growing international collaboration. With the establishment of the Sustainability Transitions Research Network (STRN) in 2009, the field became institutionalized, and the volume of publications has ever since grown to the extent that newcomers may struggle to navigate its diverse and fragmented literature.

Sustainability transitions are defined by six key characteristics. First, they are *multi-dimensional*, involving the co-evolution of technological, social, economic, and institutional elements. Second, they are *multi-actor* processes shaped by interactions among firms, users, policymakers, and civil society. Third, they are *long-term*, often unfolding over decades due to the slow emergence of radical innovations and the resilience of incumbent systems. Fourth, they are *goal-oriented*, aiming to enhance environmental performance while ensuring social and economic sustainability. Fifth, they are *conflictual* because they disrupt established interests and face resistance from powerful actors. Finally, they are *non-linear and uncertain*, with multiple competing innovations making outcomes difficult to predict. Together, these features make sustainability transitions analytically complex and resistant to conventional short-term social science approaches. Given these defining characteristics, the volume has turned to theoretical frameworks to understand how transitions unfold.

The book foregrounds the Multi-Level Perspective (MLP), now the dominant framework in Sustainability Transitions. Originating in the early 2000s, the MLP synthesizes insights from innovation studies, evolutionary economics, and the sociology of innovation to explain transitions as interactions across three levels: *niches* (protected spaces for radical innovation), *regimes* (stabilized socio-technical configurations), and *landscapes* (broader exogenous contexts such as cultural norms, macroeconomic trends, and geopolitical shocks). Transitions occur when niche innovations gain momentum, regimes face internal tensions or external pressures, and landscape dynamics create windows of opportunity. MLP highlights lock-in mechanisms, economic sunk costs, social routines, and political networks that stabilize regimes and resist radical change. Furthermore, it rejects monocausal explanations while emphasizing conjunctural and configurational causality.

The book also discusses three other frameworks, *Strategic Niche Management* (SNM), *Technological Innovation Systems* (TIS), and *Transition Management* (TM). SNM emphasizes vision-building, learning, and social networks in early innovation phases. TIS focuses on system functions such as knowledge development and resource mobilization. Finally, TM looks at governance approaches by combining visioning, experimentation, and reflexive learning. While each has distinct emphases, the book demonstrates how they complement the MLP in analysing phases of transitions.

The volume provides three major contributions. The first one lies in its systematic analysis of transition phases. Building on earlier models, it makes the distinctions between four sequential stages, namely experimentation, stabilization, diffusion, and reconfiguration. *Experimentation* involves radical innovations that initially function as "hopeful monstrosities", promising new functionalities but suffering from poor performance and high costs. Pilot projects and learning by doing are crucial at this stage, because they offer open-ended learning by doing and trial and error processes in concrete settings. Frameworks like SNM and TIS illuminate these processes.

Stabilization occurs when innovations consolidate into dominant designs, supported by field-level knowledge, codification, and niche markets. Niche actors also often articulate positive cultural discourses in this phase to legitimate innovations and attract further support.

Diffusion represents the scaling up of innovations into mainstream markets, often requiring supportive policy interventions and favorable public discourses. Here, public perceptions and cultural meanings are crucial. While positive public debates and discourses help drive diffusion, negative ones can lead to controversies and thus hamper the diffusion process.

Reconfiguration denotes system-wide restructuring, involving changes in technologies, infrastructures, cultural norms, and institutions. This reconfiguration implies that, in addition to substitution, sustainability transitions can also change in a sequential or stepwise manner.

The book illustrates these phases with both historical and contemporary cases. The transition from horse-drawn carriages to automobiles in the United States (between the 1890s and the mid-20th century) demonstrates how innovations evolve from niches to mainstream systems, reshaping entire economies and cultures. Similarly, the transition to piped water in the Netherlands (between the 1870s and 1920s) shows how technological and institutional innovations co-evolved to transform public health. Contemporary cases, especially the German *Energiewende* (energy transition), highlight the interplay of technological advances, policy instruments, and external shocks. The diffusion of wind and solar power was accelerated by the Chernobyl and Fukushima nuclear accidents, supportive feed-in tariffs, and grassroots activism. Yet the case also illustrates vulnerabilities, such as the bankruptcy of domestic producers in the face of global competition (especially from China). These examples underscore the non-linear, contested, and contingent nature of transitions.

The second major contribution of the book remains its nuanced treatment of actors. If early research tended to focus mainly on structures, the volume puts emphasis on agency, power, and diversity by examining four main actor groups represented by firms, civil society, policymakers, and users.

Firms are conceptualized both as incumbents defending existing regimes and as new entrants pioneering radical innovations. Initially seen as power struggles between small-scale sustainability innovations and dominant social technical regimes, more recent scholarship emphasizes the reorientation of incumbent regimes under pressure from regulation, public opinion, and market opportunities. The Triple Embeddedness Framework (TEF) captures how firms face simultaneous pressures from economic and socio-political environments, leading to phases of denial, incremental adjustment, hedging, and eventual reorientation. Empirical studies of the automotive and electricity industries illustrate these dynamics.

Civil society actors, including grassroots innovators and social movements, contribute by pioneering alternative practices, shaping cultural meanings, and mobilizing for justice. While their initiatives often struggle to scale, they play important roles in challenging dominant discourses and introducing new imaginaries. Public debates and framing struggles play a major role in shaping legitimacy and social acceptance.

Policymakers and states have re-emerged as central actors, particularly after recent geopolitical crises. Early emphasis on governance suggested a diminished role for the nation-state, but events such as the COVID-19 pandemic, the war in Ukraine, and the gas price crisis (in 2021 and 2022) revealed the enduring power of state intervention. The resurgence of industrial policy in the European Union (the European Green Deal in 2019) and the United States (the Inflation Reduction Act in 2023) illustrates this shift. Policy mixes, combinations of Research and Development subsidies, feed-in tariffs, regulations, and just transition measures, are central to sustainability transitions.

Users, too often neglected in early research, are now recognized as crucial actors. They play multiple roles by representing experimenters, legitimators, citizens, intermediaries, and consumers. Adoption theories, social practice theories, and domestication studies reveal the complexity of user engagement. They shape transitions through consumption, routines, and cultural acceptance.

Finally, the book highlights how acceleration, multi-system interactions, finance, international supply chains, emerging economies, and cities are reshaping debates and practices in the field. It, thus, demonstrates that sustainability transitions are not merely technical challenges but deeply socio-political and global in scope. This reflects both the complexity and urgency of global transitions.

The discussion of *acceleration* is particularly strong. It frames the paradox of needing faster transitions while recognizing the barriers in early phases when costs are high and technologies immature. The socio-technical feedback loop framework provides a nuanced lens for understanding why electric vehicle (EV) diffusion shifted from scepticism to strategic commitment within a decade. This effectively illustrates how technical improvements, policy pressures, and public debates reinforce each other to produce tipping dynamics.

Taken together, these dynamics reveal that the acceleration of sustainability transitions is marked not only by opportunities for rapid diffusion, as in the case of electric vehicles, but also by significant risks, exemplified by Spain's recent power outage. Occurring on 28 April 2025 and lasting several hours (from midday until approximately 7 a.m. the following day), this outage, now understood to have stemmed from a combination of technical deficiencies and coordination failures, including inadequate voltage control, frequency oscillations, and improper generator disconnections (Red Eléctrica de España, 2025) raised significant concerns about grid stability and system resilience in a country where 59 percent of electricity is generated from renewable sources. Although official reports did not single out the role of renewables (Red Eléctrica de España, 2025), the complexity of grid operations and the extremely high reliability standards they require (99.97 per cent for modern reliability targets) (Dunsmore, J. *et al.* 2025) keep this hypothesis in play. Given the inherent variability of solar and wind generation, Spain's substantial reliance on these renewable sources heightens the vulnerability of its electrical system to potential disruptions.

The argument on *multi-system interactions and deep transitions* adds historical and theoretical depth. By drawing parallels with past industrial revolutions, the author convincingly argues that today's net-zero pathways are characterized by cascading innovations across electricity, transport, and industrial systems. The concept of "deep transitions" raises the stakes by connecting system change to broader societal meta-rules. However, the critique that this approach risks being overly abstract and detached from contemporary socio-economic dynamics is well taken.

The treatment of *finance* is timely and insightful. By situating finance as its own regime with distinctive lock-ins, the author underscores why redirecting capital flows remains so challenging even though global financial assets were estimated at USD 461.6 trillion in 2022, of which the USD 6 trillion needed for the SDGs represents only 1.3 percent. Financial actors remain bound by established routines, short-term horizons, and risk-averse practices, which limit large-scale reorientation. Banks and institutional investors often regard emerging green innovations as too risky, favour large projects over smaller, fragmented ones, and lack the expertise to assess novel technologies. Consequently, investments concentrate in de-risked sectors such as solar, wind, and electric vehicles, while areas like building efficiency, hydrogen, and carbon capture remain underfunded. Broader structural constraints, including speculative financial logics, high transaction costs, and limited central bank engagement, further reinforce these barriers, rendering finance both indispensable and highly problematic for sustainability transitions.

The sections on emerging economies and cities highlight the need to adapt transition frameworks to local contexts. In the Global South, transitions are shaped by several key factors, of which the volume draws attention to four. First, fragmented and unstable socio-technical regimes create uncertainties that hinder planning and niche development. Second, firms and policymakers face limited resources and capabilities, with weak learning processes. Third, elite capture, corruption, and undemocratic governance constrain systemic change, even where natural conditions favour innovations such as solar or wind. Fourth, high poverty and inequality necessitate linking transitions to broader socio-economic development, while transnational actors often support niche innovations. These factors indicate that, although frameworks like the MLP remain useful, they require careful adaptation to the complex realities of emerging economies.

Regarding the processes in cities, the volume highlights significant limitations. Most early-phase initiatives (Latin America, South Korea, and Europe) are temporary, fail to scale, and have limited transformative impact. At the same time, implementation tends to be incremental, it involves weak social learning, limited citizen engagement, and a focus on reformist rather than systemic change. These patterns reveal a persistent gap between policy ambitions and practice, cautioning against wishful thinking and emphasizing the need for critical reflection on implementation challenges.

Having considered these three contributions, it is important to acknowledge the book's considerable merits, which make it a valuable reference for transition studies. In my view, the book has five major strengths. First, its synthetic overview makes it invaluable as a teaching and reference text. It consolidates an expansive body of literature into a coherent narrative without oversimplifying complexity. Second, its emphasis on the Multi-Level Perspective as a middle-range framework establishes an effective balance between theoretical abstraction and empirical relevance. Third, the integration of historical and contemporary cases enriches the conceptual discussion and grounds it in concrete examples. Fourth, its attention to actors reflects the field's maturation and responsiveness to mainstream social science debates. Finally, the reference to cross-cutting topics is a testament to the continuous expansion of the field.

That said, the volume also has some limitations that deserve attention. One limitation remains its heavy reliance on the Multi-Level Perspective. While the MLP is a well-established framework, this orientation risks narrowing theoretical innovation by overlooking alternative approaches. Its emphasis on technological efficiency and resource management, though valuable, does little to address the persistent inequalities that shape sustainability transitions, particularly in relation to energy access. A glance at global energy consumption underscores this issue. Of the 592 exajoules (EJ) consumed worldwide in 2024, Europe and North America accounted for 184 EJ, while Africa consumed only 21 EJ (Energy Institute, 2025).

This unequal distribution reflects a "law of thirds," whereby the wealthiest one-third of the global population uses roughly two-thirds of the world's energy (Lawrence, S. *et al.* 2013). Given the close relationship between energy access and economic productivity, such disparities constrain the capacity of societies to pursue long-term development and environmental stewardship. Incorporating more critical political economy perspectives that foreground these inequalities would significantly strengthen the volume's analysis.

Similarly, while the book convincingly demonstrates that incremental measures such as technological upgrades, efficiency improvements, and policy tweaks can yield benefits, recent climate data suggest they are insufficient to limit warming to 1.5 °C. In 2024, global emissions reached 40.8 $GtCO_2e$, a 1 percent increase above the target (Energy Institute, 2025). This trend suggests that continuous reliance on gradual transitions risks locking in high-carbon infrastructure, amplifying climate feedbacks, and reducing adaptive capacity. Therefore, while incremental steps are politically feasible, they must be complemented by bold systemic interventions, including local-led poverty eradication, renewable energy expansion, transport electrification, and broad behavioural and institutional shifts, to achieve the scale and pace required for the 1.5 °C target.

Furthermore, the volume treats grassroots and social innovations somewhat sceptically, emphasizing their diffusion challenges rather than their transformative potential. This risks underestimating the cultural and normative shifts they generate. Emerging from local needs and experimenting with alternative practices of energy use, mobility, or food provision (Seyfang, G. and Smith, A. 2007), such initiatives may indeed not scale quickly in market terms but nonetheless reshape expectations, values, and social norms. Over time, these local experiments can accumulate into broader cultural shifts, influencing discourse, policy, and imaginaries of sustainable futures. By privileging diffusion barriers, the analysis reinforces attraction toward large-scale, technology-driven solutions at the expense of bottom-up approaches. Attending to the political and cultural dimensions of grassroots innovation would substantially enrich the analysis.

This point becomes particularly salient when considering Global South contexts. As a Malian researcher, I find the volume's findings uneven in their applicability. Developed largely from Western European cases, the book assumes strong institutions, abundant resources, and stable governance, conditions that do not always hold in Mali or much of the Global South. For example, in Sub-Saharan Africa, where large segments of the population live in poverty (Abdulhakeem, A.K. *et al.* 2023), sustainable futures must begin with eradicating deprivation, and reliable access to energy is a crucial starting point. Evidence shows that while poor people may exist in rich countries, there are no rich countries without secure energy (IEA, IRENA, UNSD, World Bank, WHO, 2025). In this context, in addition to considering energy density for policy design, grassroots solutions (such as solar kiosks, community farming, and small-scale energy projects) are central drivers of change, even if the book dismisses them as fragile or non-scalable. The volume employs useful frameworks, but these require adaptation to contexts shaped by informal economies, weaker state capacity, and dependence on international donors.

Finally, in Central and Eastern Europe, the situation is different but also uneven. These countries are not part of the Global South, yet they remain outside the Western European core. Post-socialist legacies, dependence on coal and imported energy, and vulnerability to energy poverty (which manifests as inadequate heating or high housing costs) mean transitions face distinct barriers (Bouzarovski, S. *et al.* 2017). The book's insights can illuminate these processes, but its solutions often feel distant. Overall, while the volume provides powerful analytical tools, it does not fully address the specific challenges of regions beyond the global core, leaving much of the adaptation work to local researchers.

Despite these limitations, the book makes significant contributions to ongoing debates in socio-technical transitions research. It affirms the importance of multi-level and co-evolutionary perspectives while responding to critiques about agency, power, and justice. Its emphasis on acceleration resonates with recent reports from the International Energy Agency and the United Nations warning about closing windows of opportunity (International Energy Agency, 2021; United Nations Environment Programme, 2022). By documenting how transitions unfold through stepwise reconfiguration rather than sudden system overthrow, it highlights the role of unintended consequences in history while still acknowledging the potential for transformative change.

The book also connects with policy-oriented literatures on industrial strategy, innovation policy, and mission-oriented governance. Its discussion of state interventions situates sustainability transitions research within broader debates on post-neoliberal political economy, while its cautious treatment of de-growth and radical alternatives reflects the ongoing tension between reformist and transformative visions of sustainability. In summary, the book offers an authoritative, accessible, and critical overview of sustainability transitions research. It succeeds both in synthesizing the field for newcomers and in stimulating reflection among established scholars. By tracing the interplay of niches, regimes, and landscapes, analysing sequential phases of experimentation, stabilization, diffusion, and reconfiguration, examining the roles of diverse actors, and underscoring the importance of cross-cutting topics, it provides a robust framework for understanding socio-technical change. While its prioritization of the MLP and reconfiguration pathways limits engagement with more radical alternatives, it nonetheless equips graduate students and scholars, educators, practitioners, policymakers, and activists with valuable conceptual tools for addressing pressing sustainability challenges. In the context of escalating climate emergencies, these resources are particularly relevant for advancing clean, accessible, and affordable energy.

Bourema Diarra[1]

REFERENCES

Abdulhakeem, A.K., Abdulrahman, I.A. and Oniyide, G.D. 2023. Governance and multidimensional poverty in Sub-Saharan Africa. *African Journal of Economic Review* 11. (5): 34–49.

Bouzarovski, S., Herrero, S.T., Petrova, S., Frankowski, J., Matoušek, R. and Maltby, T. 2017. Multiple transformations: Theorizing energy vulnerability as a socio-spatial phenomenon. *Geografiska Annaler: Series B, Human Geography 99.* (1): 20–41.

Dunsmore, J., Arthur, L.M. and Kemp, R.S. 2025. *The Optimum Mix of Storage and Backup in a Highly Renewable, Highly Reliable European Electricity Grid*. arXiv: 2503.23604. https://arxiv.org/abs/2503.23604

Energy Institute, 2025. *Statistical Review of World Energy 2025*. Energy Institute. https://www.energyinst.org/statistical-review

IEA, IRENA, UNSD, World Bank, WHO, 2025. *Tracking SDG 7: The Energy Progress Report*. Washington D.C., World Bank.

International Energy Agency, 2021. *Net Zero by 2050: A Roadmap for the Global Energy Sector*. Paris, IEA.

Lawrence, S., Liu, Q. and Yakovenko, V.M. 2013. Global inequality in energy consumption from 1980 to 2010. *Entropy 15.* (12): 5565–5579.

Malthus, T. 1798. *An Essay on the Principle of Population*. London, J. Johnson in St. Paul's Church-Yard.

Meadows, D.H., Meadows, D.L., Randers, J. and Behrens III, W.W. 1972. *The Limits to Growth: A Report for the Club of Rome's Project on the Predicament of Mankind*. New York, Universe Books.

Red Eléctrica de España, 2025. *Blackout in the Spanish Peninsular Electrical System the 28th of April 2025*. Madrid, Red Eléctrica de España.

Richardson, K. *et al.* 2023. Earth beyond six of nine planetary boundaries. *Science Advances 9.* (37): eadh2458.

Seyfang, G. and Smith, A. 2007. Grassroots innovations for sustainable development: Towards a new research and policy agenda. *Environmental Politics 16.* (4): 584–603.

United Nations Environment Programme, 2022. *Emissions Gap Report 2022: The Closing Window – Climate Crisis Calls for Rapid Transformation of Societies*. Nairobi, UNEP.

[1] ELTE Eötvös Loránd University, Institute of Geography and Earth Sciences, Department of Social and Economic Geography, Budapest, Hungary. E-mail: boure@student.elte.hu

 DOI: 10.15201/hungeobull.75.1.7

Daheur, J. and Lučić, I. (eds.): Habsburg Natures: Imperial Governance and Environment in Central Europe, 1850–1918. New York/Oxford, Berghahn Books, 2026. 342 p.

Habsburg Natures offers a refreshingly innovative perspective on late Habsburg history by placing the environment at its core. The volume compellingly demonstrates how rivers, forests, animals, coal, and fodder actively shaped governance structures, imperial decline, and regional interactions throughout the Austro-Hungarian Empire from 1850 to 1918. This exemplary open-access publication, constructs a comprehensive new understanding of the empire that transcends conventional national narratives. It masterfully integrates physical environmental limitations – such as Alpine deforestation patterns, Danube silt dynamics, and Galician drought cycles – with complex political connections, delivering insights particularly valuable for geographers studying imperial peripheries, resource politics, and spatial state development. By thoughtfully emphasizing nature's diverse manifestations within a continental European empire – distinct from overseas colonial contexts – the book productively challenges readers to reconsider how biophysical realities fundamentally influenced Habsburg power dynamics. The volume traces this influence across compelling case studies, from diplomatic conflicts over river regulation to peasant uprisings triggered by forest commercialization, providing fresh methodological approaches for regional studies in Central and Eastern Europe.

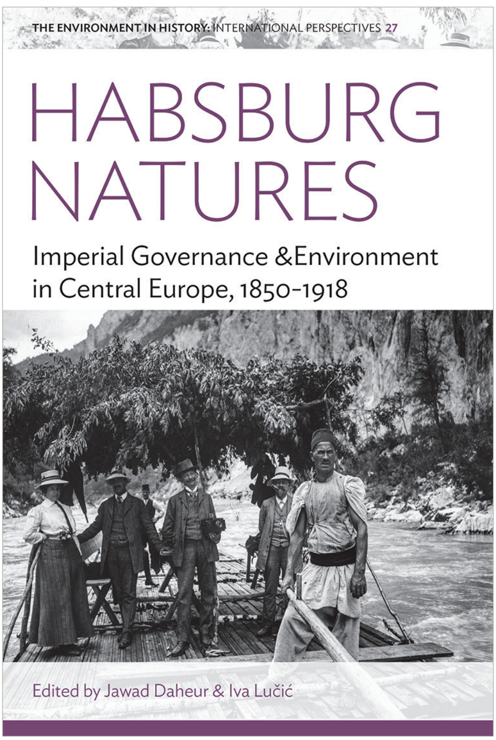

The editor's introduction expertly establishes the context, defining the "late Habsburg Empire" primarily as Austria-Hungary after 1867 and tracing its continuities back to mid-century reforms such as the 1852 Imperial Forest Act. Jawad Daheur and Iva Lučić argue that the Empire's geographical position as Europe's second-largest state – 676,615 km², 51 million people by 1910 – and its ecological diversity – from Alpine forests to Danubian floodplains – made it a laboratory for resource governance under dual sovereignty. Habsburg "internal peripheries" created inequalities through intra-imperial commodity chains, which were made political by nationalism and capitalist pressures. This arrangement is different from colonial empires that took resources from other countries. Editors Jawad Daheur, a CNRS senior researcher at CERCEC (EHESS, Paris), specialises in Central European environmental history with a focus on forests and trade, and Iva Lučić, an associate professor of Eastern European History at Stockholm University and a Pro Futura Scientia Fellow (SCAS) co-edited the volume published by Berghahn in the "Environment in History: International Perspectives" as Vol. 27. This series advances global eco-historical scholarship and publishing cutting-edge works on nature-society dynamics; this open-access volume fits seamlessly. This book, written by multiple authors because of the different languages and archives involved, brings together eleven chapters that focus on individual stories, balancing government control with local actions, and steering clear of a one-size-fits-all uniformity.

The contributions of this volume are divided into four thematic parts, each bridging material environments and institutional geographies. Part I tracks imperial entanglements inside and between empires, Part II focuses on the dynamics of cooperation and conflict, Part III provides a multispecies perspective to engineering nature and Part IV offers insights to practices of managing different kinds of resources.

Part I (*Inter/Intra Imperial Entanglements*) opens with riparian politics: Robert Shields Mevissen examines how Danube regulation projects, from the blasting of Iron Gates (1875–1890) to delta disputes after the Berlin Congress of 1878, mixing Habsburg diplomacy with policies in the crownlands. Mevissen shows that physical river dynamics – shoals, floods, and deltas – constrained navigation and forced negotiations with Romania, Serbia, and the Ottoman Empire via the European Danube Commission, while amplified internal tensions over hydraulic infrastructure funding. Jana Osterkamp's chapter discusses how melioration (land drainage and irrigation) helped states collaborate, highlighting projects in Lombardy's Po Valley and Bosnia. In the next chapter, Selçuk Dursun provides an Ottoman perspective, explaining timber poaching in Bosnia's border areas during the nineteenth century, before the Habsburg occupation in 1878.

Part II (*Cooperation and Conflict*) centres on forests, which covered more than third of the Habsburg landscapes. Iva Lučić's study of Bosnian timber exports (oak staves, trunks) shows that the "proximate colony" acted as a dividing force: after 1878, railroads directed wood to Trieste and Austrian markets, and paved a way to exclusionary campaigns in the Cisleithanian crownlands. The two case studies of this chapter demonstrate how statistics quantify frictions, while legal disputes reveal the role of private capital in imperial fissures. Gábor Egry's standout chapter on Transylvania illuminates "ecological nationalisms," where late-imperial commercialization – leasing forests to industrial firms – eroded peasant usufruct, sparking violence that peaked in 1918 revolts and persisted into Romanian rule. Communal properties (e.g. Năsăud School Fund, 91,000 acres) and noble estates fuelled clashes, as Romanian peasants invoked authenticity against Hungarian state forestry, blending material grievances with national claims. Egry extends into interwar Romania, showing Habsburg legacies in lease contracts and unified 1923 forestry laws, where state-building prioritized technocracy over redistribution. Robert Skenderović examines Croatian-Slavonian Military Border demilitarization (post-1881), where oak commercialization threatened peasants' entitlements, yet their soldier status preserved access via negotiated state management. Collectively, these chapters recast forests not as passive resources but as mediators of sovereignty, where customary rights clashed with nationalizing conflicts and exposing dualism's limits.

Part III (*Engineering Nature*) ventures into human-nonhuman entanglements, a methodological innovation for imperial history. Wolfgang Göderle's microhistory traces eleven Indian mongooses released on Mljet island (Meleda, Dalmatia) in 1910 to combat horned vipers (*Vipera ammodytes*), drawing on global knowledge – from Brockhaus encyclopaedias to Slovenian herpetology – circulated via ministries. Dalmatian civil servants mirrored human censuses with animal surveys, treating vipers as imperial threats; post-release monitoring (into the 1920s) underscores ecological legacies, with mongooses persisting despite failures. Maps of Adriatic ports (Trieste, Korčula) spatialize knowledge flows, equating administrative practices for subjects, censuses, and fauna. In the next chapter, Kristýna Kaucká reconstructs the "golden age" of bark beetle (*Ips typographus*) (1868–1876) the Šumava region, where 1846/1868 storms felled spruce, enabling infestations that ravaged aristocratic estates. Bohemian nobility lobbied for sanitation felling and railways, blending crisis response with modernization; Kaucká's life-cycle illustrations and postcards evoke the infestation's visual drama, linking pests to infrastructure debates. These chapters humanize bureaucracy, showing symmetric governance for humans and nonhumans amid globalizing science.

Part IV (*Managing Resources*) confronts scarcity politics. Jawad Daheur's quantitative reconstruction of fodder bans in 1893 and 1904 – triggered by droughts reducing hay and oilcake output—maps export chains to Germany, where Cisleithanian producers allied trans-ethnically against bans, overriding ministerial lines. Graphs of 1882–1913 exports and tables quantify crises, revealing imperial resilience, for example, via ad hoc vetoes on railway shipments or sectarian echoes. Daheur's customs data plots hay flows from Galician meadows to Prussian markets, showing the 1893 drought halved yields, prompting bans that nobles and magnates circumvented through petitions. Ségolène Plyer's Bohemian coal chapter details Ostrava-Karviná basin dynamics, where lignite and bituminous deposits fuelled regional diversity. Simone Ginrich and Martin Schmid focus on the 1852 Forest Act and aims to quantify the transitions from feudal servitudes to sustained-yield regimes, enabling wood exports that increased from 28 to 40 million m³ by 1910. While prioritizing industrial timber over peasant needs led to growing tensions and dissatisfaction among the rural population, authors suggest that uneven enforcement across crownlands sowed resentments and amplified nationalism. The conclusion of this chapter revisits these as environmental dynamics and suggests that they had their fair share in the decline of the Habsburg Empire. Part IV is exceptionally illustrated as it includes nine graphs, dual tables, QGIS maps, and photos that model biophysical teleconnections, which bind and then fracture imperial fragments.

Habsburg Nature, with its rigorous spatial analysis, integrating biophysical processes with imperial power dynamics, fills a notable gap in Habsburg environmental historiography and offers a valuable contribution for geographers and scholars of regional studies. The book includes over thirty custom QGIS maps that show Habsburg territorial expansion, Danube deltas, Transylvanian forest cover, and Bohemian coal deposits, presenting environments as important factors that influence governance and using detailed data to clearly show ecological differences. Methodologically, the actor-centred fusion of multilingual archives, quantitative sources, and visuals provides replicable templates for transregional environmental histories prioritizing flows over national silos – a real strength for scholars seeking practical models. Geographers will especially appreciate this fusion of multilingual archives and visuals, filling gaps in Habsburg environmental historiography while urging material flow analyses for timber, fodder, and coal – thrusting intra-European eco-imperial dynamics into global debates with fresh energy.

The editors' introduction frames Austria-Hungary post-1867 as a diverse "laboratory" for resource governance with ecological variety from the Alps to the Danubian plains driving innovative responses under dual sovereignty. Multilingual archives – from Czech petitions to Ottoman logs – ground microhistories like Göderle's mongoose censuses or Kaucká's Šumava beetle postcards, offering robust templates for socio-natural analysis across scales. Forestry features prominently across six of the eleven chapters, reflecting the abundance of archival sources on this theme and the pivotal role forests played in Habsburg landscapes and economies. Bosnian oak exports highlight fractures via Trieste railroads; Transylvanian leases trace peasant revolts into Romanian interwar laws; military border analysis shows peasant rights enduring post-1881. The 1852 Forest Act marks a key shift to sustained-yield forestry, boosting exports while challenging communal rights – a theme ripe for further exploration. While urban environments are mentioned briefly – especially in discussions about coal – looking more closely beyond coal could improve future research in these areas. The book also mentions connections to other empires, such as Ottoman Bosnia and Russia, which could lead to intriguing comparisons worth exploring further; using methods like material flow analysis for timber or fodder could greatly enhance the already solid research. Pre-1878 poaching or Prussian hay flows invite such extensions, globalizing Habsburg cases in parallel with Siberian taiga or tropical models.

Habsburg Natures excels in benchmarking intra-European imperialism, where "internal peripheries" like Bosnia or Galicia echoed colonies without overseas distance. Rivers drove diplomacy; disasters revealed adaptive bureaucracy. For geographers, it integrates Habsburg extraction, frontiers, and green statehood into global debates, with post-1918 extensions highlighting enduring legacies. This open-access volume in the Berghahn's Environment in History series sets a high standard, equipping scholars to reframe Central Europe's environmental histories through imperial ecologies. Its visuals, methods, and pivots – from entanglements to scarcities encouraging urban expansions and inter-imperial flows – offer transregional inspiration. Meanwhile, the volume's methodology both decentring Vienna and elevating the significance of Habsburg natures in worldwide scholarship.

Beyond its technical achievements, *Habsburg Natures* stands out as an exemplary model of collaborative scholarship, uniting an international roster of experts who deftly navigate multilingual archives to produce a cohesive narrative that transcends national boundaries and disciplinary silos. The open-access format ensures wide accessibility, democratizing cutting-edge environmental history for researchers worldwide. Overall, this book sets a new benchmark for environmental imperial histories, masterfully demonstrating how nature actively shaped Habsburg power dynamics and offering geographers invaluable tools to reframe Central European ecologies within global scholarship – a truly essential contribution that will inspire and guide future research for years to come.

Viktor Pál[1]

[1] Centre for Economic and Social History, Faculty of Arts, University of Ostrava, Ostrava, Czech Republic. E-mail: viktor.pal@osu.cz

Manuscript reviewers 2023–2025

The editors of the Hungarian Geographical Bulletin would like to thank the following experts for their assistance in reviewing manuscript submissions to our journal issues between Number 1 in 2023 and Number 4 in 2025. Their efforts and useful comments have been of great service to the authors and the journal.

Adie, Bailey Ash (Oulu)
Atak, Arif (Bursa)
Balogh, Péter (Budapest)
Barreiros, Ana M. (Lisbon)
Bayona Carrasco, Jordi (Barcelona)
Belotti, Sara (Bergamo)
Benarroch, Alicia (Granada)
Benedek, József (Cluj-Napoca)
Berghauer, Sándor (Berehove)
Bertalan, László (Debrecen)
Bilașco, Ștefan (Cluj-Napoca)
Boros, Lajos (Szeged)
Braychevskyy, Yulian (Kyiv)
Breuer, Hajnalka (Budapest)
Brönnimann, Stefan (Bern)
Buzási, Attila (Budapest)
Csapó, János (Pécs)
Cselovszki-Soltész, Petra (Budapest)
Csomós, György (Debrecen)
Czaller, László (Budapest)
Czigány, Szabolcs (Pécs)
Czimre, Klára (Debrecen)
Demeter, Gábor (Budapest)
Dezső, Zsuzsanna (Budapest)
Drbohlav, Dušan (Prague)
Dronova, Olena (Kyiv)
Dusek, Tamás (Győr)
Egedy, Tamás (Budapest)
Erőss, Ágnes (Budapest)
Fabula, Szabolcs (Szeged)
Farkas, Jenő (Kecskemét)
Fonseca, Lucinda (Lisbon)
Freytag, Tim (Freiburg)
Gál, Tamás (Szeged)
Gellér-Lukács, Éva (Budapest)
Ghafarpour, Amin (Gorgan)
Glamuzina, Nikola (Split)
Gnatiuk, Oleksiy (Kyiv)
Golovics, József (Budapest)
Gresina, Fruzsina (Budapest)
Győri, Róbert (Budapest)
Halmai, Ákos (Pécs)
Hänsel, Stephanie (Offenbach)
Harangozó, Gábor (Budapest)
Hoyk, Edit (Kecskemét)
Illés, Sándor (Budapest)
Irimiás, Anna (Budapest)
Isaac, Rami, K. (Breda)
Jakubowski, Andrzej (Lublin)
Jakubus, Monika (Poznań)
Jankiewicz, Mateusz (Toruń)
Jankó, Ferenc (Budapest)
Jastrzębska, Ewa (Warsaw)
Jóvér, Vanda (Budapest)
Juhos, Katalin (Gödöllő)
Kádár, Bálint (Budapest)
Karácsonyi, Dávid (Budapest)
Kocsis, János Balázs (Budapest)
Kołodziejczak, Małgorzata (Poznań)
Kolozsvári-Kovály, Katalin (Budapest)
Komornicki, Tomasz (Warsaw)
Kovács, Ferenc (Szeged)
Kovalcsik, Tamás (Szeged)
Kőszegi, Margit (Budapest)
Kristóf, Dániel (Budapest)
Kulcsár, Balázs (Debrecen)
Kundu, Debolina (New Delhi)
Lamego, Mariana (Rio de Janeiro)
Leibert, Tim (Leipzig)
Lendvay, Márton (Aberystwyth)
Lennert, József (Budapest)
Lóczy, Dénes (Pécs)
López Sala, Ana María (Madrid)
Łupikasza, Ewa (Katowice)
Marquardt, Editha (Heidelberg)
Mazurek, Małgorzata (Poznań)
Merabishvili, Gela (Budapest)
Mezentsev, Kostyantyn (Kyiv)
Michalkó, Gábor (Budapest)
Molnár, Ernő (Debrecen)
Molnár, Tamás (Sopron)
Mucsi, László (Szeged)
Nagy, Erika (Békéscsaba)
Nagy, Gábor (Békéscsaba)
Nagy, Gyula (Szeged)
Napierała, Tomasz (Łódz)
Négyesi, Gábor (Debrecen)
Németh, Krisztina (Budapest)
Nikolova, Valentina (Sofia)
Nováček, Aleš (České Budějovice)
Novák, Tibor (Debrecen)
Nyéki, Anikó Éva (Győr)
Nzimande, Ntombifuthi (Szeged)
Orozco-Martínez, Carolina (Barcelona)
Orusa, Tommaso (Torino)
Pawlik, Łukasz (Katowice)
Pécsek, Brigitta (Eger)
Pénzes, János (Debrecen)
Piasecki, Adam (Toruń)
Pinskwar, Iwona (Poznań)
Pirisi, Gábor (Pécs)
Plavcová, Eva (Prague)
Prokkola, Eeva-Kaisa (Oulu)
Proto, Matteo (Bologna)
Rainer, Gerhard (Passau)
Räisänen, Jouni (Helsinki)
Raucsik-Varga, Andrea (Szeged)
Reményi, Péter (Pécs)
Rietbergen, Martijn (Utrecht)
Sajter, Domagoj (Osijek)
Salim, Emmanuel (Lausanne)
Sarkadi, Noémi (Pécs)
Sipos, György (Szeged)
Soha, Tamás (Budapest)
Solarz, Marcin Wojciech (Warsaw)
Šūpule, Inese (Riga)
Szabó, Szilárd (Debrecen)
Szalai, Zoltán (Budapest)
Szatmári, Daniel (Bratislava)
Szlávecz, Katalin (Baltimore)
Tátrai, Patrik (Budapest)
Telbisz, Tamás (Budapest)
Tomay, Kyra (Pécs)
Torbenson, Max C.A. (Mainz)
Unger, János (Szeged)
Uzzoli, Annamária (Budapest)
Vaishar, Antonín (Brno)
Vavrouchová, Hana (Brno)
Vida, Zsófia (Budapest)
Vityi, Andrea (Sopron)
Weidinger, Tamás (Budapest)
Wendt, Jan Andrzej (Gdańsk)
Więckowski, Marek (Warsaw)

GUIDELINES FOR AUTHORS

Hungarian Geographical Bulletin (formerly Földrajzi Értesítő) is a double-blind peer-reviewed English-language quarterly journal publishing open access **original scientific works** in the field of physical and human geography, methodology and analyses in geography, GIS, environmental assessment, regional studies, geographical research in Hungary and Central Europe. In the regular and special issues also discussion papers, chronicles and book reviews can be published.

Manuscript requirements

We accept most word processing formats, but MSWord files are preferred. Submissions should be single spaced and use 12pt font, and any track changes must be removed. The paper completed with abstract, keywords, text, figures, tables and references should not exceed **7,000 words**.

The Cover Page of the article should only include the following information: title; author names; a footnote with the affiliations, postal and e-mail addresses of the authors in the correct order; a list of 4 to 8 keywords; any acknowledgements.

An abstract of up to **300 words** must be included in the submitted manuscript. It should state briefly and clearly the purpose and setting of the research, methodological backgrounds, the principal findings and major conclusions.

Figures and tables

Submit each illustration as a separate file. Figures and tables should be referred in the text. Numbering of figures and tables should be consecutively in accordance with their appearance in the text. Lettering and sizing of original artwork should be uniform. Convert the images to TIF or JPEG with an appropriate resolution: for colour or grayscale photographs or vector drawings (min. 300 dpi); bitmapped line drawings (min.1000 dpi); combinations bitmapped line/photographs (min. 500 dpi). Please do not supply files that are optimised for screen use (e.g., GIF, BMP, PICT, WPG). Size the illustrations close to the desired dimensions of the printed version. Be sparing in the use of tables and ensure that the data presented in tables do not duplicate results described elsewhere in the article.

REFERENCES

Please ensure that every reference cited in the text is also present in the reference list (and vice versa). Titles of non-English references should be translated in English and indicated in brackets.

Reference style

Text: In the text refer to the author's name (small capitals with initials) and year of publication. References should be arranged first chronologically and then further sorted alphabetically if necessary. More than one reference from the same author(s) in the same year must be identified by the letters 'a', 'b', placed after the year of publication.
Examples: (Ridgewell, A.J. 2002; Maher, B.A. *et al.* 2010) or Ridgewell, A.J. (2002); Maher, B.A. *et al.* (2010).

Journal papers:
Aagaard, T., Orford, J. and Murray, A.S. 2007. Environmental controls on coastal dune formation; Skallingen Spit, Denmark. *Geomorphology* 83. (1): 29–47.

Books:
Pye, K. 1987. *Aeolian Dust and Dust Deposits.* London, Academic Press.

Book chapters:
Kovács, J. and Varga, Gy. 2013. Loess. In *Encyclopedia of Natural Hazards.* Ed.: Bobrowsky, P., Frankfurt, Springer, 637–638.

Book reviews

Book reviews should be between 2,000 and 3,000 words (including references).

Submission

Submission to this journal occurs online. Please submit your article via http://ojs3.mtak.hu/index.php/hungeobull/about/submissions

All correspondence, including notification of the Editor's decision and requests for revision, takes place by e-mail.

Publisher:
HUN-REN Research Centre for Astronomy and Earth Sciences
1121 Budapest, Konkoly Thege Miklós út 15–17., Hungary

Editorial office:
Geographical Institute
HUN-REN Research Centre for Astronomy and Earth Sciences
1112 Budapest, Budaörsi út 45., Hungary
Phone, fax: +36 1 309 2628
E-mail: hungeobull@csfk.org, kovacs.zoltan@csfk.org
Distribution: GABRIELLA PETZ, petz.gabriella@csfk.org
Full text is available at https://ojs3.mtak.hu/index.php/hungeobull

Typography: ESZTER GARAI-ÉDLER
Technical staff: FANNI KOCZÓ, ANIKÓ KOVÁCS, GÁSPÁR MEZEI

Cover design: ANNA REDL
Printed by: Premier Nyomda Kft.

HU ISSN 2064–5031

Distributed by the Geographical Institute, Research Centre for Astronomy and Earth Sciences

Subscription directly at the Geographical Institute, Research Centre for Astronomy and Earth Sciences (H-1112 Budapest, Budaörsi út 45), by postal order or transfer to the account IBAN: HU24 10032000-01730841-00000000. Individual copies can be purchased in the library of the Institute at the above address.